Dissertation

Sensor Systems for Impaired Healing

Markers, Concepts and Applications for Objective Wound Assessment

Vom Fachbereich für Physik und Elektrotechnik der Universität Bremen

zur Erlangung des akademischen Grades Doktor-Ingenieur (Dr.-Ing.) genehmigte Dissertation

von

Dietmar Puchberger

Rotensterngasse 7/11, 1020, Wien

Wien, 2015

Eingereicht am: 09.02.2016
Tag des Promotionskolloquiums: 14.06.2016

Referent: Prof. Dr.-Ing. Michael J. Vellekoop
University of Bremen
Bremen, Germany

Koreferent: Prof. Dr. Franz Keplinger
Vienna University of Technology
Vienna, Austria

URN: urn:nbn:de:gbv:46-00105319-19

Diese Dissertation ist online verfügbar unter:
http://nbn-resolving.de/urn:nbn:de:gbv:46-00105319-19

Wonder is the seed of knowledge.
Francis Bacon

Contents

Summary **xi**

Kurzfassung **xiii**

Nomenclature **xv**
0.1 List of Abbreviations xv
0.2 List of Variables xvi

1 Introduction **1**
1.1 Wound Healing - A Highly Ordered Sequence of Events . . 2
1.1.1 Wound Healing Mechanisms 2
1.1.2 Impaired Healing and Chronic Wounds 4
1.2 Conventional Wound Care Techniques 5
1.3 Study Objectives 8
1.4 Outline of the Thesis 9

2 Wearable System for Direct Wound Monitoring **11**
2.1 Introduction 11
2.2 Sensor design and fabrication 15
2.3 Animal study design 18
2.4 Results and Discussion 19
2.4.1 pH Responsive Film Characterization 19
2.4.2 Multi-parameter Sensor Characterization 21
2.4.3 Wound Monitoring in Porcine Model 26
2.5 Conclusions 31

3 Enabling Technologies for Microfluidic Analyses **33**
3.1 Microfabrication Technologies 33
3.2 Rapid Prototyping by Dry Film Resist 35
3.3 Hydrogels as Functional Structures in Microfluidics 40
3.4 Conclusions 44

4 Biochemical Wound Analysis 45
4.1 Biomarkers for Impaired Healing 45
4.1.1 Conclusions 51
4.2 Microarray Chip for Biochemical Analysis 51
4.2.1 Selection of Parameters 53
4.2.2 Pressure Barriers for Selective Gel Patterning 54
4.2.3 Chip Design and Operation Principle 55
4.2.4 Hydrogels, Samples and Experiments 61
4.2.5 Results and Discussion 63
4.2.6 Matrix Metalloproteinase Enzyme Assays 63
4.2.7 Conclusions 66

5 Systems for Bacteria Analysis 69
5.1 The Pro-Inflammatory Environment 69
5.1.1 Diagnostics and Infection Control 71
5.2 Micro-Free Flow Electrophoretic Concentration of Bacteria . 72
5.2.1 Theory 74
5.2.2 Chip Design and Fabrication 75
5.2.3 Finite Element Simulations 76
5.2.4 Sample Preparation 78
5.2.5 Experimental Setup 79
5.2.6 Results and Discussion 80
5.2.7 Conclusions 83
5.3 Low Cost Bacteria Detection System 84
5.3.1 Chip Design and Fabrication 85
5.3.2 Setup and Experiments 87
5.3.3 Results and Discussion 88
5.3.4 Conclusion 89
5.4 Rapid Bacterial Testing 89
5.4.1 Device Fabrication and Operation Principle 92
5.4.2 Chemicals and Experiments 94
5.4.3 Results and Discussion 95

6 Conclusions and Outlook 107

A Wound Sensor Controller Schematic 111

B Antibiotic Reference Testing 113

C Fluorescent Image Analysis **115**

D Device Masks **117**

Acknowledgements **123**

List of Publications **125**

Bibliography **131**

About the Author **155**

Summary

In the pathological healing of chronic wounds the ordered sequence of tissue restoration is disturbed. As a consequence, chronic wounds fail to heal within months and pose a major impact on the patient by pain, odor, leakage, and the risk of infection and the health care system by its constant treatment. Introducing objective wound assessment by sensor technology into clinical routine would help to guide treatment procedures and improve the healing outcome.

The aim of this research study was the development of simple and effective concepts to evaluate the wound status at the point of care. Requirements for point of care testing include a fast and flexible device use by untrained personal, reduced time and costs, as well as reliable and easy to interpret results.

The complex nature of wounds can be divided into the different regimes of physical appearance, biochemical status and microbiological environment, which influence each other. Each regime is tackled separately in this work by identifying possible parameters for wound analysis from the literature and the design of sensor concepts to quantify these candidates.

A miniaturized, wearable sensor system for the integration in a wound dressing was developed to collect healing relevant, physiological data. The sensor measures optical reflectance, heart rate, arterial oxigenation, surface pH, moisture and temperature. The function of the sensor system was verified in a porcine wound model. A combination of surface pH, reflected infrared, and red light showed to be the most significant parameter, associated with the healing progress.

For the measurement of biochemical parameters a microfluidic platform for the preparation of biosensing hydrogels by in situ polymerization was designed. Introducing functional structures for gel patterning in the chip fabrication allows for rapid assay customization. Simple handling and functionality were illustrated by assays for matrix metalloproteinase, an important factor in chronic wound healing. In addition, the demonstrated assays for total protein concentration and cell counts indicate the possibilities for a wide range of fast and simple diagnostics.

The last part of the thesis discusses microfluidic technologies for rapid analysis of bacteria. Preconcentration of bacteria by on-chip electrophoresis and detection by a simple optical setup are presented. Furthermore, devices for rapid and parallel growth-based bacterial identification and antibiotic testing in microfluidic cultures were designed.
The presented results and demonstrated tools show that medical analysis can be improved by sensor technologies that are simple to operate and yield fast results at the point of care.

Kurzfassung

Im pathologischen Heilungsverlauf chronischer Wunden ist die geordnete Abfolge der Gewebereparatur gestört. Dadurch können chronische Wunden für Monate oder länger nicht verheilen und verursachen beträchtliche Einschränkungen des Patienten durch Schmerzen, Geruch, Exudat und das Infektionsrisiko sowie beträchtliche Kosten für die andauernde Behandlungszeit. Eine objektive Wundbewertung durch die Einführung von Sensortechnologie in die klinische Praxis würde die Behandlung und damit das Heilungsergebnis verbessern.

Das Ziel dieser Arbeit war die Entwicklung von einfachen, effektiven Konzepten zur Wundstatus-Analyse in patientennaher Labordiagnostik (Point of care testing, POCT). Die Möglichkeit eines schnellen und flexiblen Einsatzes durch ungeschultes Personal, geringer Zeit- und Kostenaufwand, sowie verlässliche und einfach zu interpretierende Ergebnisse bilden die Vorraussetzungen für POCT Systeme.

Die Komplexität von Wunden kann in die sich gegenseitig beeinflussenden Bereiche der physikalischen Beschaffenheit, den biochemischen Zustand und die mikrobiologische Umgebung unterteilt werden. In der vorliegenden Arbeit werden diese drei Bereiche unabhängig voneinander untersucht. Diese Untersuchung umfasst eine Literaturrecherche zu möglichen Parametern sowie die Realisierung von Sensorkonzepten zur Messung der identifizierten Kandidaten.

Zur Erfassung heilungsrelevanter physiologischer Daten in einem Wundverband wurde ein tragbares, miniaturisiertes Sensorsystem entwickelt. Der Sensor misst optische Reflektion, Puls, arterielle Sauerstoffsättigung, pH-Wert, Feuchtigkeit und Temperatur. Die Funktion des Sensors wurde in einem Wundheilungsmodell an Schweinen getestet. Eine Kombination aus den Werten von pH-Wert, reflektiertem Infrarot und rotem Licht zeigte die höchste Korrelation mit dem Heilungsverlauf.

Für die Messung von biochemischen Parametern wurde eine mikrofluidische Plattform mit biosensitiven Hydrogelen entworfen. Funktionelle Strukturen für die Gelstrukturierung in dieser Plattform erlauben die einfache Bereitstellung unterschiedlicher Tests.

Die einfache Handhabung und hohe Funktionalität wurde durch die Messung von Matrixmetalloproteinase, einem wichtigen Parameter in der Wundheilung, belegt. Zusätzliche Tests für Gesamtproteingehalt und Zellzählung zeigen die Möglichkeiten für eine vielseitige Diagnostik auf.
Der letzte Teil dieser Arbeit präsentiert mikrofluidische Technologien für die Analyse von Bakterien. Die Aufkonzentrieung von Bakterien durch on-chip Elektrophorese und die Detektion durch ein einfaches optisches Setup werden gezeigt. Zusätzlich wurde ein System für parallele, wachstumsbasierte Identifikation von Bakterien und Antibiotika Wirksamkeitstests entwickelt.
Die präsentierten Ergebnisse und vorgestellten Prototypen zeigten, dass medizinische Analysen durch Sensortechnologie verbessert werden können falls diese einfach und schnell genug für die Implementierung in der klinischen Praxis sind.

Nomenclature

0.1 List of Abbreviations

Symbol	Description
AHL	acyl-homoserinelactone
APS	ammonium persulfate
CFU	colony forming units
DEP	dielectrophoresis
DRIE	Deep reactive ion etching
EDTA	ethylene diamine tetraacetic acid
EM	electrophoretic mobility
EOF	electroosmotic flow
EPS	extracellular polymeric substance
FFE	free flow electrophoresis
GFP	green fluorescent protein
GLYMO	(3-Glyciyloxypropyl)trimethoxysilane
HAVE	Hyaluronic acid vinyl ester
HMPP	2-hydroxy-2-methylpropiophenone
HPMC	hydroxypropylmethylcellulose
IDE	interdigitated electrode structure
IL	interleukin
LAP	Lithium phenyl-2,4,6-trimethylbenzoylphosphinate
LB	lysogeny browth
MEMS	micro electromechanical structures
MIC	minimal inhibitory concentration

Symbol	Description
MMP	matrix metalloproteinase
MRSA	methicillin resistanst *Staphylococcus aureus*
NOS	nitric oxide synthase
Ormosil	organically modified silicate
PAAm	polyacrylamide
PDGF	platelet derived growth factor
PDMS	polydimethylsiloxane
PEG-DA	Polyethylene glycol diacrylate
pHEMA	Poly(2-hydroxyethyl methacrylate)
PMMA	poly(methyl methacylate)
pO_2	partial Oxygen pressure
POCT	point of care testing
PTFE	polytetrafluoroethylene
PVA	polyvinylalcohol
ROS	reactive oxygen species
SB	sodium borate
SpO_2	partial Oxygen pressure determined by pulse oximetry
TEOS	tetraethoxysilane
TEMED	tetramethylethylenediamine
TGF	transforming growth factor
TIMP	tissue inhibitors of metalloproteinases

0.2 List of Variables

Symbol	Description	Unit
A	area	m^2
c	concentration	mol/liter

Symbol	Description	Unit
D	diffusion coefficient	m^2/s
E	electric field strength	V/m
h	height	m
I	intensity	W/m^2
l	length	m
p, P	pressure	Pa
R	radius	m
t	time	s
v	velocity	m/s
w	width	m
γ	surface tension	N/m
θ	contact angle	$^\circ$
μ	electrophoretic mobility	m^2/Vs
σ	electrical conductivity	S/m

Chapter 1

Introduction

In the world today, sensors and sensor systems become more and more important. Over the last decades, computers have changed from specialized work tools to everyday companions. Driven by that enormous presence of computing devices, their need for interaction with the environment has led to a similar but delayed evolution of sensor systems. As a consequence, we are surrounded by a diversity of sensors, which assist us to collect information about our environment and ourselves. Health care and medical diagnostics are no exception in this development.
The global market for disposable medical sensors was estimated at 3.8 billion USD in 2013 and is expected to grow at more than 10% annually until 2020. Wearable and diagnostic strip sensors account for the biggest share of disposable medical sensors market. The growing demand of patient monitoring and disease diagnostics is driven by the increasing geriatric population and growing prevalence of chronic diseases. Home healthcare and point of care diagnostics require miniaturized, cost effective sensors, which are operated by portable and hand-held medical devices [1].
The development of new sensing concepts and diagnostic procedures contributes to the improvement of health-related quality of life for individuals and society as a whole. Extending objective measurements in medicine will help to avoid personal errors in treatment and accelerate diagnosis of complex diseases. Impaired healing and chronic wounds represent such a class of a complex disease with huge implications for the patients and the health care system. Disturbed healing often is related to comorbidities and requires individual and protracted treatment. Introducing objective and detailed wound evaluation at different levels (i.e. physical, biochemical, microbiological) would help to optimize treatment and, therefore, save costs and lives.

1.1 Wound Healing - A Highly Ordered Sequence of Events

The human skin is not only our largest organ but also a protective layer for muscles, bones and organs. It consists of two distinct layers, the outer epidermis and the underlying dermis. The epidermis mainly consists of keratinocyte cells with the stratum corneum, the outermost layer of dead cells, serving as a protective layer against pathogens. An important part of pathogen defense is the acid mantle, a pH value of the stratum corneum between 4 and 6.5.
The dermis is a thicker, underlying layer, composed of 80% collagen of dermis dry mass. Its main functions are providing mechanical strength, moisture retention, as well as blood and oxygen supply [2].
Mechanical traumas, burns, surgical incisions, and other injuries that disrupt skin and tissue are considered as wounds. Healing of a wound is a complex process to restore the functions of the skin in several distinct phases. The healing process is influenced by many systemic factors such as patient age, malnutrition, obesity or cigarette smoking. Comorbidities including vascular disorders, diabetes mellitus or malignancy can lead to impaired wound healing with risk of infections and development of chronic wounds [3]. A chronic wound fails to progress through the normal sequence of repair and is stalled in an early phase of healing without restoring functional tissue. In contrast, an acute wound heals in a timely and uncomplicated manner [2]. An overview on acute and chronic healing mechanisms is given in the following sections.

1.1.1 Wound Healing Mechanisms

Wound healing is a complex sequence of events starting from the injury until the complete closure and functional restoration of the tissue. A healed wound, however, reaches only 70% to 80% of tensile strength compared to normal skin. Usually, the healing process is divided into the four stages of hemostasis, inflammation, proliferation and remodeling [2]. The many mechanisms taking place are regulated by chemical signals between cells, namely cytokines and growth factors. Due to the large number and redundant function of these factors only the most important are mentioned in the following. For details, refer to DIEGELMANN and EVANS [4], and WERNER and GROSE [5].

Hemostasis is the first step of healing after the disruption of blood vessels. When blood fills the wound, platelets are exposed to the extracellular matrix. Upon activation, they aggregate, degranulate and form a fibrin clot to stop the bleeding. A secondary function of platelets is to release chemotactic and growth factors to initiate further steps of the healing sequence [6].

Inflammation is divided into the early and late inflammatory phase. In the early inflammatory response, neutrophils invade the wound to remove bacteria and damaged tissue by phagocytosis within 24 to 36 hours. Growth factors, such as platelet derived growth factor (PDGF) and transforming growth factor (TGF-β) play an important role in the sequence of effects by attracting and activating neutrophils.
Damaged matrix components that must be replaced are degraded by matrix metalloproteinase enzymes (MMP-2 and MMP-9), which are released by neutrophils. Monocytes are attracted to the wound site in the late inflammatory phase (48 to 72 h post-wounding) by some of the same chemotactic factors as neutrophils. Monocytes are transformed to tissue macrophages, which continue phagocytosis of pathogens and debris, and destroy remaining neutrophils. Macrophages are considered to play a key role in the transition from inflammation to repair by providing TGF-α, TGF-β as well as other cytokins for the activation of keratinocytes and fibroblasts. [6, 7]

Proliferation is the phase of reepithelialization and dermal restoration. At an early stage of repair keratinocytes at the wound edge migrate across the wound gap. Migration of keratinocytes, an important step for healing, is facilitated by MMP-1 [8]. Reepithelialization also involves keratinocyte proliferation at the wound edge to supply sufficient cells to migrate and cover the wound [6].
Dermal reconstruction starts with fibroblast migration and proliferation and is clinically characterized by granulation tissue. Fibroblasts are responsible for production of collagen and other matrix proteins. However, the collagen formation in the early stage of repair is premature and non-structured [6, 9].

Remodeling or maturation is the last step in acute wound healing and may last up to a year. Synthesis and degradation of the extracellular matrix is tightly regulated during the whole healing process.

The activity of MMPs is gradually reduced by tissue inhibitors of metalloproteinases (TIMPs), promoting matrix formation. Collagen begins to cross-link over time and the wound is contracted, leading to a matured scar with high tensile strength [7].

1.1.2 Impaired Healing and Chronic Wounds

In pathological conditions the highly ordered sequence of events described above is disturbed. Chronic wounds or ulcers are a severe problem for patients and the health care system. A chronic wound is stalled in an early phase of healing and shows no further improvement after 3 months. A chronic wound has tremendous effects on patients quality of life due to pain, malodor or leakage. In addition, it poses the risk of lethal morbidity, such as sepsis and amputation. About 1% of adult population and 3.6% of people older than 65 years are affected by lower limb ulcers [10]. Worldwide 347 million people are affected by diabetes [11]. An estimated 15% of these diabetic patients develop a diabetic foot ulcer [12]. As treatment may take up to several years and ulceration is likely to be recurrent, the economic impact on the health care system is apparent.
Chronic ulcers often result from different morbidities including venous and arterial ulcers, diabetic foot ulcers and pressure ulcers. A pressure ulcer also referred to as bedsore is an injury usually over a bony area due to constant pressure or friction. Patients with lack of sensation as with spinal cord injury are at risk to develop pressure ulcers [2].
Venous ulcers account for more than 80% of leg ulcers and result from reduced blood flow due to venous disease or calf muscle pump failure. Common risk factors are obesity and arthritis of the hip, knee or ankle [10, 13]. Venous ulcers often are triggered by traumas, such as surgeries, fractures, burns, insect bites, scratches and blunt traumas.
Arterial ulcers result from an inadequate blood supply and often occur over pressure points. Atherosclerosis is the most common underlying pathology. Diabetes is not a primary cause for ulceration but a diabetic foot ulcer may develop due to sensory neuropathy or ischaemia. Unnoticed, painless trauma are the most common reason for diabetic foot ulcers [10].
Impaired wound healing is characterized by a severe and prolonged inflammatory response. Abundance of neutrophils and increased levels of MMPs (especially MMP-9) inhibit further steps of the normal healing process.

Although it has not been fully explained why chronic wounds without infection have elevated levels of MMPs, they have shown to be key players in poor healing and regulation can facilitate the healing process [14].
All chronic wounds contain bacteria but infection is only present when a critical colonization is exceeded. The risk of infection is determined by the number of organisms, their virulence and the host resistance. A high bacterial burden or infection also creates a pro-inflammatory environment that delays healing [15]. The presence of biofilms is discussed to inhibit efficient eradication of bacteria by neutrophils and antimicrobials. Thus, some authors stress that nonhealing wounds are often related to biofilms [16].
Despite their different etiology chronic wounds show some common factors, including ischemia (reperfusion) and a sustained inflammatory environment by bacterial colonization. In addition to these factors, an altered stress response to injury in the elderly fosters the development of chronic wounds [17].

1.2 Conventional Wound Care Techniques

Wound preparation is often performed according to the **TIME** (or **DIME**) principle including **T**issue **D**ebridement, **I**nflammation and infection control, **M**oisture balance and observation of the wound **E**dge [15, 18–20].

Tissue debridement removes necrotic tissue, eschar and biofilms that shield bacterial colonies. Debridement enhances blood supply and helps to restore biological balance. Surgical debridement is considered the most effective method. If not feasible due to pain, lack of time or expertise, autolytic debridement in a moist environment is applied. [15]

Infection is clinically diagnosed. Indications for high bacterial burden or infections are:

- Nonhealing wound due to prolonged inflammatory response.
- Increased wound exudate
- Red and bleeding wound
- Necrotic tissue and debris

- Smell from the wound

As stated in Section 1.1.2, the bacterial burden of a wound can be related to the progress of healing. However, quantitative biopsies are not performed in practice because of costs, time and the risk of introducing infections [21]. Surface swabs are only used to identify resistant organisms and to guide antimicrobial therapy when an infection based on the clinical indicators has been diagnosed [15].

Moisture balance of the wound is an important issue to achieve optimal healing. It is widely accepted now that healing is promoted in a moist environment. Moisture promotes migration of keratinocytes and increases growth factor receptor density on fibroblasts [18]. However, it is important to avoid maceration of the surrounding skin by excessive wound exudate. Damage of the surrounding skin is associated with corrosive components of exudate [22]. Depending on the amount of exudate an adequate wound dressing is chosen to balance moisture. Dressings can be divided into absorbent and hydrating dressings (Table 1.1).

Edge of the wound observation is a tool to evaluate the healing progress. For example, SHEEHAN *et al.* found a 50% reduction of wound area of diabetic ulcers in 4 weeks to be a good indicator for healing within 3 months [23]. If the wound edge is not migrating after wound bed preparation according to the previous steps, reassessment of the patient is necessary to rule out other factors.
The healing progress of wounds is currently assessed dimensionally and visually. Visual observation includes physiological criteria, such as presence of necrotic tissue, exudate, epithelialization and granulation, which are subjectively valuated [24].
Dimensional measurements of length, width, area or volume are objective methods to evaluate progress of healing. Several two- and three-dimensional measurement methods have been developed. The simplest are to measure linear dimensions with a ruler or trace the wound onto a sterile, transparent film. More advanced techniques are scaled photographs and computerized stereo photogrammetry [25].

Dressing	Properties	Application
	Absorbent dressings	
Foam	Porous polyurethane, thermal insulation, permeable to gas and water, high absorbency and long wear time	Venous ulcer with high levels of exudate
Hydrofiber	Sodium carboxymethyl cellulose, provides moisture balanced milieu, slow autolysis	Moderately exudative wounds, wounds with increased bioburden
Calcium alginate	Alginate in fibers, ion exchange between exudate and dressing forms gel, hemostatic, autolytic	Moderately exudative wounds
Negative pressure wound therapy	Topical subathmospheric pressure by vacuum pump with airtight sealed foam dressing	Manage excess exudate of critically colonized wounds
	Hydrating dressings	
Hydrogel	Semipermeable, nonadherent, semitransparent, soothing on burns	Dry, sloughy wounds with mild exudate
Hydrocolloid	Hydrocolloid gel, impermeable to vapor, autolytic debridement	Chronic ulcers, burns
Film	Elastic, transparent, semipermeable polyurethane, least moisture balance	Intravenous catheters, newly healed wounds

Table 1.1: Wound dressing materials for moisture balance and indicated applications [18].

1.3 Study Objectives

As discussed in the previous sections, the assessment of chronic wounds greatly relies on subjective methods. The only widespread measurements in clinical wound care are of dimensional nature. In order to guide and evaluate wound treatment in an optimal manner, advanced methods have to be developed. Requirements for such new tools include a safe, simple and flexible operation, a clinical relevant and easy to interpret output, and cost effectiveness [26].
Due to the complexity and variety of wounds, a single parameter to determine healing has not been identified. The parameters in question might be of physical, microbiological or biochemical origin. While physical measurements mainly are performed directly at the wound site, biochemical and microbiological tests make use of a sample in the form of a swab, absorbed wound fluid, or a tissue biopsy.
The objective of this work is to identify possible approaches for fast wound assessment in a clinical setting or for home testing, generally referred to as point of care testing. Bioanalytical techniques, including point of care testing usually require a series of tasks which may include:

- Sample acquisition
- Sample pre-treatment, purification, pre-concentration
- Assay or test preparation
- Testing procedure, device operation
- Results readout and presentation

Optimization of these tasks to generate a fully integrated diagnostic system or functional, modular units is an integral part of current research. The aim of this work is to design and realize new tools for the before mentioned tasks to facilitate the determination of the status of a wound. The requirements for point of care testing call for miniaturized sensors, operated with little external equipment. The research is divided into the topics of physical in situ measurements, biochemical sample analysis, and bacterial testing, which are discussed in the following chapters. Literature reviews are included to identify possible markers and parameters.

1.4 Outline of the Thesis

Chapter 2 focuses on physical measurements directly at the wound site. It provides an introduction to wearable sensor systems and highlights relevant physical parameters. The development and fabrication of a sensor system for wound dressing integration is described, followed by data analysis of a trial, conducted at the University of Veterinary Medicine, Vienna.

Chapter 3 gives a brief introduction to rapid microfluidic diagnostics and an overview over common lab on a chip fabrication technologies. Key technologies, utilized for the fabrication of prototypes and devices, are discussed in the sections 3.2 and 3.2.

Chapter 4 is dedicated to the design and development of a microfluidic system for biochemical exudate analysis. The literature of biomarkers is reviewed in section 4.1 in order to identify promising candidates for point of care analysis. Parameter selection and design aspects are highlighted. Experimental results of the microarray for a set of analytes are presented.

Chapter 5 describes concepts for rapid microbiological analysis. A brief illustration of the microbiological wound environment is given in section 5.1. An electrophoretic method for preconcentration of bacteria is introduced in section 5.2. Based on these results, a low-cost setup for the point of care quantification of the bacterial burden is presented in section 5.3. For further bacterial analysis a microfluidic chip for rapid cultivation-based antibiotic testing and bacterial identification is covered by section 5.4.

Chapter 6 draws the main conclusions of this research and discusses further possibilities and trends.

Chapter 2

Wearable System for Direct Wound Monitoring

This chapter presents a miniaturized and disposable sensor system for integration into a wound dressing and wound status evaluation at the wound site. The introduction provides a detailed review of the literature about physical measurement methods and parameters for wound assessment as well as miniaturized sensor concepts. On this basis, a multi-parametric sensor system for wound assessment was developed.
Parts of the development of the presented sensor have been published in *Organically modified silicate film pH sensor for continuous wound monitoring*, in Proceedings IEEE Sensors 2011, ISBN: 978-1-4244-9288-6; S. 679 - 682, http://dx.doi.org/10.1109/ICSENS.2011.6127220 reprinted by permission of IEEE, ©2011 IEEE and *Characterization of a Multi-parameter Sensor for Continuous Wound Assessment*, Procedia Engineering, 47 (2012), S. 985 - 988, http://dx.doi.org/10.1016/j.proeng.2012.09.312.

2.1 Introduction

Monitoring of physiological processes by wearable devices has become of high interest in recent years. Vital signs are recorded in a continuous manner in order to monitor the health condition of an individual. Possible applications include monitoring of sport performance, gait analysis and detection of pathological events. Sensor systems for the assessment of physiological parameters such as body temperature, heart rate and electrocardiogram have been in the focus of recent research. Design parameters that have to be considered include size and weight limitations, low device costs, biocompatibility, data storage and interpretable results [27–29]. Therefore, the selection of parameters, which are accessible for

wearable devices is limited.
Besides wearable inertial sensors for gait analysis, detection of falls and monitoring of patients with Parkinson's disease [30, 31], photoplethysmography for heart rate and arterial oxygen saturation has been the single most application for optical wearables [32–38]. Application of biochemical sensors in wearable systems is limited because of difficulties with analyte sampling, transport, and washing steps [39].
A special focus of physiological measurements has been the monitoring of chronic healing wounds because of their impact on patients and the health care system [40,41]. Minimizing the amount of disturbing dressing changes while gaining vital information on the wound status is the promising goal of introducing sensor technology into wound management [42,43]. Parameters that have been in focus in conventional wound bed measurements include temperature, moisture, pH, oxygen and optical methods (visible light and near-infrared absorption). A summary of relevant parameters and their ranges is given in table 2.1. Several studies have reported on increased temperatures in chronic wound healing and infections [44–46] and temperature monitoring has been discussed as a prediction for diabetic foot ulceration [47].
Monitoring the surface pH value of the wound bed has been discussed as a potential parameter for an objective wound assessment [48–50]. In intact skin, the epidermis provides a protective layer of an acidic pH value, which is unfavorable for the growth of most pathogenic bacteria. Upon injury, an alkaline pH of the underlying tissue is present, which subsequently follows a trajectory to restore the acidic milieu of normal skin [49]. pH values measured in chronic wounds varied from a pH of 5.45 to 8.65 [51]. The pH value in wound healing is not only passively regulated but also actively influences biochemical processes, such as the activity of enzymes [48, 49]. SCHREML et al. presented a method for two-dimensional mapping of pH in wounds [52]. Concepts for miniaturized pH sensors include pH-sensitive hydrogels [53–55] and screen printed electrodes [56, 57]. In addition, colorimetric principles have proven to be very efficient for disposable sensors, as they are cost efficient and simple to read [58–60]. Organically modified sol gels (Ormosils) have shown to offer tunable properties to optimize optical pH sensors in respect to mechanical resistance and dye leaching characteristics. [61, 62].
Oxygen concentration has been shown to play a pivotal role in wound healing processes and, therefore, has been considered for therapeutic

and monitoring applications. Reactive oxygen species (ROS) from enzymatically converted oxygen are involved in cytokine release, cell motility and extracellular matrix formation [63]. SMART *et al.* [64] suggest a value of 10 to 40 mmHg for wound hypoxia in comparison with normal values of 60 to 70 mmHg. Local tissue partial oxygen pressure (pO_2) is directly determined by a Clark electrode or luminescence lifetime imaging (LLI) while indirect methods include optical methods, such as near-infrared spectroscopy [65–67]. Calculation of arterial oxygen by pulse oximetry (SpO_2) is a systemic factor and does not represent local tissue oxygenation [68, 69]. Further optical systems for skin and wound analysis include near infrared spectroscopy and laser Doppler imaging. [70–78] WEINGARTEN *et al.* report on a significant difference of absorption between healing and non-healing wounds [70–72, 79] while other studies have correlated multispectral camera images with burn wound healing rates [74].
In addition to the summarized parameters in table 2.1, moisture balance is considered of great importance in modern wound care and, besides visual inspection, the main reason for regular dressing changes [18]. Impedance and capacitive moisture measurements on skin [80–82], inside the wound dressing [83] and at the wound site have been presented [84, 85]. A commercially available sensor system to measure healing relevant parameters has been presented by MCCOLL *et al.* A strip of flexible electrodes is used to determine dressing moisture by impedance measurements [83]. Typically, planar capacitive sensors have been utilized for a wide range of applications due to design flexibility, low cost and non-invasive operation. Key design features are the total sensing area, electrode spacing and the insulation thickness [86]. Connecting the electrodes while maintaining a flat sensing area is an important issue for capacitive skin sensors. Interdigitated capacitive structures have been presented for single-point measurements of skin hydration and transepidermal water loss [80–82].

Analysis of possible parameters reveals that the variation of single values among individuals complicates healing prediction and longitudinal measurements, introducing sensor technology might be a promising approach. In this chapter a miniaturized, disposable sensor that combines the measurements of near infrared monitoring, heart rate, oxygen saturation, pH value, skin moisture and temperature is presented. The combination of

Table 2.1: Summary of parameters for objective wound assessment.

Parameter	Wound type	Result	Ref
Temperature	Neuropathic ulcers	3.84°C increase vs. contralateral foot	[44]
	Neuropathic ulcers	3.1°C increase vs. contralateral foot	[45]
	Infected venous ulcers	2.45°C periwound skin temperature increase vs. 0.22°C in non-infected	[46]
pH	Non healing ulcers	Wounds with pH $\geq$8.0 did not decrease in size, wounds with pH $\leq$7.6 decreased 30% in 2 weeks	[87]
	Pressure ulcers	Mean pH of 7.8 without epithelialization, pH 6 with epithelial tissue	[88]
	Acute and Chronic wounds	Upon healing pH value decreased from pH 8.5 to below 8	[89]
	Chronic venous ulcers	Lower wound pH in the healing group compared to non healers (6.9 vs. 7.42)	[90]
Oxygen	Chronic non-healing wounds	5 to 20 mmHg vs. 30 to 50 mmHg of control tissue	[91]
	Review study	Hypoxic wounds 10 to 40 mmHg vs. 60 to 70 mmHg normal $p_{TC}O_2$	[64]
Optical	Diabetic foot ulcers	Reduction of haemoglobin concentration during healing	[70]
	Burn wounds	Green, red and infrared imaging correlates with healing time	[74]
	Leg ulcers	remission spectra (400 - 1600 nm) correlate with clinical wound score	[76]

these values allows for a deeper insight into physiological processes than observing only a single parameter.

2.2 Sensor design and fabrication

For designing a sensor that is in contact with skin or an open wound several limitations have to be considered. Besides biocompatibility of the materials in contact with the skin and sterility of the device, a flat and soft surface is required to avoid any discomfort. In addition, the footprint should be as small as possible to allow fluid absorption into the dressing. Temperature, pH, moisture, and optical absorption, including photoplethysmography were identified as possible candidates for integration into a small sensing device that is autonomously operated. To co-integrate the individual elements, the multi-parametric sensor was assembled on a flexible printed circuit board. The sensing elements were completely encapsulated in polydimethylsiloxane (PDMS), a flexible, soft, transparent and biocompatible silicone rubber that has proven to be suitable for wearable sensor fabrication [92–94].

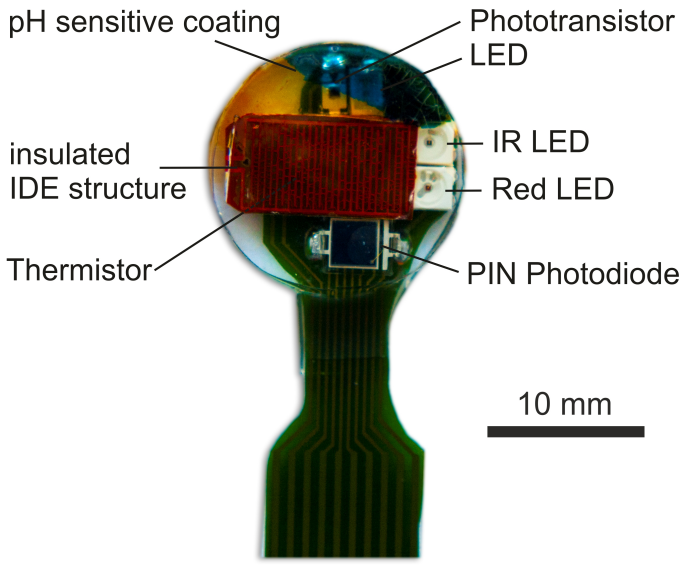

Figure 2.1: Assembled sensors for reflectance measurements, heart rate, oxygen saturation, pH value, skin moisture and temperature: The pH sensitive silicate film is illuminated by a LED and the reflected light is detected by the phototransistor. An infrared and red LED are used with a photodiode for absorption measurements and pulse oximetry. Furthermore, it comprises an insulated electrode structure for moisture monitoring and a silicon thermistor for temperature measurements.

As shown in Fig. 2.1 the disposable device comprises an infrared (850 nm, Osram, SFH4250Z) and red (645 nm, Osram, LSE6SF) light emitting diode (LED) with a photodiode (Osram, BPW34S) for absorption and pulse-oximetric measurements. The difference of extinction coefficients between oxygenated and deoxygenated blood becomes a maximum at the red and infrared wavelengths [68]. Absorption data from both LEDs was stored at a sampling rate of 20 Hz for 5 s to receive sufficient points for pulse rate calculation. A silicon thermistor (Microchip, MCP9701A) that delivers an analogue voltage of 19.5 mV/°C was utilized for temperature measurements. An insulated interdigitated capacitive (IDE) structure was used for moisture detection. The 100 µm wide IDE electrodes were fabricated with a gap of 300 µm. A 30 µm thick PDMS was used as an insulation layer on top of the electrodes, plasma activated and bonded to the bulk PDMS. As an alternative insulation, a 25 µm thick polyimide insulation foil was adhesively bonded on top of the electrodes. In order to provide a completely flat surface that is in contact with skin, the contact pads of the electrodes were bent backwards and connected under the active IDE structure.

Sol-gel technology has been widely used to immobilize chemical reagents for the design of optical sensors. Most frequently, optical transparent thin films are produced by hydrolysis of tetraethoxysilane (TEOS) or tetramethoxysilane (TMOS) in the presence of an acidic catalyst [95, 96]. Organically modified hybrid sol-gels (Ormosil) have been shown to offer advantageous characteristics for the fabrication of active thin films. Compared to inorganic thin films, Ormosils show an improved physical mechanical resistance, better adhesion, a crack-free surface and less leaching. On the other hand, response times are considerably longer [61, 62].

Tetraethoxysilane (TEOS) and (3-Glycidyloxypropyl)trimethoxysilane (GLYMO) precursors, and bromocresol green sodium salt were obtained from Sigma Aldrich. Bromocresol purple was purchased from Carl Roth. A 0.5% HCl solution was used as a catalyst in the sol formation and ethanol as a mutual solvent. The ratios of precursors and the acidic catalyst influence adhesion, pore size, physical resistance and cracking of the sol-gel films. The sol was prepared by mixing 500 µl TEOS, 50 µl GLYMO, 600 µl ethanol, 150 µl 0.5% hydrochloric acid, pH indicator dye (10 mg/ml), and stirring for 30 min. After mixing the solution was centrifuged to remove undissolved parts.

Standard microscope slides were used as substrate for the thin film characterization. The slides were rinsed with isopropanol and deionized water, and dried with nitrogen gas. 50 µl of the sol were distributed on the slides with a pipette and dried at room temperature for at least 24 hours. To determine the absorption spectra of the indicator doped thin films the glass slides were immersed in pH buffer liquids ranging from pH 3.3 to 10.6. The spectra in the visible range were recorded by an ATI Unicam UV4 UV/Vis spectrometer.
On the sensor the pH sensitive film was fabricated by dip coating the oxygen plasma activated PDMS surface, resulting in a covalently bonded thin film. A light emitting diode and a phototransistor were used for simple optical readout of the color shift of the indicator doped pH sensitive layer.
After assembly, the sensors were embedded in the center of a polyurethane foam dressing (Lohmann & Rauscher) and fixed by a thin adhesive film. The sensors were mounted in plane with the dressing surface and the connector was left at a distance to avoid additional pressure on the wound site (Fig. 2.2a-c). Dressings with integrated sensors were sterilized by ethyleneoxide gas.
The sensor is operated by a microcontroller board (Microchip, PIC18F4520), developed at the Austrian Center for Medical Innovation and Technology (ACMIT). The microcontroller drives each sensing element and stores the measurement data to a microSD card. The board is battery-powered and protected by a robust aluminum case (Fig. 2.2d). A schematic of the controller board is depicted in Appendix A.

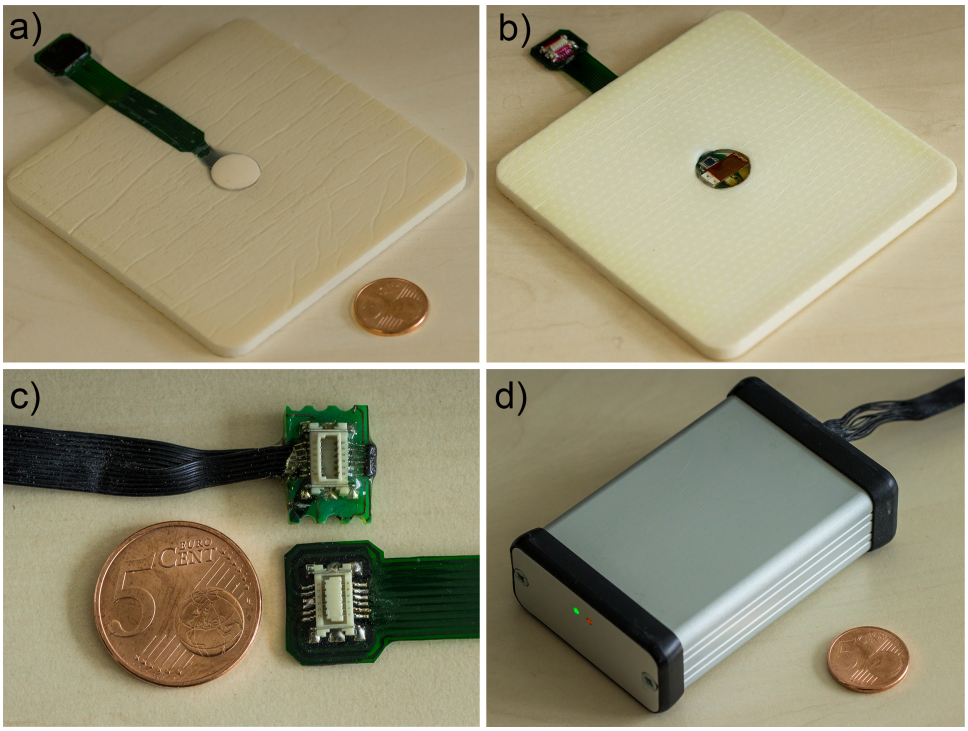

Figure 2.2: Sensor integration and control: a) The sensor is inserted from the backside into a 100 mm × 100 mm foam dressing and fixed by an adhesive film. b) The sensing area is in plane with the dressing surface and the sensor is connected outside of the dressing. c) Connection between microcontroller and disposable sensor device. d) Microcontroller for operation and data management. The controller is encased in a solid box to prevent damage in the animal study. Dimensions: 84 mm × 53 mm × 23 mm. LEDs report the state of operation.

2.3 Animal study design

Monitoring of wound healing was tested in a porcine wound healing model at the University of Veterinary Medicine Vienna. The animal experiment was approved by the Ethics Committee of the University of Veterinary Medicine Vienna and the national authority (BMWF-68.205/0049-II/3b/2012).

As an acute healing model two paravertebral split-thickness skin grafts were taken from each animal. One of the wounds was treated with a wound dressing with the integrated sensor system. The reference wound was treated with the same dressing without a sensor included. The data logger

was fixed supraspinal with cotton wool and a bandage. Dressing change was performed every 24 hours with image documentation of the wounds.
Swabs for semi-quantitative bacteriological analysis were taken every 48 hours. Cultures were prepared according to the quadrant streak method [97]. Growth was reported by 1+ (scant), growth in the first quadrant, 2+ (low), growth in the first and second quadrant, 3+ (moderate), first three quadrants and 4+ (high), growth in all quadrants. After 14 days, the experiment was stopped and biopsies were taken for histological healing assessment.

2.4 Results and Discussion

2.4.1 pH Responsive Film Characterization

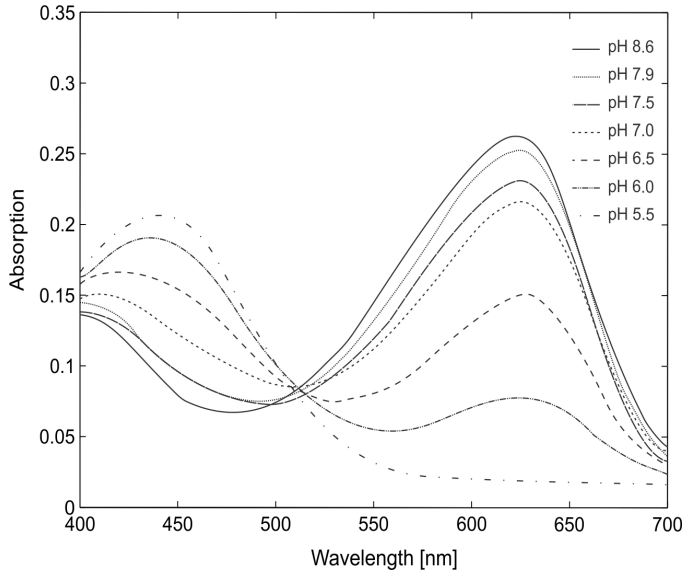

Figure 2.3: Absorption spectra of bromocresol green Ormosil film at different pH values. The second absorption peak is at 625 nm.

The pH response of the fabricated thin films was tested by absorption measurements upon exposure to different pH buffer liquids. As seen from the absorption spectra for bromocresol green in Fig. 2.3 the immobilization of the indicator dyes considerably shifts the response towards a more basic

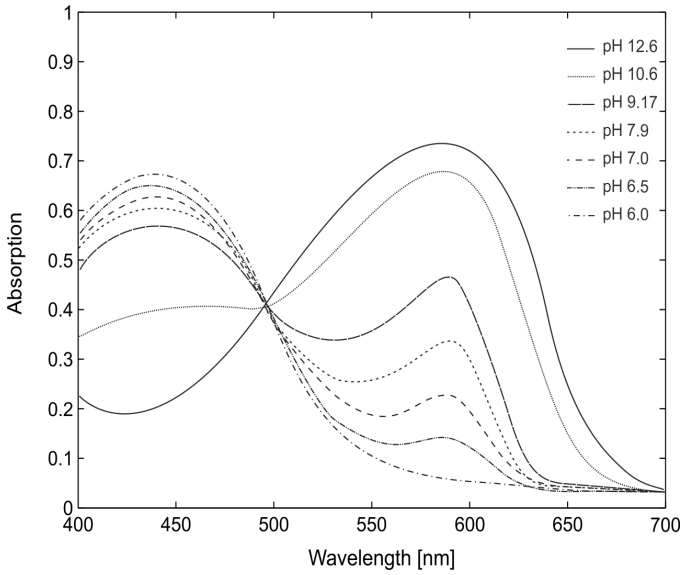

Figure 2.4: Absorption spectra of bromocresol purple Ormosil film at different pH values. The absorption peak is at about 590 nm.

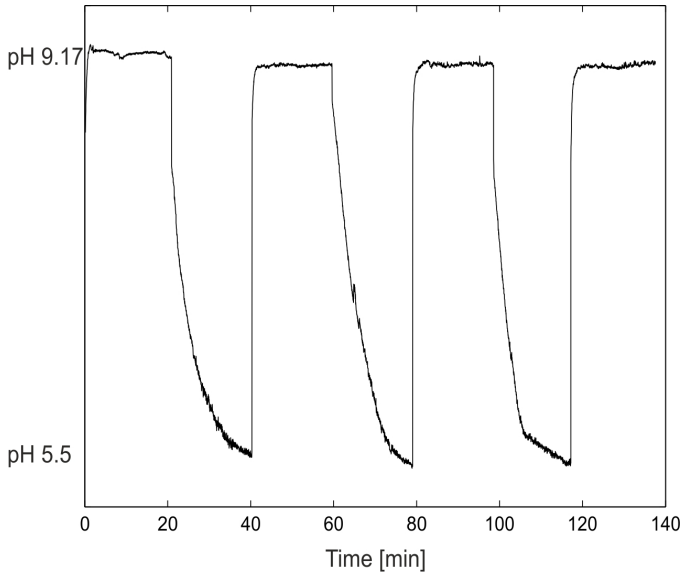

Figure 2.5: Continuous measurements with alternating exposure of the pH sensor to agar gels with pH 5.55 (boric acid) and 9.17 (sodium borate). A relatively slow but fully reversible response was observed.

regime. In comparison to the pH response of bromocresol green in solution (pH $3.8 - 5.4$) the Ormosil film showed a response in the range of pH 5.5 to about 8.6. The absorption peak is located at about 625 nm.

For bromocresol purple the pH response shifted from pH $5.2 - 6.8$ to values between about 6.5 and 11 with an absorption peak at a wavelength of 590 nm (Fig. 2.4). In respect to pH values of chronic wounds, which were determined to range from 5.45 to 8.65 [51] the bromocresol green Ormosil appeared to be very suitable to detect the pH transition from basic to acidic values during healing. The wavelength of the chip-LED for the sensor was chosen to be 626 nm to fit the second absorption peak (Fig. 2.3).

Response time and dye leaching of the film depend on the pore size, which is adjusted by precursor and catalyst ratios. The mixture of 500 µl TEOS, 50 µl GLYMO, 600 µl ethanol, 150 µl 0.5% hydrochloric acid was found to yield optimal results in terms of response time, mechanical stability and leaching of the pH responsive films. In order to test the reversibility of the pH response, the prepared films were alternately exposed to artificial wound beds, prepared of agar gels at different pH values. As seen from Fig. 2.5 the response time varied between transition from high to low pH values and vice versa and in general was considerably slower than in solution. However, a fully reversible response was observed and response time is considered to be less critical in wound monitoring as the healing takes from several days to weeks.

In respect of using the pH sensitive film material in wound monitoring, biocompatibility was proven by cultivating epithelial cells on the film. Madin-Darby canine kidney (MDCK) cells were used to compare the Ormosil film with standard cell culture petri dishes. As seen from Fig. 2.6 no difference in cell attachment after 24 hours of cultivation nor in the confluent layer after 48 hours was observed, proving that the pH film does not show any toxic side effects.

2.4.2 Multi-parameter Sensor Characterization

The individual elements of the assembled multi-parameter sensor were tested and characterized in different experiments. The temperature sensor was calibrated on a precision hotplate in a range between 32 and 42°C as seen in Fig. 2.7.

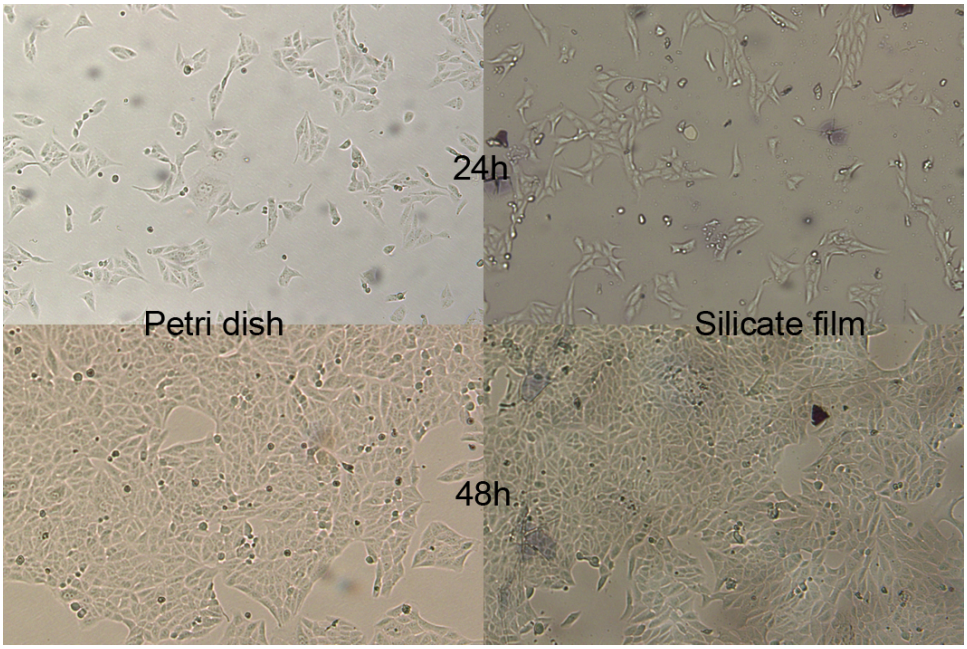

Figure 2.6: Biocompatibility test of the fabricated pH sensitive films by cultivation of MDCK cell line on the surface. A standard cell culture petri dish was used as a reference. No difference of cell growth was observed after 24 and 48 hours of incubation.

In the calibration of the pH sensor the device was immersed into different pH buffer liquids and put on skin prior to the measurement. The sensor response plotted versus pH value is shown in Fig. 2.8. A second order polynomial was fitted to the obtained data to match the non-linear characteristic.

The moisture sensor was tested by experiments on human skin. In order to vary the water content, the skin was treated either with ethanol or moistening cream prior to the experiment. Comparisons of capacitive measurements on normal and treated skin are illustrated in Fig. 2.9. While ethanol treatment resulted in drier skin and a decrease in capacitance, treatment with skin cream yielded a higher value as compared to normal skin.

Trauma induced differences in tissue absorption are visible by measurements on a knee bruise compared to the same position on the counter side and a nearby reference point on both legs as shown in Fig. 2.10. At both wavelengths the transmitted light was less on the bruise

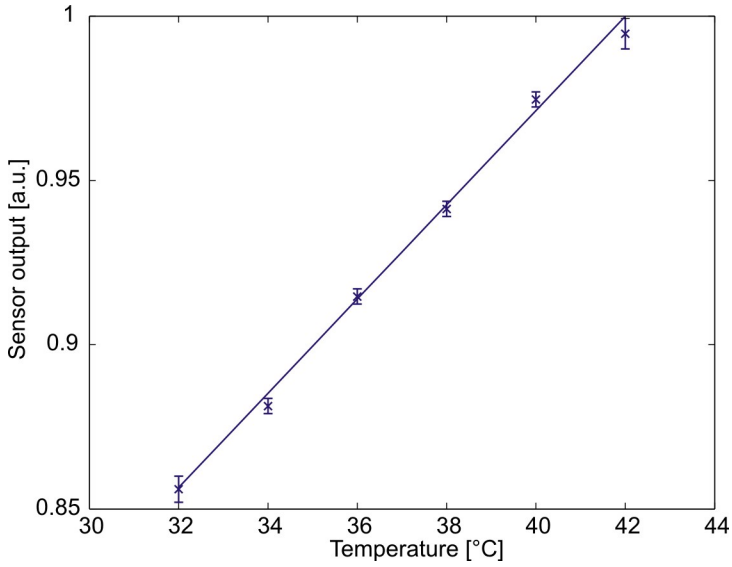

Figure 2.7: Calibration of temperature sensor on a precision hotplate between $32°C$ and $42°C$. Error bars indicate means and standard deviation of three measurements (linear correlation, $r = 0.997$, $p < 0.001$)

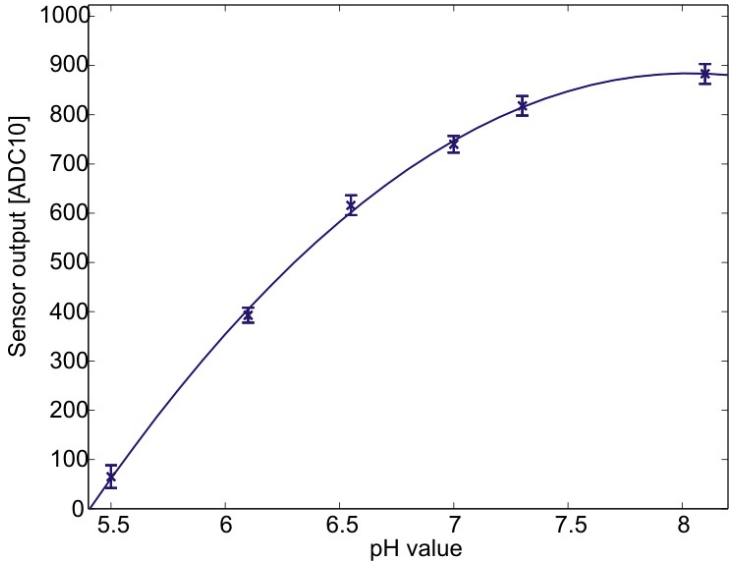

Figure 2.8: Calibration plot for pH value with 2^{nd} order polynomial fit, Spearman correlation: $r = 0.988$, $p < 0.001$.

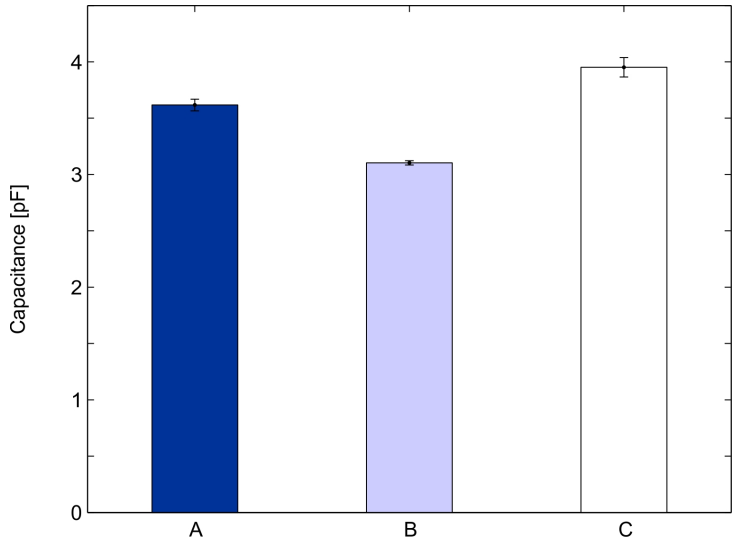

Figure 2.9: Moisture monitoring by interdigitated electrode structure with 30 μm insulation layer on human skin at different moisture levels: A) Normal skin. B) Ethanol treated skin. C) Moistening cream treated skin. ($n = 3$).

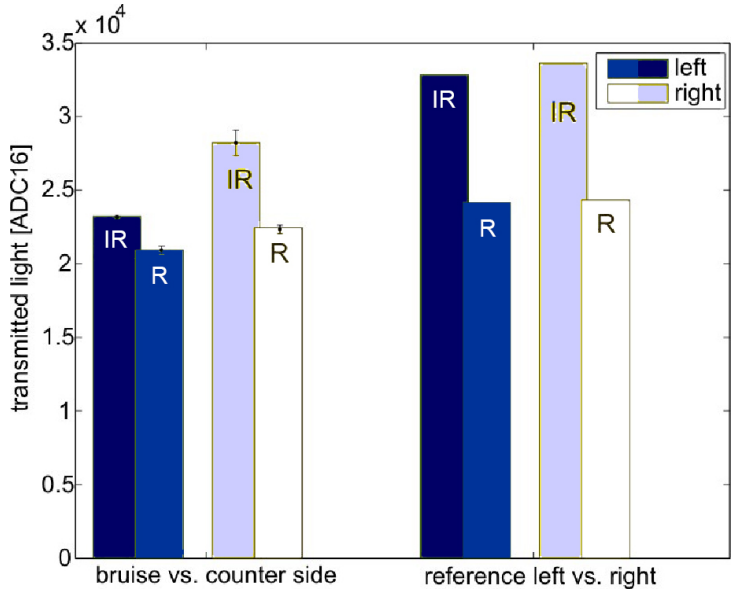

Figure 2.10: Infrared (IR) and Red (R) light absorption of tissue: A) Knee bruise (left) and control measurement on the same position on the right leg ($n = 3$). B) Nearby reference point on both legs.

then in the control measurement because of higher absorption due to the blood accumulation under the skin. However, the difference between the measurements at the infrared wavelength (850 nm) was much higher compared to red light (645 nm) as the larger penetration depth results in a bigger influence of the blood accumulation. Therefore, the absorption ratio of both wavelengths could be a suitable parameter to determine the depth of a wound.

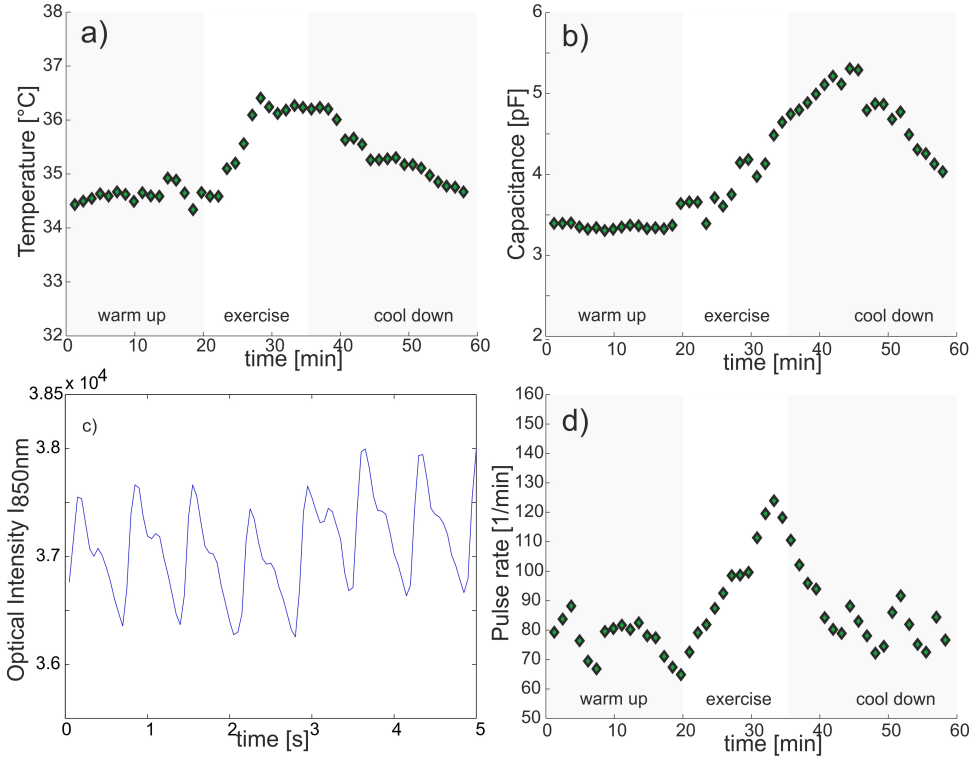

Figure 2.11: Continuous on-body trial: Sensor used for sports monitoring, mounted in a headband. a) Body temperature during warm up, exercise and cool down. b) Sweat measured by capacitive IDE structure. c) Backscattered intensity $I_{850\,\mathrm{nm}}$ for pulse rate measurement. d) Pulse rate during exercise.

In addition to the previous characterization measurements the sensor system was also used to monitor sports performance [98]. Fig. 2.11 summarizes the results of an exercise trial, divided into warm-up, exercise, and cool down phase. During the exercise the sensor and the microcontroller box were fixed in a headband, taking measurements on the forehead. Body temperature increased and decreased only with a short delay after start and

stop of exercising, respectively (Fig. 2.11a) while the sweat rate was a lot more delayed 2.11b. Recorded pulse waves for the pulse rate calculation are depicted in 2.11c. The signal is a combination of the pulsating expansion of arteries and, hence, increased absorption and the respiration rate, which modulates cardiac output [99]. The dicrotic notch, which is associated with arterial valve closure, is well visible as a characteristic dip in the wave form [100]. The calculated pulse rate, quickly following the exercise is given in Fig. 2.11d.

2.4.3 Wound Monitoring in Porcine Model

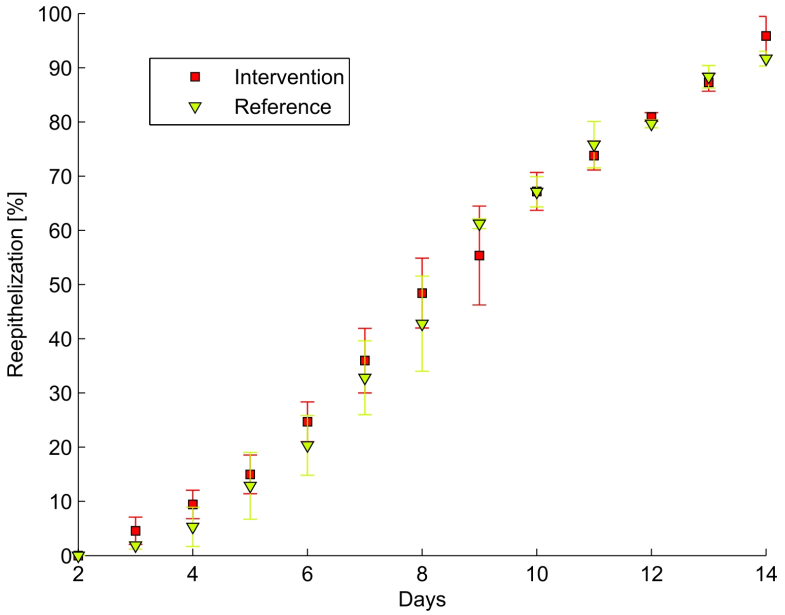

Figure 2.12: Comparison of healing rates between reference and intervention wound site. Measurements are based on reepithelialization rates determined by planimetry. No difference in healing trajectories nor in the final outcome were observed.

A comparison of the healing course of all wounds did not show any difference in healing rates between the wounds with sensor and reference wounds as observed by planimetrics and histology. The reepithelialization as obtained from planimetry is shown in 2.12. Wound images of one intervention wound during healing are given in Fig. 2.13.

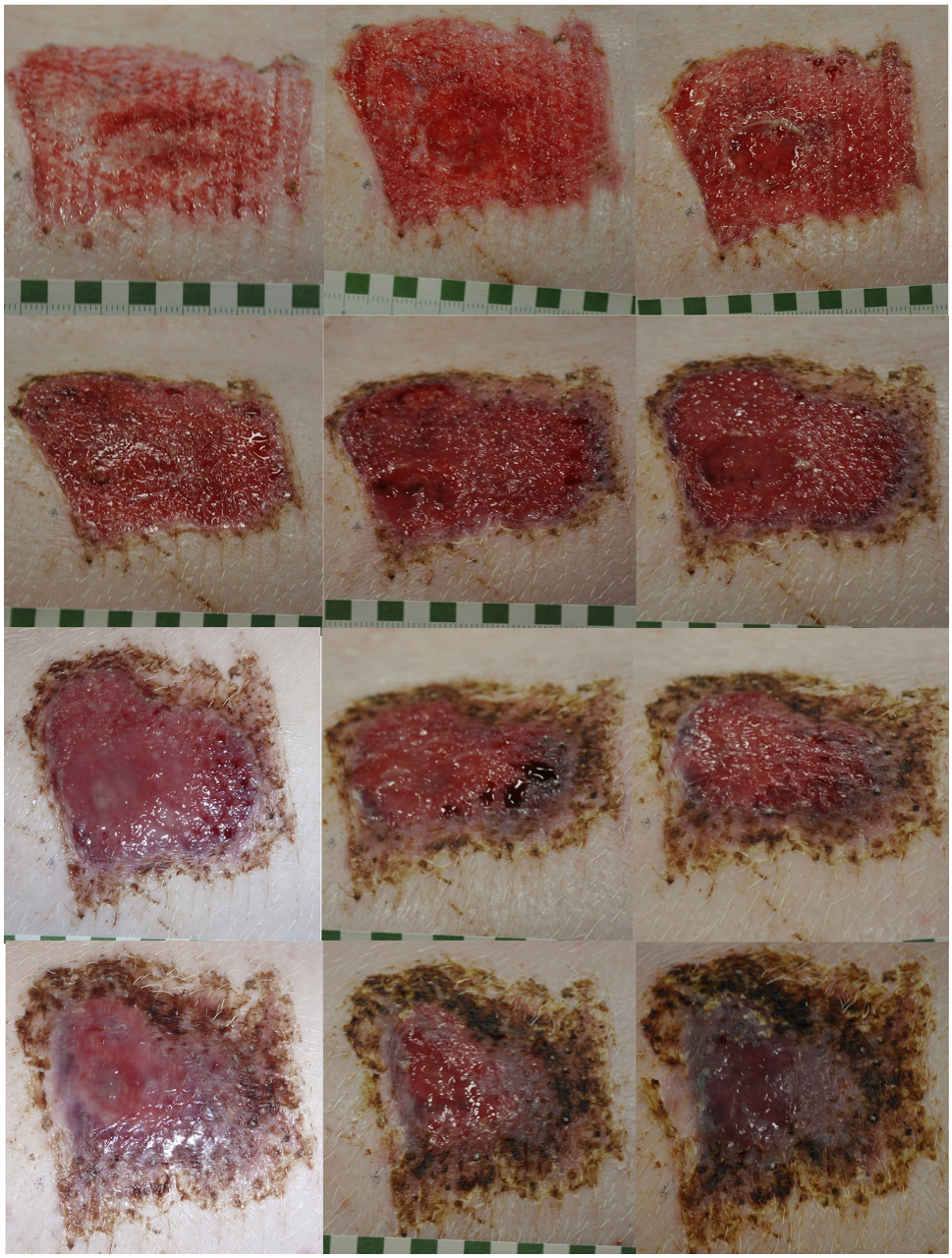

Figure 2.13: Image documentation of wounds of one animal during healing.

Semi-quantitative swab cultures according to the four quadrant streak method revealed wound colonizations by bacteria of the strains *S.aureus*

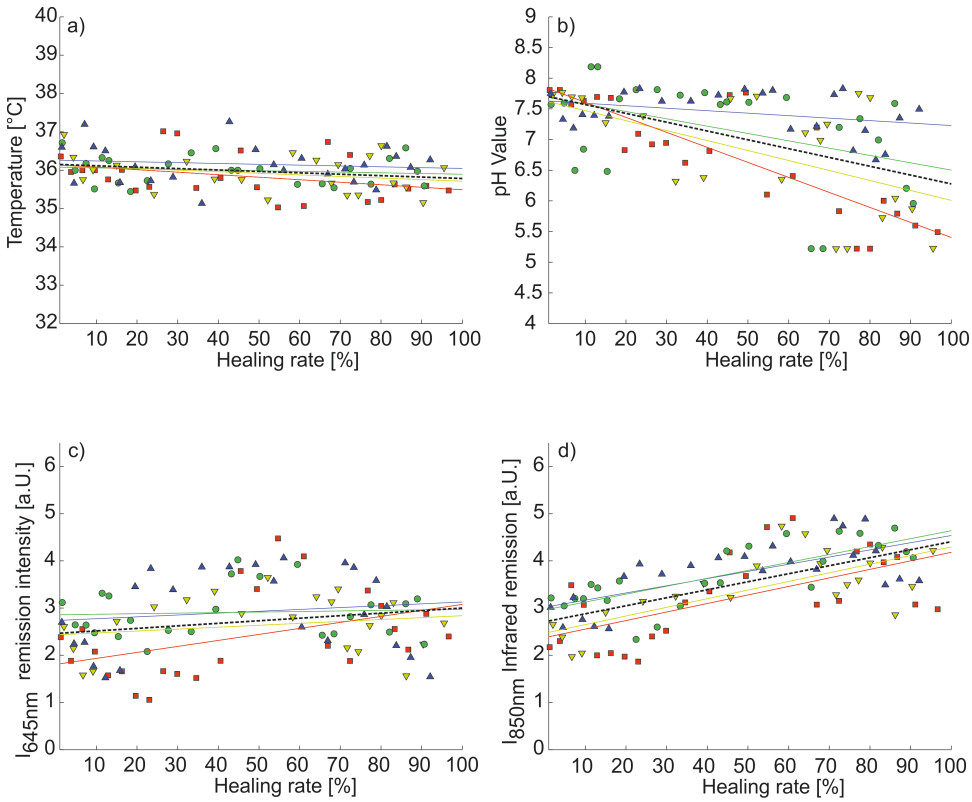

Figure 2.14: Sensor readings of all four animals plotted over wound closure. Combined linear least square regression in black. a) Temperature, combined Spearman correlation coefficient, $r = -0.23, p = 0.027$. b) pH Value, $r = -0.49, p < 0.001$. c) Red remission, $r = 0.19, p = 0.058$. d) Infrared remission, $r = 0.6580, p < 0.001$. As an isolated value infrared remission yielded the highest correlation and significance. Variations were due to variations in sensor fabrication and differences in individuals, sensor position and pressure.

and *S. hyicus* between scant and low growth (1+ to 2+). No difference in colonization between intervention and reference wounds was observed (Mann-Whitney-U test, p=0.5).

Results of the readings of all sensors on the intervention wounds of all four animals are summarized in Fig. 2.14. Calculation of arterial oxygen by pulse oximetry (SpO_2) was not used in this study because it is not a local but a systemic factor [68,69]. Sensor readings were correlated to the healing progress, expressed by reepithelialization that was determined from image analysis. Readings of the moisture sensor could not be used because of

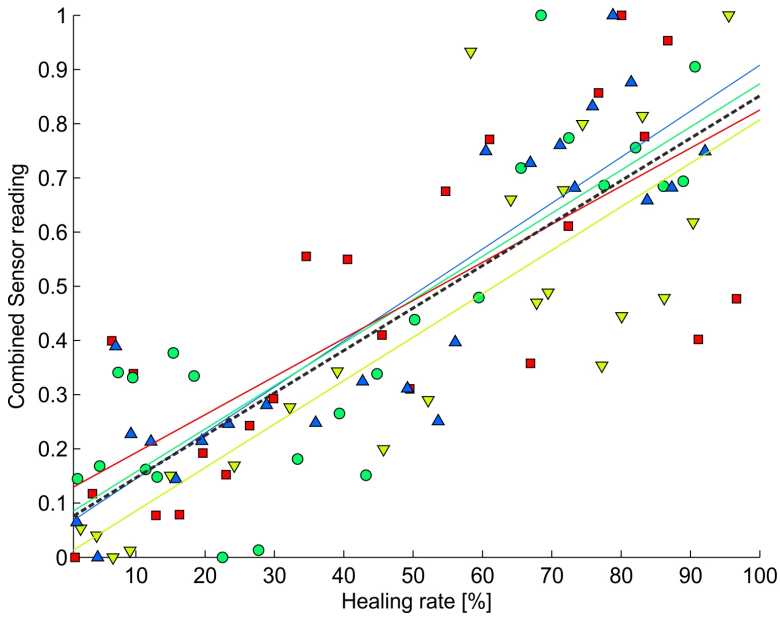

Figure 2.15: Combination of Sensor data of pH, red and infrared remission. Correlation of the combined data with healing is increased to $r = 0.83$, $p < 0.001$.

mechanical failure of the PDMS insulation. Changing the insulation to polyimide ($25\ \mu$m) showed better mechanical stability, but could not be used in this study because of the time consuming sterilization procedures.
As seen from Fig. 2.14 a, there is a negative and significant ($r = 0.23$, $p = 0.027$) correlation between temperature and wound closure. Due to a relatively high type variation of the temperature sensors this correlation is rather low. However, the temperature sensor was included to detect any temperature increase due to infections (see table 2.1), which were not present in this acute wound healing model. Other factors of influence include sensor position, sensor to tissue coupling and interindividual differences. Especially pH value readings (Fig. 2.14 b, $r = 0.49, p < 0.001$) are affected by local and interindividual variations [51, 101]. Although, two dimensional pH mapping methods might give a more accurate picture, time series of single values in the center of the wound are easier to obtain, interpret and to use in further analysis.
Optical readings of red at 645 nm and infrared (850 nm) remission intensities are summarized in Fig. 2.14 c and d, respectively. While the correlation of the lower wavelength with healing is low and insignificant (r = 0.19, p =

0.058), infrared absorption decreased during healing due to a decreasing hemoglobin concentration in the wound bed ($r = 0.6580$, $p < 0.001$). This finding is in accordance with previous studies [70].

A combination of the sensor readings was performed in order to increase the robustness of healing prediction. The combination of $(2 \cdot I_{850\text{nm}} - I_{645\text{nm}}) \cdot pH$ yielded the highest correlation coefficient of $r = 0.83$, $p < 0.001$ between healing rate and sensor output, as shown in Fig. 2.15. The difference of the backscattered intensities acts as an offset correction between different sensor modules. Introducing a third wavelength, as a common reference would be a simple step to further increase the reliability of the low cost sensor system.

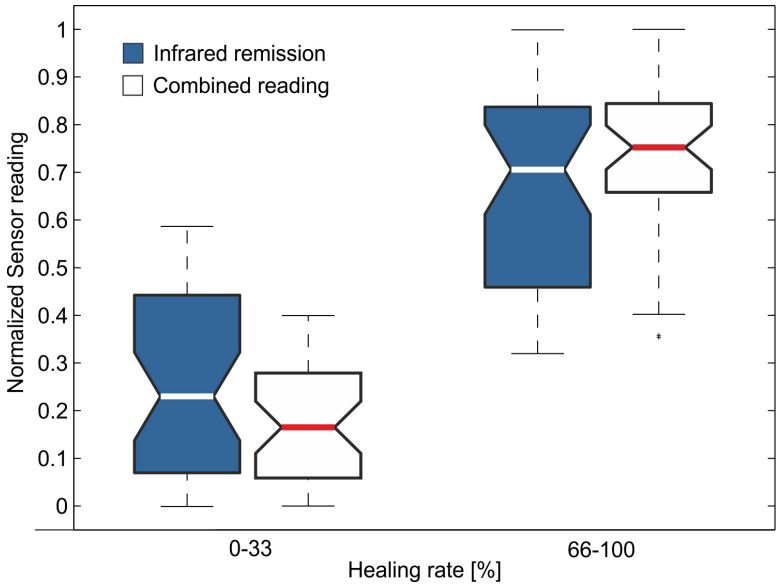

Figure 2.16: Summary of sensor readings: Combination of the different low cost sensors provides a robust method to differentiate healing phases.

The sum of all measurements in an early and late healing phase is shown in the box plot of Fig. 2.16. The plot compares the backscattered infrared intensity $I_{850\text{nm}}$ with the combined sensor signal. As indicated by the boxes, a considerable improvement of robustness in wound status characterization could be obtained by combining the individual sensor signals, which were influenced by different factors. The lines in the boxes give median values with the notches as the $5\,\%$ confidence interval.

2.5 Conclusions

A low-cost, disposable sensor system for the integration in a wound dressing has been discussed in this section. The sensor showed to be able to predict the healing of a wound within the dressing. Due to the many influencing factors, including device variations, fabrication deviations, differences in position, pressure and individual differences the combination of multiple sensor signals to a single output value proved to be advantageous for a robust wound assessment. Including sensor readings of the revised capacitive moisture sensor and introducing a third reference wavelength (e.g. at 950 nm for water absorption), robustness can further be increased. The sensor did not show any negative influence on the wound bed when a flat surface without additional pressure on the wound was ensured. As the physiological processes in healing are of rather slow nature, sensor readout intervals can be between hours and days. By fabricating all sensor functions in a thin and flexible device layer integration into a large variety of dressings could be achieved [102].
Besides the integration in a dressing for wound assessment, monitoring sports performance or vital signs of the elderly are possible fields of applications for multi-parametric physiological measurements.

Chapter 3

Enabling Technologies for Microfluidic Analyses

The desire for miniaturized diagnostic devices for point of care testing and chemical analytical tools has led to the research field of microfluidics and lab on a chip technologies. Emerging from microelectronic fabrication technologies, the field also integrates molecular chemistry, molecular biology and optics [103]. Miniaturization of diagnostic devices reduces material and chemical input. Characteristic device dimensions reach from 100 nm to 1000 µm. As the structural dimensions approach the range of analytes (<1 nm to 20 µm), effects can be utilized that are not present or very slow in the macroscopic world. A prominent example is the motion of particles in inhomogeneous electric fields, so called dielectrophoresis. Trapping, moving and separating different cell types are the main applications of dielectrophoresis in microfluidic devices [104–106].

Knowledge of available technologies for device fabrication is of fundamental importance. As a highly interdisciplinary field, microfluidic device fabrication makes use of a variety of technologies from different origin. A brief overview over existing technologies and the fabrication technologies utilized in this thesis, including rapid dry film prototyping and in-situ hydrogel polymerization, are presented to the reader in the following sections.

3.1 Microfabrication Technologies

Evolved from silicon microfabrication, microfluidic technologies have shifted towards a much broader material spectrum. A major challenge has been the fabrication of 2.5-dimensional or even 3-dimensional structures with a technology, originally developed for planar devices. Deep reactive

ion etching (DRIE) is a classical silicon micromachining technology, developed for microelectromechanical systems (MEMS) fabrication. DRIE often is used in applications in which high aspect ratios (e.g. 20:1) are required [107,108]. In fluidic applications such devices are sealed by anodic bonding of a glass layer to the structured silicon wafer.
Another popular fabrication technology is the use of SU-8, a thick epoxy-based photoresist. Unlike other photoresist materials it is used as permanent functional layer due to its chemical resistance and excellent structuring properties regarding resolution and aspect ratio [109, 110]. Closure of SU-8 microfluidic channels has been an issue and several strategies have been developed to overcome this limitation, including the use of uncrosslinked SU-8 adhesive bonding [111] and plasma-based PDMS sealing [112].
Soft lithography of PDMS is by far the most common technology in microfluidic and lab on a chip fabrication due to its simple fabrication and strong bonding to glass [113]. The two component silicone elastomer is poured over the master structure, which after curing is molded into the PDMS layer (Fig. 3.1). PDMS can be easily cut into shape, punctured for fluidic access, and bonded to glass by oxygen plasma activation.

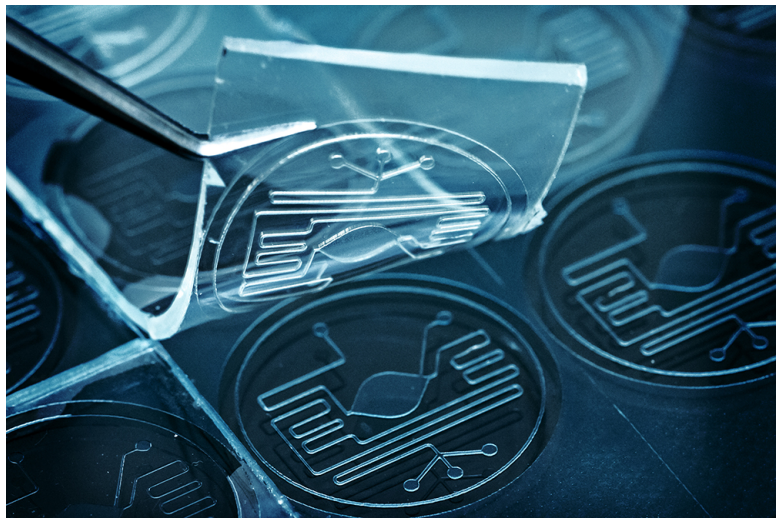

Figure 3.1: Soft lithography fabrication. A photoresist master structure is transformed into channels by silicone (PDMS) casting. Permanent sealing is achieved by oxygen plasma bonding of PDMS to glass.

Besides the above mentioned technologies a vast variety of materials and techniques have been utilized for device fabrication. The combination of multiple material properties can lead to fascinating devices. ZACCHEO and CROOKS, for example, presented a self powered sensor where enzyme digestion triggers an electrochemical reaction to indicate the enzyme concentration by a light emitting diode [114]. On the other hand, fabrication and device costs always remain an important factor as for the handling of potentially infectious agents disposable devices are required. In this respect, paper-based diagnostic devices have emerged for a variety of applications in health care, environmental monitoring or food safety [115]. In a larger scale, polymeric devices are very cost effectively fabricated by injection molding. In a research setting fabrication techniques may considerably differ from industrial production. Nevertheless, the possibility for production up-scaling should be taken into consideration during the device design. The development of a functional, disposable cartridge of low complexity operated by a mobile readout device is a promising approach in point of care testing. Advantages and/or requirements of mobile diagnostic systems can be summarized as follows [26, 116]:

- Fast and easy to interpret results
- Reliable and clinical relevant results
- Flexible device use
- Reduced sample transport and cooling
- Reduced external equipment and reagents
- Reduced analysis costs
- Simple operation for non-trained personal or home-use
- Simple calibration and quality control

3.2 Rapid Prototyping by Dry Film Resist

The lamination of dry film resist on different substrates offers a simple, yet flexible prototype fabrication with the possibility of large scale production. Dry film photoresists are provided on rolls and can be applied in a

continuous process on multiple substrates. The substrates mainly used in this study are common microscopy soda lime glass slides with dimensions of 76 mm × 26 mm × 1 mm. Main advantages of microscopy slides for prototype fabrication are their low costs and compatibility with microscope holders without further dicing. Silicon and borosilicate wafers and some polymers can be utilized likewise. Requirements for polymer use are chemical stability in the developer solution and good adhesion of the film laminate. Laser printer polyester sheets were successfully tested for device fabrication [117]. Polymeric chips can be easily machined while requiring less equipment and causing less mechanical wear in comparison to the standard substrates in microtechnology. However, for higher resilience, higher transparency, and better wetting glass substrates might be preferable. The entire fabrication process is illustrated in Fig. 3.2.

If required, the substrates are cleansed with isopropanol and deionized water. The dry film resist (*Ordyl SY300*, *Elga Europe, Italy*), a negative resist, is available in thicknesses of 17, 30 and 55 μm. It comes on a roll with protective films on both sides, allowing device fabrication without a cleanroom setting. In a first step, one of the protective films is peeled off and the resist is laminated onto the substrate by an office laminator at about 95°C. Multiple layers of the different thicknesses can be combined to obtain the desired channel height (Fig. 3.2a). The resist is UV exposed (i-line, 365 nm) through a transparency film mask (*Zitzmann GmbH, Germany*) using a mask aligner (Fig. 3.2b). Film masks are plotted with 64000 dots/inch and have a minimum line resolution of about 6.3 µm. During exposure the top protective film remains to prevent the resist from sticking to the mask and to avoid dust contamination. Before post exposure baking at 85°C for 1 min the protective sheet is removed. Depending on resist thickness and pattern dimensions (i.e. width of structures and voids) the exposure dose has to be to be adjusted. Free standing structures are more robust with higher exposure doses, while the quality of channels is better with less exposure.

The structures are developed in a solution of 75% xylene and 25% 2-butoxyethyl acetate (*Sigma-Aldrich, USA*) for 100 s under ultra sonic agitation. After the development the substrates are rinsed with isopropanol and deionized water. Holes for fluidic access to the final microfluidic chips are structured into a second layer by powder blasting (Fig. 3.2e). Size and distribution of the holes are defined by a printed transparency mask, transferred to a masking layer (*I-XE, Harke, Germany*) that is resistant

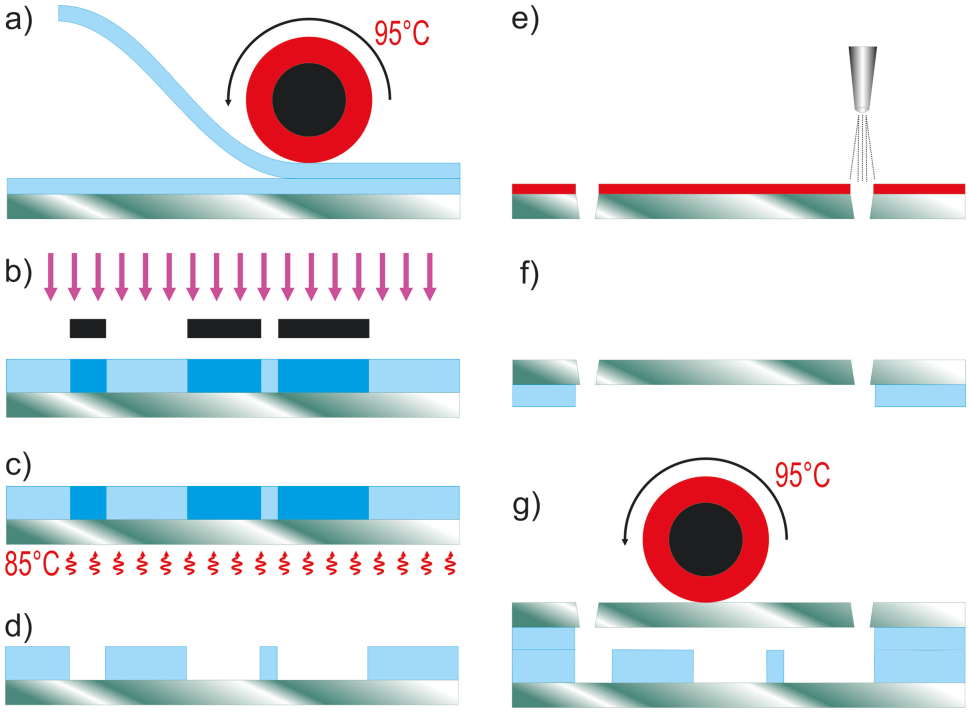

Figure 3.2: Process steps for fabrication of dry film laminate devices: a) Lamination of multiple layers of dry film resist onto the bottom substrate. b) UV exposure through a foil mask. c) Post exposure bake. d) Development of the structures under ultrasonic agitation. e) Powder blasting of access holes into the top substrate. f) Structuring of a dry film layer on the top substrate, analogous to a-d for the fabrication of three dimensional structures. g) Hot roll bonding of both parts.

to the abrasive particle jet. Aluminum oxide with 100 µm particle size is used for structuring glass and silicon in a sandblaster (*Easyblast, Bego, Germany*). The adhesive *I-XE* film is developed in warm water after UV exposure without any baking steps. As the blasting of holes by the particle jet does not cause significant substrate stress, a high density of holes without any cracking can be produced. As an example, Fig. 3.3 shows a device with 84 holes through a microscope slide, with the closest spaced only by 1 mm. One slide is processed within a few minutes only. By the masking technology holes and structures can be of any size and shape, which is a considerable advantage over drilling. Powder blasting has also been proposed for the fabrication of microfluidic [118] and MEMS structures

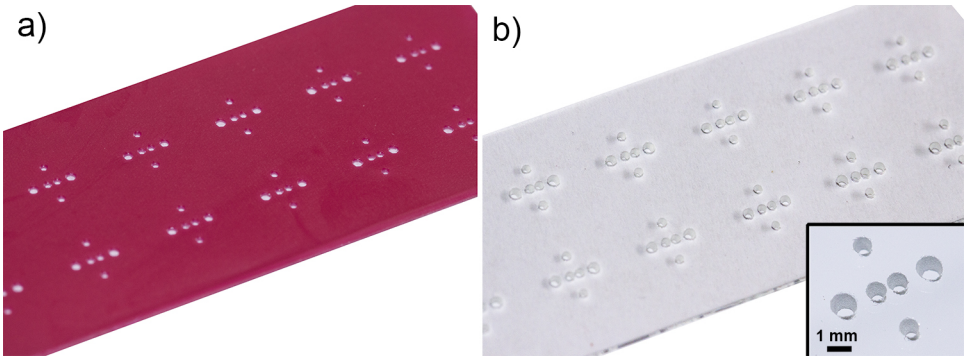

Figure 3.3: Powder blasting of access holes through a glass slide. a) Holes are precisely defined by a photosensitive resist (*I-XE, Harke, Germany*). b) Blasting of holes does not cause substrate stress. Therefore, a high density of holes can be produced without cracking.

[119].
Three dimensional features within a chip are fabricated by structuring a second functional layer on the top substrate. In contrast to any spin coated photo resists the dry film lamination technique yields a uniform resist layer over previously structured holes. Therefore, combining powder blasting as a bulk process with subsequent dry resist structuring offers great flexibility. An example of a 200 µm thin free standing beam over a 2 mm wide gap is presented in Fig. 3.4. If more than two functional layers in one device are required, lamination, exposure and development steps (Fig. 3.2 a to d) are repeated on either of the two substrate parts. Fully three dimensional networks can be realized by that layer-by-layer fabrication.

After structuring, the devices are sealed by bonding both substrate parts together. Adhesive bonding of two resist layers (Fig. 3.2 g) or a single structured layer to a glass cover is performed at a temperature of 150°C. The required bonding pressure increases with decreasing resist thickness from 20 N/cm^2 for 150 µm to 200 N/cm^2 for 10 µm. The direct adhesive bonding is the most valuable feature of dry film fabrication because other technologies, such as SU-8 require more elaborate bonding protocols to be followed [111].
A major disadvantage of the dry film lamination with *Ordyl* resist in comparison with standard SU-8 fabrication is the reduced resolution and

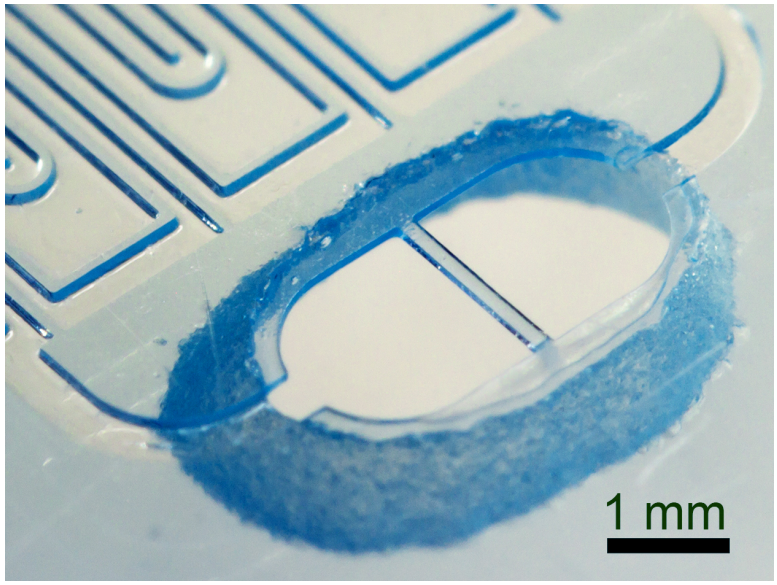

Figure 3.4: Structuring of dry film laminate over powder blasted holes. The possibility to apply a resist layer over structured substrates enables simple fabrication of free standing structures. Beam dimensions are 200 µm × 100 µm × 2 mm.

aspect ratio. The maximum resolution is about 10 µm while the aspect ratio (feature height to width) is limited at approximately 2.5. As seen from the inset in Fig. 3.5 the sidewall profile of the dryfilm resist is nearly vertical.

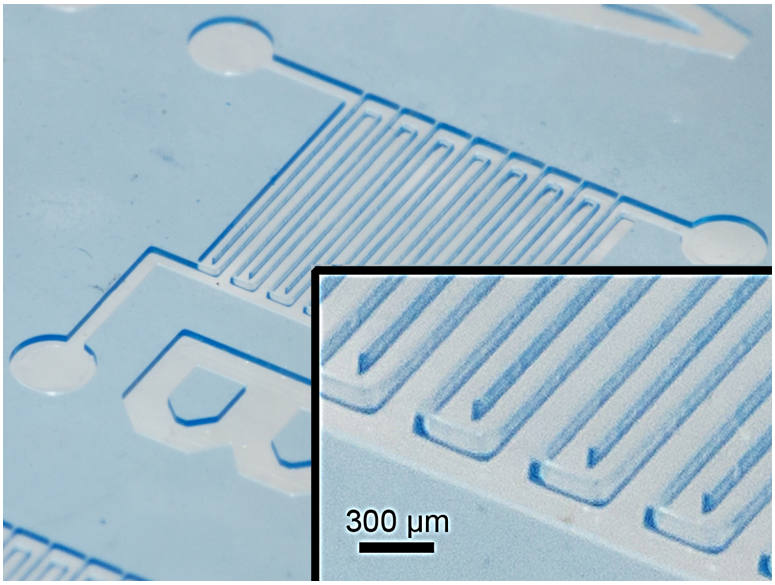

Figure 3.5: Structures with a maximum aspect ratio of 2.5. Line dimensions are 100 µm in height and 40 µm in width.

3.3 Hydrogels as Functional Structures in Microfluidics

Hydrogels are hydrophilic, cross linked polymeric networks that can absorb significant amounts of water. Gels are widely used in food industry and medicine, including applications in wound dressings, soft contact lenses, drug delivery and tissue engineering. The most important parameters of different hydrogels are their pore size, mechanical stability and biocompatibility. Gelation refers to the increased linking of macromolecular chains with decreased solubility. The gelation process can be either reversible in physically crosslinked gels or irreversible due to the covalent bonding in chemically crosslinked gels [120]. A selection of physical and chemical gels is summarized in Table 3.1.

Table 3.1: Overview of physically and chemically crosslinked hydrogel systems.

Physical Gels	**Properties**
Agarose	Gelling with hysteresis in temperature. Large pores of 50 to 600 nm for large DNA separation [121].
Gelatine	Temperature sensitive gel, used in food industry, drug capsules and as cell adhesion promoter.
Calcium alginate	Used in wound dressing applications. Approximately 10 nm pore size [122].
Polyvinylalcohol (PVA)	Crystallite induced gelling by repeated freeze thaw cycles.

Chemical Gels	**Properties**
Poly(2-hydroxyethyl methacrylate) (pHEMA)	Basic material for soft contact lenses [123].
Polyacrylamide	Predominant gel for protein and DNA separation. Toxic monomer.
Polyethylene glycol diacrylate (PEG-DA)	Available in a wide range of molecular weights to define pore size.
Hyaluronic acid vinyl ester (HAVE)	Superior biocompatibility over acrylates and methacrylates [124]

Natural polysaccharides like agarose form a gel upon cooling of hot solutions. Gels are reversely linked by helix formation of polymer fibers which are held together by hydrogen bonds. Another form of physical crosslinking is ionotropic interaction, present in calcium alginate gels. The anionic polysaccharide sodium alginate is gelled with a Ca^{2+} ion of opposite charge [125]. In contrast, chemical crosslinking is done by a free radical polymerization. In the case of polyacrylamide (PAAm) the reaction is initiated by ammonium persulfate (APS) with tetramethylethylenediamine (TEMED). TEMED accelerates free radical formation from APS. A prominent application of hydrogels are soft contact lenses. Poly(2-hydroxyethyl methacrylate) (pHEMA) is the most widely used hydrophilic polymer for contact lenses. The pHEMA hydrogel with a water content of $38\,\%$ usually is chemically crosslinked with ethylene dimethacrylate [123]. The requirements of gels for contact lenses include sufficient mechanical stability, a high oxygen permeability [126] and low protein adsorption [127]. For its improved mechanical integrity and low protein adsorption freeze-thaw crosslinked Polyvinyl alcohol (PVA) has been of interest for contact lens applications [128].
For chemical hydrogels summarized in Table 3.1, photochemical crosslinking is a popular method as it gives full control over temporal and spatial gelation. Especially in the field of tissue engineering where hydrogel scaffolds, fibers and particles are fabricated, selective curing via a mask or a focused UV light beam offers great flexibility. The gel monomer is mixed with a small amount of a photoinitiator that produces free radicals upon exposure. Photoinitiators with varying properties are available, including 2-hydroxy-2-methylpropiophenone (*Irgacure 1173*) as an efficient UV sensitive initiator for acrylate prepolymers. A mixture of eosin Y and triethanolamine has been used as a visible light sensitive composition for cell encapsulation [129]. As many photoinitiators and monomers show cytotoxic effects, initiator and monomer concentration, UV wavelength, and polymerization turnover have to be considered. Lithium phenyl-2,4,6-trimethylbenzoylphosphinate (LAP) is an efficient initiator that is sensitive at $365\,\mathrm{nm}$ and higher wavelengths that are benign to cells and shows high cytocompatibility [130]. An obstacle in photoinitiated polymerization is the quenching of radicals by molecular oxygen. This oxygen inhibition is avoided by a high UV intensity, an inert atmosphere or certain additives [131].
Tissue engineering is closely related to microfluidcs as photo lithography

and soft lithography techniques are applied for the fabrication of hydrogel scaffolds and vascular networks within the gels [132]. Furthermore, microfluidc devices for flow focusing [133] and droplet generation [134] are utilized to fabricate gel fibers and particles [135]. Vice versa, hydrogels are used in microfluidic devices to study 3-dimensional cell cultures on chip [136, 137].
Besides cell immobilization, gels in chips can fulfill several other functions. Based on their permeable network, gels find applications in membranes for sample concentration and separation [138], the generation of chemical gradients [139, 140], enzyme reactions for biosensors, and chemical sensors or actuators based on their swelling behavior [141, 142]. A gel membrane, incorporated in a capillary electrophoresis device has been utilized to block bulk flow and allow convenient sample handling in continuous operation mode [143]. Fig. 3.6 shows the gel, separating a channel for sample and buffer, while ions can migrate through the nanoporous gel barrier.

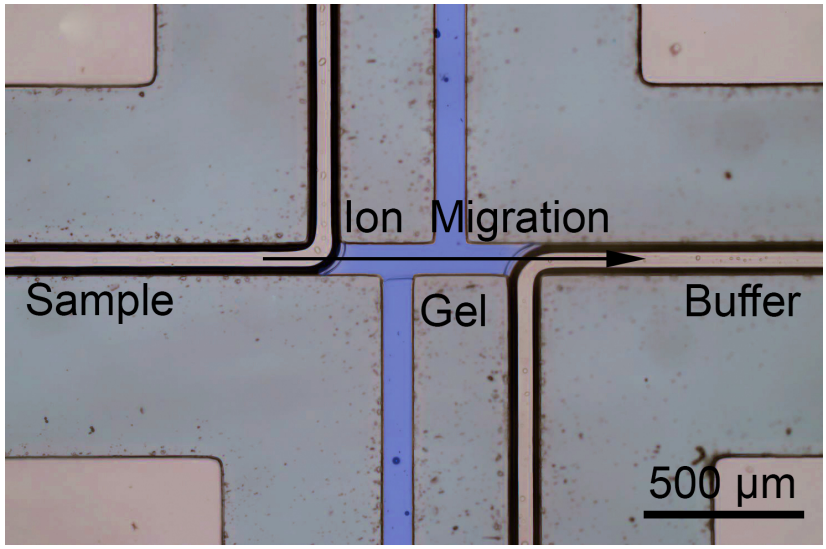

Figure 3.6: In-situ polymerized hydrogel barrier (blue) in capillary electrophoresis chip for continuous operation. Sample and buffer are independently changed [143].

3.4 Conclusions

The presented technologies and methods represent only a small fraction of nowadays available fabrication techniques. Depending on the requirements of the application, traditional MEMS technologies, PDMS soft lithography or laser milling of polymers might be applied. Detailed overviews of those fabrication methods can be found elsewhere [144, 145]. Three-dimensional polymer printing could play an important role in future fabrication processes. However, issues like limited resolution, long writing times, removal of uncrosslinked resin and autofluorescence are limiting its current use [146].

In-situ polymerization of hydrogels enables the simple fabrication of membranes and diffusion networks in microfluidic devices. In addition, a degree of freedom can be left to the user, as gels are easily customized with functional entities, like chemical reagents, enzymes or cells.

The need for cost efficient, disposable devices in point of care diagnostics certainly will stimulate polymer- and paper-based fabrication techniques. Home healthcare further will profit from the ubiquitous computing power of smartphones, as an enormous potential for hand-held readout devices. With their integrated cameras, network possibilities and the intuitive user interface smartphones could be a trigger for wide spread acceptance of lab on a chip devices [147, 148].

Chapter 4

Biochemical Wound Analysis

Following the discussion of fabrication technologies in chapter 3, this chapter presents the design, fabrication, and experimental results of a microfluidic device for biochemical exudate analysis. As a prerequisite, the realization of a lab on a chip requires the identification of appropriate diagnostic parameters. The section 4.1 reviews recent literature of biomarkers for healing that are found in wound exudate.
Section 4.2 describes the development of a microfluidic platform for biochemical analyses. Parts of this section have been published in *Single-step design of hydrogel-based microfluidic assays for rapid diagnostics*, Lab Chip, 2014, 14, 378-383, http://dx.doi.org/10.1039/C3LC50944C, reproduced by permission of The Royal Society of Chemistry.

4.1 Biomarkers for Impaired Healing

Identification of healing relevant growth factors, cytokines, and enzymes has been in the focus of recent research. A multitude of these biomolecules are present in a wound, and their expressions show a temporal and interdependent regulation [5]. A summary of biomarkers, identified in different studies is given by Table 4.1.
An imbalance of pro- and anti-inflammatory factors is considered a main reason for persistent inflammation and poor healing as a consequence. Abundance of neutrophils and their secreted enzymes have been shown to inhibit further steps of the normal healing process. During the normal course of healing a high level of tissue degrading matrix metalloproteinases (MMPs) activity decreases as the wound progresses [149, 150]. Several studies presented a significant increased concentration and activation of MMPs, especially MMP-9 in poor healing wounds [9, 14, 15, 151–159]. SCHULTZ and MAST [153] reported a 116-fold higher MMP activity in

chronic compared to acute wound fluids. After the chronic ulcers began to heal MMP activity decreased. This increase is linked to the inflammatory response since MMP-9 is expressed by neutrophils and macrophages. In addition, chronic wound fluid shows decreased levels of tissue inhibitor of metalloproteinase (TIMP-1) and a reduction of transforming growth factor (TGF-β). High wound fluid concentrations of MMP-9 and large MMP-9 to TIMP-1 ratios can predict poor healing. A simple test for these risk factors could be useful to assist healing prognostication [153, 154]. Although it has not been fully explained why chronic wounds without infection have elevated levels of MMPs, they have shown to be key players in poor healing [152]. A possible explanation might be previously undetected biofilm contamination of clinically non-infected wounds [160].
Negative pressure wound therapy has been discussed to create an environment of low protease and neutrophil elastase levels by continuously removing wound fluid and proteases therein [154, 161]. Together with matrix metalloproteinases, other enzymes, including neutrophil elastase, myeloperoxidase and lysozyme have been related with poor healing [162, 163].
Interleukins, a group of cytokines show a concentation shift in non-healing wounds. For instance, IL-1, a pro-inflammatory cytokine and its inhibitor IL-1ra did show an increased ratio in infected and non-healing wounds [101, 153, 164]. TRENGOVE *et al.* reported on elevated levels of IL-1, IL-6 and TNF-α in wound fluids of nonhealing foot ulcers [165]. Furthermore, levels of IL-6 and TNF-α were found to correlate with bacterial burden, and hence, useful to detect infections [166]. Anti-inflammatory factors IL-2 and IL-5 also were presented as infection markers in diabetic foot ulcers. The commonly used bioburden level of 10^6 CFU per ml wound fluid was used to define infection. Levels of IL-2 and IL-5 were significantly decreased above this critical colonization [167]. Similar results of increasing pro inflammatory IL-1 and IL-6 and decreasing anti-inflammatory IL-2 and IL-5 during healing was found by FINNERTY *et al.* in a mouse burn wound model [168].
Nutritional markers, including albumin, total protein, zinc, and glucose levels were studied in a clinical trial with pressure ulcers for their potential as healing markers. Albumin levels siginificantly increased as the wounds moved into proliferation phase compared to the inflammatory phase. In addition, glucose levels were reduced in infected ulcers [169]. JAMES *et al.* found significant differences of total protein and albumin levels in wound

fluids of healing and non-healing leg ulcers [170].
Another group of molecules which have been in discussion to greatly influence the healing process are reactive oxygen species (ROS), including hydrogen peroxide (H_2O_2), the superoxide anion ($O_2^{\cdot -}$) and the hydroxyl radical ($OH^{\cdot}$). ROS are generated in the respiratory burst of phagocytic cells to neutralize pathogens. Because of their cytotoxic effects, ROS require a tight control by the enzymes catalase, glutathione peroxidase, and superoxide dismutase (SOD). Disbalances in the regulation lead to oxidative stress and potential tissue damage [171–174]. Due to their short lifetime and high reactivity, direct measurement of ROS in wounds is difficult [172]. However, increased levels of steady-state H_2O_2 have been measured in inflammatory phase and chronic wound mouse models [175, 176]. Indirect measurements determine oxidative damage products as isoprostane, allantoin or protein carbonyl [177–179]. Regulating enzymes including catalase, superoxide dismutase and total antioxidant capacity might be determined as well [176, 178]. In addition to ROS, nitric oxide, its reactive species (RNS) and the producing enzymes nitric oxide synthase (NOS) are discussed as being important molecules in healing [174, 180].

Although several reports suggest an increased oxidative stress in chronic wounds (Table 4.1), currently only little data is available and more research is required to validate oxidative stress biomarkers for clinical use.
BROWNE *et al.* [181] showed that the bacterial burden, expressed in CFU/g tissue, is related to the rate of healing. Despite the lack of clinical infection signs, a bacterial load of $\geq 10^6$ CFU/g resulted in impaired healing. PIERPONT *et al.* presented the bacterial burden as a useful marker to individualize treatment. With increased bacterial burden the frequency of an active dressing application was increased [182]. The presence of biofilms is discussed to inhibit efficient eradication of bacteria by neutrophils and antimicrobials. Thus, some authors stress that nonhealing wounds are often related to biofilms [16, 183]. Signaling molecules of bacteria in biofilms, relevant for quorum sensing by acyl-homoserinelactone molecules (AHL) have been utilized to detect bacteria and the formation of biofilms. Quorum inhibition, on the other hand aims to disrupt the communication of bacteria and hence avoid formation of biofilms [184, 185]. MOOR *et al.* [158] and LIU *et al.* [157] have also shown an association between high bacterial levels and elevated MMP-9 concentration.

Table 4.1: Summary of studies, utilizing different biomarkers for wound assessment.

Biomarker	Wound type	Result	Ref.
Enzymes			
MMP-2	Chronic leg ulcer vs. acute wounds	$5-10\times$ activity	[186]
	Pressure ulcers vs. acute wounds	$10\times$ level	[187]
MMP-9	Chronic leg ulcer vs. acute wounds	$5-10\times$ activity	[186]
	Infected vs. non-infected (post-operative, pressure ulcers, blisters)	significantly increased	[163]
	Pressure ulcers vs. acute wounds	$25\times$ level	[187]
	Healing diabetic foot ulcers	significant decrease	[8, 157]
MMP-9/ TIMP-1	Pressure ulcer during healing	significant decrease	[188]
	Healing diabetic foot ulcers	significant decrease	[157]
Neutrophil elastase	Infected vs. non-infected (post-operative, pressure ulcers, blisters)	significantly increased	[163]
	V.A.C treated burn wounds	significant decrease	[189]
	Surgical wounds, infected	significantly increased	[190]
Lysozyme	Infected vs. non-infected (post-operative, pressure ulcers, blisters)	activity $12.85\times$, concentration $13.55\times$ increased	[163]

Biomarker	Wound type	Result	Ref.
Enzymes			
Arginase	Chronic venous ulcers	increased vs normal skin	[191]
	Diabetic ulcers	increased vs normal skin	[192]
Cytokines			
IL-1	Venous leg ulcers nonhealing vs. healing	significantly increased	[165]
	Infected venous leg ulcers	significantly increased with $> 10^6$ CFU/ml	[167]
IL-1ra/ IL-1	Chronic vs. acute wounds	7:1 vs. 480:1	[153]
IL-2, IL-5	Infected diabetic foot ulcers	Significantly decreased with $> 10^6$ CFU/ml	[167]
IL-6	Venous leg ulcers nonhealing vs. healing	significantly increased	[165]
	Infected venous leg ulcers	significantly increased with $> 10^6$ CFU/ml	[167]
	Infected aterial and venous leg ulcers	elevated with bacterial load and infection	[166]
TNF-α	Venous leg ulcers nonhealing vs. healing	significantly increased	[165]
	Infected venous leg ulcers	significantly increased with $> 10^6$ CFU/ml	[167]
P55/ TNF-α	Chronic vs. acute wounds	4:1 vs. 12:1	[153]

Other			
Bacterial counts	Rat chronic wound model	CFU/g more frequent treatment	[182]
	Diabetic foot ulcer	Wound closure inverse proportional CFU/g	[193]
Protein	Pressure ulcers during healing	Significant albumin level increase	[169]
	Healing vs. nonhealing leg ulcers	Increased total protein and albumin levels	[170]
	Acute wounds vs. venous ulcers	Increased total protein concentration	[179]
Oxidative stress, ROS	Chronic leg ulcers vs. acute	Elevation of allantoin : uric acid ratio	[177]
	Chronic wound mouse model	Increased SOD and H_2O_2 levels	[176]
	Non-healing venous ulcers	Increased ferritin vs. healing ulcers and acute wounds. Increased isoprostane vs. acute wounds	[178]
Nitro-oxidative stress, NO	Chronic venous ulcers vs. normal skin	Increased NOS activity	[191]
	Diabetic foot ulcer	increased total NOS activity vs. normal and diabetic skin	[192]
	Chronic wounds (mixed etiology)	NOx levels discriminate worsening from progressing wounds	[194]

4.1.1 Conclusions

As seen from the summary in Table 4.1 a multitude of biomarkers for impaired healing have been analyzed and proposed for wound assessment. Due to the diversity of study approaches and wound types identification of a single superior marker is difficult. However, there is consensus that a prolonged elevated enzyme activity of tissue degrading MMPs is a sign for impaired healing. Unfortunately, Table 4.1 also reveals that only quantitative tests may be applied rather than qualitative detection of a species, as for example human chorionic gonadotropin (hCG) in a home pregnancy test. As the activity levels vary during normal healing and differ from person to person even the determination of a certain threshold is problematic.
However, a timely determination of proteinase activity in the wound would enable clinicans to evaluate the wound therapy and make informed decisions on further treatment [195].
A promising approach for the design of a robust point of care indicator would be the combination of a set of parameters, in order to gain a reference value. Such a combination depends on the envisioned application, the method of sampling and the available technologies.

4.2 Microarray Chip for Biochemical Analysis

For the success of microfluidic devices in point-of-care diagnostics, easy handling and fast operation are key points [196, 197]. Incorporation of hydrogels in microfluidic chips has been shown to enable simple, parallel and sensitive biosensing. Sensors for measurements of glucose [198–200], phenol [201], organophosphates [202] and urea [203] have been presented. Hydrogels are a suitable matrix to store reagents [204, 205], proteins [201, 202, 206, 207], DNA [208, 209], and cells [136, 137, 210–214] on microchips without a loss of activity.
In contrast to paper-based microfluidics, which has been investigated for mainly colorimetric ready-to-use diagnostic devices [115, 215], hydrogel chips offer more flexibility for complex samples such as cell suspensions and for sensitive optical detection methods. Unlike sensors based on surface immobilization, a hydrogel contains the sensing reagent in a three-dimensional matrix and allows diffusion of the analyte through the pores of

the gel. The diffusion time of reagents t is determined by

$$t \propto \frac{l^2}{D} \tag{4.1}$$

where l is the diffusion length and D the diffusion coefficient of the molecule of interest. Since the diffusion length l is determined by the size of the hydrogel structures, their dimensions have to be relatively small, i.e., in the micrometer range to enable reactions within a reasonable short time. Furthermore, the pore size of the gel has to be large enough to facilitate diffusion.

In situ polymerization of gel particles within a microfluidic chip has been the preferred fabrication method. An advantage of this procedure over conventional bead assays is that an exact number of particles or amount of reagent can be placed in a chip. Photosensitive polyethlyene glycol diacrylate (PEG-DA) has found broad application as a biocompatible hydrogel in tissue engineering [132, 135] and allows photostructuring as well as pore size tuning over a wide range. Pore sizes of PEG-based hydrogels can be tuned by varying the molecular weight and concentration of the PEG-DA precursor. If pore sizes of up to micrometers are required, polyethylene glycol in different molecular weights can be added as a porogen [216]. These tuning opportunities allow immobilization and handling of a wide range of species from small molecules up to cells.

PEG-DA microgel structures have to be fabricated by UV exposure through a mask [199, 200, 213, 217] or stepwise by a focused beam [218–221]. Another fabrication method for hydrogel assays is the prefabrication of gel beads by a droplet generator [198, 210, 222–224]. However, all these methods have in common that they require a subsequent washing step to remove unreacted precursor. Furthermore, in-situ gel assays need an additional surface modification step to improve gel adhesion to the chip [136, 200–205, 208, 212]. Elaborate preparations and need for external operation compromise the usability of such microfluidic diagnostic tools.

This chapter presents a microfluidic platform, which allows for in-situ polymerization of hydrogel microstructures in a single step without surface modification and washing steps. Furthermore, no external operation is required to initiate a reaction. The first reagent is mixed with the gel precursor and introduced into the chip only in predefined regions. The regions of the gel micropattern and analyte are defined by capillary pressure barriers within the chip. An advancing fluid meniscus is pinned to a

barrier and advances along it instead of crossing it. This concept of laplace pressure barriers has been presented earlier for controlled priming [225–227], valving [228] and pressure driven batch mixing [229, 230].

4.2.1 Selection of Parameters

As previously discussed, the assessment of the biochemical status of impaired healing wounds would be a promising tool to guide wound treatment. As the healing mechanisms are complex and wound status cannot be determined by a single marker, defining a set of markers would be the most promising approach for diagnostic tools [26]. From the markers identified in section 4.1 mainly enzyme activity, protein concentration, albumin, glucose and cell counts are available for direct detection in a single step. In addition, many other selective fluorescent probes, as for reactive oxygen species (ROS), as well as other enzymatic sensing principles are available. Relevant levels of markers from the literature are summarized in table 4.2. The inability of clinicians to measure these markers in an efficient manner has prevented wound care to keep pace with scientific results. Therefore, quantitative and parallel diagnostics at the point-of-care would be an important tool to guide and evaluate clinical treatment of chronic wounds [231].

Table 4.2: Literature values of biomarkers for wound assessment

Marker	healing (non-infected)	non-healing (infected)
Collagenases (µg/ml) [232]	0.76	22.8
active MMP-9 (µg/ml) [157]	1.18 ± 1.21	2.9 ± 1.64
Lysozyme (µg/ml) [163]	1.79 ± 1.22	24.2 ± 9.2
Total protein (mg/ml) [170]	44.3 ± 8.8	30 ± 7.6
Albumin (mg/ml) [170]	25 ± 2.3	17 ± 4.3
Glucose (mM) [169]	$5 - 7.6$	$0.3 - 1$
Bacteria counts (CFU/ml) [193, 233]	$< 10^6$	$> 10^6$

The functionality of the preseted microfluidic device is demonstrated by assays of matrix metalloproteinase 9 (MMP-9), protein concentration and white blood cell counts.

4.2.2 Pressure Barriers for Selective Gel Patterning

The function of the pressure barriers is best illustrated by considering the model of a burst valve, a rectangular channel with a sudden expansion with the angle β as illustrated in Fig. 4.1 and described by CHO *et al.* [234]. The pressure drop across the liquid/air interface can be determined by the Laplace-Young equation as follows:

$$\Delta p = P_{\mathrm{i}} - P_{\mathrm{o}} = \gamma(\frac{1}{R_{\mathrm{w}}} + \frac{1}{R_{\mathrm{h}}}) \tag{4.2}$$

In this equation γ is the surface tension and R_{w} and R_{h} are the radii of the meniscus curvature. With the geometrical substitutes $R_{\mathrm{w}} = \frac{w}{2\cos\theta_{\mathrm{s}}}$ and $R_{\mathrm{h}} = \frac{h}{2\cos\theta_{\mathrm{v}}}$ equation 4.2 yields

$$\Delta p = 2\gamma(\frac{\cos\theta_{\mathrm{s}}}{w} + \frac{\cos\theta_{\mathrm{v}}}{h}) \tag{4.3}$$

where w and h denote width and height of the channel with θ_s and θ_v the contact angles of side walls and vertical walls. A positive value for the pressure difference in Equation 4.3 indicates spontaneous imbibition into the channel. In contrast, in a hydrophobic channel ($\theta > 90°$) the sign changes, meaning that external pressure has to be applied to drive the liquid into the channel. When a liquid interface is moving, the contact angle increases above the static equilibrium contact angle θ_{e}. A critical advancing contact angle ($\theta_{\mathrm{A}} > \theta_{\mathrm{e}}$) is required for the movement, thus the minimum pressure to move the liquid is bigger than in the equilibrium. Considering the meniscus reaching the sudden expansion, the contact angle with the new wall θ_{n} is reduced to $\theta_{\mathrm{n}} = \theta_{\mathrm{A}} - \beta$ (Fig. 4.1). The meniscus stops instantly because $\theta_{\mathrm{n}} < \theta_{\mathrm{A}}$ i.e. the meniscus is pinned. When the contact line bulges until $\theta_{\mathrm{n}} = \theta_{\mathrm{A}}$ the valve bursts and the liquid flow continues to the right in Fig. 4.1. At this point the contact angle with the left wall is $\theta_{\mathrm{I}} = \theta_{\mathrm{A}} + \beta$ with a maximum of $180°$. The Young-Laplace equation for the pinned meniscus can be rewritten as

$$\Delta p = 2\gamma(\frac{\cos\theta_{\mathrm{A}}}{w} + \frac{\cos\theta_{\mathrm{I}}}{h}) \tag{4.4}$$

with a maximum pressure the valve can withstand at $\theta_{\mathrm{Imax}} = min\{\theta_{\mathrm{A}} + \beta, 180°\}$. According to Equation 4.4 the factors influencing the maximum pressure for a robust meniscus pinning and in consequence the liquid guiding (where $w \gg h$ and $\theta_{\mathrm{I}} = \theta_{\mathrm{A}} + \beta$) are: The surface tension of

the liquid γ, the contact angle at the expansion θ_A, the opening angle β and the channel height h. In the case of liquid guiding by the dry film structures $\beta = 90°$, given by the sidewall profile of the dry resist, while θ_A depends on the resist material and the liquid, and γ on the liquid only. Therefore, only h, the relative height of the resist structure remains as a free design parameter.

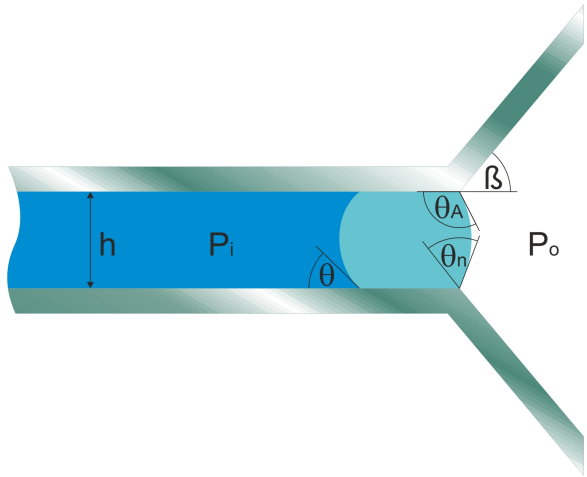

Figure 4.1: Illustration of a burst valve for meniscus pinning consisting of a rectangular channel (height *h*, width *w*) with a sudden expansion at an angle β.

4.2.3 Chip Design and Operation Principle

The principle of the device is illustrated in Fig. 4.2. Analogous to the burst valve model, a fluid meniscus is pinned to a capillary pressure barrier and propagates along it instead of crossing it (Fig. 4.2b). Therefore, liquid occupies only regions that are defined by the barriers within the chip. After injection and UV curing of the sensing hydrogel, the analyte autonomously fills the chamber interdigitated to the gel micro structures by capillary action (Fig. 4.2a). This principle of selective, interdigitated fluid structuring allows effective mixing of small liquid batches without any external operation.
Microfluidic chips were fabricated on a microscope glass slide (76 mm × 26 mm) by hot roll lamination of dry film photoresist, which allows fast, cost efficient, and parallel processing. Sixteen devices were fabricated on a slide in a size and distance according to a 96 well plate in order to be compatible with standard fluorescence reader equipment.

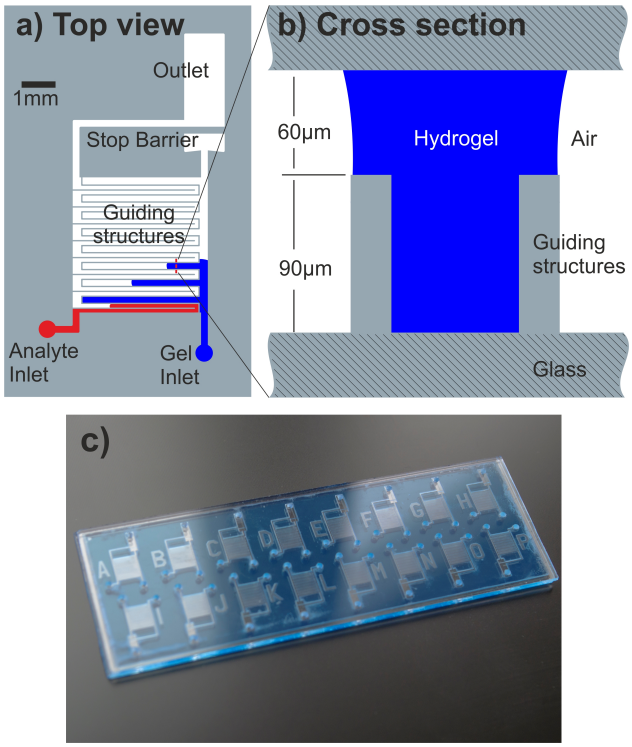

Figure 4.2: Illustration of chip design. a) Top view: The device is prepared by injecting the sensing hydrogel via one inlet (blue). After curing, the analyte fills the chamber interdigitated to the gel and void-free (red). b) Cross section: Capillary pressure barriers enable reliable liquid guiding. c) Assembled device with 16 reaction chambers (microscope slide format). Dry film resist is sandwiched inbetween glass slides. Device masks are shown in Appendix D.

In the first fabrication step a layer of 90 µm dry film resist (Ordyl SY300, Elga Europe) was laminated onto the bottom glass slide. The microfluidic chambers and pressure barriers were structured by standard photolithography. Inlet and outlet holes were powder-blasted into the top glass layer. Afterwards, a 60 µm dry film layer was laminated and structured onto the top glass. Both glass slides were aligned by eye and the two resist surfaces were bonded by hot roll lamination. An assembled device is depicted in Fig. 4.2c.

After preparation of the chip with a gel for the desired assay, the reaction is initiated by adding a drop of the sample to the analyte inlet (Fig. 4.2a). The chip concept enables reactions with a minimum of reagent and sample

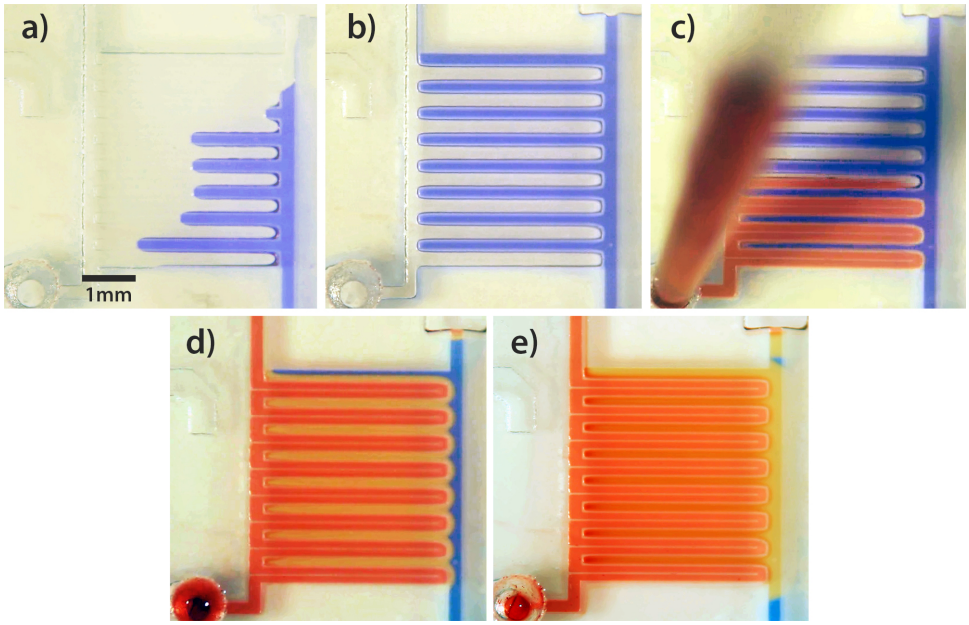

Figure 4.3: Visualization of an assay reaction. a) Only 1 µl of the the sensing hydrogel is required to prepare the chip. b) Device is ready for the assay with bromophenol blue pH indicator dye, immobilized in the UV cured hydrogel. c) Citric acid (pH 2) colored with cochineal red is topping up the chip interdigitated to the gel in order to have short diffusion paths. d) Fast (around 3 s) shift from blue to yellow of the pH indicator dye. e) Diffusion of the cochineal red dye into the hydrogel takes some time due to its molecular weight (MW 604). Picture taken after 120 s).

volume per test. In comparison to conventional assays, only a fraction (1.5 µl) of sample per test is required. Preparation procedures and reaction dynamics are illustrated in Fig.4.3. The device in Fig. 4.3a was prepared with a pH sensitive dye (bromophenol blue) incorporated in the hydrogel. Bromophenol blue exhibits a shift from blue to yellow at a pH value below 3. Citric acid (pH 2) with cochineal red (a red food dye) with a molecular weight of 604 was added to the chip to start the reaction (Fig. 4.3c). Due to the hydrophilic nature of the gel the device fills completely automatic and void-free by capillary action. The fast response of bromophenol blue to the acidic environment is visible in Fig. 4.3d. On the other hand, diffusion of the cochineal red molecules into the gel structures takes a bit longer. As seen in the picture Fig. 4.3e, which was taken 2 min after the start of the experiment, the red dye diffused into the hydrogel fingers. This

result shows the dependencies of reaction dynamics on the molecule size and gel porosity. To yield assays with reasonable short response times (e.g. minutes), the gel composition has to be adjusted to the sample. By varying the molecular weight of the PEG-DA precursor or addition of a polyethyleneglycol porogen the pore size and hence diffusion dynamics can be customized. Since the gel microstructures occupy about half the active chip area (16 mm^2), the device is compatible with macroscopic readout equipment such as digital cameras, photodiodes or plate readers.

4.2.3.1 Device Dimensions Analysis

Analyses of influencing device geometries and hydrogel properties were performed in order to optimize the defined filling of the devices and reaction performance. Interdependencies of design parameters are illustrated in Fig. 4.4. External limiting factors are given in red for upper limits and green for lower limits. According to equation 4.1, the reaction speed depends on the width of the gel structures. A main tradeoff is given by gel finger width for fast diffusion and the liquid volume in the chip for convenient handling in terms of pipetting and evaporation (Fig. 4.4). The quadratic increase of diffusion time with gel width narrows the design window. On the other hand, the channel height is closely related to the structure dimensions by a robust guiding and the maximum aspect ratio. Several experiments with varying parameters were performed to optimize the mixing structure design.

Table 4.3: Hydrogel contact angle measurements on glass and photoresist surface (Ordyl SY300) in dependence of PEG-DA 700 concentration in water.

PEG-DA concentration	0%	20%	40%	60%	80%
glass	11.5	14.5	20	35	38
Ordyl	68	47	40	37	27

Contact angles of gel precursors on glass and the resist surface depend on the amount of polymer content, thus effecting the guiding by the hydrophobic resist structures patterned on the hydrophilic glass surface. Contact angle measurements in dependence on PEG-DA concentrations are shown in table 4.3.

As the contact angle difference between glass and the photoresist decreases with increasing polymer content, the step height of the resist structures has to be increased for a reliable guiding (reduced h in equation

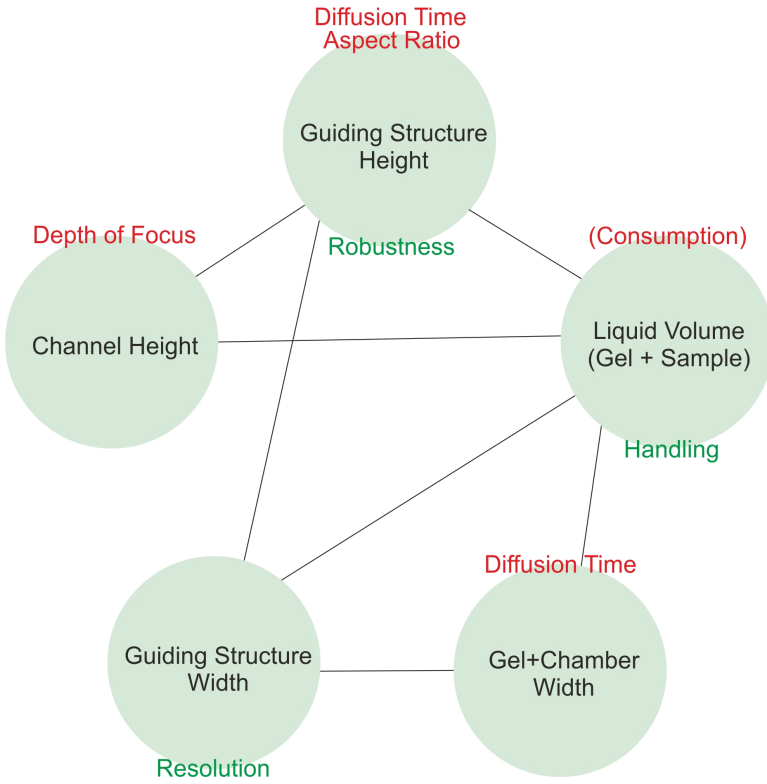

Figure 4.4: Interdependence of device design parameters with external upper and lower limits.

4.4). In practice, a step height larger than $60\,\%$ of the chamber height showed robust guiding for the tested precursor solutions. With that structure height definition, the reliable performance was independent on the chamber height, tested from 65 µm to 150 µm. However, the total chamber height is limited by the maximum aspect ratio ($\approx 2.5h/w$) of the resist material for the guiding structures. In Fig. 4.5 the advancing menisci on top of the guiding structures to the top glass surface can be seen. At the PEG-DA concentration of $20\,\%$ a clear difference in wetting on both surfaces is observable in the inset.

As given by the diffusion law, the gel finger width tremendously influences the reaction speed as illustrated in Fig. 4.6. The three test structures contain finger structures with widths of 450 µm, 300 µm and 225 µm, respectively. Both, the pH reaction as well as the red dye diffusion become considerably faster as the gel finger width decreases.

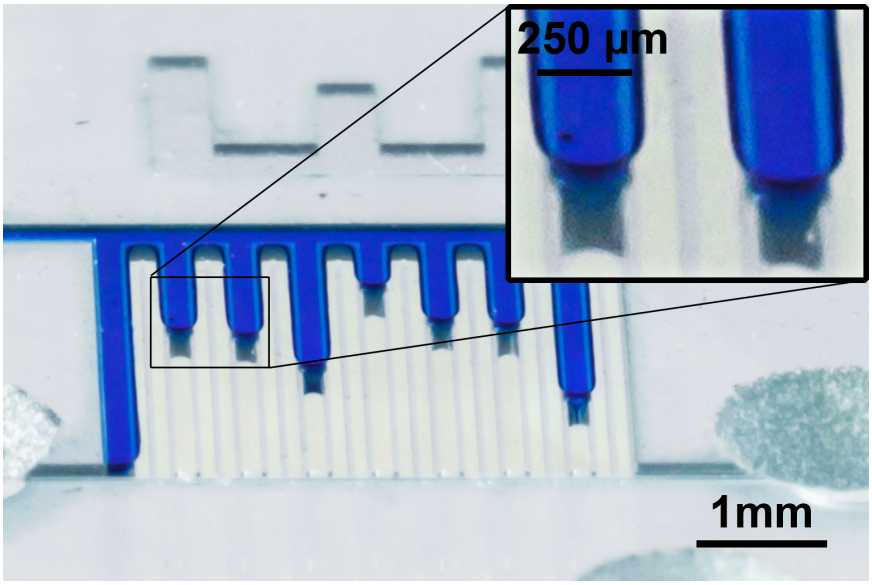

Figure 4.5: Advancing fluid menisci pinned to the resist guiding structures, allowing selective and well defined structuring of the hydrogel in a micrometer range for fast reagent interaction. Gel finger width: 250 µm. PEG-DA Prepolymere content is 20 %.

The remaining gel interface height on top of the structures has only minor influence on the assay speed. Fig. 4.7 compares the reaction speeds of devices with 20 µm and 50 µm gel interface with only little differences in color change within the same time. However, an evident difference in Fig. 4.7 is the increasing intensity with total chamber height, which is advantageous for readout.

Although minimizing the gel width increases the diffusion speed, a limit is given by the gel interface height. As seen from Fig. 4.8a, large structures are robustly filled by low guiding structures ($h = 40\,\%$). However, as the dimensions of the stretched meniscus approaches the lateral gel dimension (feature size), a critical corner is formed that is prone to overflow and device failure (Fig. 4.8b).
Dimensions of the reaction chamber of 4 mm $\times$ 4 mm with 250 µm finger width, 90 µm high guiding structures and 60 µm gel interface showed to be

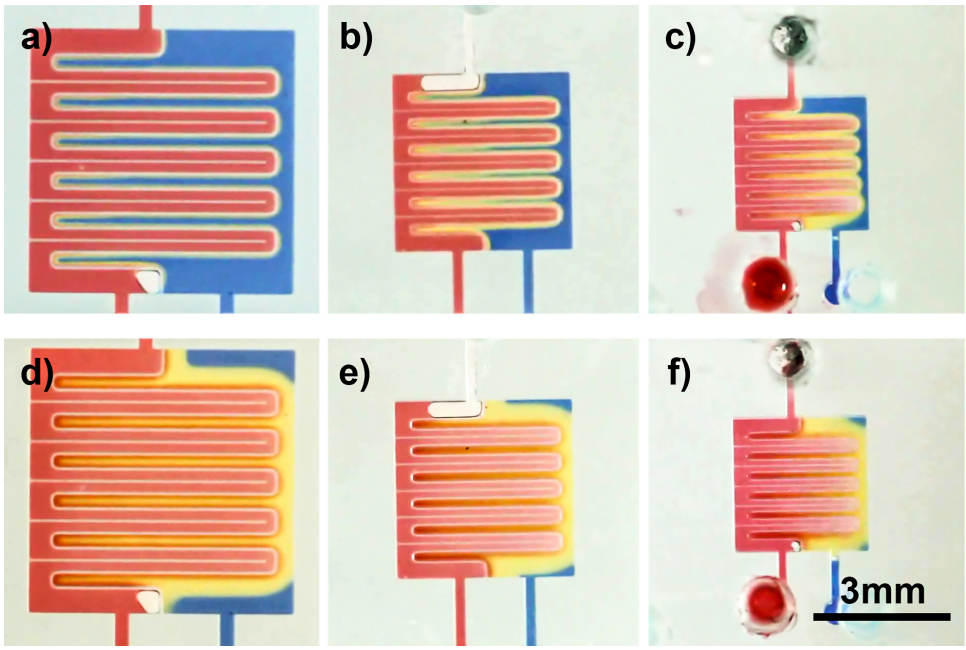

Figure 4.6: Test structures showing the influence of the chip geometry on the reaction speed. a-c) Picture taken 3 s after sample injection. a) 6 mm chamber 450 µm fingers. b) 4 mm chamber 300 µm fingers. c) 3 mm chamber 225 µm fingers. d-f) 2 min after sample injection.

a reliable trade-off of the mentioned aspects and ensure reliable guiding of liquids with different wetting properties due to varying content of monomers or solvents.

4.2.4 Hydrogels, Samples and Experiments

The hydrogel consisted of polyethylene glycol diacrylate (PEG-DA) with a 2-hydroxy-2-methylpropiophenone (HMPP) photoinitiator. For the proteinase assays the hydrogel precursor was prepared by dissolving PEG-DA with a molecular weight of 6000 in Tris-HCl buffer (pH 7.6) at 10% w/v. The HMPP photoinitiator was added at a concentration of 1.5% v/v. An autoquenching fluorescein conjugate proteinase substrate (DQ Gelatin, Invitrogen) was mixed with the gel precursor at 10% v/v. Upon cleavage of the substrate by the proteinase, fluorescence intensity, corresponding to the enzyme activity can be measured.
Colorimetric protein detection was achieved by a color shift of bromophenol

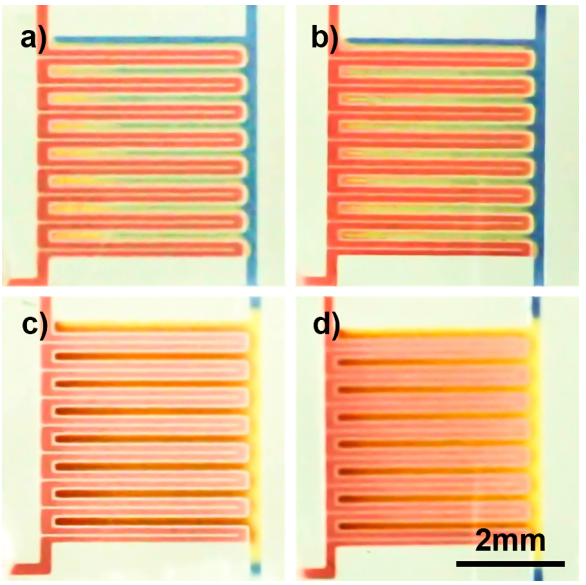

Figure 4.7: Reaction speed in dependence of relative guiding structure height. a, c) 90 µm guiding structure, 20 µm gel interface (110 µm total channel height). b, d) 90 µm guiding structure, 60 µm gel interface (150 µm total channel height). a, b) 3 s after sample injection. c, d) 2 min after sample injection. The relative height of the guiding structure only slightly influences the reaction speed. However, color intensity increases with total channel height.

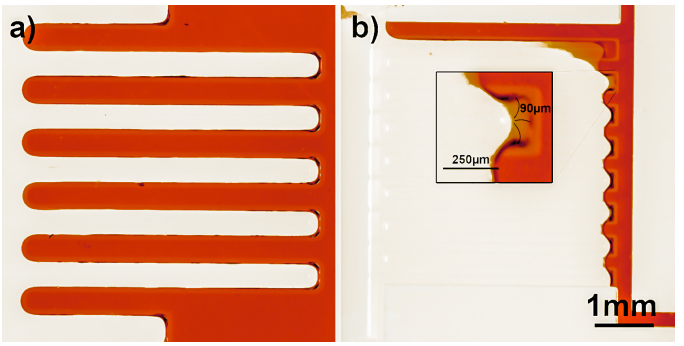

Figure 4.8: Influence of feature size on liquid guiding effect. Guiding structures are 60 µm high in 150 µm chambers. a) Large structures enable reliable filling even with the guiding structure height of 40 %. b) As the vertical meniscus dimensions (≈90 µm in the inset) increase in relation to the feature size, a critical corner is formed, which is prone to overflow .

blue upon interaction with protein in an acidic environment [235]. Stock solutions for the colorimetric protein assay were prepared as follows: A) PEG-DA, molecular weight 700 mixed with 2% v/v HMPP. B) Bromophenol blue in deionized water at 10 mg/ml. C) Polyethylene gylcol (PEG), MW 8000 in deionized water 50% w/w. The gel was mixed in ratios 1:2:1 (A:B:C).
Fluorescent protein assay gels were prepared by mixing 20% w/v PEG-DA 6000, 1.5% v/v HMPP and 5% v/v of a protein specific dye (Qubit, Invitrogen) in the provided buffer.
Gel for cell counts consisted of 5 µM Syto-9 in 20% w/v PEG-DA 6000, 1.5% v/v HMPP in Tris/HCl buffer.
Blood samples were obtained from healthy volunteers, recruited at the Austrian Institute of Technology with informed consent. All experiments were performed in compliance with the relevant laws and institutional guidelines of the Austrian Institute of Technology, approved by the ethics board of the city of Vienna, Austria.
After introduction of the gel into the chip, it was cured by flood exposure at 365 nm in a UV nail dryer for 30 s. The chips were sealed with tape and stored cool and dark until use. Samples for standard curves were prepared by serial dilutions of *Clostridium histolyticum* collagenase type IV (MMP-9) and bovine serum albumin. Cochineal red was obtained from a local pharmacy, all other chemicals were ordered from Sigma Aldrich unless other mentioned. Fluorescence detection was done by a camera mounted on a Nikon Eclipse 80i fluorescence microscope with a B-2A filter set. In addition, readings with a fluorescence spectrometer (Perkin Elmer LS55) were conducted.

4.2.5 Results and Discussion

4.2.6 Matrix Metalloproteinase Enzyme Assays

The functionality of the microfluidic chips for diagnostic applications is presented by assaying matrix metalloproteinase 9. Depending on the enzyme activity the collagene substrate in the hydrogel is cleaved and a green fluorescence signal is emitted (inset Fig. 4.9a). Results of three independent experiments are plotted in Fig. 4.9a. Mean values and standard deviation of image histograms are shown. As seen from the plot, the sensitivity of the assay increases with incubation time. For concentrations

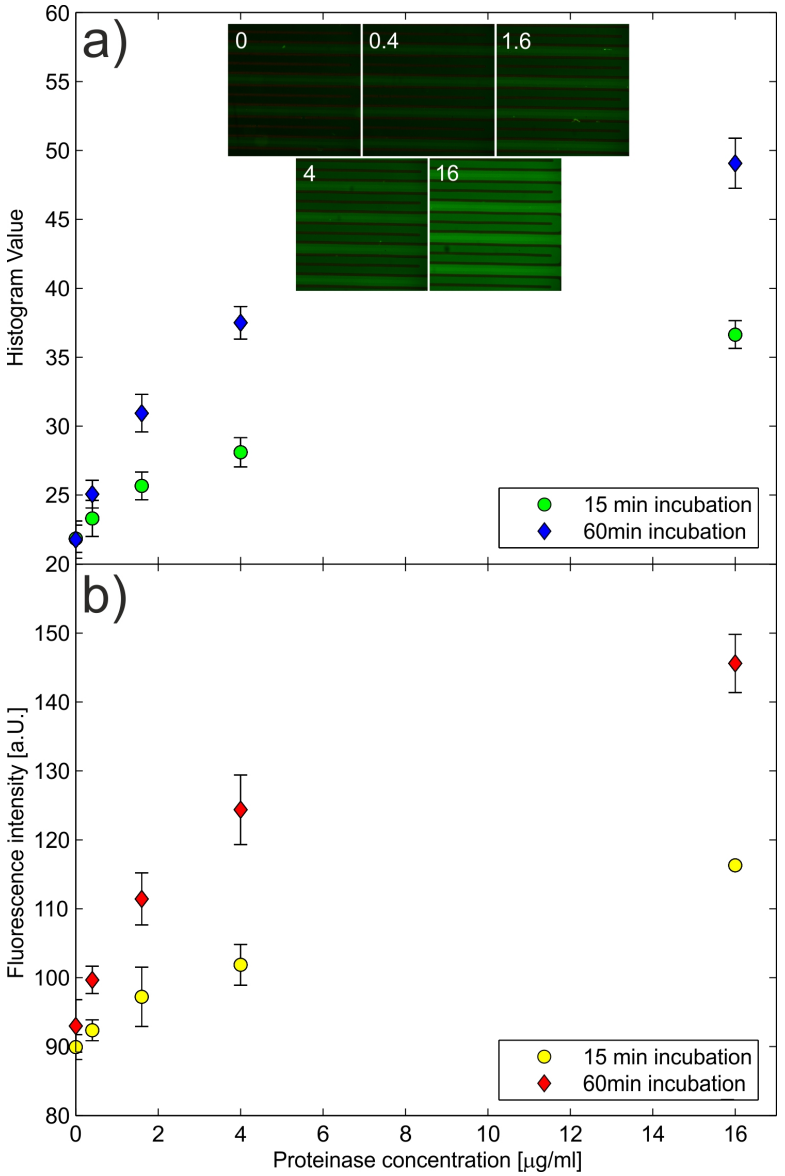

Figure 4.9: Data evaluation of fluorescent images of the metalloproteinase assay. Mean histogram values are plotted versus enzyme activity of MMP-9. a) Results of 3 consecutive experiments are summarized. Data shows results after 15 min and 60 min of incubation. b) Readings of a fluorescence plate reader are in good agreement with image analysis. (excitation 490 nm, slit 5, emission 525 nm slit 10, 515 nm cut-off)

in the range of 10 µg/ml an incubation time of only 15 min is sufficient. With increasing incubation time, the limit of detection can be decreased. Following the guidelines of the Clinical and Laboratory Standards Institute [236] a rough estimation of the limit of detection at an incubation time of 60 min gives

$$L_{\mathrm{D}} = \frac{mean_{\mathrm{blank}} + 1.645\sigma_{\mathrm{blank}} + 1.645\sigma_{\mathrm{lowC}}}{sensitivity} = 0.47\mu g/ml \qquad (4.5)$$

which is well below the values given in table 4.2. Readings with a fluorescence plate reader are shown in Fig. 4.9b to demonstrate compatibility with standard laboratory equipment. As seen, results are in good agreement with image analysis.

4.2.6.1 Protein Concentration

Comparison of fluorescent and colorimetric total protein concentration measurements are summarized in Fig. 4.10. Serial dilutions of bovine serum albumin were used for calibration. Incubation time after sample introduction was 10 min. The sensitivity of the fluorescent assay (Fig. 4.10a) is much higher compared to the colorimetric method, with a corresponding L_{D} of 0.02 mg/ml. On the other hand, colorimetric analyses are simply done by evaluating histogram values of the digital photograph. As seen from the inset in Fig. 4.10b, the blue color intensity increases with increasing protein concentration. Limit of detection in this case calculates to 0.14 mg/ml, which still is well below the concentrations found in wound fluid samples (compare table 4.2).

4.2.6.2 White Blood Cell Count

The device is capable to handle complex samples as shown by an experiment with whole blood, collected by a finger prick from a healthy volunteer (Fig. 4.11). 2 µl were serially diluted 3 and 12 times. Syto-9, a cell permeable DNA fluorescent dye was incorporated into the gel. After an incubation time of 15 min white blood cells were labeled green fluorescent. As mature red blood cells do not contain a nucleus and DNA, the white blood cells are brightly visible. Counting the number of white blood cells has diagnostic applications in diseases such as leukemia [237], coronary heart disease [238], and systemic infection diagnostics. Furthermore, cell counts in wound fluid could be of additional value as excessive neutrophil

invasion corresponds with wound severity [239]. Wound fluid analysis by performing the three presented fluorescent assays on a chip could give clinicians a quick and robust tool to estimate chronic wound status. All three assays can be performed on the same chip with equal fluorescent detection (filter set 450-490/500/515).

4.2.7 Conclusions

A new method for the rapid preparation of hydrogel-based bioassays in a single step has been demonstrated in this chapter. The simple handling and operation allows the end user to customize the microfluidic chip for different biosensing applications. As the chip dimensions define the reaction volume, pipetting errors by the user can be excluded. Compatibility with standard equipment was proven, which is an important step towards clinical acceptance.

By the simple dry film process the chips can be produced by any standard facility. Future large scale production could also be achieved by hot embossing methods, as the guiding effect does not necessitate different wetting properties.

The presented enzyme, protein and cell assays indicate the vast amount of possibilities for biochemical testing. Hydrogel-based assays are especially suitable for enzyme activity, enzymatic sensing and direct target labeling assays, allowing for instantaneous readout. However, hydrogels also support antibody binding within the three-dimensional matrix, with the specific advantages of maintaining excellent stability and yielding higher signals than planar assay due to higher loading [210, 240]. Performing homogeneous immunoassays would enable detection of specific rare protein markers in the same rapid manner as the presented assays [241].

The evolution of user friendly microfluidics will yield analytical tools in clinical applications. Combining several analytical tests on a single slide offers the possibility to obtain multi-parametric analysis at the point-of-care. Such tests will help to investigate complex diseases such as chronic wound healing, where many factors contribute to stalled healing.

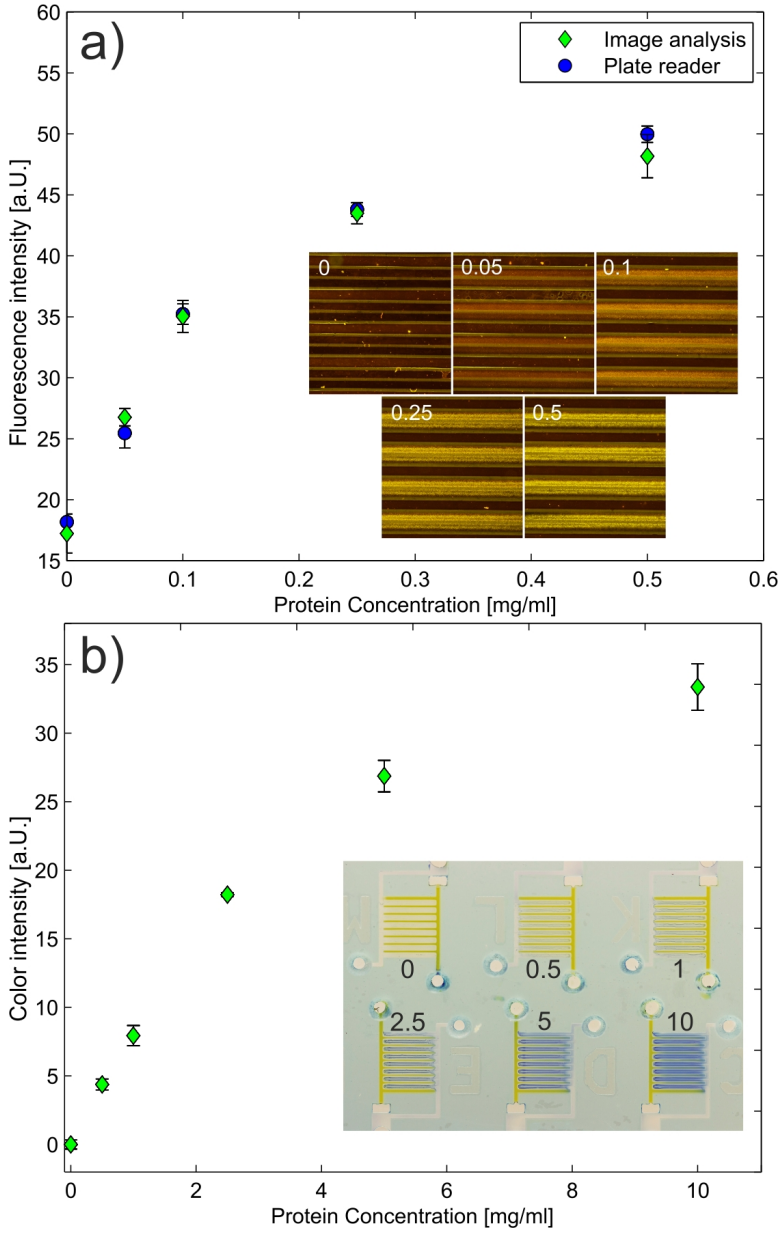

Figure 4.10: Total protein concentration assays. a) Fluorescent protein assay results from image analysis and plate reader (excitation 490 nm, slit 5, emission 560 nm slit 20, 515 nm cut-off). b) Colorimetric protein assay. Bromophenol blue exhibits a color shift from yellow to blue in an acidic environment upon addition of protein. All experiments were conducted in triplets, readings were done after 10 min of incubation time.

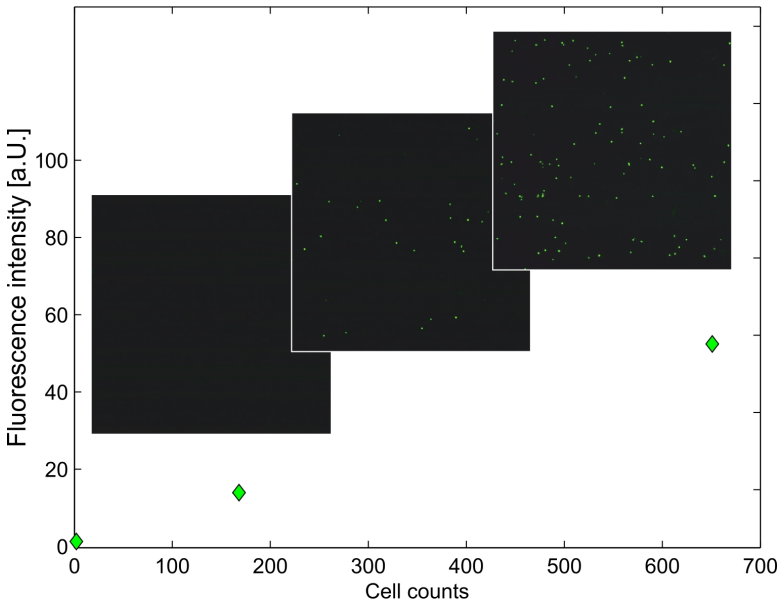

Figure 4.11: Handling of complex samples: Fluorescent staining of white blood cells with Syto-9 in a blood sample. Fluorescence image intensity is plotted against an automated cell count. From left to right: Negative control, 12-fold and 3-fold dilution of a drop of whole blood.

Chapter 5
Systems for Bacteria Analysis

Bacteria play an important role in delayed healing, as briefly mentioned in chapter 4.1. Not only do they pose the risk for life-threatening infections but also influence the wound environment by affecting pH levels, releasing enzymes, and forming of biofilms. Section 5.1 discusses the inflammatory environment promoted by bacteria in chronic wounds.
Efficiency in detecting local infections and testing antibiotic susceptibility are of utmost importance. A concept for the concentration of bacteria for use in molecular diagnostics is presented in section 5.2, published in *Microfluidic concentration of bacteria by on-chip electrophoresis*, Biomicrofluidics 5, 044111, 2011, http://dx.doi.org/10.1063/1.3664691, reproduced by permission of AIP Publishing.
Based on these results, a low-cost detection system to determine total bacteria counts was developed (5.3), published in *Rapid detection of bacteria by low-cost microfluidic system*, Proceedings of Smart Systems Integration, Apprimus Verlag, Aachen, (2014), ISBN: 978-3-86359-201-1; S. 323 - 328.
Developed methods for advanced antibiotic testing and bacteria identification are presented in section 5.4, published in *Hydrogel-based microfluidic incubator for microorganism cultivation and analyses*, Biomicrofluidics 9, 014127, 2015, http://dx.doi.org/10.1063/1.4913647, reproduced by permission of AIP Publishing.

5.1 The Pro-Inflammatory Environment

The chronic open wound offers a sustained gateway for bacteria. Therefore, all chronic wounds contain bacteria from the environment, the surrounding skin, or endogenous sources, including mucous membranes [242]. A critical aspect to healing is the grade of bacterial invasion, which can be divided into surface contamination, superficial colonization, deeper tissue infection,

and the systemic sepsis. The risk of an infection can be described by the following relation:

$$\text{Infection} = \frac{\text{Number of organisms} \times \text{Organism virulence}}{\text{Host resistance}}. \tag{5.1}$$

Besides number and type of bacteria, the ability of the immune response to prevent bacterial damage is the most important factor. Cardiovascular diseases, poor nutrition, medication, smoking, or diabetes all may interfere with the host immune system. Acute infections are diagnosed by the classic terms of calor, rubor, dolor, tumor, and functio laesa (heat, redness, pain, swelling and function loss). For diagnosing chronic wound infection additional clinical signs include red and bleeding granulation tissue, delayed healing, exudate, necrotic tissue, increased temperature, smell, and new areas of breakdown. [15, 243, 244]
However, for wounds without those signs of infection that still refuse to heal biofilm formation has been a possible explanation. A biofilm is defined as a community of bacteria that adheres to a surface and is embedded in an extracellular polymeric substance (EPS). The inability of the immune system to eradicate bacteria, protected by the EPS is believed to be a reason for the persistent inflammatory response in chronic wounds [16, 244, 245].
Investigation of chronic leg ulcers revealed the presence of two to five different bacteria with the presence of *Staphylococcus aureus* in 93.5%, *Enterococcus faecalis* in 71.7%, *Pseudomonas aeruginosa* in 52.2%, coagulase-negative staphylococci, such as *Staphylococcus epidermis* in 45.7% and anerobic species in 39.1% of the observed ulcers [246]. Observations of a broader range of wound types also yields a wider variation of bacteria but *S. aureus* and *P. aeruginosa* remain among the most prevalent and most discussed species as a reason for delayed healing [242, 247–249]. In contrast to coagulase-negative staphylococci, *S. aureus* is pathogenic due to the virulence factors coagulase, protein A, leukocidine, enzymes as catalase and different toxins. In addition *S. aureus* has the ability to form biofilms, and it may show antibiotic resistance (methicillin resistanst *S. aureus*, MRSA) with major consequences for the treatment procedures in order to avoid further spread [250]. In addition to *S. aureus* also *P. aeruginosa* has the ability to form biofilms. Wound colonization with *P. aeruginosa* has shown to result in delayed healing [251, 252]. In wounds that harbored large *P. aeruginosa* aggregates, alginate was found to build the EPS [253], which prevents phagocytosis, acts as a scavenger of oxygen

radicals, and binds cationic antibiotics [16]. The virulence factors produced by the bacteria in biofilms interfere with the host immune response and foster the release of pro-inflammatory cytokines and proteases [245].

5.1.1 Diagnostics and Infection Control

Determining the bacterial load of a wound has for long been discussed as a measure for delayed healing [242]. A tissue bacterial count of 10^5 to 10^6 CFU/g has been suggested as a quantitative measure for delayed healing. However, the sampling method highly influences the result and and has been discussed in literature. While some authors have argued that tissue biopsies yield a precise microbiological representation of the wound, non-invasive, faster and safer surface swabs according to the Levine technique have become the gold standard [2, 233, 242, 254–256]. At least at the first presentation of the patient swabs are recommended to record the bacterial spectrum of the wound [247]. In addition, when signs of infection are present, identification of pathogens and antibiotic sensitivity testing is recommended [257]. Although molecular methods have been proposed for bacterial identification, antibiotic sensitivity testing requires growth based methods in any case [258, 259]. Despite the presence and importance of anerobic bacteria in chronic wound infections, anerobic microbiological analysis are not performed routeinely in many facilities due to time consuming, elaborate and expensive culturing [242, 249].

A direct and simple method of biofilm identification does not exist but fluorescent in situ hybridization with confocal laser scanning microscopy can be used to visualize biofilms in chronic wound biopsies [253, 260].
Biofilm-based wound care is a combination of sharp debridement and strategies to inhibit reformation of biofilms. For optimal treatment after debridement, rapid methods to identify bacteria and their antibiotic susceptibility are required. Different topical antiseptics have been evaluated for the treatment of biofilm containing wounds. A class of agents including lactoferrin, xylitol, and ethylene diamine tetraacetic acid (EDTA) especially targets the inhibition of biofilm formation [50, 261, 262]. In this respect quorum sensing, a chemical communication among bacteria, is an important mechanism in biofilm formation and poses an exciting and attractive possibility for biofilm inhibition. [184, 185, 263].
Observing equation 5.1 reveals that not all contributors to infection are

accessible for measurements. Currently, only methods for bacterial counts and identification are available. However, infection is diagnosed by clinical signs of the immune response and bacterial analysis is only performed if these clinical signs of infection are present. The role of anerobic bacteria in delayed healing often is neglected, while methods for identification and treatment of biofilms currently still are under investigation. Routinely performed bacterial tests and controls of the microbiological wound environment would be of great benefit to get a complete picture of the chronic wound for research and therapy. Therefore, rapid tools for bacterial analysis are required together with standardized sampling methods.

5.2 Micro-Free Flow Electrophoretic Concentration of Bacteria

Miniaturized diagnostic systems for analysis of infectious pathogens have been widely investigated over the last two decades [103, 264]. Amplification-based systems such as real-time PCR have been in the focus of this research. For applications at point-of-care or resource poor environments automated and easy to handle sample preparation techniques have to be developed. Sample preparation for nucleic acid testing includes concentration of the pathogens and extraction of nucleic acids. Commonly applied procedures for nucleic acid extraction require a large number of reagents and preparation steps, limiting applications in rapid pathogen testing [265]. Recently, a microfluidic chip for lysis of target species and isolation of RNA was presented [266]. Due to the small volumes of such devices and the low analyte concentration of real-world samples, a preconcentration step is required. Conventional concentration techniques are based on centrifugation, membrane filtering or capturing by functionalized magnetic beads [267]. For the success of microfluidc diagnositic platforms automated, easy to handle and readily combinable functional units have to be developed [268].
The three main concepts for chip-based pathogen concentration are physical trapping, functionalized particles and electrokinetic techniques [264]. Physical traps for bacteria are fabricated by shallow channels or arrays of microbeads [269, 270]. Although these devices are simple, clogging and capturing of small pathogens such as viruses are major difficulties.

Antibody-coated particles have been used to selectively bind to the target species. These particles are trapped in microchannels by physical barrieres [271] or magnetic fields [272–274]. The capture efficiency strongly depends on the quality of the coatings and proper mixing of particles and analytes. For a successful integration and an increased capture efficiency, further advances in bead modification and controllability of the magnetic field have to be made [275, 276].
The electrokinetic principles, dielectrophoresis (DEP) and electrophoresis have the advantage to be electrically controllable and easy to integrate [268]. Both methods depend on the conductivity of the liquid medium. Hence, analysis of swab-derived pathogens, transferred to the medium is the preferable application over direct use of physiological samples. Swabs are the most common method for identification of wound infections in clinical diagnostics [277]. Other applications of swabs are the detection of respiratory infections [278], and contaminated food and environmental surfaces [279].
Dielectrophoresis has widely been used for preconcentration and separation of cells and bacteria [106]. Many of them direct cells to certain positions within a prefilled chip [280–284] rather than reducing the volume. A number of DEP traps and separators have been optimized for continuous operation by careful scaling of the device and electrode dimensions to the analyte, as the dielectrophoretic force depends on the volume of the biological particles [285–291]. As analyzed by KUCZENSKI et al. [287] the high field strengths required to manipulate bacteria can strongly affect their viability. In addition, high fields induce disturbing effects such as electrothermal flow and AC electroosmosis [283, 292, 293].
Bacteria and viruses exhibit a negative charge at physiological pH values. Therefore, electrophoretic concentration has the advantage to be universally applicable for a wide range of pathogens. Free flow electrophoresis (FFE) including isoelectric focusing (IEF) and zone electrophoresis (ZE) has been used to separate biological particles [294–297] but has received considerably less attention for the concentration of bacteria or viruses. YAGER *et al.* and BALASUBRAMANIAN *et al.* presented microfluidic devices for continuous concentration and capture of bacteria. [298–300]
Previously, a device for the concentration of bacteria was developed. A factor of 17.8 for gram positive bacteria was achieved within 30 min. Besides the throughput also the capture efficiency was still unsatisfyingly at around 80 % [301]. Herein, the influencing factors are analyzed and an

optimized device and method for concentration of bacteria by means of FFE is presented. A highly efficient but gentle concentration of gram negative bacteria, which are far more sensitive to lysis is demonstrated. Together with the earlier developed chip for lysis and nucleic acid isolation [266] the presented method can lead to rapid analysis of swab-derived pathogens.

5.2.1 Theory

Bacterial cells exhibit a negative surface charge due to ionized carboxylate and phosphoryl groups and therefore experience a force in an electric field. The resulting migration velocity is proportional to the electric field,

$$\vec{v} = \mu \vec{E} \tag{5.2}$$

where μ is defined as the electrophoretic mobility (EM). Electrophoretic mobilities of bacteria are typically in the range of -1 to $-4 \cdot 10^{-8}\,\mathrm{m^2/Vs}$ and are highest at low ionic strength of the medium [302–304]. The pH has a minor influence above a value of 6, at which mobilities are almost constant [305].
The major side-effect, influencing the motion of bacteria is due to electroosmotic flow (EOF). The EOF is caused by the interaction of an electric field with the double layer formed at the liquid/glass interface. The high surface-to-volume ratio in microfluidic channels causes EOF to have a major influence on micro-electrophoretic techniques. The electric field moves the liquid boundary layer towards the cathode and drags the bulk fluid along. Since the channel is closed in the direction of the electric field, a circular flow develops that interferes the electrophoretic migration of bacteria. Cationic surfactants have been used to suppress EOF [298]. As these surfactants are known biocides they have to be avoided to ensure high bacterial yield.

Polymeric additives, such as hydroxypropyl methylcellulose (HPMC) can be used to suppress electroosmotic flow. HPMC acts as a dynamic coating, increasing the viscosity within the double layer and reducing the surface charge density at the channel wall. By adding 0.1% w/w methylcellulose CUI *et al.* have reduced the EOF by a factor of 10 [306].

5.2.2 Chip Design and Fabrication

Formation of bubbles at the electrodes due to electrolysis and, as a consequence, the unstable performance is one of the main limiting factors of μFFE. To overcome this problem a variety of strategies have been developed, including different buffer additives, membrane barriers, or multiple depths designs [307, 308]. In the presented device the concept of phaseguides was used to prevent bubbles from blocking the current paths and to enable controlled filling of the chip. Phaseguides are stripes of resist within the channel to control an advancing liquid-air meniscus as discussed in section 4.2.2.

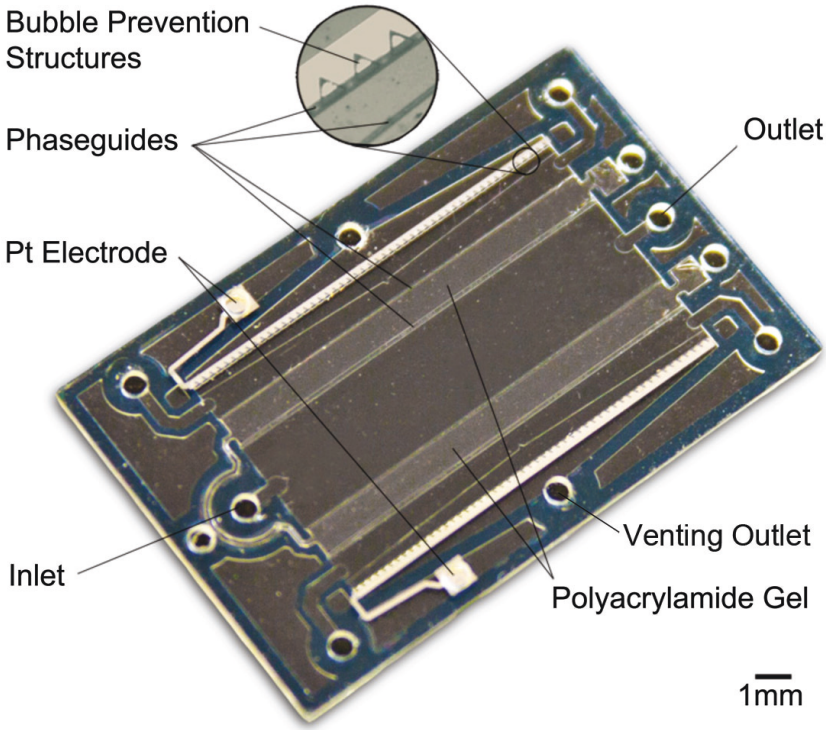

Figure 5.1: Photograph of the microfluidic chip: Phaseguides are used to ensure controlled filling of polyarcylamide gel. Triangular structures are placed on top of the electrodes to expulse bubbles to the venting outlet. Device dimensions are $14\,\text{mm} \times 22\,\text{mm}$ with $120\,\mu\text{m}$ channel height. The concentration channel, defined by gel barriers measures $3.5\,\text{mm} \times 15\,\text{mm}$. Device masks are shown in Appendix D.

The chip design is illustrated in Fig. 5.1. Polyacrylamide gel is introduced via phaseguides to define the concentration channel. The nanoporous gel polymerizes without shrinking. It is used to collect the target species, which are driven through the chip by a continuous flow while electrical current passes through the gel matrix. The phaseguides at the electrodes act as a pressure barrier, preventing gas bubbles to cross (zoom circle in Fig. 5.1). Furthermore, for a bubble that develops between two triangles, the pressure drop across the larger liquid/gas interface is lower than across the smaller surface. Thus, the bubble tends to grow towards the open end of the triangles and leaves the channel through the venting hole.
Two 4-inch, 500 µm thick glass wafers were used as the base material of the devices. Platinum electrodes were structured on the bottom substrate by a standard lift-off process. Holes for fluidic access were drilled through the top substrate. The microfluidic structures of the device were formed within a dry film resist layer (*Ordyl SY330*). The resist with a thickness of 30 µm was laminated onto one substrate in multiple layers at $95°$C and photolithographically patterned. Two layers were laminated and exposed to obtain phaseguides of 60 µm height. Another two layers were added to form the channels and the bubble expulsion structures of a total height of 120 µm (Fig. 5.1). After resist development the top substrate was bonded at a pressure of 60 N/cm^2 and a temperature of $95°$C without the need of further adhesives. For details of dry film resist chip fabrication refer to VULTO *et al.* [309]. Finally, the bonded wafers were diced into single devices of 14 mm $\times$ 22 mm dimensions.
After fabrication, a 16% polyacrylamide gel (40% Acrylamid/Bisacrylamid 19:1, sodium borate) was filled into the chips. The gel was crosslinked with ammonium persulfate (APS) and tetramethylethylenediamine (TEMED) in a nitrogen-flooded chamber. Afterwards, the devices were filled with SB medium to avoid dehydration of the gel until use.

5.2.3 Finite Element Simulations

To optimize the parameters of the concentration method, bacterial trajectories were calculated by finite element simulations in *COMSOL Multiphysics* and *MATLAB*. The stationary velocity of the pressure driven flow was evaluated by a 3-dimensional model of the microfluidic channel. For the calculation of the electric field distribution and the corresponding electroosmotic flow a 2D model was sufficient because the field was

uniform along the channel. The simulation results were used in a *MATLAB* script to calculate the resulting bacteria motion by summing up the pressure driven flow, EOF and the electrophoretic migration at discrete time steps. Simulation parameters were matched to the experimental settings. The zeta potential, $\zeta = -75\,\mathrm{mV}$ of glass with $1\,\mathrm{mM}$ sodium borate was taken from LEE *et al.* [310].

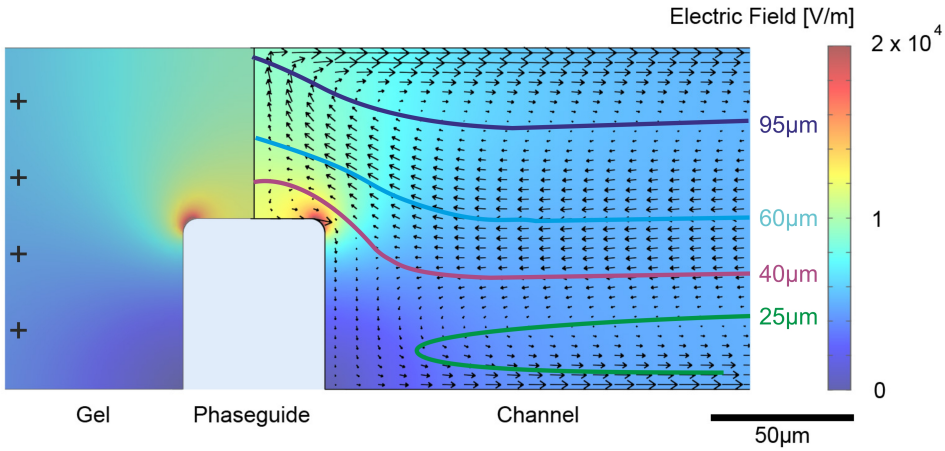

Figure 5.2: Finite element simulations of the concentration process: Cross section at the anodic side of the channel. Surface plot: Electic field distribution. Arrows: Electroosmotic flow. Lines: Trajectories corresponding to Fig. 5.3. Simulation parameters: Electric current I=230 µA, zeta potential $\zeta = -75\,\mathrm{mV}$, medium conductivity $\sigma_{SB} = 250\,\mu\mathrm{S/cm}$

Results of the finite element simulations of the concentration process are shown in Fig. 5.2 and Fig. 5.3. The surface plot in Fig. 5.2 shows the electric field distribution at the anodic gel/channel interface. From a distance of the interface the electric field takes a constant value of $5111\,\mathrm{V/m}$. The arrows indicate direction and velocity of the electroosmotic flow. As it induces a circular bulk flow it is independent of the phaseguide. The performance limiting influence of EOF is illustrated by the trajectories in Fig. 5.3.

Bacteria enter the channel from the left at different vertical starting points. Close to the top and bottom glass surface the electroosmotic velocity outweighs the oppositely directed electrophoretic migration and bacteria are

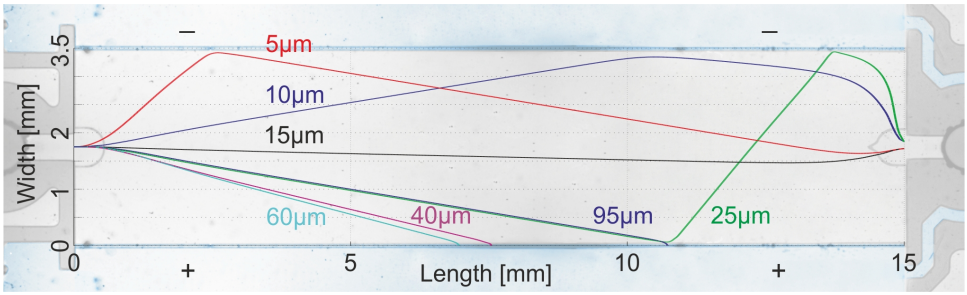

Figure 5.3: Trajectory simulations of bacteria under the influence of EOF at different heights: Close to the glass surface EOF dominates over the electrophoretic force and bacteria are swept out instead of being captured at the gel. Simulation parameters: Flow rate 15 µl/min, electrophoretic mobility $\mu = -2 \cdot 10^{-8}\mathrm{m}^2/\mathrm{Vs}$.

moved towards the cathode. Due to the circular flow they turn around at the gel barrier and migrate towards the anode. However, before being captured at the anode by the electric field these bacteria are swept out of the channel ($h = 5\,\mu$m, $10\,\mu$m, $15\,\mu$m). As EOF is reversed towards the vertical center (Fig. 5.2) both, the electrophoretic force and EOF are directed towards the anode and bacteria are collected at the gel as desired ($h = 40\,\mu$m, $60\,\mu$m, $95\,\mu$m).

When EOF is suppressed by addition of hydroxypropylmethylcellulose (HPMC) all trajectories end at the gel, independent of the height of the phaseguide. These results verify that the electric field of $5111\,\mathrm{V/m}$ is sufficient to capture bacteria at the given flow rate of $15\,\mu$l/min. Upon variation of the flow rate the electric field has to be set accordingly. With the drag force of the flow and the perpendicular electrophoretic force, the capture efficiency follows a linear relationship.

5.2.4 Sample Preparation

Two different strains of *E. coli*, namely *K12* and *XL1-blue* were used as model organisms. *K12* cultures were grown overnight for $14\,$h to $16\,$h in lysogeny browth (LB) medium at $37°$C in a shaking incubator. To receive log-phase bacteria, $5\,\mu$l of the culture were transferred to $5\,$ml of fresh LB medium and incubated for $2.5\,$hours.

For better insight into the concentration and resuspension process green fluorescent bacteria were utilized. *XL1-blue* cells were transformed with pBAD vector harbouring genes for expression of green fluorescent protein

(GFP) and ampicillin resistance. Since GFP expression induced by arabinose takes between 8 and 24 hours it is not possible to receive log-phase fluorescent bacteria. Therefore, the *XL1-blue* cells were grown on LB agar with 0.5% w/w arabinose and 50 µg/ml ampicillin.
The samples were suspended in sodium borate (SB), which is proposed by BRODY and KERN [311] to be a superior electrophoresis medium. Gram-negative bacteria exposed to EDTA show an enhanced membrane leakage giving rise to bacterial death rate [312]. Therefore, SB medium appeared to be more suitable for bacterial concentration experiments. The solution consisted of 1 mM sodium tetraborate. The pH was adjusted to 8.5 by addition of boric acid. The final conductivity was adjusted to $\sigma_{\mathrm{SB}} = 250\,\mu$S/cm. In addition, hydroxypropyl methylcellulose was added in a concentration of 0.1% w/w to effectively suppress electroosmotic flow. Prior to the experiments the bacteria were washed in SB and diluted to a final concentration of about $5 \cdot 10^4$ CFU/ml. This concentration was the minimum to have sufficient bacteria in the waste for enumeration.

5.2.5 Experimental Setup

For fluidic and electrical access the chip was placed into an acrylic holder. The setup was placed on a microscope table to follow the experiments (Fig. 5.4). As part of the construction of a portable system, a miniaturized electroosmotic pump (*Nano Fusion Technologies*) was used in this study. Since the working liquid of the pump had to be deionized water, the sample was introduced into a tube and pumped indirectly through the chip. The concentration experiments were conducted at the maximum flow rate of the electroosmotic pump of 15 µl/min.

To avoid electrolyte exhaustion, the electrode chambers were rinsed with fresh buffer. A constant current was applied to the electrodes to maintain a stable electric field and a constant migration velocity throughout the experiments.
The maximum concentration factor of 61.54 was determined by the used sample volume of 400 µl and the chip volume of 6.5 µl. With the flow rate of 15 µl/min the experiments lasted approximately 27 min.
The drop plate method was used for enumeration because of less time and material needed compared to the spread plate method [313]. The sample reference was plated prior the experiments to avoid overestimation of the concentration factor due to lysis during the experiments. 100 µl of the

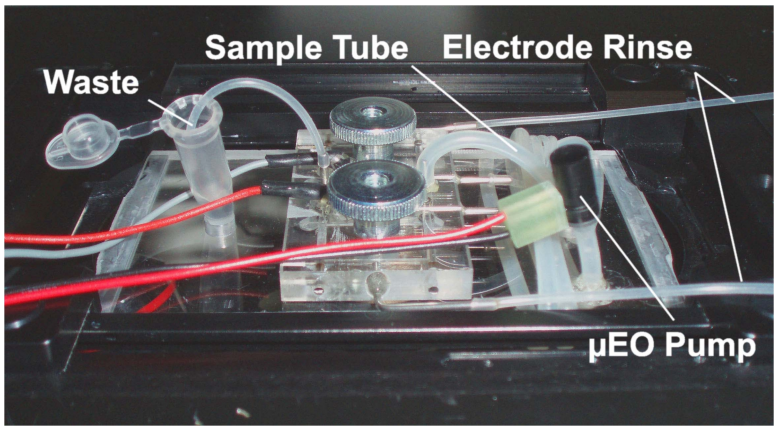

Figure 5.4: Experimental setup: Chip in acrylic holder, sealed by two knurled screws. An electroosmotic pump (*Nano Fusion Technologies*) drives the sample into the chip. The electrode chambers are hydrostatically flushed with medium.

sample (=$\mathrm{Vol_{ref}}$) were 10-fold serially diluted in LB medium and 16 drops of 10 µl of each dilution step were plated for enumeration. After collecting the bacteria at the gel, a negative current was applied to resuspend them to the medium. The chip volume was emptied with a pipette, transferred to 993.5 µl LB, serially diluted and plated. The waste was plated without dilution to receive sufficient colony forming units (CFU). After incubating the agar plates overnight, the CFU were counted and the capture efficiency C, concentration factor f_c, and recovery rate R were calculated as follows:

$$C = 1 - \frac{CFU_\mathrm{waste}}{CFU_\mathrm{ref}} \cdot \frac{Vol_\mathrm{ref}}{Vol_\mathrm{waste}} \tag{5.3a}$$

$$f_\mathrm{c} = \frac{CFU_\mathrm{chip}}{CFU_\mathrm{ref}} \cdot \frac{Vol_\mathrm{ref}}{Vol_\mathrm{chip}} \tag{5.3b}$$

$$R = f_\mathrm{c} \cdot \frac{Vol_\mathrm{chip}}{Vol_\mathrm{sample}}. \tag{5.3c}$$

5.2.6 Results and Discussion

Bacterial viability in the electrophoresis medium was tested by suspending *E. coli XL1-blue* in SB and TBE buffers. The bacteria were plated immediately after suspending as a reference and after 30 min and 60 min at room temperature. Compared to previously used gram positive bacteria,

gram negative *E. coli* are far more sensitive to lysis [301]. Furthermore, Fig. 5.5 shows a significant decrease of viable cells in TBE between 30 min and 60 min, whereas the cell number in SB medium almost remained constant within this time frame. Thus, SB turned out to be the better choice for electrophoresis experiments with gram negative bacteria.

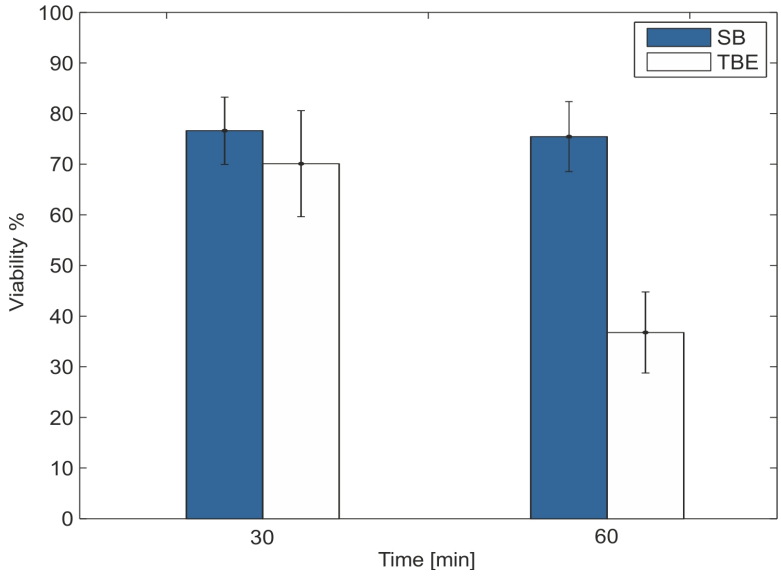

Figure 5.5: Comparison of *E. coli XL1-blue* viability in SB and TBE. The faster decrease of viable, culturable bacteria in TBE confirmed that SB is the favorable medium for electrophoretic experiments. The bars represent mean values of three independent time series.

As shown by the simulation in Fig. 5.3 the influence of electroosmosis decreases the capture efficiency of the device. During experiments without HPMC a part of the bacteria visibly followed the simulated trajectories and were swept out of the channel. Thus, the capture efficiency C according to Eq. 5.3a considerably decreased without the addition of HPMC as a dynamic coating.

The influence of EOF depends on the flow rate and the strength of the electric field. In addition to previous results [301], three concentration experiments of *E. coli XL1-blue* at 15 µl/min without HPMC showed an capture efficiency of $87 \pm 7\%$. In contrast, in experiments with 0.1% HPMC and the same species the efficiency was $98.4 \pm 1\%$ as summarized in Table 5.1. By supressing EOF the earlier found non-linear variations of the capture efficiency [301] could not be observed anymore.

Five independent experiments were conducted with *E. coli XL1-blue* and *E. coli K12*. The details of the concentration experiments are presented in Table 5.1. Capture efficiencies for both strains were around $99\,\%$ with small deviations. Variation of parameters, such as the medium conductivity and the flow rate of the µEO pump gave rise to these deviations. The mean value of recovery R was $81.5 \pm 3.6\%$ for *XL1-blue* with a corresponding concentration factor f_c of 50.2 ± 2.2. Experiments with the *K12* strain showed a mean recovery rate of $77 \pm 2.8\%$ and a 47.4 ± 1.7-fold concentration. All experiments were conducted at a flow rate of 15 µl/min for a time of 26 min 40 s.

Table 5.1: Results of five indepenent concentration experiments for *E. coli XL-1 blue* and *E. coli K12*, respectively.

E. coli XL-1 blue		
Capture Efficiency C	Recovery Rate R	Concentration Factor f_c
98.9 %	77.3 %	47.6
99.3 %	81.1 %	49.9
97.5 %	82.4 %	50.7
99.1 %	87.1 %	53.6
97.1 %	79.7 %	49.05
$98.4 \pm 1\,\%$	$81.5 \pm 3.6\,\%$	50.2 ± 2.2

E. coli K12		
Capture Efficiency C	Recovery Rate R	Concentration Factor f_c
99.6 %	72.2 %	44.4
99.8 %	79.1 %	48.7
99.9 %	77.2 %	47.5
99.4 %	78.9 %	48.5
98.6 %	77.5 %	47.7
$99.5 \pm 0.5\,\%$	$77 \pm 2.8\,\%$	47.4 ± 1.7

The resuspension process is depicted in Fig. 5.6 for the fluorescent *E. coli XL1-blue*. Accumulation of bacteria at the gel barrier at the end of the experiment is shown in Fig. 5.6(a). The recovery rates depended on the number of viable and culturable bacteria in the chip and their adherence to the gel. Excellent visibilty of the fluorescent bacteria enabled to optimize

the resuspension process. A small current of $-50\,\mu A$ to $-100\,\mu A$ applied for 1 min was found to yield optimal resuspension results. Bacterial viability of the initial sample was checked at the end of each experiment. For *E.coli K12* the mean viability after experiments was $89 \pm 5.7\%$. The viability of *Xl1-blue* showed a higher variation ($90.8 \pm 10.7\%$) because growth on agar plates was not as reproducible as growth of log-phase *K12* in LB medium. Comparison of the viability and recovery rates reveals a mean loss of 12% for *K12* and 9.3% for *XL1-blue*. After inversion of the electric field, the bacteria were resuspended to the medium. As seen from Fig. 5.6(b) the loss can be addressed to irreversible adherence of bacteria to the gel. Thus, it can be concluded that the method itself did not affect bacterial viability, which is important to prevent nucleic acids from enzymatic degradation.
For comparison, HALLE *et al.* [299] reported concentration factors of 1.8 for vegetative bacteria and 4.5 for bacterial spores in 9 min 30 s. BALASUBRAMANIAN *et al.* [300] showed the concentration of bacteria with an efficiency up to 99.9% and a maximum concentration factor of 14.2 in 1 h.
In contrast to other concepts, bacteria were captured at the implemented gel barrier. Keeping bacteria away from the electrodes prevents electrode fouling and decreasing capture performance over time. Besides the concentration, subsequent access to the sample is of main importance but often neglected. The controlled release of bacteria from the gel barrier delivers a concentrated sample for further use. Growth based enumeration proved that the presented method keeps bacteria viable and culturable. After recovering the sample, target molecules can be cleared in the previously developed RNA extraction chip. Neither the used gel nor hydroxypropylmethylcellulose inhibit subsequent PCR amplification. [266, 314]

5.2.7 Conclusions

A system for on-chip electrophoretic concentration of pathogens to a small volume, required for microfluidic, PCR-based detection systems has been presented. *E. coli* were continuously collected at an embedded polyacrylamide gel, separating the concentration channel from the electrodes. Thus, bacteria were prevented from exposure to high field strengths and electrolysis products at the electrodes.
In comparison to previous works [298–301] several advances were obtained:

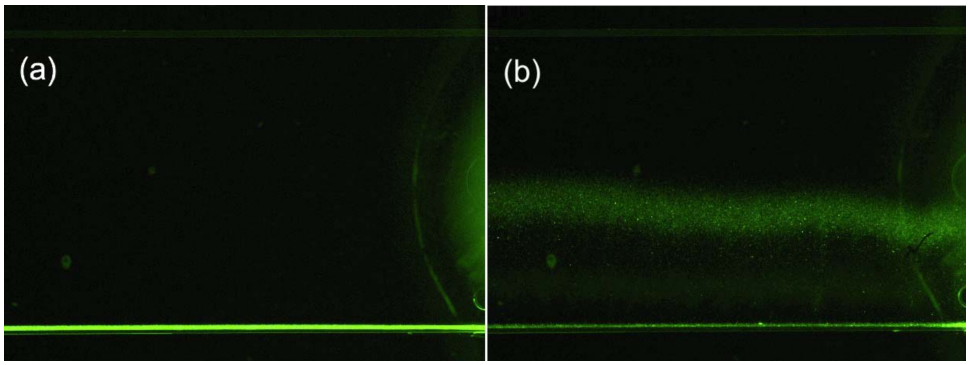

Figure 5.6: Resuspension of fluorescent *E.coli XL1-blue*. (a) Accumulation at the end of the experiment. (b) Application of $-50\,\mu$A for 1 min to detach bacteria.

The small chip volume of $6.5\,\mu$l and the flow rate of $15\,\mu$l/min enabled high concentration factors in less than $27\,$min while maintaining capture efficiencies up to $99\,\%$ by supression of EOF. Recovering viable and culturable bacteria from the chip yielded factors of 50.2 ± 2.2 for *E. coli XL1-blue* and 47.4 ± 1.7 for *E. coli K12*. Phaseguides of half the channel height effectively prevented bubbles from blocking current paths and did away with the elaborate deposition of platinum black. Sodium borate was shown to be the superior medium for the concentration experiments.
The experimental results show the great potential of free flow electrophoresis for the concentration of pathogens. Avoiding resuspension and transfer of the analyte would further increase the concentration factor, and save time and material. Integration of preconcentration, cell lysis, and nucleic acid isolation and analysis on a single device is a promising step towards rapid identification of pathogens.

5.3 Low Cost Bacteria Detection System

In the previous section a powerful method for the concentration of bacteria at the point-of-care was presented. In addition to the discussed molecular detection methods after a concentration step, direct detection of the total amount of bacteria is thinkable. A high bacterial burden or infection creates a pro-inflammatory environment that delays healing as discussed in section 5.1. Analysis of wound swabs have shown that a bioburden of > 37000 bacteria per swab can predict chronic wound infection and

delayed healing [233]. Cultivation on agar plates is the golden standard for bacterial analysis but is laborious and results are not available within 24 hours or more. Rapid bacterial detection methods would help to improve wound treatment and reduce the risk for patients. Fluorescence is the most utilized detection method in biological analysis. However, conventional fluorescence methods include the use of expensive equipment, such as flow cytometers, epifluorescence microscopes or fluorescence spectrometers.
The availability of computing power and excellent cameras in consumer electronic devices, such as mini computers and smartphones, gives the possibility to design smart and readily available diagnostic devices [315]. Herein, the rapid enumeration of bacteria by utilizing a Raspberry pi mini computer in combination with a disposable microfluidic chip is demonstrated. Bacteria are stained and concentrated to a small volume by an electrophoretic force, where they are detected by the simple optical system.

5.3.1 Chip Design and Fabrication

The design of the microfluidic chip is illustrated in Fig. 5.7. It consists of two 100 µm wide fluidic channels, which are separated by a nanoporous hydrogel membrane. Each channel is supplied by a single fluidic reservoir with a partition strip for bubble free filling, as indicated by the white arrow in Fig. 5.7. With this design, different fluid levels, evaporation or tilted placement do not induce a disturbing flow once the reservoirs are filled (5.8a). The sample reservoir can take 100 µl of liquid, avoiding the use of fluidic connections and pumps.

The third inlet is used to introduce a photocurable hydrogel (Fig. 5.8b), which is acting as a nanoporous membrane. At a physiological pH bacterial cells exhibit a negative surface charge and, therefore, experience a force in an electric field. When a DC voltage (U_c) is applied across the two reservoirs, bacteria migrate towards the hydrogel (Fig. 5.7 green arrow) and are collected and concentrated at the gel interface. With the reservoir volume of 100 µl and the detection volume of about 1 nl a theoretical concentration factor of 10^5 is obtained. In contrast to other nanoporous membranes, which are difficult to cointegrate with the fluidic system, the hydrogel membrane has the advantage to keep the chip fabrication very simple.
The microfluidic chips were fabricated on a poly(methyl methacylate) (PMMA) substrate, laser-cut to a format of 76 mm × 26 mm. Channel

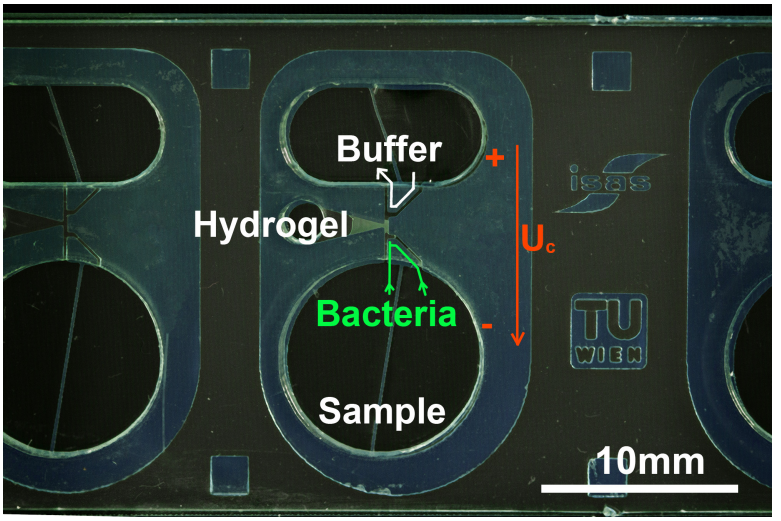

Figure 5.7: Microfluidic electrophoresis chip: Reservoirs for sample and buffer are separated by a hydrogel membrane. By applying a DC voltage between the reservoirs, bacteria are concentrated and detected at the gel barrier. Device masks are shown in Appendix D.

structures were fabricated into an acrylic dry film photoresist (Ordyl SY300, Elga Europe). This technology enables rapid and cost efficient prototyping. A layer of 150 µm dry film resist was laminated on a PMMA slide and structured by standard photolithography.

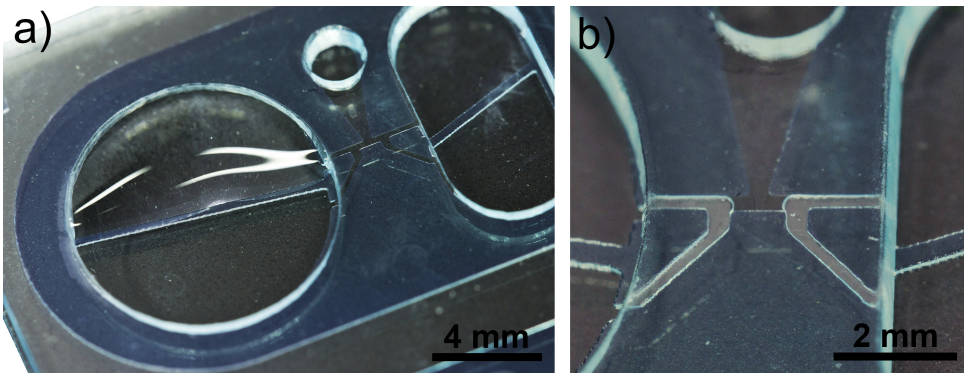

Figure 5.8: Microfluidic electrophoresis chip: a) Partition strip for filling the channels from a single reservoir. b) Injection of hydrogel in the third inlet forms the membrane.

Fluidic access holes and reservoirs were laser-cut into a second PMMA slide. Finally, the two slides were bonded by hot roll lamination. Four individual devices were fabricated on a slide. The nanoporous hydrogel consisted of 20% polyethyleneglycol diacrylate MW 700 (with 1.5% 2-hydroxy-2-methyl-propiophenone as a photo initiator) in sodium borate buffer liquid. 0.4 µl of the gel precursor were injected into the chips and cured by exposure to 365 nm UV light for 30 s.

5.3.2 Setup and Experiments

The buffer liquid for the electrophoretic concentration of bacteria was prepared by 5 mM sodium tetraborate (Sigma Aldrich) adjusted to a pH of 8.5 by adding boric acid. The final conductivity of the buffer was 750 µS/cm.

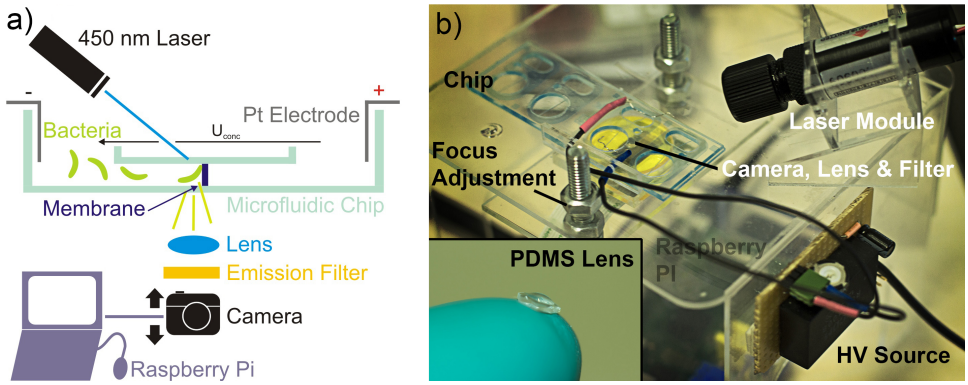

Figure 5.9: Detection system consisting of a Raspberry pi with CMOS camera, equipped with a longpass filter (515 nm) and a PDMS lens. A blue diode laser (450 nm) is used for fluorescent excitation. Concentration voltage U_c = 120 V is provided by a DC high voltage converter.

Samples were prepared from cultures of 6 different *E. coli* strains (Symbioflor 2) and 10 strains of *E. faecalis* (Symbioflor 1). Bacteria were cultivated on agar plates with 1.5% agar and 20 g/l lysogenic broth (Carl Roth). Before the experiments, a culture was taken from the plate, suspended in the electrophoresis buffer and serially diluted. Bacteria were fluorescently labeled with nucleic acid binding dyes. Syto 9 (Invitrogen) (ex 480/em 505) penetrates all bacteria and renders them green fluorescent. For total bacteria enumeration the samples were incubated with a working concentration of 1 µM Syto 9 for 15 min.

The experimental setup is depicted in Fig. 5.9. The chip is placed into the holder and the focus of the camera module adjusted, if required. The electrodes are immersed in the open chip reservoirs, in order to allow release of electrolytically formed gas bubbles. A DC/DC converter (Recom R05-100B) provides the electrophoretic concentration voltage U_c of 120 V. Fluorescence is excited by the 450 nm diode laser (Laser Roithner), which is directly coupled into the chip at a shallow angle. A longpass filter with 515 nm cut-on wavelength is placed above the camera module. The magnifying lens was fabricated by rapidly curing a drop of polydimethylsiloxane (PDMS) on a hotplate at 80°C. Total costs of the setup are summarized in Table 5.2.
An experiment was started by applying the concentration voltage to the reservoirs. The camera was set to take a picture after 5 min for subsequent fluorescence intensity measurements. As a reference, a part of the sample was serially diluted and plated on agar plates for enumeration by the drop plate method [313].

Table 5.2: Approximate costs of the detection system

Raspberry pi + camera module	55 €
Laser module	170 €
Longpass filter	30 €
DC/DC converter	29 €
Power supply	5 €
Housing	5 €
Total	294 €

5.3.3 Results and Discussion

Detection of different concentrations of bacteria is illustrated in Fig. 5.10. As seen in the sequence of Fig. 5.10 a, bacteria were concentrated at the hydrogel, yielding a bright fluorescent signal. Fluorescence intensity increased with colony forming units log(CFU/ml) according to the fitted power function (Fig. 5.10 b). The last point was excluded from the fit, as the intensity was saturating at such high concentrations. Intensities were evaluated after 5 min. In order to increase sensitivity, the experiment time can simply be extended. Selectivity towards other organisms is given by the negative charge of bacteria as well as the fluorescent dye, which especially is staining bacteria but not yeasts.

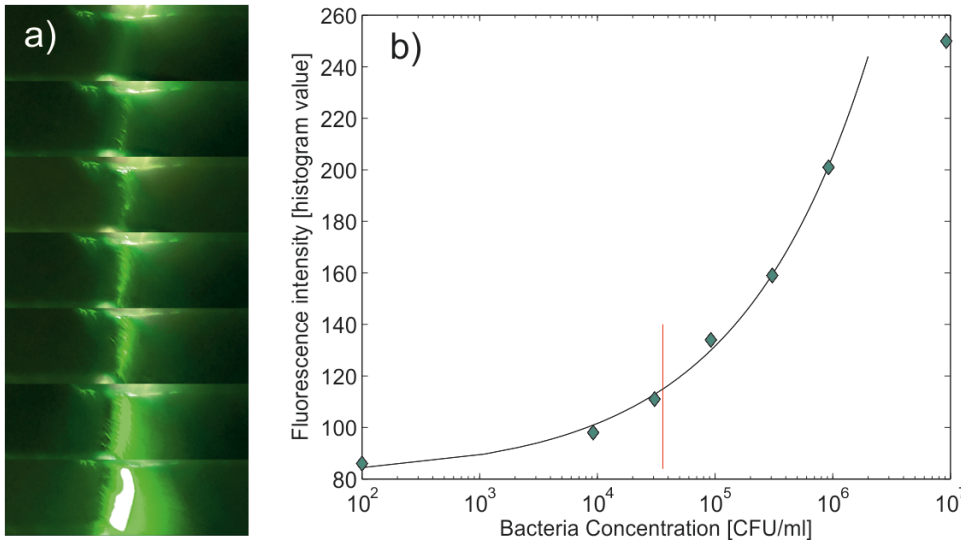

Figure 5.10: a) Enrichment of E.coli bacteria at the gel membrane. The corresponding concentrations are indicated by the red diamonds. b) Fluorescence intensity is plotted over concentration values. The red line marks the critical value of swab-derived bacteria for wound infection. Experiment time: 5 min.

5.3.4 Conclusion

With the presented system the detection of bacteria in a fast and simple manner was demonstrated. The threshold of 37000 bacteria for wound infection diagnostics can be detected within a few minutes. The simple design in combination with a nanoporous hydrogel allows fabrication on a disposable polymer substrate. By rearranging the mechanical setup the principle can also be applied to any other available devices, such as smartphones or tablets. The combination of smart microfluidic systems with widespread consumer electronics can revolutionize common analytical procedures by enabling rapid and simple analysis for many applications in health care diagnostics and environmental monitoring.

5.4 Rapid Bacterial Testing

As discussed in section 5.1, growth based methods are required for antibiotic sensitivity testing of bacteria. As the growth is macroscopically detected, these methods generally are slow. However, microfluidic culturing

techniques are able to overcome these limitations. Cultivating different cell types on microfluidic devices outperforms conventional culture methods in many ways. The major advantage is that the systems in the microscale can provide tightly controlled culture conditions, mimicking the in vivo environment of cells [316]. The possibilities of coculturing multiple cell types while studying their interactions has led to the emerging subfield of organs on chip [317]. In addition, microfabrication technologies enable cointegration of online analysis and manipulation concepts, such as micro electrodes and optoelectronic devices [226, 318–320]. Key issues in microfluidic cell cultures are the need for defined cell seeding, supply of nutrients and gases, as well as keeping the cells in place. Adherently grown cells are either attached to the bottom surface in 2-dimensional cultures or immobilized in 3-dimensional hydrogel structures [137, 321–325]. Cells that are growing in suspension usually are trapped by physical barriers while the culture chamber is perfused with fresh medium [319, 326, 327]. The shear stress induced by the constant fluid flow can have adverse effects on sensitive cells. In addition, small species, such as microorganisms with diameters down to 0.5 µm are difficult to trap. Devices for shear-free cultures make use of dead-end growing chambers with diffusive medium supply from a microfluidic channel. Seeding strategies, including injection through the chip cover [328], high pressure [329], or application of a vacuum [330, 331] can be complex, while harvesting of cells after an experiment is hardly possible.

The majority of microfluidic cell culturing chips are fabricated in PDMS because of its inherent oxygen permeability. [113, 323–325, 332–341]. Some report on partial 3D cell culture patterning by arrays of posts [323–325], requiring delicate injection pressure control [323] and, therefore, preventing wide spread application. At the same time PDMS has several other disadvantages. Due to its hydrophobic nature, difficulties with priming, trapped air bubbles, and adsorption of proteins and dyes can arise. Furthermore, unstable surface properties and leaching of uncrosslinked oligomers have been reported [113, 339, 340]. A variety of surface modification techniques have been developed to overcome those issues but they complicate fabrication and again reduce oxygen permeability [342]. Other device concepts utilize polymeric membranes in hybrid fabricated devices for nutrient [321, 343, 344] and oxygen supply [345].

In chapter 4, a method for maskless microstructuring of hydrogels in a microfluidic chamber for batch mixing in biochemical analysis has been established. In this section, the hydrogel structuring is adopted to fabricate micro culturing chambers in microfluidic chips enabling complete feeding control (gases and liquids) and on-chip analysis. Trapping suspended microorganisms (or cells) inside a closed hydrogel micro chamber yields many advantages in operation:

(i) Leaving cells in suspension while nutrients, antibiotics, and indicator dyes are provided in the gel does not require any sample treatment and offers the potential for self contained and customized bacterial testing.

(ii) Autonomous priming by the hydrophilic nature of the chip does not require external pressure and pumping, an essential benefit to gain acceptance in clinical use.

(iii) During cell growth, oxygen is allowed to diffuse from the air-filled part of the chip through the gel to the micro chambers where the cells are seeded, yielding simple control over normoxia or hypoxia.

(iv) Capturing the suspended growing microorganisms in a permeable gel chamber for subsequent diffusive staining allows for a much simpler fabrication technology because the minimum feature size is not governed by cell size as in conventional trapping devices (e.g. in PDMS). The open space enables safe and simple in-situ drug delivery by reducing operation to only one pipetting step. Only small batches of reagents and short incubation times (by short diffusion lengths) are required while no external pressure is disturbing the culture (e.g. disrupting cellular chains by introduced flow).

(v) The mechanical guiding structures inherently offer the possibility for simple cell seeding and medium supply in continuous cultures by utilizing the difference of two-phase and laminar flow [346].
Antibiotic resistances of pathogenic bacteria have become a major health care problem, threatening the achievements of modern medicine [347]. Cultivation of bacteria on agar plates has been the golden standard for bacterial analysis but the method is laborious and time consuming. CHEN et

al. have shown that the high ratio of (oxygen permeable) surface to volume in microfluidic channels facilitates bacterial growth [341]. Several rapid, microfluidic methods for antibiotic testing have been proposed, including easy to handle devices with colorimetric readout [331, 348], analysis of dielectrophoretic behavior [349], polymerase chain reaction [350] and continuous flow chips with immobilized samples [329, 351–354].

As recently stated by WHITESIDES [196] and CHIN et al. [355] a more general acceptance of microfluidic devices requires simple methodology and handling as well as alternative fabrication methods. Sacrificing oxygen permeability of PDMS-based devices for advantageous handling, priming, and fabrication requires an alternative solution for oxygenation. With the hydrogel oxygenation concept and the extra benefits of on-chip reagent storage and diffusive in-situ analysis of microorganisms in suspension the presented device adds significant value to microbiological analysis.

5.4.1 Device Fabrication and Operation Principle

As previously described in section 3.2, the microfluidic devices were fabricated by hot roll lamination, enabling fast, parallel and cost efficient fabrication. A schematic of the fabrication workflow is shown in Fig. 3.2. Plug-in connectors for polytetrafluoroethylene (PTFE) tubes were made of PDMS, punched through with a needle and bonded over the inlet holes by oxygen plasma treatment.
The function of the device is illustrated in Fig. 5.11. A single chip consists of three functional regions, defined by Laplace pressure barriers (phaseguides) to guide liquid filling. A hydrogel is injected into the chip to define the growth chambers and allow gas diffusion from the outer part of the chip (Fig. 5.11 A). The schematic cross section in Fig. 5.11 B illustrates the principle of the phaseguide structures of 100 µm height and 40 µm width. An advancing liquid is induced to move along the guiding strips by the sudden capillary pressure change at the structures.

Diffusion time of a chemical species scales with the diffusion distance squared. In order to maximize oxygen influx and reduce diffusion time in subsequent cell staining, the distance through the gel to the culture should be minimized. This design input leads to the narrow finger structure, surrounded by a thin gel rim. A minimum width is given by practical aspects, including the maximum resolution and aspect ratio of dry film

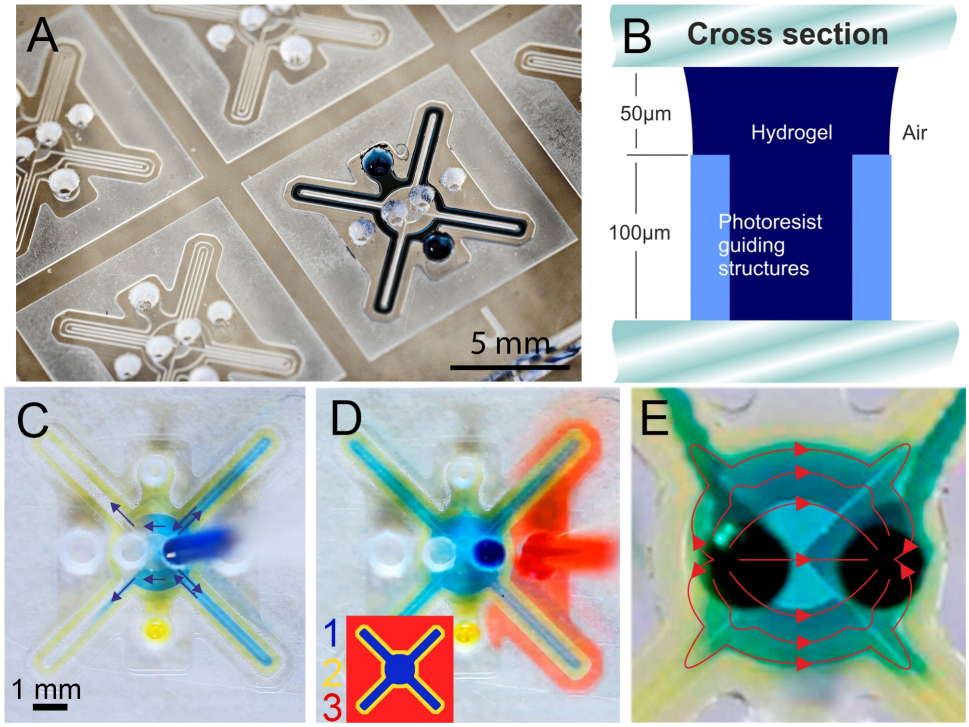

Figure 5.11: Operation principles of the microfluidic cell culture device. A: Photograph of a gel pre-filled chip. The gel (in blue) defines the growth chamber, in which the sample is injected. The outer part remains empty to allow oxygen diffusion through the gel to the culture. B: Cross section of the chip, showing the principle of phaseguides. C: Sample injection with void-free filling of the micro chambers along the phaseguide structures. D: Injection of a chemical reagent (region 3, in red) and diffusion through the gel (yellow, 2) to the culture (blue, 1). E: Continuous operation: Once the device is filled (yellow) a laminar flow is established with diffusive medium supply to the finger structures (blue). Device masks are shown in Appendix D.

laminate, robustness of the guiding effect, and minimum liquid amounts for convenient pipetting. Previously, a value of 60% guiding structure height for robust on-chip patterning of complex gel networks was determined (chapter 4).

Four culture chambers are designed in a symmetric shape with inlet holes in the center of the closed gel structure. The chambers are 250 µm wide and surrounded by another 250 µm of gel. With this design the device contains about 1.6 µl hydrogel and sample.

For static cell cultures the sample is injected into the central region 1 (Fig. 5.11 C) after the chip is prepared with the gel. For in-situ analysis or chemical stimulus after incubation, a reagent is injected in the outer section 3 (Fig. 5.11 D) and allowed to diffuse through the gel into the culture.
In a continuous experiment, at first the sample fills the empty chamber along the guiding structures. Once the chamber is full, the liquid flows in a laminar regime, indicated by the red streamlines in Fig. 5.11 E with negligible flow in the finger structures. This concept allows for cell seeding and medium supply via the same inlet without any additional operation steps.

5.4.2 Chemicals and Experiments

Unless otherwise stated, chemicals were ordered from *Carl Roth* (Germany). The hydrogel was prepared of deionized water with $0.4\,\%$ low melt agarose. In a standard procedure the gel was autoclaved and cooled down to $45\,°$C at which it was kept until injection into the chips. In order to cure the gel, the chips were cooled down to $4\,°$C.
For the glucose assay, L+ glucose was added to the gel precursor in a concentration of $250\,$mM. The sample, which was subsequently injected into the gel-prepared chip, consisted of glucose oxidase ($500\,$U/ml, *Sigma Aldrich*), horseradish peroxidase ($100\,$U/ml) and potassium iodide ($50\,$mM).
For bacterial testing the gel was prepared with $20\,$mg/ml lysogenic broth (LB). Gram negative *E. coli* (HB 101), *B. amyloliquefaciens* (FZB42) and gram positive *E. faecalis* (DSM 16440) were cultivated on LB agar plates. Samples were prepared by diluting a colony in $10\,$mM phosphate buffered saline (PBS). For enumeration, serial dilutions were plated according to the drop based method [313].
Stock solutions of ampicillin and gentamicin antibiotics were prepared in concentrations of $5\,$mg/ml, $500\,$µg/ml and $50\,$µg/ml for minimal inhibitory concentration experiments. Aliquotes were added to vials of $1\,$ml gel at $45\,°$C to give the final antibiotic concentrations in a range from 0 to $128\,$µg/l. About 1.8 µl of gel were injected into each chip, the whole device was sealed with tape and stored at $4\,°$C.
Bacterial samples were injected into the chips with different antibiotic concentrations and subsequently incubated at $35\,°$C in normal air for $3\,$hours. After incubation, the cell permeable nucleic acid stain Syto-9 ($10\,$µM, *Invitrogen*) and gram positive specific hexidium iodide ($10\,$µM, *Invitrogen*) in DI water were added to the outer part of the chip and

incubated for 15 min. Images were taken with a fluorescence microscope (Ex 470/30, Dm 495, Em 530 LP) with a mounted Nikon D5100 camera. Image analysis was performed in *Image J* to quantify bacterial growth (see Appendix C for details).
For colorimetric readout of bacterial growth, 20 mg/ml lactose (*Sigma Aldrich*) and 2 mg/ml bromcresol purple were added to the gel precursor.
For the demonstration of enzyme assays a fluorescent substrate (DQ Gelatin, Invitrogen) was used to determine the presence of bacterial gelatinase. For analysis, the substrate (100 µg/ml in Tris HCl buffer) was injected in chip region 3 after bacterial growth and incubated. Readings were performed after 15 min.
Reference susceptibility testing was performed, using the disk diffusion method according to the standards of the Clinical and Laboratory Standards Institute [356]. Agar plates were prepared with unsupplemented Mueller Hinton agar. Bacteria suspensions were adjusted to 10^8 CFU/ml (0.5 McFarland standard). Agar plates were inoculated by evenly spreading bacteria with a swab. 6 mm filter discs, loaded with 10 µg antibiotic were placed on the agar plate. Incubation time was 16 to 18 hours. The zone of inhibition was measured as visible by the unaided eye.
S. cerevisiae was obtained as a fresh package (*Hagold*) and directly suspended in PBS prior to the experiments. Continuous flow of 50 mg/ml YPD medium was provided by a syringe pump at 1 µl/min. Cells were cultured at room temperature, followed by time lapse photography on a microscope. Fluorescent live/dead staining was performed at the end of the experiment by adding 10 µM propidium iodide and 20 µM Syto 9.

5.4.3 Results and Discussion

Previously utilized photoinitiated hydrogels were evaluated for use in this study. Polyethylene glycol diacrylate, polyethylene glycol dimethacrylate, and hyaluron acid vinyl ester [124] were investigated. Due to oxygen inhibition of the radical polymerization in the small structures, complete polymerization was only possible in a nitrogen environment, complicating the gel structuring. On the other hand, incomplete polymerized gels showed to be a major reason for decreased biocompatibility as acrylate monomers are toxic to bacteria, resulting in reduced growth. While sufficiently cured gels did show good biocompatibility, these gels posed another severe drawback by activating the fluorescent DNA dyes, making

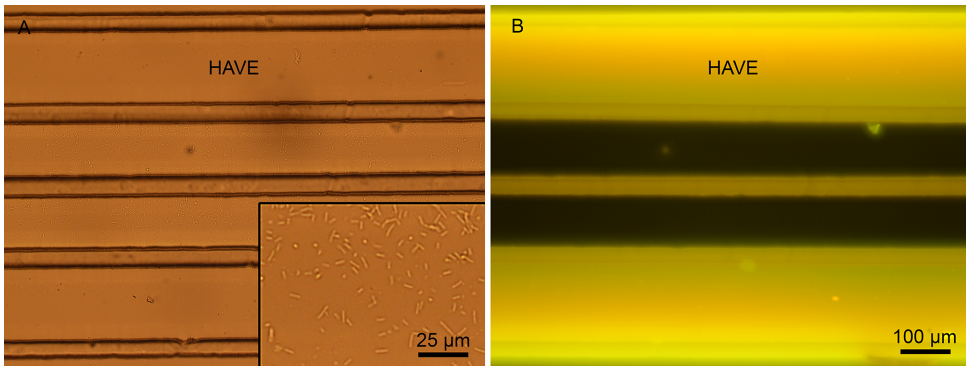

Figure 5.12: Growth of *E. coli* in hyaluronic acid vinyl ester (HAVE) hydrogel chamber. Although bacteria showed excellent growth, DNA fluorescent dyes were activated by the gel itself, making in-situ staining impossible.

in-situ staining impossible (5.12). Therefore, use of low melt agarose gels was an advantageous alternative as the gelling temperature allowed handling with pipettes and chips at room temperature. Gels were prepared in analogy to conventional petri dishes with the gel chamber fabrication in only one pipetting step with subsequent cooling. The fabricated device showed excellent autonomous priming and robust guiding. Because of the thin finger structure diffusion of a subsequently added drug was completed within few minutes.

5.4.3.1 Oxygen Supply

The chosen chip dimensions are governed by the trade-off between diffusion time and reliable filling. Oxygen diffusion from the empty part of a growth chip towards the cell culture was calculated in a finite element simulation in *Comsol Multiphysiscs 4.4* (Fig. 5.13 A). With a diffusion coefficient of molecular oxygen in agar [357] of $2.36 \cdot 10^{-9}\,\mathrm{m^2/s}$, the concentration in the culture chamber is over 90% of that in the surrounding air within 2 min. An oxygen dependent glucose oxydase enzyme reaction was used to visualize the oxygen influx through the gel (Fig. 5.13 B). According to the following equation [358], glucose oxidase catalyzes the oxidation of glucose to hydrogen peroxide. Further, horseradish peroxidase catalyzes the reaction of hydrogen peroxide with potassium iodide to brown iodine:

$$\mathrm{Glucose} + \mathrm{O_2} + \mathrm{H_2O} \xrightarrow{\text{Glucose Oxidase}} \mathrm{Gluconic\ Acid} + \mathrm{H_2O_2}$$

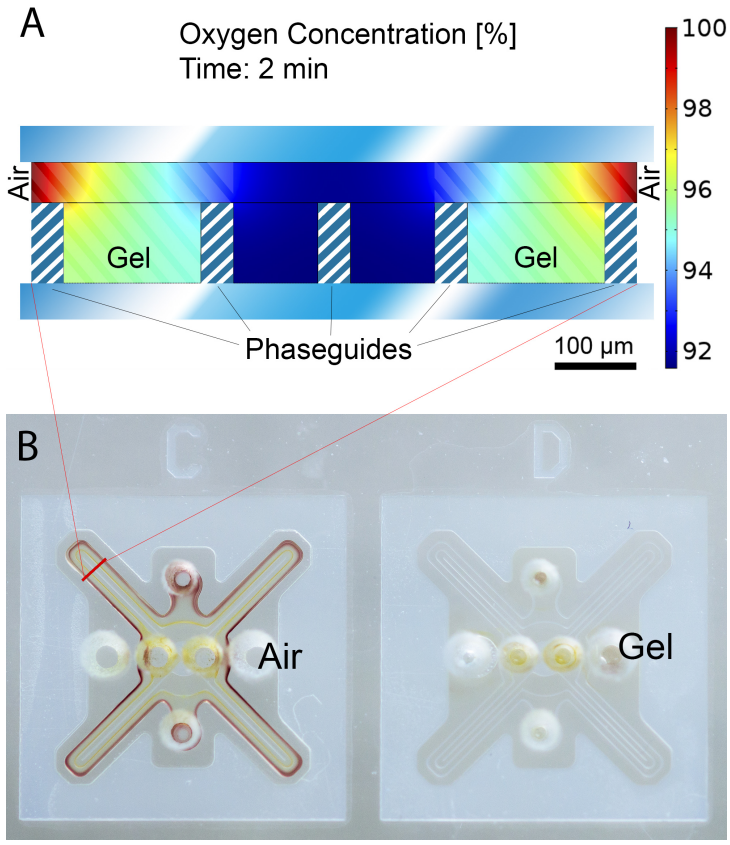

Figure 5.13: Illustration of oxygen supply. A: Finite element simulation *(Comsol Multiphysics 4.4)* of oxygen diffusion through the gel. Within 2 min the oxygen concentration in the center is 92 % of the concentration in air. B: Visualization of oxygen influx through the gel by a glucose assay. In chip C the outer part was left empty to allow ambient oxygen to diffuse into the gel while in chip D it was also filled with the glucose gel. The absence of ambient oxygen in D inhibited the enzymatic color reaction.

$$H_2O_2 + \text{Potassium Iodide} \xrightarrow{\text{HRP}} \text{Iodine} + H_2O$$

The devices were prepared with a glucose containing gel and the enzyme mix was introduced into the gel well. While in device C of Fig. 5.13B the region 3 remained empty, it was filled up in device D to remove ambient

oxygen. As seen from the color difference in both devices, there was no reaction taking place in the finger structures of device D due to the absence of ambient oxygen. To show the influence of ambient oxygen on bacteria, aerobic Gram positive *B. amyloliquefaciens* were cultured in two chambers in an analogous configuration. The comparison of bacterial growth after 10 hours in an aerobic and anaerobic chamber is shown in Fig. 5.14. For the anaerobic growth condition the chip region 3 in Fig. 5.14A was filled with culture medium. At the end, the medium was removed and both cultures were stained. This experiment confirms the simple and effective possibility to control aerobic and anaerobic growth conditions.

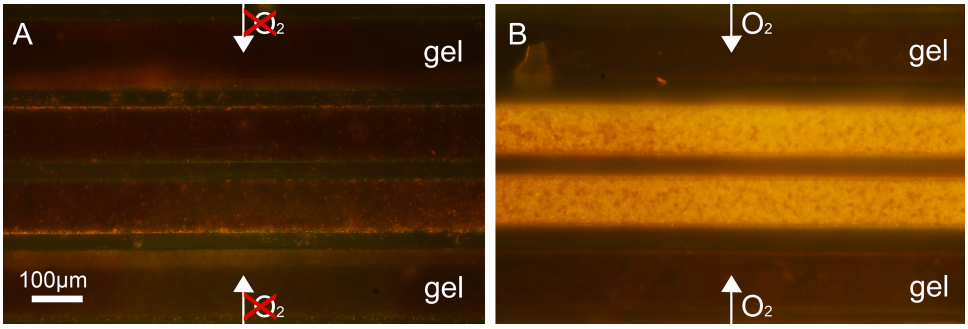

Figure 5.14: Cultivation of aerobic growing *B. amyloliquefaciens*. A: Ambient oxygen was removed from device by filling region 3 with culture medium. B: Oxygen was allowed to diffuse to the culture from the open space.

5.4.3.2 Bacterial Analysis

The simplest way to verify bacterial growth in a microfluidic chip is the application of a colorimetric change. Lactose fermenting bacteria, such as *E. coli* produce an acid which induces a color change of a present pH indicator dye. A yellow color shift of bromophenol purple by a growing *E. coli* culture is shown in Fig. 5.15. However, a major disadvantage of the colorimetric readout is the dependence on the initial bacteria concentration, which results in a time dependence to grow a large enough colony that induces the color reaction. As a consequence, colorimetric devices are usually incubated over night to get a definite answer [331, 348]. For this reason, all further experiments were done with in-situ fluorescent staining of bacterial samples.

Figure 5.15: Colorimetric assay of lactose fermenting bacteria. Serial dilutions of *E. coli* were incubated to show the impact of the initial concentration on the assay. Image was taken after 5 hours incubation time. Initial sample concentrations: H: $2.5 \cdot 10^7$ Colony forming units (CFU) per ml. I: $2.5 \cdot 10^6$ CFU/ml. J: $2.5 \cdot 10^5$ CFU/ml. Only for the highest concentration a definite prove of growth was present.

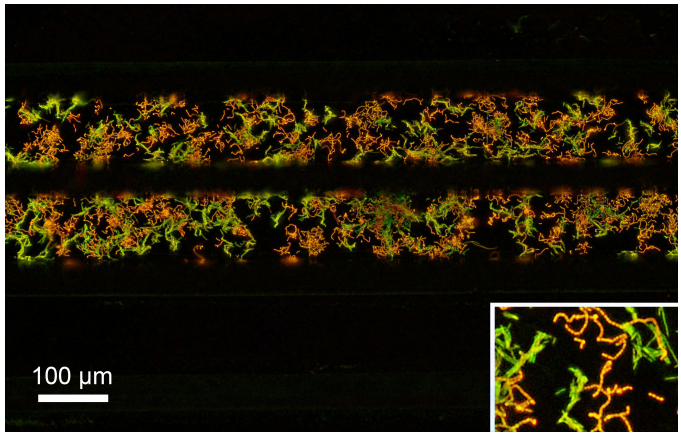

Figure 5.16: Simultaeous growth of Gram positive *E. faecalis* (orange) and Gram negative *E. coli* (green). Staining with cell permeable Syto 9 and Gram positive specific hexidium iodide. In the inset the different phenotypes (cocci and rods) are well visible.

Microfluidic devices are well suited for fluorescent readout because the low channel height minimizes common medium autofluorescence and fits to the focus depth of a microscope. In addition, the structure of the presented chips allows for convenient in-situ staining after an experiment.

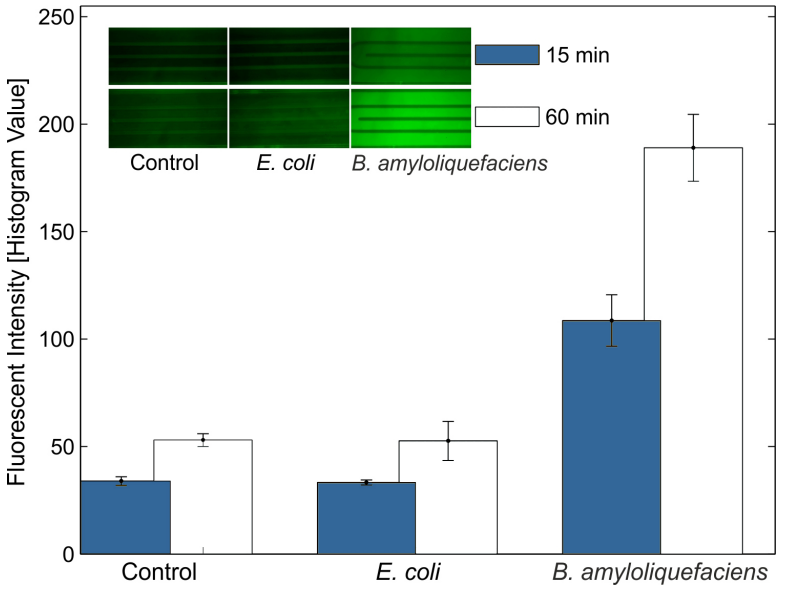

Figure 5.17: Proof of enzyme expression of a bacterial culture in the chip. In contrast to a control chip without bacteria and an *E. coli* culture *B. amyloliquefaciens* express gelatinase, which can be detected by the fluorescent substrate within minutes.

Differential staining with Syto 9 and hexidium iodide not only yields the number of bacteria and their phenotype but also shows the Gram type in mixed cultures [359], altogether valuable information for analysis of clinical samples. Fig. 5.16 illustrates the simultaneous cultivation of Gram positive *E. faecalis*, which appear as orange cocci and Gram negative *E. coli* as green rods. In addition to the direct staining methods, enzymatic assays for bacteria identification can be performed in the chip. A bacterial gelatinase test is presented in Fig. 5.17. In contrast to *E. coli*, *B. amyloliquefaciens* cultures produce gelatinase that cleaves the injected substrate to yield high fluorescence. In clinical application a gelatinase test is used to differentiate pathogenic *S. aureus* from nonpathogenic *S. epidermis* and can take up to several days. [97]

As a reference for antibiotic susceptibility experiments, the used bacteria strains were tested by the standardized disk diffusion method. Interpretive reference values for inhibition zones and minimal inhibitory concentrations (MIC) are given in Appendix B. Growth inhibition zones

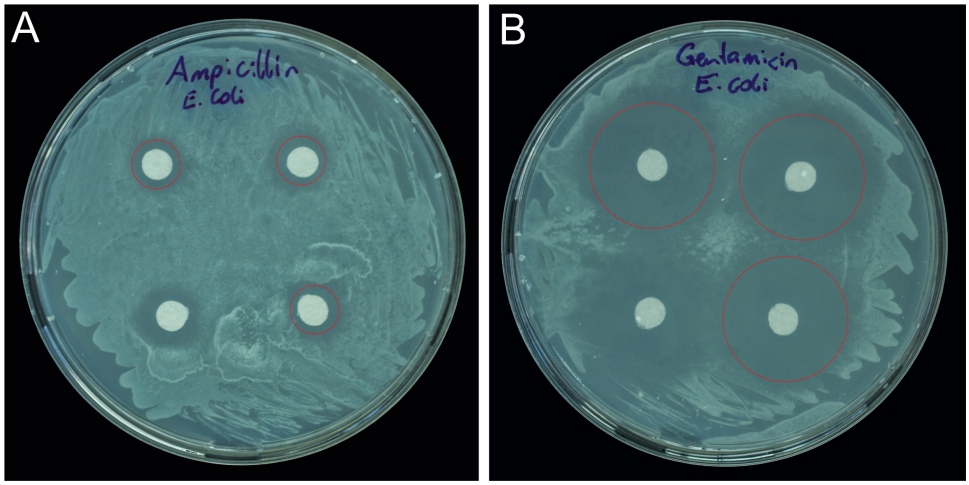

Figure 5.18: Disk diffusion antibiotic susceptibility testing of *E. coli* (HB 101). A: Ampicillin with 10 mm inhibition zone. B: Gentamicin with 25 mm inhibition zone.

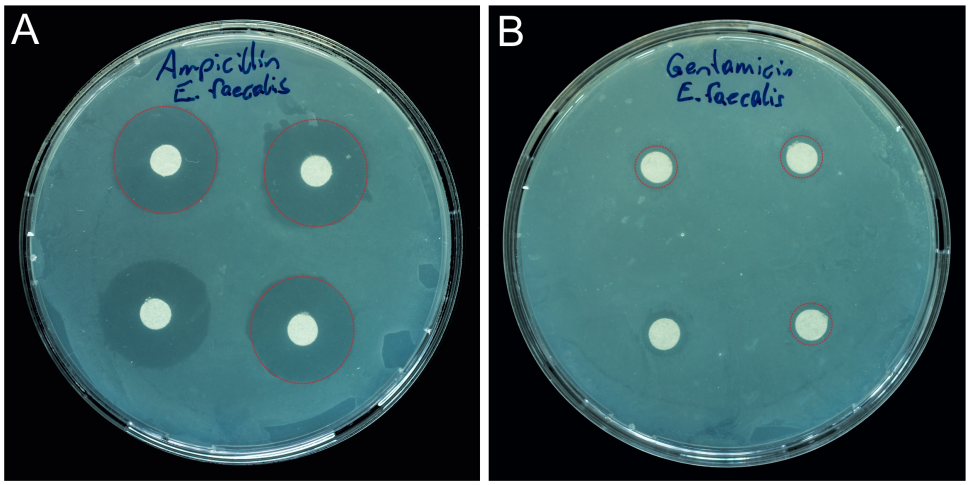

Figure 5.19: Disk diffusion antibiotic susceptibility testing of *E. faecalis* (DSM 16440). A: Ampicillin with 21 mm inhibition zone. B: Gentamicin with 8.5 mm inhibition zone.

around the filter discs are clearly visible in the images of the agar plates in Fig. 5.18 for *E. coli* and Fig. 5.19 for *E. faecalis*.

Table 5.3: Summary of antibiotic susceptibility results of the two tested strains.

	Ampicillin	**Gentamicin**
E. coli (HB 101)	**R** MIC $\geq$32 μg/ml	**S** MIC $\leq$4 μg/ml
E.faecalis (DSM 16440)	**S** MIC $\leq$8 μg/ml	**R** NA

Results of the tested strains are summarized in Table 5.3. *E. coli* showed to be resistant against Ampicillin with a minimal inhibitory concentration (MIC) $\geq$ 32 µg/ml while susceptible to Gentamicin. On the other hand *E. faecalis* was susceptible to Ampicillin and resistant to Gentamicin, as to all aminoglycosides [356].

For antibiotic susceptibility tests, bacteria samples were introduced in 7 cultivation chambers that were prepared with antibiotic concentrations from 0 to 128 µg/ml. A control value of injected bacteria was recorded before incubation. Results of the experiments are summarized in Fig. 5.20 for *E. coli* and Fig. 5.21 for *E. faecalis*. Comparing efficacy of antibiotics for each strain reveals that the rapid microfluidic method robustly determines susceptibility with MIC concentrations in accordance with the standard reference methods. As seen from the inset in Fig. 5.20A *E. coli* growth was not inhibited at low Ampicillin concentrations but rather the bacteria grew in long chains. This chain formation has been associated with defense mechanisms against antibiotics, limiting their bactericidal effects [360]. The fast and dramatic response to culture conditions in the microenvironment is remarkable.

5.4.3.3 Continuous Culturing

In addition to static cultures the same device can be used for long-term culturing of suspended cells with continuous supply of fresh medium. The continuous configuration was tested by culturing *S. cerevisiae*. A tube with continuous medium supply by a syringe pump was attached to the inlet. A small number of cells were seeded into the device (Fig. 5.22A) with the first few microliters, filling the chip. Once a laminar flow was established, fresh medium flowed by the finger structures, supplying the cells by diffusion, as shown in Fig. 5.11 E. Without any additional steps the cells were seeded and supplied with medium via the same inlet.

By the constant supply of fresh medium and removal of produced gas, the culture was able to grow to a very high concentration (Fig. 5.22C). After the experiment, viability was verified in-situ by fluorescent live/dead staining. Only a low number of dead cells were stained by propidium iodide as seen in Fig. 5.22C, revealing remarkably high viability. The possibility to expose the culture to chemicals without disrupting the continuous experiment yields many possibilities for drug testing experiments.

5.4.3.4 Conclusions

Microfluidic cell culturing techniques have made a tremendous progress in the recent years and led to a entirely new field of research. With the presented design we overcome a number of critical issues in the culturing of suspended cells, including autonomous priming, sample preparation, capturing microorganisms - fabrication resolution, in-situ drug delivery, nutrients supply and oxygen control.
The in-situ polymerized hydrogel adds an enormous degree of freedom to fabrication and handling of on-chip cell cultures. For further analysis, enzyme assays can be run on the culturing device, just by one additional pipetting step. Culture medium agar for chip injection can be prepared by microbiologists just as conventional petri dishes with various nutrients and drugs. Devices that are prepared in advance constitute a sample-in/answer-out system for the end user. With fourteen culture chambers on a convenient microscope format, parallel testing with a minimum of samples and reagents can be performed. Phaseguide assisted seeding and subsequent diffusive medium supply, enables shear-free cell cultures with the least possible complexity.

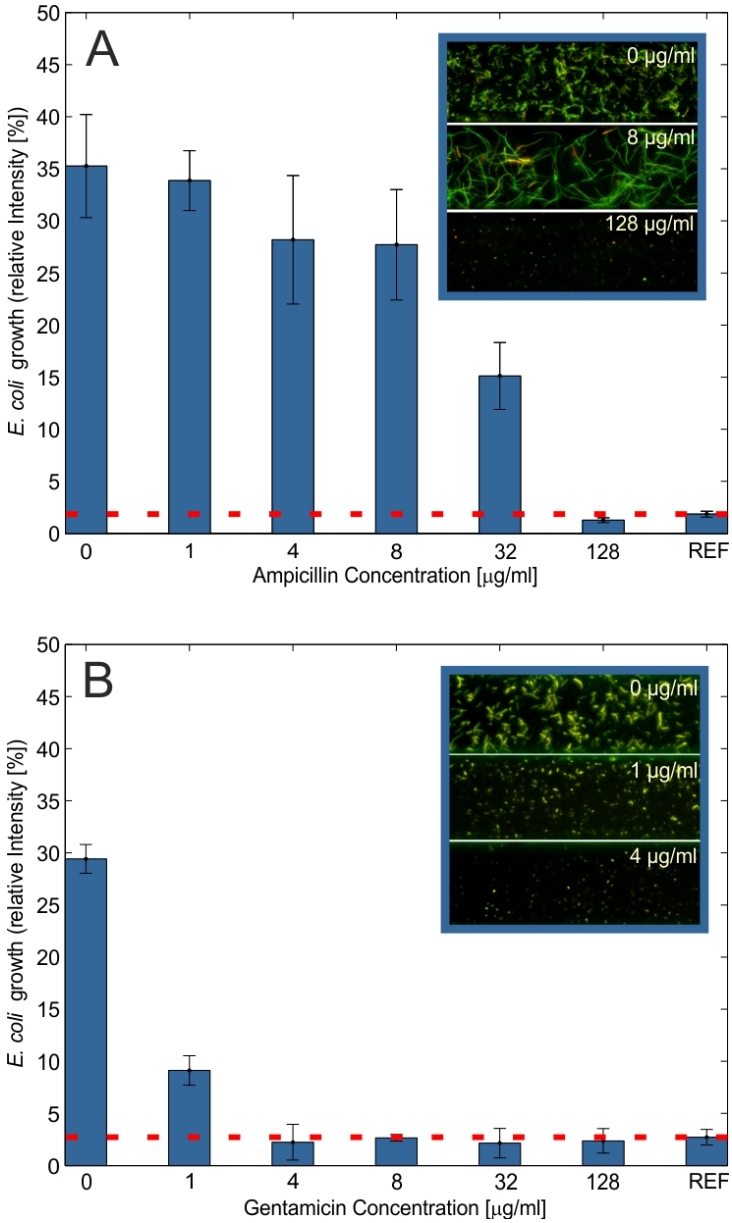

Figure 5.20: Antibiotic testing of *E. coli*, incubated with varying concentrations of antibiotics. Bars represent mean growth values of 4 culture wells. Reference values were recorded before incubation. A: *E. coli* showed to be resistant against *Ampicillin*. The inset shows formation of long chains as a defense mechanism, limiting antibiotic efficiency. B: Gentamicin effectively inhibited *E. coli* growth at all concentrations > 1 µg/ml.

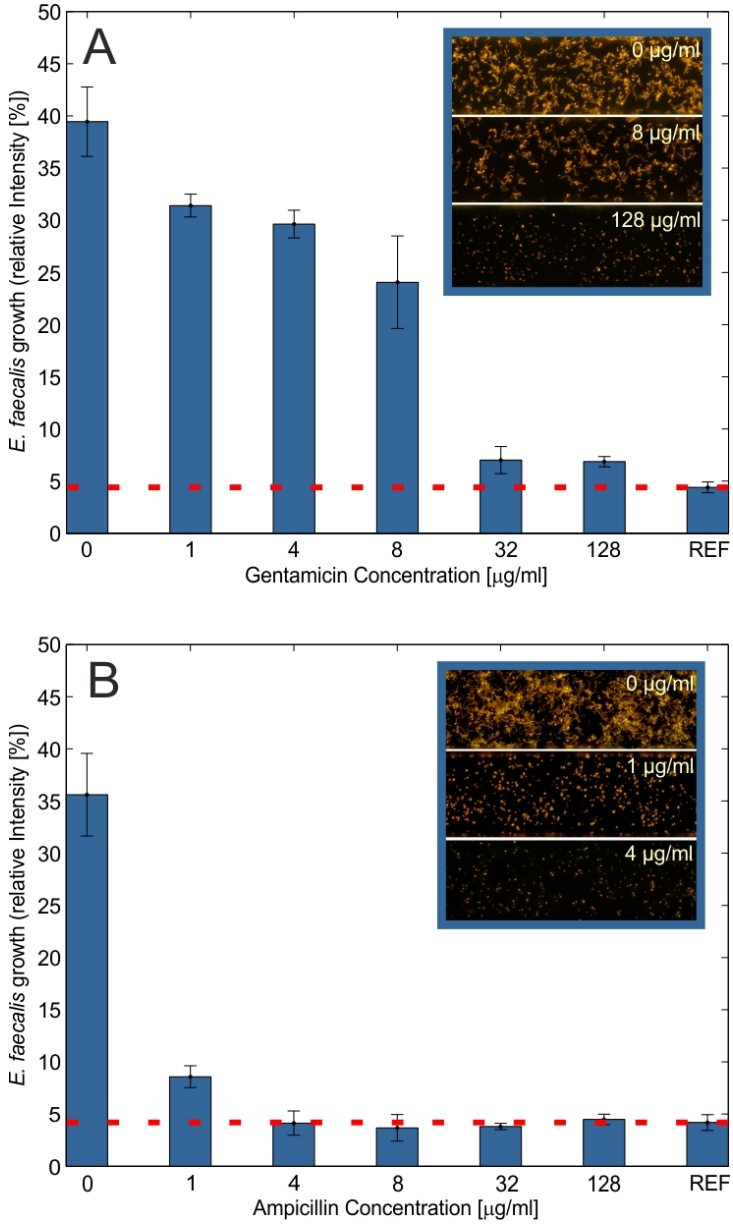

Figure 5.21: Antibiotic testing of *E. faecalis*, incubated with varying concentrations of antibiotics. Bars represent mean growth values of 4 culture wells. A: Inhibition of *E. faecalis* growth by Ampicillin $> 1\,\mu g/ml$. B: *E. faecalis* resistance against Gentamicin at all concentrations.

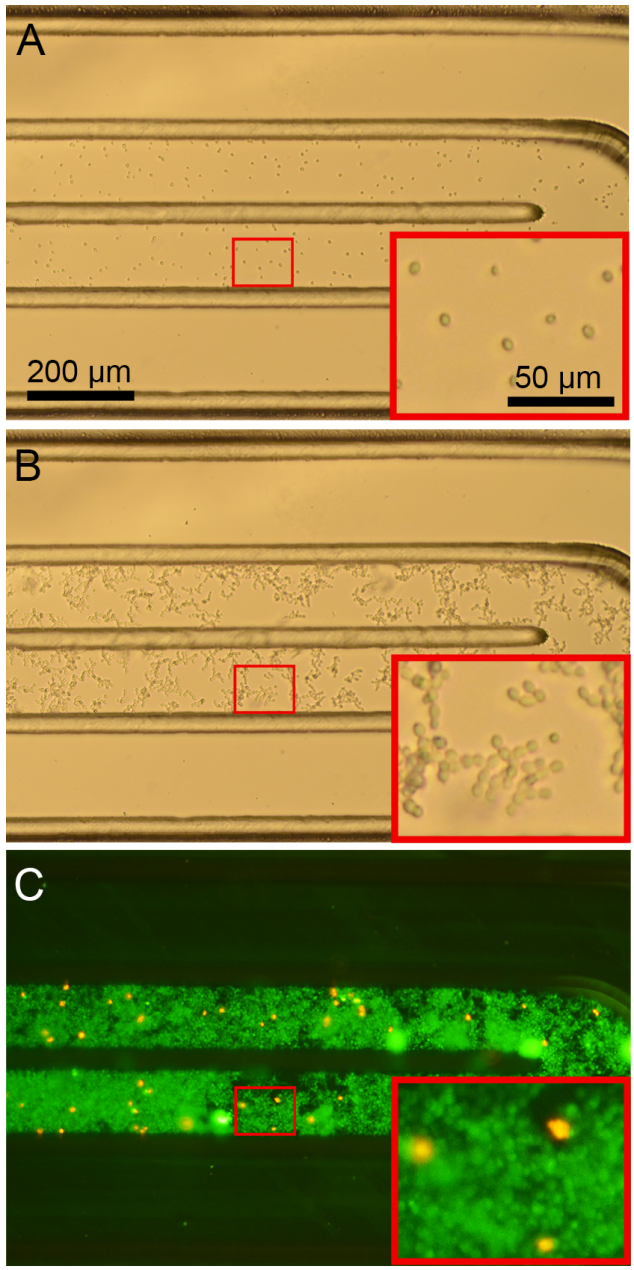

Figure 5.22: Continuous culturing of *S. cerevisiae* cells. A: Seeding of a small number of cell into the chip. B: The culture 10 hours after experiment start. C: High cell concentration after 20 hours of cultivation without loosing viability. Medium flow rate 0.5 µl/min.

Chapter 6
Conclusions and Outlook

The development of different methods and approaches towards an objective wound assessment has been the focus of this research. As discussed in the literature review sections (1, 2.1, 4.1 and 5.1) wounds can show very different characteristics depending on their etiology, including surgical incisions, burns, arterial and venous diseases, diabetes and bedsores. The many different reasons for the development of chronic or impaired healing wounds call for a personalized, patient-centered wound care. Or, as put another way by SIBBALD *et al.* [15],

Treatment of the whole patient before the hole in the patient

is required. Driven by the implications for the world wide health care systems, optimal treatment of non-healing wounds, infections and drug resistant bacteria have moved in the focus of clinical practice and research. While the treatment of chronic wounds accounts for a substantial part of the health care budget [361], the spread of antibiotic resistances put the developments of modern medicine at risk [347]. These challenges in clinical care, require a deeper understanding of the involved factors and, therefore, call for novel diagnostic approaches. In order to gather useful information about the wound-to-treat many different approaches have been followed and wound research has become a multidisciplinary research field.

The research conducted in this thesis summarizes the main aspects of wound healing and presents monitoring approaches by means of physical (Chapter 2), biochemical (Chapter 4) and microbiological methods (Chapter 5). Despite the different approaches and origin of analytes, they interfere with each other in the complex wound environment. As an example, the pH value directly affects the activity of enzymes within wound. On the other hand, the present microbes produce a certain microenvironment of pH and extracellular proteins and enzymes. Thus, in their collective the presented methods could help to generate a detailed picture of each wound type. The aim of the developments has been to provide tools for rapid and

simple analysis at the point of care. Complexity of analysis and the related time and costs have prevented wound analysis from general application in clinical care or even in larger clinical studies. Because of the variation among wounds, longitudinal measurements are considered to be superior over single point measurements. With the results a practitioner should be able to determine the progress of healing to assess treatment or be warned of adverse developments.

Temperature, pH value, moisture, and optical tissue properties have shown to give a vital set of parameters that can be integrated into a single miniaturized sensing device and simultaneously determined in the wound bed. A proof of concept was demonstrated by experiments in a porcine wound healing model. Further sensor optimization and clinical studies in human wounds should be the first steps in further developments of integrated wound sensing.

In-situ hydrogel polymerization was presented as a powerful tool in the development of biochemical analytic devices. A microfluidic platform for the implementation of parallel assays has been designed, fabricated, and successfully tested with measurements of enzyme activity, protein concentration, and white blood cell concentration. Design and fabrication of a hand-held readout instrument and clinical tests are tasks to be performed in the future. Delivery of a standard device with a customizable polymerization kit could pave the way for novel tools in biological research.

Handling living cells and microorganisms on microfluidic chips is an exciting field of research with manifold manipulation possibilities that otherwise would not be thinkable or extremely complex. Herein, novel concepts for especially detecting and analyzing bacteria are introduced. Increasing analytic efficiency and reducing the requirement of bulk equipment has driven these efforts.

Within the last years the understanding of impaired healing considerably has improved with new approaches, such as the investigation of biofilms. Some aspects still are controversially discussed among the medical experts for their implications in chronic wounds. However, awareness of a global problem and the need for further research in all aspects of chronic wounds including fundamental healing processes, therapy and diagnostics has dramatically increased.

Depending on the type of analysis, the method of sampling has a huge impact on the results. In order to receive comparable results in research, standardized sampling techniques are required [362]. While for bacterial

analyses the Levine swab has become the preferred technique [2, 233, 242, 254–256], for biochemical POC analysis wound fluid absorption on filter paper appears to be the most suitable method [158, 179, 363]. By applying these standards, accurate evaluation of a set of parameters and introduction in clinical routine could be imagined [362]. The results in this thesis demonstrate that sensor technology can be a key enabling factor in this process to gain further understanding of chronic wound healing and eventually improve treatment procedures.

Appendix A

Wound Sensor Controller Schematic

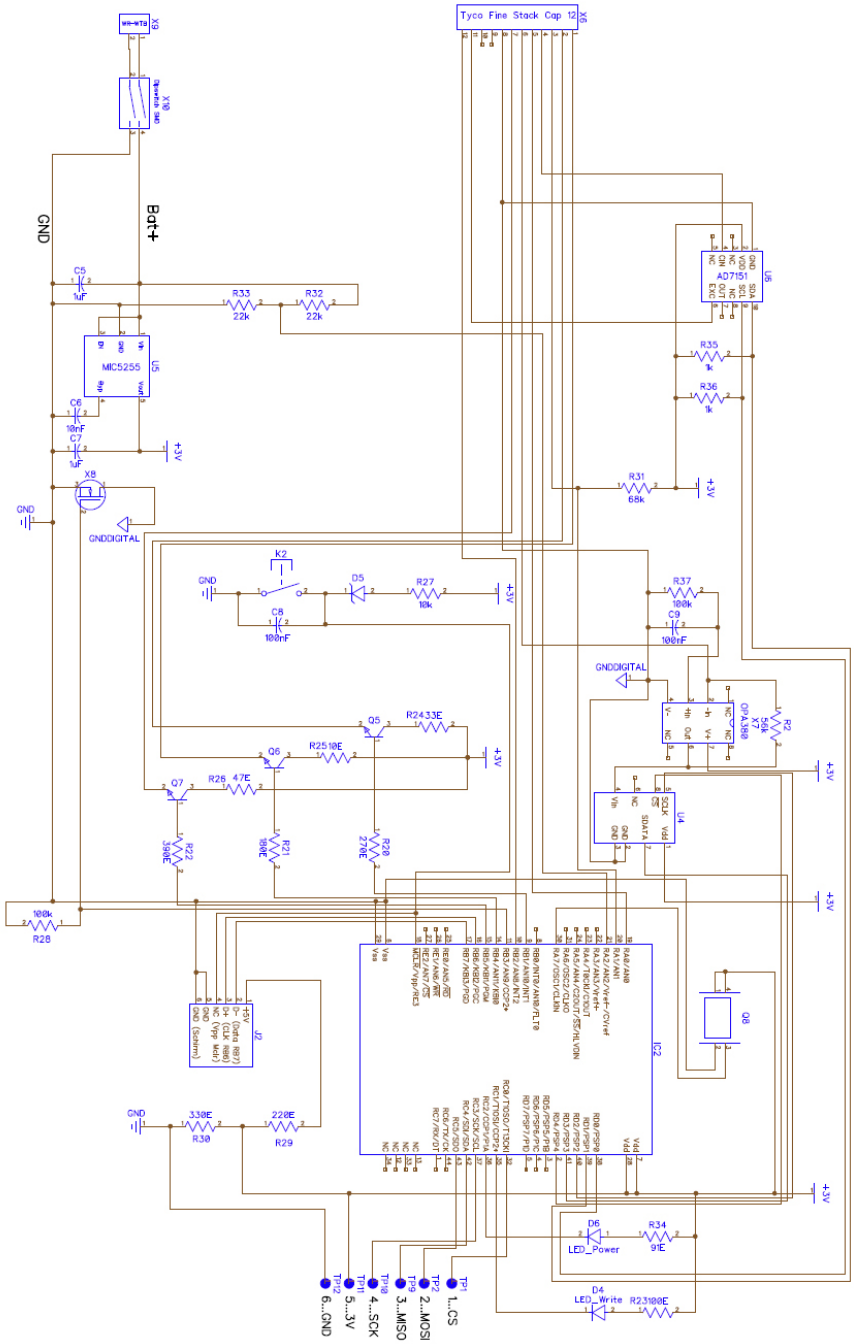

Figure A.1: Schematic of the microcontroller circuit.

Appendix B
Antibiotic Reference Testing

Table B.1: Interpretation of inhibition zone values of the disk diffusion test and corresponding minimal inhibitory concentration (MIC). Diameters are given for **S**usceptible, **I**ntermediate and **R**esistant characterization [356].

E. coli (Enterobacteriaceae)

		Diameter (mm)			**MIC** (µg/ml)		
Antimicrobial Agent	**Amount**	**S**	**I**	**R**	**S**	**I**	**R**
Ampicillin	10 µg	≥17	14-16	≤13	≤8	16	≥32
Gentamicin	10 µg	≥15	13-14	≤12	≤4	8	≥16

E. faecalis (Enterococcus)

		Diameter (mm)			**MIC** (µg/ml)		
Antimicrobial Agent	**Amount**	**S**	**I**	**R**	**S**	**I**	**R**
Ampicillin	10 µg	≥17	-	≤16	≤8	-	≥16
Gentamicin		isolates should not be reported as susceptible					

Appendix C

Fluorescent Image Analysis

Fluorescent images are analyzed in Image J. Area fraction of bacteria in the image is an appropriate measure because individual counts are prone to underestimate growth at high concentrations and clustering. After splitting channels and subtracting background a threshold for black&white is applied. The relative area of bacteria is measured.

Image J macro:

```
dir=getDirectory("Choose a Directory");print(dir);

resDir=dir + "\Result\\";

print(resDir);
File.makeDirectory(resDir);
list = getFileList(dir);

run("Set Measurements...", "
area_fraction display redirect=None decimal=3");

for (i=0; i<list.length; i++) {
 if (endsWith(list[i], ".jpg")){
 print(i + ": " + dir+list[i]);
 open(dir+list[i]);
 imgName=getTitle();
 baseNameEnd=indexOf(imgName, ".jpg");
 baseName=substring(imgName, 0, baseNameEnd);

 run("Split Channels");
 selectWindow(imgName + " (green)");
 //green/red for Gram negative/positive staining

 run("Subtract Background...", "rolling=30");
```

```
  setAutoThreshold("Default dark");
  //run("Threshold...");

  setOption("BlackBackground", false);
  setThreshold(20, 255); //Threshold to be adjusted
  makeRectangle(81, 186, 3072, 231); //define ROI

  run("Measure");

  saveAs("Jpg", resDir+baseName + "-green.jpg");
  run("Close All");
}}
```

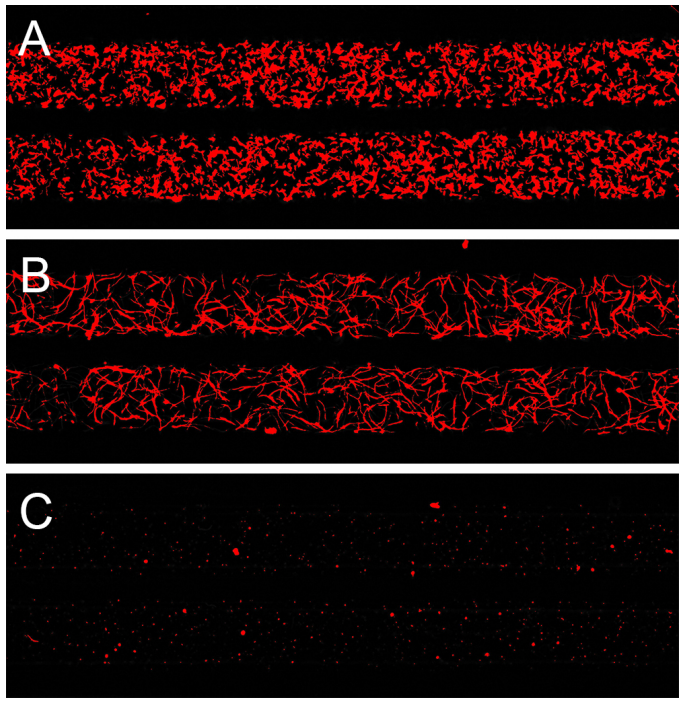

Figure C.1: Extracted images for bacterial growth determination. Example of *E. coli* at different Ampicillin concentrations: A: 0 µg/ml. B: 8 µg/ml. C: 128 µg/ml. Relative area occupied by bacteria is measured.

Appendix D
Device Masks

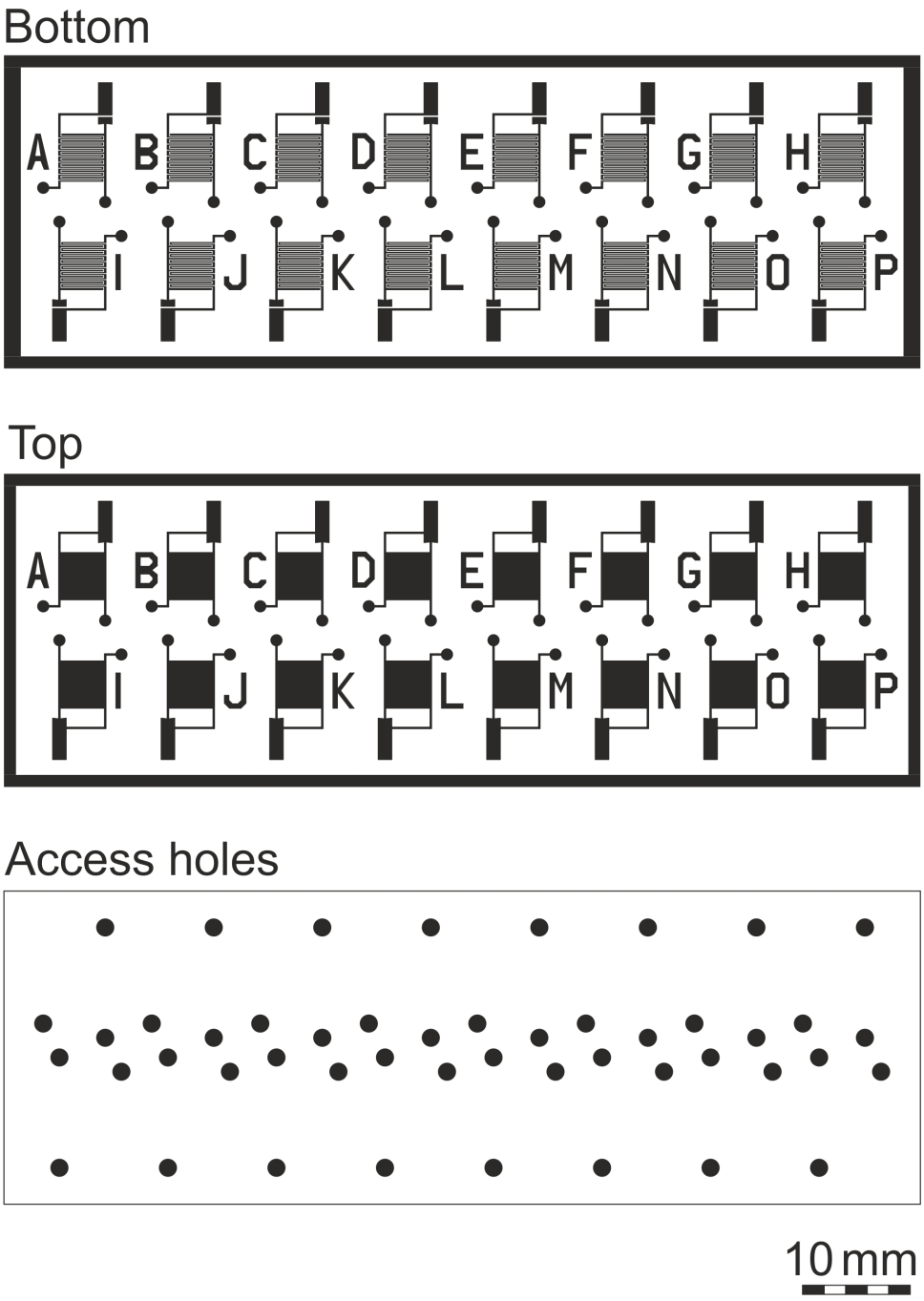

Figure D.1: Microarray Chip for Biochemical Analysis. Section 4.2

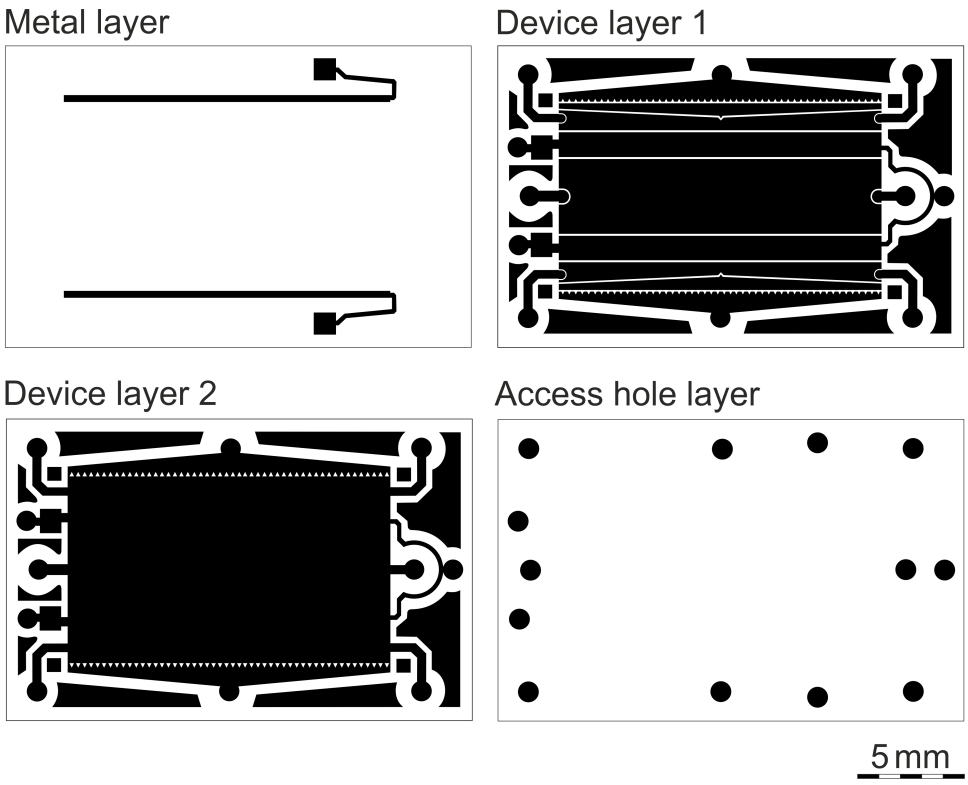

Figure D.2: µFFE chip. Section 5.2

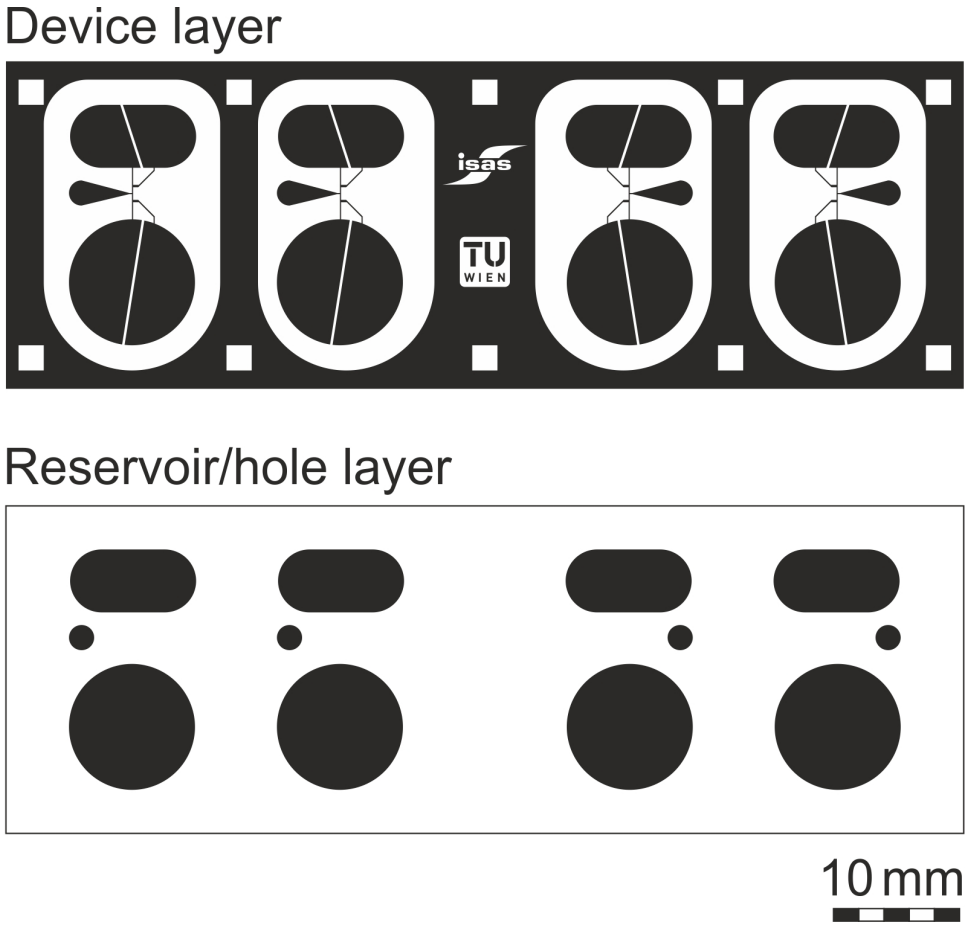

Figure D.3: Low cost bacteria detection chip. Section 5.3

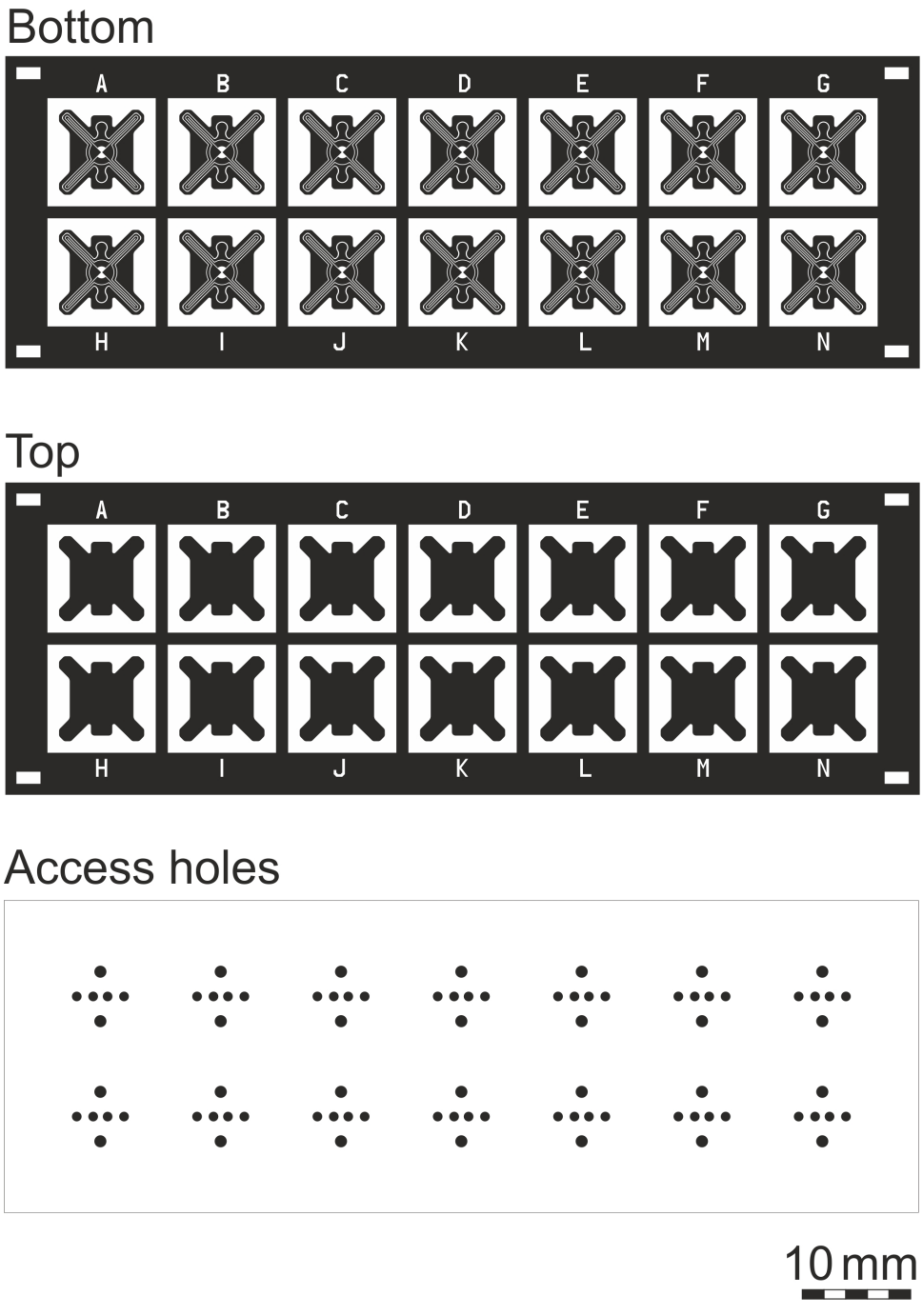

Figure D.4: Rapid Bacterial Testing chip. Section 5.4

Acknowledgements

It is the people we meet on the way who shape our paths. It is my great pleasure to thank those who have contributed to the journey of this work. First of all, I would like to express my gratitude to my supervisor Michael Vellekoop for giving me the opportunity to join his research group as a Ph.D. student. His guidance and support over the last years with the freedom for my ideas, created a great work environment. In numerous discussions he always found the right, motivating words.
I would like to thank Franz Keplinger who especially supported me in the late period of my work. Thank you for all the corrections, advices and off-topic discussions.
Many thanks to Gerald Urban for the opportunity to work in his group at the Department of Microsystems Engineering, University of Freiburg.
The work presented in this thesis was supported by the Austrian Center for Medical Innovation and Technology (ACMIT), which is funded within the scope of the COMET Competence Centers for Excellent Technologies program of the Austrian Government. Particular thanks go to Christian Krutzler and Nikolaus Dellantoni for their support and fruitful discussions.
The author also gratefully acknowledges funding from the European Union in the framework of the EU Marie Curie Research Training Network (MRTN): On-Chip Cell Handling and Analysis, CellCheck (MRTN-CT-2006-035854) and the Optifert project (FP7-OPTIFERT-286772).
Many thanks to all my colleagues and friends who have contributed with scientific debates, great teamwork, enjoyable lunchbreaks, and after work acctivities. In particular, I thank my colleagues Sander van den Driesche, Emanuel Weber, and Lukas Brandhoff from the University of Bremen, Christoph Haiden, Anna Haller, Georgis Kokkinis, and Martin Smolka from the Technical University of Vienna and Susann Podszun, Helene Heinz, and Carsten Hermann from the University of Freiburg. Additional thanks go to all project partners for the valuable discussions and fruitful cooperations.
Furhtermore, thanks to all technicians, especially Peter Svasek, who shared their knowledge in microfabrication and technology.

Finally, I am grateful to my family for their care and understanding and, above all, I would like to thank my wife, Michaela for believing in me and her continuous love throughout the years.

List of Publications

Journal Papers

D. Puchberger-Enengl, S. van den Driesche, C. Krutzler, F. Keplinger, M.J. Vellekoop: *Hydrogel-based microfluidic incubator for microorganism cultivation and analyses*; Biomicrofluidics, 9 (2015), 014127; S. 1 - 9.

D. Puchberger-Enengl, C. Krutzler, F. Keplinger, M.J. Vellekoop: *Single-step design of hydrogel-based microfluidic assays for rapid diagnostics*; Lab on a Chip, 14 (2014), 2; S. 378 - 383.

D. Puchberger-Enengl, S. Podszun, H. Heinz, C. Hermann, P. Vulto, G. Urban: *Microfluidic concentration of bacteria by on-chip electrophoresis*; Biomicrofluidics, 5 (2011), 044111; S. 1 - 10.

M. Smolka, D. Puchberger-Enengl, M. Bipoun, A. Klasa, M. Kiczkajlo, W. Smiechowski, P. Sowinski, C. Krutzler, F. Keplinger, M.J. Vellekoop: *A mobile lab-on-a-chip device for on-site soil nutrient analysis*; Precision Agriculture, (2016), 1-17.

A.E.M. Haller, A. Spittler, L. Brandhoff, H. Zirath, D. Puchberger-Enengl, F. Keplinger, M.J. Vellekoop: *Microfluidic Vortex Enhancement for on-Chip Sample Preparation*; Micromachines, 6 (2015), 2; 13 S.

E. Weber, D. Puchberger-Enengl, F. Keplinger, M.J. Vellekoop: *In-line characterization and identification of micro-droplets on-chip*; Optofluidics, 1 (2013), S. 11 - 18.

S. Van den Driesche, V. Rao, D. Puchberger-Enengl, W. Witarski, M. Vellekoop: *Continuous cell from cell separation by traveling wave dielectrophoresis*; Sensors and Actuators B, 170 (2012), S. 207 - 214.

International Conferences

D. Puchberger-Enengl, C. Krutzler, M. Binder, C. Rohrer, K. Schrder, F. Keplinger, M.J. Vellekoop: *Characterization of a Multi-parameter Sensor for Continuous Wound Assessment*; Eurosensors XXVI, Krakow, Poland; 09.09.2012 - 12.09.2012; in: Procedia Engineering, 47 (2012), S. 985 - 988.

D. Puchberger-Enengl, C. Krutzler, F. Keplinger, M.J. Vellekoop: *Rapid detection of bacteria by low-cost microfluidic system*; Smart Systems Integration (SSI) 2014, Wien; 26.03.2014 - 27.03.2014; in: Smart Systems Integration, Apprimus Verlag, Aachen, (2014), ISBN: 978-3-86359-201-1; S. 323 - 328.

D. Puchberger-Enengl, C. Krutzler, M. Vellekoop: *Organically modified silicate film pH sensor for continous wound monitoring*; IEEE Sensors, Limerick, Ireland; 28.10.2011 - 31.10.2011; in: Proceedings IEEE Sensors 2011, (2011), ISBN: 978-1-4244-9288-6; S. 679 - 682.

D. Puchberger-Enengl, S. van den Driesche, C. Krutzler, F. Keplinger, M.J. Vellekoop: *Microfluidic cell culturing by hydrogel-based diffusion/perfusion*; Transducers & Eurosensors XXVII, Barcelona; 16.06.2013 - 20.06.2013; in: Transducers & Eurosensors XXVII, (2013), ISBN: 978-1-4673-5983-2; S. 2094 - 2097.

D. Puchberger-Enengl, M. Vellekoop: *On-chip concentration of microorganisms by free flow electrophoresis*; Eurosensors XXV, Athens, Greece; 04.09.2011 - 07.09.2011; in: Procedia Engineering, 25 (2011), S. 1249 - 1252.

D. Puchberger-Enengl, M. Bipoun, M. Smolka, C. Krutzler, F. Keplinger, M.J. Vellekoop: *Hydrogel plug for independent sample and buffer handling in continuous microchip capillary electrophoresis*; SPIE Microtechnologies International Symposium, Grenoble; 24.04.2013 - 26.04.2013; in: Proceedings of SPIE, Proc. SPIE 8763, Smart Sensors, Actuators, and MEMS VI, 87631B (May 17, 2013), 8763 (2013).

S. van den Driesche, J. V. Pimentel, D. Puchberger-Enengl, L. Brandhoff, M.J. Vellekoop: *Easy-to-realise polyvinylsiloxane microfluidic connectors for PDMS chips*; Eurosensors XXIX, (2015) Freiburg, Germany; 06.09.-09.09.2015; in Procedia Engineering, (accepted for publication).

M. Smolka, D. Puchberger-Enengl, M. Bipoun, G. Fercher, A Klasa, C. Krutzler, F. Keplinger, M.J. Vellekoop: *A new injection method for soil nutrient analysis in capillary electrophoresis*; SPIE Microtechnologies International Symposium, Grenoble; 24.04.2013 - 26.04.2013; in: Proceedings of SPIE, Proc. SPIE 8763, Smart Sensors, Actuators, and MEMS VI, (2013).

C. Haiden, T. Wopelka, M. Jech, E. Weber, D. Puchberger-Enengl, F. Keplinger, M.J. Vellekoop: *A microfluidic system for visualisation of individual sub-micron particles by light scattering*; Eurosensors XXVI, Krakow, Poland; 09.09.2012 - 12.09.2012; in: Procedia Engineering, 47 (2012), S. 680 - 683.

E. Weber, D. Puchberger-Enengl, M. Vellekoop: *In-line characterization of micro-droplets based on partial light reflection at the solid-liquid interface*; ASME International Conference on Nanochannels, Microchannels, and Minichannels ICNMM2012, Puerto Rico, USA; 08.07.2012 - 12.07.2012; in: ASME 2012 10th International Conference on Nanochannels, Microchannels, and Minichannels, (2012).

S. Van den Driesche, S. Rao, D. Puchberger-Enengl, W. Witarski, M. Vellekoop: *Continuous separation of viable cells by travelling wave dielectrophoresis*; Eurosensors XXIV, September 5-8, 2010, Linz, Austria; Procedia Engineering, 5 (2010), S. 41 - 44.

S. Van den Driesche, A.E.M. Haller, D. Puchberger-Enengl, W. Witarski, M. Vellekoop: *Cell-Cell Separation of Suspended-grown Cells by Interdigitated Triangular Electrodes Based on Negative Dielectrophoresis*; The Second Conf. on Advances in Microfluidics and Nanofluidics & Asia-Pacific Intl. Symposium on Lab on Chip, Singapore; 05.01.2011 - 07.01.2011; in: Proceedings AMN-APLOC 2011, (2011), ISBN: 978-981-08-7722-4; S. 22 - 23.

S. Van den Driesche, H. Zirath, D. Puchberger-Enengl, F. Iuliano, H. Wiesinger-Mayr, M. Vellekoop: *Separation of biological cells and bacteria by gradient electrodes*; EUROSENSORS, Athens, Greece; 09.09.2011 - 14.09.2011; in: Procedia Engineering, 25 (2011), S. 705 - 708. Procedia Engineering, 5 (2010), S. 41 - 44.

Patent applications

D. Puchberger-Enengl, M. Binder, K zer, C. Rohrer: *Verfahren zur berwachung der wundheilung*; Patent: Austria, Nr. PCT/AT/2013/000132; filed: 06.09.2012, registered: 13.08.2013.

Other Publications

D. Puchberger-Enengl, C. Krutzler, M. Binder, C. Rohrer, F. Keplinger, M.J. Vellekoop: *Multi-parametric physiological measurements for sports monitoring*; ICT meets Medicine and Health ICTMH2013, Bremen; 19.03.2013 - 20.03.2013;

D. Puchberger-Enengl, E. Weber, C. Krutzler, M. Vellekoop: *Flexible Microfluidics: Low cost fabrication of plastic lab-on-a-chip devices*; Informationstagung Mikroelektronik (ME), Wien; 23.04.2012 -

24.04.2012; in: Tagungsband zur Informationstagung 2012, (2012), ISBN: 978-3-85133-071-7; 4 S.

D. Puchberger-Enengl, S. van den Driesche, C. Krutzler, F. Keplinger, M.J. Vellekoop: *Microfluidic Incubator for Rapid Bacterial Testing*; 2nd Austrian Biomarker Symposium 2014 Early Diagnostics, Wien; 31.03.2014 - 01.04.2014.

D. Puchberger-Enengl, S. Van den Driesche, V. Rao, W. Witarski, M. Vellekoop: *Cell separation in a continuous flow by traveling wave*; GMe Forum 2011, Vienna, Austria; 14.04.2011 - 15.04.2011; in: GMe Forum 2011 - Proceedings, (2011), ISBN: 978-3-901578-23-6; S. 99 - 104.

S. Hakenberg, S. Podszun, D. Puchberger-Enengl, H. Heinz, C. Hermann, P. Vulto, G. Dame, G. Urban: *Microfluidic enrichment of viable bacteria by electrophoretic deflection in a chip for pathogen detection*; BMT 2011, Freiburg; 27.09.2011 - 30.09.2011.

Bibliography

[1] Grand View Research, "Disposable Medical Sensors Market Analysis By Product (Wearable, Strip, Implantable, Invasive Sensors), By Technology (Temperature, Pressure, Accelerometers, Biosensors), By Application (Monitoring, Therapeutic, Diagnostic) And Segment Forecasts To 2020," Grand View Research, Tech. Rep., 2014. [Online]. Available: http://www.grandviewresearch.com/industry-analysis/disposable-medical-sensors-industry

[2] S. Baranoski and E. A. Ayello, Eds., *Wound Care Essentials: Practice Principles*, 2nd ed. Philadelphia: Lippincott, 2008.

[3] M. N. Menke, N. B. Menke, C. H. Boardman, and R. F. Diegelmann, "Biologic therapeutics and molecular profiling to optimize wound healing." *Gynecologic oncology*, vol. 111, no. 2 Suppl, pp. S87–91, nov 2008. doi:10.1016/j.ygyno.2008.07.052. [Online]. Available: http://www.pubmedcentral.nih.gov/articlerender.fcgi?artid=2592097{&}tool=pmcentrez{&}rendertype=abstract

[4] R. Diegelmann, "Wound healing: an overview of acute, fibrotic and delayed healing," *Frontiers in Bioscience*, vol. 9, no. 1-3, p. 283, 2004. doi:10.2741/1184. [Online]. Available: http://www.bioscience.org/2004/v9/af/1184/list.htm

[5] S. Werner and R. Grose, "Regulation of wound healing by growth factors and cytokines." *Physiological reviews*, vol. 83, no. 3, pp. 835–70, jul 2003. doi:10.1152/physrev.00031.2002. [Online]. Available: http://www.ncbi.nlm.nih.gov/pubmed/12843410

[6] J. Li, J. Chen, and R. Kirsner, "Pathophysiology of acute wound healing." *Clinics in dermatology*, vol. 25, no. 1, pp. 9–18, 2007. doi:10.1016/j.clindermatol.2006.09.007. [Online]. Available: http://www.ncbi.nlm.nih.gov/pubmed/17276196

[7] T. Velnar, T. Bailey, and V. Smrkolj, "The wound healing process: an overview of the cellular and molecular mechanisms." *The Journal of international medical research*, vol. 37, no. 5, pp. 1528–42, 2009. [Online]. Available: http://www.ncbi.nlm.nih.gov/pubmed/19930861

[8] M. Muller, C. Trocme, B. Lardy, F. Morel, S. Halimi, and P. Y. Benhamou, "Matrix metalloproteinases and diabetic foot ulcers: the ratio of MMP-1 to TIMP-1 is a predictor of wound healing." *Diabetic medicine : a journal of the British Diabetic Association*, vol. 25, no. 4, pp. 419–426, 2008.

[9] L. Braiman-Wiksman, I. Solomonik, R. Spira, and T. Tennenbaum, "Novel insights into wound healing sequence of events." *Toxicologic pathology*, vol. 35, no. 6, pp. 767–79, jan 2007. doi:10.1080/01926230701584189. [Online]. Available: http://www.ncbi.nlm.nih.gov/pubmed/17943650

[10] N. J. M. London and R. Donnelly, "Ulcerated lower limb," *BMJ : British Medical Journal*, vol. 320, no. 7249, pp. 1589–1591, 2000.

[11] G. Danaei, M. M. Finucane, Y. Lu, G. M. Singh, M. J. Cowan, C. J. Paciorek, J. K. Lin, F. Farzadfar, Y.-H. Khang, G. A. Stevens, M. Rao, M. K. Ali, L. M. Riley, C. A. Robinson, and M. Ezzati, "National, regional, and global trends in fasting plasma glucose and diabetes prevalence since 1980: systematic analysis of health examination surveys and epidemiological studies with 370 country-years and 27 million participants." *Lancet*, vol. 378, no. 9785, pp. 31–40, jul 2011. doi:10.1016/S0140-6736(11)60679-X. [Online]. Available: http://www.ncbi.nlm.nih.gov/pubmed/21705069

[12] H. Brem and M. Tomic-Canic, "Cellular and molecular basis of wound healing in diabetes." *The Journal of clinical investigation*, vol. 117, no. 5, pp. 1219–22, may 2007. doi:10.1172/JCI32169

[13] C. K. Sen, G. M. Gordillo, S. Roy, R. Kirsner, L. Lambert, T. K. Hunt, F. Gottrup, G. C. Gurtner, and M. T. Longaker, "Human skin wounds: a major and snowballing threat to public health and the economy." *Wound repair and regeneration : official publication of the Wound Healing Society [and] the European Tissue Repair Society*, vol. 17, no. 6, pp. 763–71, 2009. doi:10.1111/j.1524-475X.2009.00543.x. [Online]. Available: http://www.pubmedcentral.nih.gov/articlerender.fcgi?artid=2810192{&}tool=pmcentrez{&}rendertype=abstract

[14] S. McLennan, D. Min, and D. Yue, "Matrix metalloproteinases and their roles in poor wound healing in diabetes." *Wound Practice & Research*, vol. 16, no. 3, pp. 116–121, 2008. [Online]. Available: http://search.ebscohost.com/login.aspx?direct=true{&}profile=ehost{&}scope=site{&}authtype=crawler{&}jrnl=18376304{&}AN=34374632{&}h=CSOE/ARDjP3Bf7F3DnPtRGMv8/CTtYVJ3WEa6gvACNGgGJ9c/V/Gi3Lj37GaEB81+4KTBsxFInE9Z4cZXLEn/A=={&}crl=c

[15] R. Sibbald, K. Woo, and E. Ayello, "Wound bed preparation : DIM before DIME," *Wound Healing Southern Africa*, vol. 1, no. 1, pp. 29–34, 2008.

[16] A. Widgerow, "Persistence of the chronic wound implicating biofilm," *Wound Healing Southern Africa*, vol. 1, no. 2, pp. 5–8, 2008.

[17] T. Mustoe, "Understanding chronic wounds: a unifying hypothesis on their pathogenesis and implications for therapy," *The American Journal of Surgery*, vol. 187, no. 5, pp. S65–S70, may 2004. doi:10.1016/S0002-9610(03)00306-4. [Online]. Available: http://linkinghub.elsevier.com/retrieve/pii/S0002961003003064

[18] D. Okan, K. Woo, E. A. Ayello, and G. Sibbald, "The role of moisture balance in wound healing." *Advances in skin & wound care*, vol. 20, no. 1, pp. 39–53; quiz 53–55, 2007. doi:10.1097/00129334-200701000-00014

[19] L. Foley, "The application of TIME (wound bed preparation principles) in the management of a chronic heel ulcer," *Primary Intention*, vol. 12, no. 4, pp. 163–165, 2004. [Online]. Available: http://search.informit.com.au/fullText;dn=676104029907942;res=IELHEA

[20] E. Lahnsteiner and J. Lohninger, "Wundbehandlung - Eine interdisziplinäre Herausforderung," in *Manual der Wundheilung*, 2007th ed., T. Wild and J. Auböck, Eds. Vienna: Springer, 2007, ch. 30. [Online]. Available: http://link.springer.com/chapter/10.1007/978-3-211-69454-1{_}32

[21] S. J. Landis, "Chronic wound infection and antimicrobial use." *Advances in skin & wound care*, vol. 21, no. 11, pp. 531–40; quiz 541–2, nov 2008. doi:10.1097/01.ASW.0000323578.87700.a5. [Online]. Available: http://www.ncbi.nlm.nih.gov/pubmed/18981758

[22] K. Woo, E. Ayello, and R. Sibbald, "The skin and periwound skin disorders and management," *Wound Healing Southern Africa*, vol. 2, no. 2, pp. 1–6, 2009. [Online]. Available: http://www.woundhealingsa.co.za/index.php/WHSA/article/view/58

[23] P. Sheehan, P. Jones, A. Caselli, J. M. Giurini, and A. Veves, "Percent change in wound area of diabetic foot ulcers over a 4-week period is a robust predictor of complete healing in a 12-week prospective trial," *Diabetes Care*, vol. 26, no. 6, pp. 1879–1882, 2003.

[24] S. Barber, "A clinically relevant wound assessment method to monitor healing progression." *Ostomy/wound management*, vol. 54, no. 3, pp. 42–49, 2008.

[25] A. Fette, "A clinimetric analysis of wound measurement tools," 2006. [Online]. Available: http://www.worldwidewounds.com/2006/january/Fette/Clinimetric-Analysis-Wound-Measurement-Tools.html

[26] World Union of WoundHealing Societies (WUWHS), "Principles of best practice: Diagnostics and wounds. A consensus document," London, 2008. [Online]. Available: http://scholar.google.com/scholar?hl=en{&}btnG=Search{&}q=intitle:Principles+of+best+practice:+Diagnostics+and+wounds.+Aconsensus+documen{#}0

[27] M. Chan, D. Estève, J.-Y. Fourniols, C. Escriba, and E. Campo, "Smart wearable systems: current status and future challenges." *Artificial intelligence in medicine*, vol. 56, no. 3, pp. 137–56, nov 2012. doi:10.1016/j.artmed.2012.09.003

[28] S. Patel, H. Park, P. Bonato, L. Chan, and M. Rodgers, "A review of wearable sensors and systems with application in rehabilitation." *Journal of neuroengineering and rehabilitation*, vol. 9, no. 1, p. 21, jan 2012. doi:10.1186/1743-0003-9-21

[29] S. C. Mukhopadhyay, "Wearable Sensors for Human Activity Monitoring: A Review," *IEEE Sensors Journal*, vol. 15, no. 3, pp. 1321–1330, mar 2015. doi:10.1109/JSEN.2014.2370945

[30] Y.-L. Hsu, P.-C. J. Chung, W.-H. Wang, M.-c. Pai, C.-Y. Wang, C.-w. Lin, H.-L. Wu, and J.-S. Wang, "Gait and balance analysis for patients with Alzheimer's disease using an inertial-sensor-based wearable instrument." *IEEE journal of biomedical and health informatics*, vol. 18, no. 6, pp. 1822–30, nov 2014. doi:10.1109/JBHI.2014.2325413

[31] P. Bonato, "Wearable sensors and systems. From enabling technology to clinical applications." *IEEE engineering in medicine and biology magazine : the quarterly magazine of the Engineering in Medicine & Biology Society*, vol. 29, no. 3, pp. 25–36, 2010. doi:10.1109/MEMB.2010.936554

[32] Y. Mendelson and B. D. Ochs, "Noninvasive pulse oximetry utilizing skin reflectance photoplethysmography." *IEEE transactions on bio-medical engineering*, vol. 35, no. 10, pp. 798–805, oct 1988. doi:10.1109/10.7286

[33] S. Takatani and J. Ling, "Optical oximetry sensors for whole blood and tissue," *IEEE Engineering in Medicine and Biology Magazine*, vol. 13, no. 3, pp. 347–357, jul 1994. doi:10.1109/51.294005

[34] H. H. Asada, P. Shaltis, A. Reisner, S. Rhee, and R. C. Hutchinson, "Mobile monitoring with wearable photoplethysmographic biosensors." *IEEE engineering in medicine and biology magazine : the quarterly magazine of the Engineering in Medicine & Biology Society*, vol. 22, no. 3, pp. 28–40, 2003.

[35] S. B. Duun, R. G. Haahr, K. Birkelund, and E. V. Thomsen, "A Ring-Shaped Photodiode Designed for Use in a Reflectance Pulse Oximetry Sensor in Wireless Health Monitoring Applications," *IEEE Sensors Journal*, vol. 10, no. 2, pp. 261–268, feb 2010. doi:10.1109/JSEN.2009.2032925

[36] R. Haahr, S. Duun, and M. Toft, "An electronic patch for wearable health monitoring by reflectance pulse oximetry," *IEEE Transactions on Biomedical Circuits and Systems*, vol. 6, no. 1, pp. 45–53, 2012. doi:10.1109/TBCAS.2011.2164247

[37] Y. K. Lee, J. Jo, and H. S. Shin, "Development and Evaluation of a Wristwatch-Type Photoplethysmography Array Sensor Module," *IEEE Sensors Journal*, vol. 13, no. 5, pp. 1459–1463, may 2013. doi:10.1109/JSEN.2012.2235424

[38] a. Pantelopoulos and N. Bourbakis, "A Survey on Wearable Sensor-Based Systems for Health Monitoring and Prognosis," *IEEE Transactions on Systems, Man, and Cybernetics, Part C (Applications and Reviews)*, vol. 40, no. 1, pp. 1–12, jan 2010. doi:10.1109/TSMCC.2009.2032660

[39] S. Coyle, K.-T. Lau, N. Moyna, D. O'Gorman, D. Diamond, F. Di Francesco, D. Costanzo, P. Salvo, M. G. Trivella, D. E. De Rossi, N. Taccini, R. Paradiso, J.-A. Porchet, A. Ridolfi, J. Luprano, C. Chuzel, T. Lanier, F. Revol-Cavalier, S. Schoumacker, V. Mourier, I. Chartier, R. Convert, H. De-Moncuit, and C. Bini, "BIOTEX–biosensing textiles for personalised healthcare management." *IEEE transactions on information technology in biomedicine : a publication of the IEEE Engineering in Medicine and Biology Society*, vol. 14, no. 2, pp. 364–70, mar 2010. doi:10.1109/TITB.2009.2038484

[40] T. R. Dargaville, B. L. Farrugia, J. a. Broadbent, S. Pace, Z. Upton, and N. H. Voelcker, "Sensors and imaging for wound healing: A review." *Biosensors & bioelectronics*, pp. 1–13, sep 2012. doi:10.1016/j.bios.2012.09.029

[41] N. Mehmood, A. Hariz, R. Fitridge, and N. H. Voelcker, "Applications of modern sensors and wireless technology in effective wound management." *Journal of biomedical materials research. Part B, Applied biomaterials*, vol. 102, no. 4, pp. 885–95, may 2014. doi:10.1002/jbm.b.33063

[42] D. Puchberger-Enengl, C. Krutzler, and M. J. Vellekoop, "Organically modified silicate film pH sensor for continuous wound monitoring," in *2011 IEEE SENSORS Proceedings*, no. 86578. IEEE, oct 2011, pp. 679–682. doi:10.1109/ICSENS.2011.6127220

[43] M. Ochoa, R. Rahimi, and B. Ziaie, "Flexible sensors for chronic wound management." *IEEE reviews in biomedical engineering*, vol. 7, pp. 73–86, jan 2014. doi:10.1109/RBME.2013.2295817

[44] D. G. Armstrong and L. a. Lavery, "Monitoring neuropathic ulcer healing with infrared dermal thermometry," *The Journal of Foot and Ankle Surgery*, vol. 35, no. 4, pp. 335–338, jul 1996. doi:10.1016/S1067-2516(96)80083-4

[45] D. Armstrong and L. Lavery, "Infrared dermal thermometry for the high-risk diabetic foot," *Physical Therapy*, vol. 77, no. 2, 1997.

[46] M. Fierheller and R. G. Sibbald, "A clinical investigation into the relationship between increased periwound skin temperature and local wound infection in patients with chronic leg ulcers." *Advances in skin & wound care*, vol. 23, no. 8, pp. 369–79; quiz 380–1, aug 2010. doi:10.1097/01.ASW.0000383197.28192.98

[47] V. J. Houghton, V. M. Bower, and D. C. Chant, "Is an increase in skin temperature predictive of neuropathic foot ulceration in people with diabetes? A systematic review and meta-analysis." *Journal of foot and ankle research*, vol. 6, no. 1, p. 31, jan 2013. doi:10.1186/1757-1146-6-31

[48] G. Gethin, "The significance of surface pH in chronic wounds," *Wounds A Compendium Of Clinical Research And Practice*, vol. 3, no. 3, pp. 52–55, 2007.

[49] L. A. Schneider, A. Korber, S. Grabbe, and J. Dissemond, "Influence of pH on wound-healing: a new perspective for wound-therapy?" *Archives of dermatological research*, vol. 298, no. 9, pp. 413–20, feb 2007. doi:10.1007/s00403-006-0713-x

[50] S. L. Percival, S. McCarty, J. a. Hunt, and E. J. Woods, "The effects of pH on wound healing, biofilms, and antimicrobial efficacy." *Wound repair and regeneration : official publication of the Wound Healing Society [and] the European Tissue Repair Society*, vol. 22, no. 2, pp. 174–86, 2014. doi:10.1111/wrr.12125

[51] J. Dissemond, M. Witthoff, T. C. Brauns, D. Haberer, and M. Goos, "[pH values in chronic wounds. Evaluation during modern wound therapy]." *Der Hautarzt; Zeitschrift für Dermatologie, Venerologie, und verwandte Gebiete*, vol. 54, no. 10, pp. 959–65, oct 2003. doi:10.1007/s00105-003-0554-x

[52] S. Schreml, R. J. Meier, O. S. Wolfbeis, M. Landthaler, R.-M. Szeimies, and P. Babilas, "2D luminescence imaging of pH in vivo," *Proceedings of the National Academy of Sciences*, vol. 108, no. 6, pp. 2432–2437, jan 2011. doi:10.1073/pnas.1006945108

[53] S. Pasche, S. Angeloni, R. Ischer, M. Liley, J. Luprano, and G. Voirin, "Wearable Biosensors for Monitoring Wound Healing," *Advances in Science and Technology*, vol. 57, pp. 80–87, 2008. doi:10.4028/www.scientific.net/AST.57.80

[54] V. Sridhar and K. Takahata, "A hydrogel-based passive wireless sensor using a flex-circuit inductive transducer," *Sensors and Actuators A: Physical*, vol. 155, no. 1, pp. 58–65, oct 2009. doi:10.1016/j.sna.2009.08.010

[55] A. Nocke, A. Schröter, C. Cherif, and G. Gerlach, "Miniaturized textile-based multi-layer ph-sensor for wound monitoring applications," *Autex Research Journal*, vol. 12, no. 1, pp. 20–22, jan 2012. doi:10.2478/v10304-012-0004-x

[56] J. Phair, L. Newton, C. McCormac, M. F. Cardosi, R. Leslie, and J. Davis, "A disposable sensor for point of care wound pH monitoring." *The Analyst*, vol. 136, no. 22, pp. 4692–5, nov 2011. doi:10.1039/c1an15675f

[57] S. Milne and P. Connolly, "Development of wearable sensors for tailored patient wound care," in *Annual International Conference of the IEEE Engineering in Medicine and Biology Society (EMBC)*. Chicago: IEEE, 2014, pp. 618–621.

[58] S. Trupp, M. Alberti, T. Carofiglio, E. Lubian, H. Lehmann, R. Heuermann, E. Yacoub-George, K. Bock, and G. Mohr, "Development of pH-sensitive indicator dyes for the preparation of micro-patterned optical sensor layers," *Sensors and Actuators B: Chemical*, vol. 150, no. 1, pp. 206–210, sep 2010. doi:10.1016/j.snb.2010.07.015

[59] D. Morris, S. Coyle, Y. Wu, K. T. Lau, G. Wallace, and D. Diamond, "Bio-sensing textile based patch with integrated optical detection system for sweat monitoring," *Sensors and Actuators B: Chemical*, vol. 139, no. 1, pp. 231–236, may 2009. doi:10.1016/j.snb.2009.02.032. [Online]. Available: http://linkinghub.elsevier.com/retrieve/pii/S0925400509001270

[60] V. F. Curto, C. Fay, S. Coyle, R. Byrne, C. OToole, C. Barry, S. Hughes, N. Moyna, D. Diamond, and F. Benito-Lopez, "Real-time sweat pH monitoring based on a wearable chemical barcode micro-fluidic platform incorporating ionic liquids," *Sensors and Actuators B: Chemical*, vol. 171-172, pp. 1327–1334, aug 2012. doi:10.1016/j.snb.2012.06.048

[61] R. Makote and M. Collinson, "Organically modified silicate films for stable pH sensors," *Analytica chimica acta*, vol. 394, no. April, pp. 195–200, 1999.

[62] S. Jurmanović, Š. Kordić, M. D. Steinberg, and I. M. Steinberg, "Organically modified silicate thin films doped with colourimetric pH indicators methyl red and bromocresol green as pH responsive solgel hybrid materials," *Thin Solid Films*, vol. 518, no. 8, pp. 2234–2240, feb 2010. doi:10.1016/j.tsf.2009.07.158

[63] G. M. Gordillo and C. K. Sen, "Revisiting the essential role of oxygen in wound healing," *The American Journal of Surgery*, vol. 186, no. 3, pp. 259–263, sep 2003. doi:10.1016/S0002-9610(03)00211-3

[64] D. Smart, M. Bennett, and S. Mitchell, "Transcutaneous oximetry, problem wounds and hyperbaric oxygen therapy," *Diving and Hyperbaric Medicine Journal*, vol. 36, no. 2, pp. 72–86, 2006.

[65] S. Schreml, R. M. Szeimies, L. Prantl, S. Karrer, M. Landthaler, and P. Babilas, "Oxygen in acute and chronic wound healing." *The British journal of dermatology*, vol. 163, no. 2, pp. 257–68, aug 2010. doi:10.1111/j.1365-2133.2010.09804.x

[66] L. Martinez, "A non-invasive spectral reflectance method for mapping blood oxygen saturation in wounds," in *Applied Imagery Pattern Recognition Workshop Proceedings*. Washington, DC: IEEE, 2002.

[67] T. Seki and M. Fujioka, "Regional tissue oxygen saturation measured by near-infrared spectroscopy to assess the depth of burn injuries," *International Journal of Burns and Trauma*, vol. 4, no. 1, pp. 40–44, 2014.

[68] M. Nitzan and H. Taitelbaum, "The measurement of oxygen saturation in arterial and venous blood," *IEEE Instrumentation & Measurement Magazine*, vol. 11, no. 3, pp. 9–15, jun 2008. doi:10.1109/MIM.2008.4534373

[69] F. Gottrup, "Oxygen in wound healing and infection." *World journal of surgery*, vol. 28, no. 3, pp. 312–5, mar 2004. doi:10.1007/s00268-003-7398-5

[70] M. S. Weingarten, M. Neidrauer, A. Mateo, X. Mao, J. E. McDaniel, L. Jenkins, S. Bouraee, L. Zubkov, K. Pourrezaei, and E. S. Papazoglou, "Prediction of wound healing in human diabetic foot ulcers by diffuse near-infrared spectroscopy: A pilot study," *Wound Repair and Regeneration*, vol. 18, no. 2, pp. 180–185, mar 2010. doi:10.1111/j.1524-475X.2010.00583.x

[71] E. S. Papazoglou, M. S. Weingarten, L. Zubkov, M. Neidrauer, and K. Pourrezaei, "Assessment of diabetic foot ulcers with diffuse near infrared methodology," *2008 8th IEEE International Conference on BioInformatics and BioEngineering*, pp. 1–5, oct 2008. doi:10.1109/BIBE.2008.4696754

[72] E. S. Papazoglou, M. S. Weingarten, L. Zubkov, L. Zhu, S. Tyagi, and K. Pourrezaei, "Optical properties of wounds: diabetic versus healthy tissue." *IEEE transactions on bio-medical engineering*, vol. 53, no. 6, pp. 1047–55, jun 2006. doi:10.1109/TBME.2006.873541

[73] A. Garcia-Uribe, K. C. Balareddy, J. Zou, and L. V. Wang, "Micromachined Fiber Optical Sensor for In Vivo Measurement of Optical Properties of Human Skin," *IEEE Sensors Journal*, vol. 8, no. 10, pp. 1698–1703, oct 2008. doi:10.1109/JSEN.2008.2003306

[74] M. a. Afromowitz, J. B. Callis, D. M. Heimbach, L. a. DeSoto, and M. K. Norton, "Multispectral imaging of burn wounds: a new clinical instrument for evaluating burn depth." *IEEE transactions on bio-medical engineering*, vol. 35, no. 10, pp. 842–50, oct 1988. doi:10.1109/10.7291

[75] R. Moza, J. M. Dimaio, and J. Melendez, "Deep-tissue dynamic monitoring of decubitus ulcers: wound care and assessment." *IEEE engineering in medicine and biology magazine : the quarterly magazine of the Engineering in Medicine & Biology Society*, vol. 29, no. 2, pp. 71–7, 2010. doi:10.1109/MEMB.2009.935721. [Online]. Available: http://www.ncbi.nlm.nih.gov/pubmed/20659843

[76] W. D. Schmidt, K. Liebold, D. Fassler, and U. Wollina, "Contact-free spectroscopy of leg ulcers: principle, technique, and calculation of spectroscopic wound scores." *The Journal of investigative dermatology*, vol. 116, no. 4, pp. 531–5, apr 2001. doi:10.1046/j.1523-1747.2001.01297.x

[77] M. Attas and M. Hewko, "Visualization of cutaneous hemoglobin oxygenation and skin hydration using near infrared spectroscopic imaging," *Skin Research and Technology*, vol. 7, pp. 238–245, 2001.

[78] F. W. H. Kloppenberg, G. I. J. M. Beerthuizen, and H. J. Duis, "Perfusion of burn wounds assessed by Laser Doppler Imaging is related to burn depth and healing time," *Burns*, vol. 27, pp. 359–363, 2001.

[79] M. S. Weingarten, E. S. Papazoglou, L. Zubkov, L. Zhu, M. Neidrauer, G. Savir, K. Peace, J. G. Newby, and K. Pourrezaei, "Correlation of near infrared absorption and diffuse reflectance spectroscopy scattering with tissue neovascularization and collagen concentration in a diabetic rat wound healing model." *Wound repair and regeneration : official publication of the Wound Healing Society [and] the European Tissue Repair Society*, vol. 16, no. 2, pp. 234–42, 2008. doi:10.1111/j.1524-475X.2008.00364.x

[80] N. Sekiguchi, T. Komeda, H. Funakubo, R. Chabicovsky, J. Nicolics, and G. Stangl, "Microsensor for the measurement of water content in the human skin," *Sensors and Actuators B: Chemical*, vol. 78, no. 1-3, pp. 326–330, aug 2001. doi:10.1016/S0925-4005(01)00834-6

[81] T. HUANG, J. CHOU, T. SUN, and S. HSIUNG, "A device for skin moisture and environment humidity detection," *Sensors and Actuators B: Chemical*, vol. 134, no. 1, pp. 206–212, aug 2008. doi:10.1016/j.snb.2008.04.030

[82] B. Valentin, M. Mündlein, R. Chabicovsky, J. Nicolics, and S. Member, "A Novel Transepidermal Water Loss Sensor," *IEEE Sensors Journal*, vol. 6, no. 4, pp. 1022–1026, 2006. doi:http://dx.doi.org/10.1109/JSEN.2006.877976

[83] D. Mccoll, M. Macdougall, L. Watret, and P. Connolly, "Monitoring moisture without disturbing the wound dressing," *Wounds A Compendium Of Clinical Research And Practice*, vol. 5, no. 3, pp. 2–6, 2009.

[84] M. J. Goretsky, A. P. Supp, D. G. Greenhalgh, G. D. Warden, and S. T. Boyce, "Surface electrical capacitance as an index of epidermal barrier properties of composite skin substitutes and skin autografts." *Wound repair and regeneration : official publication of the Wound Healing Society [and] the European Tissue Repair Society*, vol. 3, no. 4, pp. 419–25, 1995. doi:10.1046/j.1524-475X.1995.30406.x

[85] S. a. Weber, N. Watermann, J. Jossinet, J. A. Byrne, J. Chantrey, S. Alam, K. So, J. Bush, S. O'Kane, and E. T. McAdams, "Remote wound monitoring of chronic ulcers." *IEEE transactions on information technology in biomedicine : a publication of the IEEE Engineering in Medicine and Biology Society*, vol. 14, no. 2, pp. 371–7, mar 2010. doi:10.1109/TITB.2010.2042605

[86] X. Hu and W. Yang, "Planar capacitive sensors designs and applications," *Sensor Review*, vol. 30, no. 1, pp. 24–39, 2010. doi:10.1108/02602281011010772

[87] G. T. Gethin, S. Cowman, and R. M. Conroy, "The impact of Manuka honey dressings on the surface pH of chronic wounds." *International wound journal*, vol. 5, no. 2, pp. 185–94, jun 2008. doi:10.1111/j.1742-481X.2007.00424.x

[88] Tsukada K, Tokunaga K, Iwama T, and Mishima Y, "The pH changes of pressure ulcers related to the healing process of wounds," *Wounds A Compendium Of Clinical Research And Practice*, vol. 4, no. 1, pp. 16–20, 1992.

[89] V. K. Shukla, D. Shukla, S. K. Tiwary, S. Agrawal, and A. Rastogi, "Evaluation of pH measurement as a method of wound assessment." *Journal of wound care*, vol. 16, no. 7, pp. 291–4, jul 2007. doi:10.12968/jowc.2007.16.7.27062

[90] G. Roberts, A. Chumley, and R. Mani, "The wound milieu in venous ulcers further observations," in *Zeitschrift für Wundheilung, Sonderheft 02/2005*, Stuttgart, 2005.

[91] P. Sheffield, "Measuring tissue oxygen tension: a review." *Undersea & hyperbaric medicine*, vol. 25, no. 3, pp. 179–188, 1998.

[92] J.-H. Moon, D. H. Baek, Y. Y. Choi, K. H. Lee, H. C. Kim, and S.-H. Lee, "Wearable polyimidePDMS electrodes for intrabody communication," *Journal of Micromechanics and Microengineering*, vol. 20, no. 2, p. 025032, feb 2010. doi:10.1088/0960-1317/20/2/025032

[93] D. P. J. Cotton, I. M. Graz, and S. P. Lacour, "A Multifunctional Capacitive Sensor for Stretchable Electronic Skins," *IEEE Sensors Journal*, vol. 9, no. 12, pp. 2008–2009, dec 2009. doi:10.1109/JSEN.2009.2030709. [Online]. Available: http://ieeexplore.ieee.org/lpdocs/epic03/wrapper.htm?arnumber=5311007

[94] H.-C. Jung, J.-H. Moon, D.-H. Baek, J.-H. Lee, Y.-Y. Choi, J.-S. Hong, and S.-H. Lee, "CNT/PDMS composite flexible dry electrodes for long-term ECG monitoring." *IEEE transactions on bio-medical engineering*, vol. 59, no. 5, pp. 1472–9, may 2012. doi:10.1109/TBME.2012.2190288

[95] F. R. Zaggout, "Encapsulation of Bromocresol Green pH Indicator into a Sol Gel Matrix," *Journal of Dispersion Science and Technology*, vol. 26, no. 6, pp. 757–761, nov 2005. doi:10.1081/DIS-200063087

[96] S. Wu, W. Cheng, Y. Qiu, Z. Li, S. Shuang, and C. Dong, "Fiber optic pH sensor based on mode-filtered light detection," *Sensors and Actuators B: Chemical*, vol. 144, no. 1, pp. 255–259, jan 2010. doi:10.1016/j.snb.2009.10.058

[97] H. Prescott, *Laboratory exercises in microbiology*, 5th ed. New York: McGraw-Hill Companies, 2002.

[98] D. Puchberger-Enengl, C. Krutzler, M. Binder, C. Rohrer, F. Keplinger, and M.J. Vellekoop, "Multi-parametric physiological measurements for sports monitoring," in *ICT meets Medicine and Health ICTMH2013*, 2013.

[99] K. H. Shelley, D. H. Jablonka, A. a. Awad, R. G. Stout, H. Rezkanna, and D. G. Silverman, "What is the best site for measuring the effect of ventilation on the pulse oximeter waveform?" *Anesthesia and analgesia*, vol. 103, no. 2, pp. 372–7, table of contents, aug 2006. doi:10.1213/01.ane.0000222477.67637.17. [Online]. Available: http://www.ncbi.nlm.nih.gov/pubmed/16861419

[100] T. Lewis, "The factors influencing the prominence of the dicrotic wave," *The Journal of Physiology*, vol. 34, no. 6, pp. 414–429, oct 1906. doi:10.1113/jphysiol.1906.sp001165. [Online]. Available: http://doi.wiley.com/10.1113/jphysiol.1906.sp001165

[101] S. Schreml, R.-M. Szeimies, L. Prantl, M. Landthaler, and P. Babilas, "Wound healing in the 21st century." *Journal of the American Academy of Dermatology*, vol. 63, no. 5, pp. 866–81, nov 2010. doi:10.1016/j.jaad.2009.10.048. [Online]. Available: http://www.ncbi.nlm.nih.gov/pubmed/20576319

[102] D.-H. Kim, N. Lu, R. Ma, Y.-S. Kim, R.-H. Kim, S. Wang, J. Wu, S. M. Won, H. Tao, A. Islam, K. J. Yu, T.-i. Kim, R. Chowdhury, M. Ying, L. Xu, M. Li, H.-J. Chung, H. Keum, M. McCormick, P. Liu, Y.-W. Zhang, F. G. Omenetto, Y. Huang, T. Coleman, and J. A. Rogers, "Epidermal electronics." *Science*, vol. 333, no. 6044, pp. 838–43, aug 2011. doi:10.1126/science.1206157

[103] G. M. Whitesides, "The origins and the future of microfluidics." *Nature*, vol. 442, no. 7101, pp. 368–373, 2006.

[104] S. van den Driesche, V. Rao, D. Puchberger-Enengl, W. Witarski, and M. J. Vellekoop, "Continuous cell from cell separation by traveling wave dielectrophoresis," *Sensors and Actuators B: Chemical*, vol. 170, pp. 207–214, jul 2012. doi:10.1016/j.snb.2011.01.012. [Online]. Available: http://linkinghub.elsevier.com/retrieve/pii/S0925400511000293

[105] S. Kostner, S. van den Driesche, W. Witarski, S. Pastorekova, and M. J. Vellekoop, "Guided Dielectrophoresis: A Robust Method for Continuous Particle and Cell Separation," *IEEE Sensors Journal*, vol. 10, no. 9, pp. 1440–1446, sep 2010. doi:10.1109/JSEN.2010.2044787. [Online]. Available: http://ieeexplore.ieee.org/xpls/abs{_}all.jsp?arnumber=5482072http://ieeexplore.ieee.org/lpdocs/epic03/wrapper.htm?arnumber=5482072

[106] R. Pethig, "Review Article-Dielectrophoresis: Status of the theory, technology, and applications." *Biomicrofluidics*, vol. 4, no. 2, jan 2010. doi:10.1063/1.3456626. [Online]. Available: http://www.pubmedcentral.nih.gov/articlerender.fcgi?artid=2917862{&}tool=pmcentrez{&}rendertype=abstract

[107] C. Iliescu, H. Taylor, M. Avram, J. Miao, and S. Franssila, "A practical guide for the fabrication of microfluidic devices using glass and silicon." *Biomicrofluidics*, vol. 6, no. 1, pp. 16 505–1 650 516, mar 2012. doi:10.1063/1.3689939. [Online]. Available: http://scitation.aip.org/content/aip/journal/bmf/6/1/10.1063/1.3689939http://www.pubmedcentral.nih.gov/articlerender.fcgi?artid=3365353{&}tool=pmcentrez{&}rendertype=abstract

[108] A. Haller, A. Spittler, L. Brandhoff, H. Zirath, D. Puchberger-Enengl, F. Keplinger, and M. Vellekoop, "Microfluidic Vortex Enhancement for on-Chip Sample Preparation," *Micromachines*, vol. 6, no. 2, pp. 239–251, feb 2015. doi:10.3390/mi6020239. [Online]. Available: http://www.mdpi.com/2072-666X/6/2/239/

[109] P. Abgrall, V. Conedera, H. Camon, A.-M. Gue, and N.-T. Nguyen, "SU-8 as a structural material for labs-on-chips and microelectromechanical systems." *Electrophoresis*, vol. 28, no. 24, pp. 4539–51, dec 2007. doi:10.1002/elps.200700333. [Online]. Available: http://www.ncbi.nlm.nih.gov/pubmed/18072221

[110] a. D. Campo and C. Greiner, "SU-8: a photoresist for high-aspect-ratio and 3D submicron lithography," *Journal of Micromechanics and Microengineering*, vol. 17, no. 6, pp. R81–R95, jun 2007. doi:10.1088/0960-1317/17/6/R01. [Online]. Available: http://stacks.iop.org/0960-1317/17/i=6/a=R01?key=crossref.5f54d4397fa259758a20d0ac229f2a2c

[111] P. Svasek, E. Svasek, B. Lendl, and M. Vellekoop, "Fabrication of miniaturized fluidic devices using SU-8 based lithography and low temperature wafer bonding," *Sensors and Actuators A: Physical*, vol. 115, no. 2-3, pp. 591–599, sep 2004. doi:10.1016/j.sna.2004.03.055. [Online]. Available: http://linkinghub.elsevier.com/retrieve/pii/S0924424704002389

[112] Z. Zhang, P. Zhao, G. Xiao, B. R. Watts, and C. Xu, "Sealing SU-8 microfluidic channels using PDMS." *Biomicrofluidics*, vol. 5, no. 4, pp. 46 503–465 038, dec 2011. doi:10.1063/1.3659016. [Online]. Available: http://www.pubmedcentral.nih.gov/articlerender.fcgi?artid=3364813{&}tool=pmcentrez{&}rendertype=abstract

[113] E. Berthier, E. W. K. Young, and D. Beebe, "Engineers are from PDMS-land, Biologists are from Polystyrenia." *Lab on a chip*, vol. 12, no. 7, pp. 1224–37, apr 2012. doi:10.1039/c2lc20982a. [Online]. Available: http://www.ncbi.nlm.nih.gov/pubmed/22318426

[114] B. A. Zaccheo and R. M. Crooks, "Self-powered sensor for naked-eye detection of serum trypsin." *Analytical chemistry*, vol. 83, no. 4, pp. 1185–8, feb 2011. doi:10.1021/ac103115z. [Online]. Available: http://pubs.acs.org/doi/abs/10.1021/ac103115zhttp://www.ncbi.nlm.nih.gov/pubmed/21247067

[115] A. K. Yetisen, M. S. Akram, and C. R. Lowe, "Paper-based microfluidic point-of-care diagnostic devices." *Lab on a chip*, vol. 13, no. 12, pp. 2210–51, jun 2013. doi:10.1039/c3lc50169h. [Online]. Available: http://www.ncbi.nlm.nih.gov/pubmed/23652632

[116] VDE Verband der Elektrotechnik, "DEUTSCHE NORMUNGS-ROADMAP Mobile Diagnostiksysteme," VDE Verband er Elektrotechnik, Frankfurt, Tech. Rep., 2015. [Online]. Available: https://www.vde.com/DE/FG/DGBMT/ARBEITSGEBIETE/PROJEKTE/MOBINOSTIK/ARBEITSPAKETE{_}VDE/Seiten/Roadmap-Mobile-Diagnostiksysteme.aspx

[117] D. Puchberger-Enengl, C. Krutzler, E. Weber, and M. J. Vellekoop, "Flexible Microfluidics : Low cost fabrication of plastic lab-on-a-chip devices," in *Tagungsband zur Informationstagung Mikroelektronik 2012*, K. U. Christoph Grimm, Bernhard Jakoby, Peter Reichel, Erwin Schoitsch, Ed. Vienna: OVE Österreichischer Verband für Elektrotechnik, 2012, pp. 90–93.

[118] A. Sayah, P.-A. Thivolle, V. K. Parashar, and M. a. M. Gijs, "Three-dimensional mixers with non-planar microchannels in a monolithic glass substrate using oblique powder blasting," *Journal of Micromechanics and Microengineering*, vol. 20, no. 8, p. 085028, aug 2010. doi:10.1088/0960-1317/20/8/085028. [Online]. Available: http://stacks.iop.org/0960-1317/20/i=8/a=085028?key=crossref.ddb0bcf2b158df779cceb66a9f357a43

[119] E. Belloy, A. Sayah, and M. Gijs, "Powder blasting for three-dimensional microstructuring of glass," *Sensors and Actuators A: Physical*, vol. 86, no. 3, pp. 231–237, nov 2000. doi:10.1016/S0924-4247(00)00447-7. [Online]. Available: http://www.sciencedirect.com/science/article/pii/S0924424700004477http://linkinghub.elsevier.com/retrieve/pii/S0924424700004477

[120] J. M. Rosiak and F. Yoshii, "Hydrogels and their medical applications," *Nuclear Instruments and Methods in Physics Research Section B: Beam Interactions with Materials and Atoms*, vol. 151, no. 1-4, pp. 56–64, may 1999. doi:10.1016/S0168-583X(99)00118-4. [Online]. Available: http://www.sciencedirect.com/science/article/pii/S0168583X99001184http://linkinghub.elsevier.com/retrieve/pii/S0168583X99001184

[121] J. Narayanan, J.-Y. Xiong, and X.-Y. Liu, "Determination of agarose gel pore size: Absorbance measurements vis a vis other techniques," *Journal of Physics: Conference Series*, vol. 28, pp. 83–86, jan 2006. doi:10.1088/1742-6596/28/1/017. [Online]. Available: http://stacks.iop.org/1742-6596/28/i=1/a=017?key=crossref.e43ad292c5e6d3b06e4be889d01ddc90

[122] W. Stewart and H. E. Swaisgood, "Characterization of calcium alginate pore diameter by size-exclusion chromatography using protein standards," *Enzyme and Microbial Technology*, vol. 15, no. 11, pp. 922–927, nov 1993. doi:10.1016/0141-0229(93)90167-Z. [Online]. Available: http://www.sciencedirect.com/science/article/pii/014102299390167Zhttp://linkinghub.elsevier.com/retrieve/pii/014102299390167Z

[123] J. Michalek, R. Hobzova, M. Pradny, and M. Duskova, "Hydrogels Contact Lenses," in *Biomedical Applications of Hydrogels Handbook*, R. M. Ottenbrite, K. Park, and T. Okano, Eds. New York, NY: Springer New York, 2010, ch. Hydrogels, pp. 303–316. doi:10.1007/978-1-4419-5919-5_16. [Online]. Available: http://link.springer.com/10.1007/978-1-4419-5919-5

[124] X.-h. Qin, P. Gruber, M. Markovic, B. Plochberger, E. Klotzsch, J. Stampfl, A. Ovsianikov, and R. Liska, "Enzymatic synthesis of hyaluronic acid vinyl esters for two-photon microfabrication of biocompatible and biodegradable hydrogel constructs," *Polym. Chem.*, vol. 5, no. 22, pp. 6523–6533, aug 2014. doi:10.1039/C4PY00792A. [Online]. Available: http://dx.doi.org/10.1039/c4py00792ahttp://xlink.rsc.org/?DOI=C4PY00792A

[125] S. Gulrez, "Hydrogels: methods of preparation, characterisation and applications," in *Progress in Molecular and Environmental Bioengineering*, A. Carpi, Ed. InTech, 2011, ch. 5. doi:10.5772/24553. [Online]. Available: http://core.kmi.open.ac.uk/download/pdf/388451

[126] P. C. Nicolson and J. Vogt, "Soft contact lens polymers: an evolution," *Biomaterials*, vol. 22, no. 24, pp. 3273–3283, dec 2001. doi:10.1016/S0142-9612(01)00165-X. [Online]. Available: http://www.sciencedirect.com/science/article/pii/S014296120100165Xhttp://linkinghub.elsevier.com/retrieve/pii/S014296120100165X

[127] J. Bohnert and T. Horbett, "Adsorption of proteins from artificial tear solutions to contact lens materials," *Investigative Ophthalmology & Visual Science*, vol. 29, no. 3, pp. 362–373, 1988. [Online]. Available: http://www.iovs.org/content/29/3/362.short

[128] C. Hassan and N. Peppas, "Structure and applications of poly (vinyl alcohol) hydrogels produced by conventional crosslinking or by freezing/thawing methods," *Advances in Polymer Science*, vol. 153, pp. 37–65, 2000. [Online]. Available: http://link.springer.com/chapter/10.1007/3-540-46414-X{_}2

[129] C. S. Bahney, T. J. Lujan, C. W. Hsu, M. Bottlang, J. L. West, and B. Johnstone, "Visible light photoinitiation of mesenchymal stem cell-laden bioresponsive hydrogels," *European Cells and Materials*, vol. 22, pp. 43–55, 2011.

[130] B. D. Fairbanks, M. P. Schwartz, C. N. Bowman, and K. S. Anseth, "Photoinitiated polymerization of PEG-diacrylate with lithium phenyl-2,4,6-trimethylbenzoylphosphinate: polymerization rate and cytocompatibility." *Biomaterials*, vol. 30, no. 35, pp. 6702–7, dec 2009. doi:10.1016/j.biomaterials.2009.08.055. [Online]. Available: http://www.pubmedcentral.nih.gov/articlerender.fcgi?artid=2896013{&}tool=pmcentrez{&}rendertype=abstract

[131] Y. Yagci, S. Jockusch, and N. J. Turro, "Photoinitiated Polymerization: Advances, Challenges, and Opportunities," *Macromolecules*, vol. 43, no. 15, pp. 6245–6260, aug 2010. doi:10.1021/ma1007545. [Online]. Available: http://pubs.acs.org/doi/abs/10.1021/ma1007545

[132] N. Annabi, J. W. Nichol, X. Zhong, C. Ji, S. Koshy, A. Khademhosseini, and F. Dehghani, "Controlling the Porosity and Microarchitecture of Hydrogels for Tissue Engineering," *Tissue Engineering Part B: Reviews*, vol. 16, no. 4, pp. 371–383, aug 2010. doi:10.1089/ten.teb.2009.0639. [Online]. Available: http://www.pubmedcentral.nih.gov/articlerender.fcgi?artid=2946907{&}tool=pmcentrez{&}rendertype=abstracthttp://www.liebertonline.com/doi/abs/10.1089/ten.teb.2009.0639

[133] G. Hairer and M. J. Vellekoop, "An integrated flow-cell for full sample stream control," *Microfluidics and Nanofluidics*, vol. 7, no. 5, pp. 647–658, mar 2009. doi:10.1007/s10404-009-0425-6. [Online]. Available: http://link.springer.com/10.1007/s10404-009-0425-6

[134] E. Weber, D. Puchberger-Enengl, F. Keplinger, and M. J. Vellekoop, "In-line characterization and identification of micro-droplets on-chip," *Optofluidics, Microfluidics and Nanofluidics*, vol. 1, no. 1, pp. 11–18, jan 2014. doi:10.2478/optof-2013-0002. [Online]. Available: http://www.degruyter.com/view/j/optof.2014.1.issue-1/optof-2013-0002/optof-2013-0002.xml

[135] B. G. Chung, K.-H. Lee, A. Khademhosseini, and S.-H. Lee, "Microfluidic fabrication of microengineered hydrogels and their application in tissue engineering." *Lab on a chip*, vol. 12, no. 1, pp. 45–59, jan 2012. doi:10.1039/c1lc20859d. [Online]. Available: http://www.ncbi.nlm.nih.gov/pubmed/22105780

[136] D. Gao, J. Liu, H.-B. Wei, H.-F. Li, G.-S. Guo, and J.-M. Lin, "A microfluidic approach for anticancer drug analysis based on hydrogel encapsulated tumor cells." *Analytica chimica acta*, vol. 665, no. 1, pp. 7–14, apr 2010. doi:10.1016/j.aca.2010.03.015. [Online]. Available: http://www.ncbi.nlm.nih.gov/pubmed/20381684

[137] S. J. Trietsch, G. D. Israëls, J. Joore, T. Hankemeier, and P. Vulto, "Microfluidic titer plate for stratified 3D cell culture." *Lab on a chip*, jul 2013. doi:10.1039/c3lc50210d. [Online]. Available: http://www.ncbi.nlm.nih.gov/pubmed/23887749

[138] J. de Jong, R. G. H. Lammertink, and M. Wessling, "Membranes and microfluidics: a review." *Lab on a chip*, vol. 6, no. 9, pp. 1125–39, sep 2006. doi:10.1039/b603275c. [Online]. Available: http://www.ncbi.nlm.nih.gov/pubmed/16929391

[139] S.-Y. Cheng, S. Heilman, M. Wasserman, S. Archer, M. L. Shuler, and M. Wu, "A hydrogel-based microfluidic device for the studies of directed cell migration," *Lab on a Chip*, vol. 7, no. 6, p. 763, 2007. doi:10.1039/b618463d. [Online]. Available: http://pubs.rsc.org/en/content/articlehtml/2007/lc/b618463dhttp://xlink.rsc.org/?DOI=b618463d

[140] S. Cosson, S. Allazetta, and M. P. Lutolf, "Patterning of cell-instructive hydrogels by hydrodynamic flow focusing." *Lab on a chip*, vol. 13, no. 11, pp. 2099–105, may 2013. doi:10.1039/c3lc50219h. [Online]. Available: http://www.ncbi.nlm.nih.gov/pubmed/23598796

[141] M. Guenther and G. Gerlach, *Hydrogel Sensors and Actuators*, ser. Springer Series on Chemical Sensors and Biosensors, G. Gerlach and K.-F. Arndt, Eds. Berlin, Heidelberg: Springer Berlin Heidelberg, 2010, vol. 6. doi:10.1007/978-3-540-75645-3. [Online]. Available: http://link.springer.com/10.1007/978-3-540-75645-3

[142] A. Döring, W. Birnbaum, and D. Kuckling, "Responsive hydrogels - structurally and dimensionally optimized smart frameworks for applications in catalysis, micro-system technology and material science." *Chemical Society reviews*, may 2013. doi:10.1039/c3cs60031a. [Online]. Available: http://www.ncbi.nlm.nih.gov/pubmed/23677178

[143] D. Puchberger-Enengl, M. Bipoun, M. Smolka, C. Krutzler, F. Keplinger, and M. J. Vellekoop, "Hydrogel plug for independent sample and buffer handling in continuous microchip capillary electrophoresis," in *Proc. SPIE 8763, Smart Sensors, Actuators, and MEMS VI*, U. Schmid, J. L. Sánchez de Rojas Aldavero, and M. Leester-Schaedel, Eds., vol. 8763, may 2013, p. 87631B. doi:10.1117/12.2018088. [Online]. Available: http://proceedings.spiedigitallibrary.org/proceeding.aspx?doi=10.1117/12.2018088

[144] P. Abgrall and A.-M. Gué, "Lab-on-chip technologies: making a microfluidic network and coupling it into a complete microsystema review," *Journal of Micromechanics and Microengineering*, vol. 17, no. 5, pp. R15–R49, may 2007. doi:10.1088/0960-1317/17/5/R01. [Online]. Available: http://stacks.iop.org/0960-1317/17/i=5/a=R01?key=crossref.c24504191bbdbbc35f746483f719698a

[145] G. Fiorini and D. Chiu, "Disposable microfluidic devices: fabrication, function, and application," *BioTechniques*, vol. 38, no. March, pp. 429–446, 2005. [Online]. Available: http://www.biotechniques.com/multimedia/archive/00004/BTN{_}A{_}05383RV02{_}O{_}4116a.pdf

[146] P. F. O'Neill, A. Ben Azouz, M. Vázquez, J. Liu, S. Marczak, Z. Slouka, H. C. Chang, D. Diamond, and D. Brabazon, "Advances in three-dimensional rapid prototyping of microfluidic devices for biological applications." *Biomicrofluidics*, vol. 8, no. 5, p. 052112, sep 2014. doi:10.1063/1.4898632. [Online]. Available: http://www.ncbi.nlm.nih.gov/pubmed/25538804

[147] D. Erickson, D. O'Dell, L. Jiang, V. Oncescu, A. Gumus, S. Lee, M. Mancuso, and S. Mehta, "Smartphone technology can be transformative to the deployment of lab-on-chip diagnostics." *Lab on a chip*, vol. 14, no. 17, pp. 3159–64, sep 2014. doi:10.1039/c4lc00142g. [Online]. Available: http://www.ncbi.nlm.nih.gov/pubmed/24700127

[148] A. Ozcan, "Mobile phones democratize and cultivate next-generation imaging, diagnostics and measurement tools." *Lab on a chip*, pp. 3187–3194, mar 2014. doi:10.1039/c4lc00010b. [Online]. Available: http://www.ncbi.nlm.nih.gov/pubmed/24647550

[149] M. S. Agren, "Gelatinase activity during wound healing." *The British journal of dermatology*, vol. 131, no. 5, pp. 634–40, dec 1994. [Online]. Available: http://www.ncbi.nlm.nih.gov/pubmed/7999593

[150] E. a. Baker and D. J. Leaper, "Profiles of matrix metalloproteinases and their tissue inhibitors in intraperitoneal drainage fluid: relationship to wound healing." *Wound repair and regeneration : official publication of the Wound Healing Society [and] the European Tissue Repair Society*, vol. 11, no. 4, pp. 268–74, 2003. [Online]. Available: http://www.ncbi.nlm.nih.gov/pubmed/12846914

[151] M. Weckroth, A. Vaheri, J. Lauharanta, T. Sorsa, and Y. T. Konttinen, "Matrix Metalloproteinases, Gelatinase and Collagenase, in Chronic Leg Ulcers." *Journal of Investigative Dermatology*, vol. 106, no. 5, pp. 1119–1124, may 1996. doi:10.1111/1523-1747.ep12340167. [Online]. Available: http://www.nature.com/doifinder/10.1111/1523-1747.ep12340167

[152] M. Muller, C. Trocme, F. Morel, S. Halimi, and P. Y. Benhamou, "Increased matrix metalloproteinase-9 predicts poor wound healing in diabetic foot ulcers: Response to Liu et al." *Diabetes care*, vol. 32, no. 11, p. e138, nov 2009. doi:10.2337/dc09-0770. [Online]. Available: http://www.ncbi.nlm.nih.gov/pubmed/19875601

[153] G. Schultz and B. Mast, "Molecular analysis of the environments of healing and chronic wounds: cytokines, proteases and growth factors," *Primary Intention*, vol. 2, pp. 7–14, 1999. [Online]. Available: http://www.awma.com.au/journal/0701{_}01.pdf

[154] D. Gibson and G. Schultz, "Chronic wound diagnostic for matrix metalloproteinase," *Wound Healing Southern Africa*, vol. 2, no. 2, pp. 68–70, 2009.

[155] E. a. Rayment, Z. Upton, and G. K. Shooter, "Increased matrix metalloproteinase-9 (MMP-9) activity observed in chronic wound fluid is related to the clinical severity of the ulcer." *The British journal of dermatology*, vol. 158, no. 5, pp. 951–61, may 2008. doi:10.1111/j.1365-2133.2008.08462.x. [Online]. Available: http://www.ncbi.nlm.nih.gov/pubmed/18284390

[156] M. J. Reiss, Y.-P. Han, E. Garcia, M. Goldberg, H. Yu, and W. L. Garner, "Matrix metalloproteinase-9 delays wound healing in a murine wound model." *Surgery*, vol. 147, no. 2, pp. 295–302, feb 2010. doi:10.1016/j.surg.2009.10.016. [Online]. Available: http://www.pubmedcentral.nih.gov/articlerender.fcgi?artid=2813947{&}tool=pmcentrez{&}rendertype=abstract

[157] Y. Liu, D. Min, T. Bolton, and V. Nubé, "Increased matrix metalloproteinase-9 predicts poor wound healing in diabetic foot ulcers," *Diabetes care*, vol. 32, no. 1, pp. 1734–1736, 2009. doi:10.2337/dc08-0763. [Online]. Available: http://care.diabetesjournals.org/content/32/1/117.short

[158] A. N. Moor, D. J. Vachon, and L. J. Gould, "Proteolytic activity in wound fluids and tissues derived from chronic venous leg ulcers." *Wound repair and regeneration : official publication of the Wound Healing Society [and] the European Tissue Repair Society*, vol. 17, no. 6, pp. 832–9, 2009. doi:10.1111/j.1524-475X.2009.00547.x. [Online]. Available: http://www.ncbi.nlm.nih.gov/pubmed/19903304

[159] E. R. Utz, E. a. Elster, D. K. Tadaki, F. Gage, P. W. Perdue, J. a. Forsberg, A. Stojadinovic, J. S. Hawksworth, and T. S. Brown, "Metalloproteinase expression is associated with traumatic wound failure." *The Journal of surgical research*, vol. 159, no. 2, pp. 633–9, apr 2010. doi:10.1016/j.jss.2009.08.021. [Online]. Available: http://www.ncbi.nlm.nih.gov/pubmed/20056248

[160] A. D. Widgerow, "Chronic wound fluid–thinking outside the box." *Wound repair and regeneration : official publication of the Wound Healing Society [and] the European Tissue Repair Society*, vol. 19, no. 3, pp. 287–91, 2011. doi:10.1111/j.1524-475X.2011.00683.x. [Online]. Available: http://www.ncbi.nlm.nih.gov/pubmed/21518088

[161] A. Iuonut, G. Dindelegan, and C. Ciuce, "Proteases as biomarkers in wound healing," *Timisoara Medical Journal*, vol. 1, no. 2, pp. 65–73, 2011. [Online]. Available: http://tmj.ro/article.php?art=368079722132831

[162] S. A. Eming, M. Koch, A. Krieger, B. Brachvogel, S. Kreft, L. Bruckner-Tuderman, T. Krieg, J. D. Shannon, and J. W. Fox, "Differential proteomic analysis distinguishes tissue repair biomarker signatures in wound exudates obtained from normal healing and chronic wounds." *Journal of proteome research*, vol. 9, no. 9, pp. 4758–66, sep 2010. doi:10.1021/pr100456d. [Online]. Available: http://www.ncbi.nlm.nih.gov/pubmed/20666496

[163] A. Hasmann, E. Wehrschuetz-Sigl, G. Kanzler, U. Gewessler, E. Hulla, K. P. Schneider, B. Binder, M. Schintler, and G. M. Guebitz, "Novel peptidoglycan-based diagnostic devices for detection of wound infection." *Diagnostic microbiology and infectious disease*, vol. 71, no. 1, pp. 12–23, sep 2011. doi:10.1016/j.diagmicrobio.2010.09.009. [Online]. Available: http://www.ncbi.nlm.nih.gov/pubmed/21388768

[164] T. M. Battaglia, J. F. Masson, M. R. Sierks, S. P. Beaudoin, J. Rogers, K. N. Foster, G. A. Holloway, and K. S. Booksh, "Quantification of cytokines involved in wound healing using surface plasmon resonance," *Analytical Chemistry*, vol. 77, no. 21, pp. 7016–7023, 2005.

[165] N. J. Trengove, H. Bielefeldt-Ohmann, and M. C. Stacey, "Mitogenic activity and cytokine levels in non-healing and healing chronic leg ulcers," *Wound Repair and Regeneration*, vol. 8, no. 1, pp. 13–25, 2000.

[166] A. Ambrosch, R. Lobmann, A. Pott, and J. Preißler, "Interleukin-6 concentrations in wound fluids rather than serological markers are useful in assessing bacterial triggers of ulcer inflammation," *International Wound Journal*, vol. 5, no. 1, pp. 99–106, 2008.

[167] B. Stephens, P. and Moseley, R. and Clark, R. and Cullen, "DIAGNOSTIC MARKERS OF WOUND INFECTION," 2008. [Online]. Available: http://www.google.im/patents/WO2008119974A1?cl=ja

[168] C. C. Finnerty, R. Przkora, D. N. Herndon, and M. G. Jeschke, "Cytokine expression profile over time in burned mice," *Cytokine*, vol. 45, no. 1, pp. 20–25, 2009.

[169] S. Iizaka, H. Sanada, T. Minematsu, M. Oba, G. Nakagami, H. Koyanagi, T. Nagase, C. Konya, and J. Sugama, "Do nutritional markers in wound fluid reflect pressure ulcer status?" *Wound repair and regeneration : official publication of the Wound Healing Society [and] the European Tissue Repair Society*, vol. 18, no. 1, pp. 31–7, 2010. doi:10.1111/j.1524-475X.2009.00564.x. [Online]. Available: http://www.ncbi.nlm.nih.gov/pubmed/20082679

[170] T. J. James, M. a. Hughes, G. W. Cherry, and R. P. Taylor, "Simple biochemical markers to assess chronic wounds." *Wound repair and regeneration : official publication of the Wound Healing Society [and] the European Tissue Repair Society*, vol. 8, no. 4, pp. 264–9, 2000. [Online]. Available: http://www.ncbi.nlm.nih.gov/pubmed/11013017

[171] S. Schreml, M. Landthaler, M. Schäferling, and P. Babilas, "A new star on the H2O2rizon of wound healing?" *Experimental dermatology*, vol. 20, no. 3, pp. 229–31, mar 2011. doi:10.1111/j.1600-0625.2010.01195.x. [Online]. Available: http://www.ncbi.nlm.nih.gov/pubmed/21323744

[172] M. Wlaschek and K. Scharffetter-Kochanek, "Oxidative stress in chronic venous leg ulcers," *Wound Repair and Regeneration*, vol. 13, no. 5, pp. 452–461, sep 2005. doi:10.1111/j.1067-1927.2005.00065.x. [Online]. Available: http://doi.wiley.com/10.1111/j.1067-1927.2005.00065.x

[173] N. Bryan, H. Ahswin, N. Smart, Y. Bayon, S. Wohlert, and J. A. Hunt, "Reactive oxygen species (ROS) - a family of fate deciding molecules pivotal in constructive inflammation and wound healing ." *European Cells and Materials*, vol. 24, pp. 249–26, 2012.

[174] A. Soneja, M. Drews, and T. Malinski, "Role of nitric oxide, nitroxidative and oxidative stress in wound healing," *Pharmacological Reports*, vol. 57, pp. 108–119, 2005. [Online]. Available: http://rabbit.if-pan.krakow.pl/pjp/pdf/2005/s{_}108.pdf

[175] S. Roy, S. Khanna, K. Nallu, T. K. Hunt, and C. K. Sen, "Dermal wound healing is subject to redox control." *Molecular therapy : the journal of the American Society of Gene Therapy*, vol. 13, no. 1, pp. 211–20, jan 2006. doi:10.1016/j.ymthe.2005.07.684. [Online]. Available: http://www.pubmedcentral.nih.gov/articlerender.fcgi?artid=1389791{&}tool=pmcentrez{&}rendertype=abstract

[176] S. Dhall, D. Do, M. Garcia, D. S. Wijesinghe, A. Brandon, J. Kim, A. Sanchez, J. Lyubovitsky, S. Gallagher, E. a. Nothnagel, C. E. Chalfant, R. P. Patel, N. Schiller, and M. Martins-Green, "A novel model of chronic wounds: importance of redox imbalance and biofilm-forming bacteria for establishment of chronicity." *PloS one*, vol. 9, no. 10, p. e109848, jan 2014. doi:10.1371/journal.pone.0109848. [Online]. Available: http://www.pubmedcentral.nih.gov/articlerender.fcgi?artid=4196950{&}tool=pmcentrez{&}rendertype=abstract

[177] T. J. James, M. A. Hughes, G. W. Cherry, and R. P. Taylor, "Evidence of oxidative stress in chronic venous ulcers," *Wound Repair and Regeneration*, vol. 11, no. 3, pp. 172–176, may 2003. doi:10.1046/j.1524-475X.2003.11304.x. [Online]. Available: http://doi.wiley.com/10.1046/j.1524-475X.2003.11304.x

[178] S. Yeoh-Ellerton and M. C. Stacey, "Iron and 8-isoprostane levels in acute and chronic wounds." *The Journal of investigative dermatology*, vol. 121, no. 4, pp. 918–25, oct 2003. doi:10.1046/j.1523-1747.2003.12471.x. [Online]. Available: http://www.ncbi.nlm.nih.gov/pubmed/14632213

[179] R. Moseley, J. R. Hilton, R. J. Waddington, K. G. Harding, P. Stephens, and D. W. Thomas, "Comparison of oxidative stress biomarker profiles between acute and chronic wound environments." *Wound repair and regeneration : official publication of the Wound Healing Society [and] the European Tissue Repair Society*, vol. 12, no. 4, pp. 419–29, 2004. doi:10.1111/j.1067-1927.2004.12406.x. [Online]. Available: http://www.ncbi.nlm.nih.gov/pubmed/15260807

[180] M. B. Witte and A. Barbul, "Role of nitric oxide in wound repair," *The American Journal of Surgery*, vol. 183, no. 4, pp. 406–412, apr 2002. doi:10.1016/S0002-9610(02)00815-2. [Online]. Available: http://www.sciencedirect.com/science/article/pii/S0002961002008152http://linkinghub.elsevier.com/retrieve/pii/S0002961002008152

[181] A. C. Browne, M. Vearncombe, and R. G. Sibbald, "High bacterial load in asymptomatic diabetic patients with neurotrophic ulcers retards wound healing after application of Dermagraft." University of Toronto, Toronto, Canada., Tech. Rep. 10, 2001. [Online]. Available: http://cawc.net/images/uploads/resources/Sibbald{_}bact.pdf

[182] Y. N. Pierpont, M. G. Uberti, F. Ko, M. C. Robson, C. a. Smith, T. E. Wright, and W. G. Payne, "Individualized, targeted wound treatment based on the tissue bacterial level as a biological marker." *American journal of surgery*, vol. 202, no. 2, pp. 220–4, aug 2011. doi:10.1016/j.amjsurg.2010.09.009. [Online]. Available: http://www.ncbi.nlm.nih.gov/pubmed/21185550

[183] C. M. Mouës, A. W. van Toorenenbergen, F. Heule, W. C. Hop, and S. E. R. Hovius, "The role of topical negative pressure in wound repair: expression of biochemical markers in wound fluid during wound healing." *Wound repair and regeneration*, vol. 16, no. 4, pp. 488–94, 2008. doi:10.1111/j.1524-475X.2008.00395.x. [Online]. Available: http://www.ncbi.nlm.nih.gov/pubmed/18638266

[184] M. Hentzer, K. Riedel, T. B. Rasmussen, A. Heydorn, J. B. Andersen, M. R. Parsek, S. a. Rice, L. Eberl, S. Molin, N. Høiby, S. Kjelleberg, and M. Givskov, "Inhibition of quorum sensing in Pseudomonas aeruginosa biofilm bacteria by a halogenated furanone compound." *Microbiology (Reading, England)*, vol. 148, no. Pt 1, pp. 87–102, jan 2002. [Online]. Available: http://www.ncbi.nlm.nih.gov/pubmed/11782502

[185] L. C. M. Antunes, R. B. R. Ferreira, M. M. C. Buckner, and B. B. Finlay, "Quorum sensing in bacterial virulence." *Microbiology (Reading, England)*, vol. 156, no. Pt 8, pp. 2271–82, aug 2010. doi:10.1099/mic.0.038794-0. [Online]. Available: http://www.ncbi.nlm.nih.gov/pubmed/20488878

[186] A. B. Wysocki, L. Staiano-Coico, and F. Grinnell, "Wound fluid from chronic leg ulcers contains elevated levels of metalloproteinases MMP-2 and MMP-9." *The Journal of investigative dermatology*, vol. 101, no. 1, pp. 64–68, 1993.

[187] D. R. Yager, L. Y. Zhang, H. X. Liang, R. F. Diegelmann, and I. K. Cohen, "Wound fluids from human pressure ulcers contain elevated matrix metalloproteinase levels and activity compared to surgical wound fluids." *The Journal of investigative dermatology*, vol. 107, no. 5, pp. 743–748, 1996.

[188] G. P. Ladwig, M. C. Robson, R. Liu, M. A. Kuhn, D. F. Muir, and G. S. Schultz, "Ratios of activated matrix metalloproteinase-9 to tissue inhibitor of matrix metalloproteinase-1 in wound fluids are inversely correlated with healing of pressure ulcers," *Wound Repair and Regeneration*, vol. 10, no. 1, pp. 26–37, 2002.

[189] R. H. Caulfield, M. P. H. Tyler, J. M. Austyn, P. Dziewulski, and D. A. McGrouther, "The relationship between protease/anti-protease profile, angiogenesis and re-epithelialisation in acute burn wounds." *Burns : journal of the International Society for Burn Injuries*, vol. 34, no. 4, pp. 474–86, jun 2008. doi:10.1016/j.burns.2007.07.012. [Online]. Available: http://www.ncbi.nlm.nih.gov/pubmed/17980970

[190] H. P. Hofer, E. Kukovetz, W. Petek, F. Schweighofer, R. Wildburger, and R. J. Schaur, "Released PMN elastase: an indicator of postsurgical uneventful wound healing and early inflammatory complications. A contribution to the search for objective criteria in wound healing monitoring." *Injury*, vol. 26, no. 2, pp. 103–6, mar 1995. [Online]. Available: http://www.ncbi.nlm.nih.gov/pubmed/7721460

[191] S. A. Abd-El-Aleem, M. W. J. Ferguson, I. Appleton, S. Kairsingh, E. B. Jude, K. Jones, C. N. McCollum, and G. W. Ireland, "Expression of nitric oxide synthase isoforms and arginase in normal human skin and chronic venous leg ulcers," *The Journal of Pathology*, vol. 191, no. 4, pp. 434–442, aug 2000. doi:10.1002/1096-9896(2000)9999:9999¡::AID-PATH654¿3.0.CO;2-S. [Online]. Available: http://doi.wiley.com/10.1002/1096-9896(2000)9999:9999⟨::AID-PATH654⟩3.0.CO;2-S

[192] E. Jude, A. Boulton, M. Ferguson, and I. Appleton, "The role of nitric oxide synthase isoforms and arginase in the pathogenesis of diabetic foot ulcers: possible modulatory effects by transforming growth factor beta 1," *Diabetologia*, vol. 42, pp. 748–757, 1999. [Online]. Available: http://link.springer.com/article/10.1007/s001250051224

[193] L. Xu, S. V. McLennan, L. Lo, A. Natfaji, T. Bolton, Y. Liu, S. M. Twigg, and D. K. Yue, "Bacterial load predicts healing rate in neuropathic diabetic foot ulcers." *Diabetes care*, vol. 30, no. 2, pp. 378–80, feb 2007. doi:10.2337/dc06-1383. [Online]. Available: http://www.ncbi.nlm.nih.gov/pubmed/17259515

[194] S. F. Bernatchez, V. Menon, J. Stoffel, S.-A. H. Walters, W. E. Lindroos, M. C. Crossland, L. G. Shawler, S. P. Crossland, and J. V. Boykin, "Nitric oxide levels in wound fluid may reflect the healing trajectory." *Wound repair and regeneration : official publication of the Wound Healing Society [and] the European Tissue Repair Society*, vol. 21, no. 3, pp. 410–7, 2013. doi:10.1111/wrr.12048. [Online]. Available: http://www.ncbi.nlm.nih.gov/pubmed/23627618

[195] D. J. Gibson and G. S. Schultz, "Molecular Wound Assessments: Matrix Metalloproteinases." *Advances in wound care*, vol. 2, no. 1, pp. 18–23, feb 2013. doi:10.1089/wound.2011.0359. [Online]. Available: http://www.pubmedcentral.nih.gov/articlerender.fcgi?artid=3623589{&}tool=pmcentrez{&}rendertype=abstract

[196] G. M. Whitesides, "Cool, or simple and cheap? Why not both?" *Lab on a chip*, vol. 13, no. 1, pp. 11–3, jan 2013. doi:10.1039/c2lc90109a. [Online]. Available: http://www.ncbi.nlm.nih.gov/pubmed/23165967

[197] L. Gervais and E. Delamarche, "Toward one-step point-of-care immunodiagnostics using capillary-driven microfluidics and PDMS substrates," *Lab on a Chip*, vol. 9, no. 23, 2009. doi:10.1039/b906523g. [Online]. Available: http://pubs.rsc.org/EN/content/articlehtml/2009/lc/b906523g

[198] C. Kantak, Q. Zhu, S. Beyer, T. Bansal, and D. Trau, "Utilizing microfluidics to synthesize polyethylene glycol microbeads for Förster resonance energy transfer based glucose sensing." *Biomicrofluidics*, vol. 6, no. 2, pp. 22 006–220 069, jun 2012. doi:10.1063/1.3694869. [Online]. Available: http://www.pubmedcentral.nih.gov/articlerender.fcgi?artid=3360714{&}tool=pmcentrez{&}rendertype=abstract

[199] D. Choi, E. Jang, J. Park, and W. Koh, "Development of microfluidic devices incorporating non-spherical hydrogel microparticles for protein-based bioassay," *Microfluidics and nanofluidics*, pp. 703–710, 2008. doi:10.1007/s10404-008-0303-7. [Online]. Available: http://link.springer.com/article/10.1007/s10404-008-0303-7

[200] E. Jang, S. Kim, and W.-G. Koh, "Microfluidic bioassay system based on microarrays of hydrogel sensing elements entrapping quantum dot-enzyme conjugates." *Biosensors & bioelectronics*, vol. 31, no. 1, pp. 529–36, jan 2012. doi:10.1016/j.bios.2011.11.033. [Online]. Available: http://www.ncbi.nlm.nih.gov/pubmed/22177543

[201] E. Jang, K. J. Son, B. Kim, and W.-G. Koh, "Phenol biosensor based on hydrogel microarrays entrapping tyrosinase and quantum dots." *The Analyst*, vol. 135, no. 11, pp. 2871–8, nov 2010. doi:10.1039/c0an00353k. [Online]. Available: http://www.ncbi.nlm.nih.gov/pubmed/20852777

[202] V. K. Yadavalli, W.-G. Koh, G. J. Lazur, and M. V. Pishko, "Microfabricated protein-containing poly(ethylene glycol) hydrogel arrays for biosensing," *Sensors and Actuators B: Chemical*, vol. 97, no. 2-3, pp. 290–297, feb 2004. doi:10.1016/j.snb.2003.08.030. [Online]. Available: http://linkinghub.elsevier.com/retrieve/pii/S0925400503007172

[203] W.-G. Koh and M. Pishko, "Immobilization of multi-enzyme microreactors inside microfluidic devices," *Sensors and Actuators B: Chemical*, vol. 106, no. 1, pp. 335–342, apr 2005. doi:10.1016/j.snb.2004.08.025. [Online]. Available: http://linkinghub.elsevier.com/retrieve/pii/S092540050400557X

[204] L. Lin, Z. Gao, H. Wei, H. Li, F. Wang, and J.-M. Lin, "Fabrication of a gel particle array in a microfluidic device for bioassays of protein and glucose in human urine samples." *Biomicrofluidics*, vol. 5, no. 3, pp. 34 112–3 411 210, sep 2011. doi:10.1063/1.3623412. [Online]. Available: http://www.pubmedcentral.nih.gov/articlerender.fcgi?artid=3364827{&}tool=pmcentrez{&}rendertype=abstract

[205] N. Y. Lee, Y. K. Jung, and H. G. Park, "On-chip colorimetric biosensor based on polydiacetylene (PDA) embedded in photopolymerized poly(ethylene glycol) diacrylate (PEG-DA) hydrogel," *Biochemical Engineering Journal*, vol. 29, no. 1-2, pp. 103–108, apr 2006. doi:10.1016/j.bej.2005.02.025. [Online]. Available: http://linkinghub.elsevier.com/retrieve/pii/S1369703X05001762

[206] Q. Wang, Z. Yang, L. Wang, M. Ma, and B. Xu, "Molecular hydrogel-immobilized enzymes exhibit superactivity and high stability in organic solvents." *Chemical communications (Cambridge, England)*, no. 10, pp. 1032–4, mar 2007. doi:10.1039/b615223f. [Online]. Available: http://www.ncbi.nlm.nih.gov/pubmed/17325796

[207] V. a. Pedrosa, J. Yan, A. L. Simonian, and A. Revzin, "Micropatterned Nanocomposite Hydrogels for Biosensing Applications," *Electroanalysis*, vol. 23, no. 5, pp. 1142–1149, may 2011. doi:10.1002/elan.201000654. [Online]. Available: http://doi.wiley.com/10.1002/elan.201000654

[208] J. Liu, D. Gao, H.-F. Li, and J.-M. Lin, "Controlled photopolymerization of hydrogel microstructures inside microchannels for bioassays." *Lab on a chip*, vol. 9, no. 9, pp. 1301–5, may 2009. doi:10.1039/b819219g. [Online]. Available: http://www.ncbi.nlm.nih.gov/pubmed/19370254

[209] I. V. Dimitrov, E. B. Petrova, R. G. Kozarova, M. D. Apostolova, and C. B. Tsvetanov, "A mild and versatile approach for DNA encapsulation," *Soft Matter*, vol. 7, no. 18, p. 8002, 2011. doi:10.1039/c1sm05805c. [Online]. Available: http://xlink.rsc.org/?DOI=c1sm05805c

[210] K. G. Lee, T. J. Park, S. Y. Soo, K. W. Wang, B. I. I. Kim, J. H. Park, C.-S. Lee, D. H. Kim, and S. J. Lee, "Synthesis and utilization of E. coli-encapsulated PEG-based microdroplet using a microfluidic chip for biological application." *Biotechnology and bioengineering*, vol. 107, no. 4, pp. 747–51, nov 2010. doi:10.1002/bit.22861. [Online]. Available: http://www.ncbi.nlm.nih.gov/pubmed/20632371

[211] W.-G. Koh, A. Revzin, and M. V. Pishko, "Poly(ethylene glycol) hydrogel microstructures encapsulating living cells." *Langmuir : the ACS journal of surfaces and colloids*, vol. 18, no. 7, pp. 2459–62, apr 2002. [Online]. Available: http://www.ncbi.nlm.nih.gov/pubmed/12088033

[212] D. R. Albrecht, V. L. Tsang, R. L. Sah, and S. N. Bhatia, "Photo- and electropatterning of hydrogel-encapsulated living cell arrays." *Lab on a chip*, vol. 5, no. 1, pp. 111–8, jan 2005. doi:10.1039/b406953f. [Online]. Available: http://www.ncbi.nlm.nih.gov/pubmed/15616749

[213] J. Heo, K. J. Thomas, G. H. Seong, and R. M. Crooks, "A microfluidic bioreactor based on hydrogel-entrapped E. coli: cell viability, lysis, and intracellular enzyme reactions." *Analytical chemistry*, vol. 75, no. 1, pp. 22–6, jan 2003. [Online]. Available: http://www.ncbi.nlm.nih.gov/pubmed/12530814

[214] Y.-J. Eun, A. S. Utada, M. F. Copeland, S. Takeuchi, and D. B. Weibel, "Encapsulating bacteria in agarose microparticles using microfluidics for high-throughput cell analysis and isolation." *ACS chemical biology*, vol. 6, no. 3, pp. 260–6, mar 2011. doi:10.1021/cb100336p. [Online]. Available: http://www.pubmedcentral.nih.gov/articlerender.fcgi?artid=3060957{&}tool=pmcentrez{&}rendertype=abstract

[215] X. Li, D. R. Ballerini, and W. Shen, "A perspective on paper-based microfluidics: Current status and future trends." *Biomicrofluidics*, vol. 6, no. 1, pp. 11 301–1 130 113, mar 2012. doi:10.1063/1.3687398. [Online]. Available: http://www.pubmedcentral.nih.gov/articlerender.fcgi?artid=3365319{&}tool=pmcentrez{&}rendertype=abstract

[216] A. G. Lee, C. P. Arena, D. J. Beebe, and S. P. Palecek, "Development of macroporous poly(ethylene glycol) hydrogel arrays within microfluidic channels." *Biomacromolecules*, vol. 11, no. 12, pp. 3316–24, dec 2010. doi:10.1021/bm100792y. [Online]. Available: http://www.pubmedcentral.nih.gov/articlerender.fcgi?artid=3006031{&}tool=pmcentrez{&}rendertype=abstract

[217] H. M. Simms, C. M. Brotherton, B. T. Good, R. H. Davis, K. S. Anseth, and C. N. Bowman, "In situ fabrication of macroporous polymer networks within microfluidic devices by living radical photopolymerization and leaching." *Lab on a chip*, vol. 5, no. 2, pp. 151–7, feb 2005. doi:10.1039/b412589d. [Online]. Available: http://www.ncbi.nlm.nih.gov/pubmed/15672128

[218] C. L. Lewis, Y. Lin, C. Yang, A. K. Manocchi, K. P. Yuet, P. S. Doyle, and H. Yi, "Microfluidic fabrication of hydrogel microparticles containing functionalized viral nanotemplates." *Langmuir : the ACS journal of surfaces and colloids*, vol. 26, no. 16, pp. 13 436–41, aug 2010. doi:10.1021/la102446n. [Online]. Available: http://www.pubmedcentral.nih.gov/articlerender.fcgi?artid=2922968{&}tool=pmcentrez{&}rendertype=abstract

[219] L. N. Kim, S.-e. Choi, J. Kim, H. Kim, and S. Kwon, "Single exposure fabrication and manipulation of 3D hydrogel cell microcarriers." *Lab on a chip*, vol. 11, no. 1, pp. 48–51, jan 2011. doi:10.1039/c0lc00369g. [Online]. Available: http://www.ncbi.nlm.nih.gov/pubmed/20981360

[220] S. E. Chung, W. Park, S. Shin, S. A. Lee, and S. Kwon, "Guided and fluidic self-assembly of microstructures using railed microfluidic channels." *Nature materials*, vol. 7, no. 7, pp. 581–7, jul 2008. doi:10.1038/nmat2208. [Online]. Available: http://www.ncbi.nlm.nih.gov/pubmed/18552850

[221] D. C. Appleyard, S. C. Chapin, R. L. Srinivas, and P. S. Doyle, "Bar-coded hydrogel microparticles for protein detection: synthesis, assay and scanning." *Nature protocols*, vol. 6, no. 11, pp. 1761–74, nov 2011. doi:10.1038/nprot.2011.400. [Online]. Available: http://www.ncbi.nlm.nih.gov/pubmed/22015846

[222] W.-H. Tan and S. Takeuchi, "Monodisperse Alginate Hydrogel Microbeads for Cell Encapsulation," *Advanced Materials*, vol. 19, no. 18, pp. 2696–2701, sep 2007. doi:10.1002/adma.200700433. [Online]. Available: http://doi.wiley.com/10.1002/adma.200700433

[223] R. F. Shepherd, J. C. Conrad, S. K. Rhodes, D. R. Link, M. Marquez, D. a. Weitz, and J. a. Lewis, "Microfluidic assembly of homogeneous and Janus colloid-filled hydrogel granules." *Langmuir : the ACS journal of surfaces and colloids*, vol. 22, no. 21, pp. 8618–22, oct 2006. doi:10.1021/la060759+. [Online]. Available: http://www.ncbi.nlm.nih.gov/pubmed/17014093

[224] C.-h. Choi, J. Jung, T. Hwang, and C. Lee, "In situ microfluidic synthesis of monodisperse PEG microspheres," *Macromolecular Research*, vol. 17, no. 3, pp. 163–167, 2009. [Online]. Available: http://link.springer.com/article/10.1007/BF03218673

[225] F. Goldschmidtboeing, M. Rabold, and P. Woias, "Strategies for void-free liquid filling of micro cavities," *Journal of Micromechanics and Microengineering*, vol. 16, no. 7, pp. 1321–1330, jul 2006. doi:10.1088/0960-1317/16/7/029. [Online]. Available: http://stacks.iop.org/0960-1317/16/i=7/a=029?key=crossref.3ac3f0e14c666dbc23cc111391da0bad

[226] D. Puchberger-Enengl, S. Podszun, H. Heinz, C. Hermann, P. Vulto, and G. a. Urban, "Microfluidic concentration of bacteria by on-chip electrophoresis." *Biomicrofluidics*, vol. 5, no. 4, pp. 44 111–4 411 110, dec 2011. doi:10.1063/1.3664691. [Online]. Available: http://www.pubmedcentral.nih.gov/articlerender.fcgi?artid=3246011{&}tool=pmcentrez{&}rendertype=abstract

[227] P. Vulto, S. Podszun, P. Meyer, C. Hermann, A. Manz, and G. a. Urban, "Phaseguides: a paradigm shift in microfluidic priming and emptying." *Lab on a chip*, vol. 11, no. 9, pp. 1596–602, may 2011. doi:10.1039/c0lc00643b. [Online]. Available: http://www.ncbi.nlm.nih.gov/pubmed/21394334

[228] G. Takei, M. Nonogi, A. Hibara, T. Kitamori, and H.-B. Kim, "Tuning microchannel wettability and fabrication of multiple-step Laplace valves." *Lab on a chip*, vol. 7, no. 5, pp. 596–602, may 2007. doi:10.1039/b618851f. [Online]. Available: http://www.ncbi.nlm.nih.gov/pubmed/17476378

[229] J. Melin, G. Gimenéz, N. Roxhed, W. van der Wijngaart, and G. Stemme, "A fast passive and planar liquid sample micromixer." *Lab on a chip*, vol. 4, no. 3, pp. 214–9, jun 2004. doi:10.1039/b314080f. [Online]. Available: http://www.ncbi.nlm.nih.gov/pubmed/15159781

[230] S. Hakenberg, M. Hügle, M. Weidmann, F. Hufert, G. Dame, and G. a. Urban, "A phaseguided passive batch microfluidic mixing chamber for isothermal amplification." *Lab on a chip*, vol. 12, no. 21, pp. 4576–80, oct 2012. doi:10.1039/c2lc40765e. [Online]. Available: http://www.ncbi.nlm.nih.gov/pubmed/22952055

[231] R. J. Snyder, B. Cullen, and L. T. Nisbet, "An audit to assess the perspectives of US wound care specialists regarding the importance of proteases in wound healing and wound assessment." *International wound journal*, pp. 1–10, jul 2012. doi:10.1111/j.1742-481X.2012.01040.x. [Online]. Available: http://www.ncbi.nlm.nih.gov/pubmed/22846380

[232] N. J. Trengove, M. C. Stacey, S. Macauley, N. Bennett, J. Gibson, F. Burslem, G. Murphy, and G. Schultz, "Analysis of the acute and chronic wound environments: the role of proteases and their inhibitors," *Wound Repair and Regeneration*, vol. 7, no. 6, pp. 442–452, nov 1999. doi:10.1046/j.1524-475X.1999.00442.x. [Online]. Available: http://doi.wiley.com/10.1046/j.1524-475X.1999.00442.x

[233] S. E. Gardner, R. a. Frantz, C. L. Saltzman, S. L. Hillis, H. Park, and M. Scherubel, "Diagnostic validity of three swab techniques for identifying chronic wound infection." *Wound repair and regeneration : official publication of the Wound Healing Society [and] the European Tissue Repair Society*, vol. 14, no. 5, pp. 548–57, 2006. doi:10.1111/j.1743-6109.2006.00162.x. [Online]. Available: http://www.ncbi.nlm.nih.gov/pubmed/17014666

[234] H. Cho, H.-Y. Kim, J. Y. Kang, and T. S. Kim, "How the capillary burst microvalve works." *Journal of colloid and interface science*, vol. 306, no. 2, pp. 379–85, feb 2007. doi:10.1016/j.jcis.2006.10.077. [Online]. Available: http://www.sciencedirect.com/science/article/pii/S0021979706009969http://www.ncbi.nlm.nih.gov/pubmed/17141795

[235] Y. J. Wei, K. a. Li, and S. Y. Tong, "The interaction of Bromophenol Blue with proteins in acidic solution." *Talanta*, vol. 43, no. 1, pp. 1–10, jan 1996. doi:10.1016/0039-9140(95)01683-X. [Online]. Available: http://www.ncbi.nlm.nih.gov/pubmed/18966456

[236] D. a. Armbruster and T. Pry, "Limit of blank, limit of detection and limit of quantitation." *The Clinical biochemist. Reviews / Australian Association of Clinical Biochemists*, vol. 29 Suppl 1, no. August, pp. S49–52, aug 2008. [Online]. Available: http://www.pubmedcentral.nih.gov/articlerender.fcgi?artid=2556583{&}tool=pmcentrez{&}rendertype=abstract

[237] E. H. Estey, "Acute myeloid leukemia: 2012 update on diagnosis, risk stratification, and management." *American journal of hematology*, vol. 87, no. 1, pp. 89–99, jan 2012. doi:10.1002/ajh.22246. [Online]. Available: http://www.ncbi.nlm.nih.gov/pubmed/22180162

[238] G. Twig, A. Afek, A. Shamiss, E. Derazne, D. Tzur, B. Gordon, and A. Tirosh, "White blood cell count and the risk for coronary artery disease in young adults." *PloS one*, vol. 7, no. 10, p. e47183, jan 2012. doi:10.1371/journal.pone.0047183. [Online]. Available: http://www.pubmedcentral.nih.gov/articlerender.fcgi?artid=3470580{&}tool=pmcentrez{&}rendertype=abstract

[239] R. F. Diegelmann, "Excessive neutrophils characterize chronic pressure ulcers." *Wound repair and regeneration : official publication of the Wound Healing Society [and] the European Tissue Repair Society*, vol. 11, no. 6, pp. 490–5, 2003. [Online]. Available: http://www.ncbi.nlm.nih.gov/pubmed/14617291

[240] Y. Lee, H. J. Lee, K. J. Son, and W.-G. Koh, "Fabrication of hydrogel-micropatterned nanofibers for highly sensitive microarray-based immunosensors having additional enzyme-based sensing capability," *Journal of Materials Chemistry*, vol. 21, no. 12, p. 4476, 2011. doi:10.1039/c0jm03881d. [Online]. Available: http://xlink.rsc.org/?DOI=c0jm03881d

[241] T. Kreisig, R. Hoffmann, and T. Zuchner, "Homogeneous fluorescence-based immunoassay detects antigens within 90 seconds." *Analytical chemistry*, vol. 83, no. 11, pp. 4281–7, jun 2011. doi:10.1021/ac200777h. [Online]. Available: http://www.ncbi.nlm.nih.gov/pubmed/21495669

[242] P. G. Bowler, B. I. Duerden, and D. G. Armstrong, "Wound microbiology and associated approaches to wound management." *Clinical microbiology reviews*, vol. 14, no. 2, pp. 244–69, apr 2001. doi:10.1128/CMR.14.2.244-269.2001. [Online]. Available: http://cmr.asm.org/content/14/2/244.shorthttp://www.pubmedcentral.nih.gov/articlerender.fcgi?artid=88973{&}tool=pmcentrez{&}rendertype=abstract

[243] S. E. Gardner, R. A. Frantz, and B. N. Doebbeling, "The validity of the clinical signs and symptoms used to identify localized chronic wound infection," *Wound Repair and Regeneration*, vol. 9, no. 3, pp. 178–186, may 2001. doi:10.1046/j.1524-475x.2001.00178.x. [Online]. Available: http://doi.wiley.com/10.1046/j.1524-475x.2001.00178.x

[244] T. Bjarnsholt, K. Kirketerp-Møller, P. Ø. Jensen, K. G. Madsen, R. Phipps, K. Krogfelt, N. Høiby, and M. Givskov, "Why chronic wounds will not heal: a novel hypothesis." *Wound repair and regeneration : official publication of the Wound Healing Society [and] the European Tissue Repair Society*, vol. 16, no. 1, pp. 2–10, 2007. doi:10.1111/j.1524-475X.2007.00283.x. [Online]. Available: http://www.ncbi.nlm.nih.gov/pubmed/18211573

[245] R. D. Wolcott, D. D. Rhoads, and S. E. Dowd, "Biofilms and chronic wound inflammation." *Journal of wound care*, vol. 17, no. 8, pp. 333–41, aug 2008. doi:10.12968/jowc.2008.17.8.30796. [Online]. Available: http://www.ncbi.nlm.nih.gov/pubmed/18754194

[246] K. Gjødsbøl, J. J. Christensen, T. Karlsmark, B. Jørgensen, B. M. Klein, and K. A. Krogfelt, "Multiple bacterial species reside in chronic wounds: a longitudinal study," *International Wound Journal*, vol. 3, no. 3, pp. 225–231, sep 2006. doi:10.1111/j.1742-481X.2006.00159.x. [Online]. Available: http://doi.wiley.com/10.1111/j.1742-481X.2006.00159.x

[247] F. Jockenhöfer, V. Chapot, M. Stoffels-Weindorf, A. Körber, J. Klode, J. Buer, B. Küpper, A. Roesch, and J. Dissemond, "Bacterial spectrum colonizing chronic leg ulcers: a 10-year comparison from a German wound care center." *Journal der Deutschen Dermatologischen Gesellschaft = Journal of the German Society of Dermatology : JDDG*, vol. 12, no. 12, pp. 1121–7, dec 2014. doi:10.1111/ddg.12540. [Online]. Available: http://www.ncbi.nlm.nih.gov/pubmed/25482696

[248] A. J. Mangram, T. C. Horan, M. L. Pearson, L. C. Silver, and W. R. Jarvis, "Guideline for Prevention of Surgical Site Infection, 1999," *American Journal of Infection Control*, vol. 27, no. 2, pp. 97–134, apr 1999. doi:10.1016/S0196-6553(99)70088-X. [Online]. Available: http://linkinghub.elsevier.com/retrieve/pii/S019665539970088X

[249] L. J. Bessa, P. Fazii, M. Di Giulio, and L. Cellini, "Bacterial isolates from infected wounds and their antibiotic susceptibility pattern: some remarks about wound infection." *International wound journal*, vol. 12, no. 1, pp. 47–52, feb 2015. doi:10.1111/iwj.12049. [Online]. Available: http://www.ncbi.nlm.nih.gov/pubmed/23433007

[250] J. Dissemond, "Methicillin resistant Staphylococcus aureus (MRSA): Diagnostic, clinical relevance and therapy." *Journal der Deutschen Dermatologischen Gesellschaft = Journal of the German Society of Dermatology : JDDG*, vol. 7, no. 6, pp. 544–51; quiz 552–3, jun 2009. doi:10.1111/j.1610-0387.2009.07015.x. [Online]. Available: http://www.ncbi.nlm.nih.gov/pubmed/19302228

[251] S. M. Madsen, H. Westh, L. Danielsen, and V. T. Rosdahl, "Bacterial colonization and healing of venous leg ulcers," *APMIS*, vol. 104, no. 7-8, pp. 895–899, jul 1996. doi:10.1111/j.1699-0463.1996.tb04955.x. [Online]. Available: http://doi.wiley.com/10.1111/j.1699-0463.1996.tb04955.x

[252] J. N. Jacobsen, A. S. Andersen, M. K. Sonnested, I. Laursen, B. Jorgensen, and K. A. Krogfelt, "Investigating the humoral immune response in chronic venous leg ulcer patients colonised with Pseudomonas aeruginosa." *International wound journal*, vol. 8, no. 1, pp. 33–43, feb 2011. doi:10.1111/j.1742-481X.2010.00741.x. [Online]. Available: http://www.ncbi.nlm.nih.gov/pubmed/21091636

[253] K. Kirketerp-Møller, P. Ø. Jensen, M. Fazli, K. G. Madsen, J. Pedersen, C. Moser, T. Tolker-Nielsen, N. Høiby, M. Givskov, and T. Bjarnsholt, "Distribution, organization, and ecology of bacteria in chronic wounds." *Journal of clinical microbiology*, vol. 46, no. 8, pp. 2717–22, aug 2008. doi:10.1128/JCM.00501-08. [Online]. Available: http://www.pubmedcentral.nih.gov/articlerender.fcgi?artid=2519454{&}tool=pmcentrez{&}rendertype=abstract

[254] K. Gjødsbøl, M. E. Skindersoe, J. J. Christensen, T. Karlsmark, B. Jørgensen, A. M. Jensen, B. M. Klein, M. K. Sonnested, and K. A. Krogfelt, "No need for biopsies: comparison of three sample techniques for wound microbiota determination." *International wound journal*, vol. 9, no. 3, pp. 295–302, jul 2012. doi:10.1111/j.1742-481X.2011.00883.x. [Online]. Available: http://www.ncbi.nlm.nih.gov/pubmed/22067000

[255] M. E. Smith, N. Robinowitz, P. Chaulk, and K. Johnson, "Comparison of chronic wound culture techniques: swab versus curetted tissue for microbial recovery." *British journal of community nursing*, vol. Suppl, no. 9 0, pp. S22–6, sep 2014. doi:10.12968/bjcn.2014.19.Sup9.S22. [Online]. Available: http://www.pubmedcentral.nih.gov/articlerender.fcgi?artid=4267254{&}tool=pmcentrez{&}rendertype=abstract

[256] J. Dissemond, "[Chronic wounds and bacteria. Clinical relevance, detection and therapy]." *Der Hautarzt; Zeitschrift für Dermatologie, Venerologie, und verwandte Gebiete*, vol. 65, no. 1, pp. 10–4, jan 2014. doi:10.1007/s00105-013-2635-9. [Online]. Available: http://www.ncbi.nlm.nih.gov/pubmed/24343032

[257] M. Rüttermann, A. Maier-Hasselmann, B. Nink-Grebe, and M. Burckhardt, "Local treatment of chronic wounds: in patients with peripheral vascular disease, chronic venous insufficiency, and diabetes." *Deutsches Ärzteblatt international*, vol. 110, no. 3, pp. 25–31, jan 2013. doi:10.3238/arztebl.2013.0025. [Online]. Available: http://www.pubmedcentral.nih.gov/articlerender.fcgi?artid=3566621{&}tool=pmcentrez{&}rendertype=abstract

[258] A. M. Misic, S. E. Gardner, and E. a. Grice, "The Wound Microbiome: Modern Approaches to Examining the Role of Microorganisms in Impaired Chronic Wound Healing." *Advances in wound care*, vol. 3, no. 7, pp. 502–510, jul 2014. doi:10.1089/wound.2012.0397. [Online]. Available: http://www.pubmedcentral.nih.gov/articlerender.fcgi?artid=4086514{&}tool=pmcentrez{&}rendertype=abstract

[259] R. D. Wolcott and S. E. Dowd, "A rapid molecular method for characterising bacterial bioburden in chronic wounds." *Journal of wound care*, vol. 17, no. 12, pp. 513–6, dec 2008. doi:10.12968/jowc.2008.17.12.31769. [Online]. Available: http://www.ncbi.nlm.nih.gov/pubmed/19052515

[260] S. Malic, K. E. Hill, A. Hayes, S. L. Percival, D. W. Thomas, and D. W. Williams, "Detection and identification of specific bacteria in wound biofilms using peptide nucleic acid fluorescent in situ hybridization (PNA FISH)." *Microbiology (Reading, England)*, vol. 155, no. Pt 8, pp. 2603–11, aug 2009. doi:10.1099/mic.0.028712-0. [Online]. Available: http://www.ncbi.nlm.nih.gov/pubmed/19477903

[261] R. Wolcott, J. Kennedy, and S. Dowd, "Regular debridement is the main tool for maintaining a healthy wound bed in most chronic wounds," *Journal of Wound Care*, vol. 18, no. 2, pp. 54–56, feb 2009. doi:10.12968/jowc.2009.18.2.38743. [Online]. Available: http://www.magonlinelibrary.com/doi/abs/10.12968/jowc.2009.18.2.38743

[262] D. D. Rhoads, R. W. Wolcott, K. F. Cutting, and S. L. Percival, "Evidence of Biofilms in Wounds and the Potential Ramifications," *Image (Rochester, N.Y.)*, pp. 1–15, 2007.

[263] M. E. Sesto Cabral, A. N. Ramos, A. J. Macedo, D. S. Trentin, J. Treter, R. H. Manzo, and J. C. Valdez, "Formulation and quality control of semi-solid containing harmless bacteria by-products: chronic wounds pro-healing activity." *Pharmaceutical development and technology*, vol. 00, no. 00, pp. 1–8, jul 2014. doi:10.3109/10837450.2014.938858. [Online]. Available: http://www.ncbi.nlm.nih.gov/pubmed/25004009

[264] C. Lui, N. C. Cady, and C. a. Batt, "Nucleic Acid-based Detection of Bacterial Pathogens Using Integrated Microfluidic Platform Systems." *Sensors (Basel, Switzerland)*, vol. 9, no. 5, pp. 3713–44, 2009. doi:10.3390/s90503713. [Online]. Available: http://www.pubmedcentral.nih.gov/articlerender.fcgi?artid=3297159{&}tool=pmcentrez{&}rendertype=abstract

[265] M. A. Dineva, L. MahiLum-Tapay, and H. Lee, "Sample preparation: a challenge in the development of point-of-care nucleic acid-based assays for resource-limited settings." *The Analyst*, vol. 132, no. 12, pp. 1193–1199, 2007.

[266] P. Vulto, G. Dame, U. Maier, S. Makohliso, S. Podszun, P. Zahn, and G. A. Urban, "A microfluidic approach for high efficiency extraction of low molecular weight RNA." *Lab on a chip*, vol. 10, no. 5, pp. 610–6, mar 2010. doi:10.1039/b913481f. [Online]. Available: http://www.ncbi.nlm.nih.gov/pubmed/20162236

[267] M. Zourob, S. Elwary, and A. Turner, *Principles of Bacterial Detection: Biosensors, Recognition Receptors and Microsystems*, M. Zourob, S. Elwary, and A. Turner, Eds. Springer, 2008. [Online]. Available: http://www.springerlink.com/index/10.1007/978-0-387-75113-9

[268] S. Haeberle and R. Zengerle, "Microfluidic platforms for lab-on-a-chip applications." *Lab on a chip*, vol. 7, no. 9, pp. 1094–110, sep 2007. doi:10.1039/b706364b. [Online]. Available: http://www.ncbi.nlm.nih.gov/pubmed/17713606

[269] L. Zhu, Q. Zhang, H. Feng, S. Ang, F. S. Chau, and W.-T. Liu, "Filter-based microfluidic device as a platform for immunofluorescent assay of microbial cells." *Lab on a chip*, vol. 4, no. 4, pp. 337–41, aug 2004. doi:10.1039/b401834f. [Online]. Available: http://www.ncbi.nlm.nih.gov/pubmed/15269801

[270] N. Bao and C. Lu, "A microfluidic device for physical trapping and electrical lysis of bacterial cells," *Applied Physics Letters*, vol. 92, no. 21, p. 214103, 2008. doi:10.1063/1.2937088. [Online]. Available: http://link.aip.org/link/APPLAB/v92/i21/p214103/s1{&}Agg=doi

[271] X. Guan, H. J. Zhang, Y. N. Bi, L. Zhang, and D. L. Hao, "Rapid detection of pathogens using antibody-coated microbeads with bioluminescence in microfluidic chips," *Biomedical Microdevices*, vol. 12, no. 4, pp. 683–691, 2010.

[272] K.-Y. Lien, W.-C. Lee, H.-Y. Lei, and G.-B. Lee, "Integrated reverse transcription polymerase chain reaction systems for virus detection." *Biosensors & bioelectronics*, vol. 22, no. 8, pp. 1739–1748, 2007. doi:10.1016/j.bios.2006.08.010

[273] N. Beyor, T. S. Seo, P. Liu, and R. A. Mathies, "Immunomagnetic bead-based cell concentration microdevice for dilute pathogen detection," *Biomedical Microdevices*, vol. 10, no. 6, pp. 909–917, 2008.

[274] P. Grodzinski, J. Yang, R. H. Liu, and M. D. Ward, "A modular microfluidic system for cell pre-concentration and genetic sample preparation," *Biomedical Microdevices*, vol. 5, no. 4, pp. 303–310, 2003.

[275] C. Yi, C. W. Li, S. Ji, and M. Yang, "Microfluidics technology for manipulation and analysis of biological cells," pp. 1–23, 2006.

[276] S. Derveaux, B. G. Stubbe, K. Braeckmans, C. Roelant, K. Sato, J. Demeester, and S. C. De Smedt, "Synergism between particle-based multiplexing and microfluidics technologies may bring diagnostics closer to the patient." *Analytical and bioanalytical chemistry*, vol. 391, no. 7, pp. 2453–67, aug 2008. doi:10.1007/s00216-008-2062-4. [Online]. Available: http://www.pubmedcentral.nih.gov/articlerender.fcgi?artid=2516543{&}tool=pmcentrez{&}rendertype=abstract

[277] H. Patten, "Identifying wound infection: taking a wound swab," *Wound Essentials*, vol. 5, pp. 64–66, 2010. [Online]. Available: http://scholar.google.com/scholar?hl=en{&}btnG=Search{&}q=intitle:IDENTIFYING+WOUND+INFECTION:+TAKING+A+SWAB{#}2

[278] T. J. Meerhoff, M. L. Houben, F. E. J. Coenjaerts, J. L. L. Kimpen, R. W. Hofland, F. Schellevis, and L. J. Bont, "Detection of multiple respiratory pathogens during primary respiratory infection: Nasal swab versus nasopharyngeal aspirate using real-time polymerase chain reaction," *European Journal of Clinical Microbiology and Infectious Diseases*, vol. 29, no. 4, pp. 365–371, 2010.

[279] K. Scherer, D. Mäde, L. Ellerbroek, J. Schulenburg, R. Johne, and G. Klein, "Application of a Swab Sampling Method for the Detection of Norovirus and Rotavirus on Artificially Contaminated Food and Environmental Surfaces," *Food and Environmental Virology*, vol. 1, no. 1, pp. 42–49, jan 2009. doi:10.1007/s12560-008-9007-0. [Online]. Available: http://link.springer.com/10.1007/s12560-008-9007-0

[280] C.-P. Jen and H.-H. Chang, "A handheld preconcentrator for the rapid collection of cancerous cells using dielectrophoresis generated by circular microelectrodes in stepping electric fields A handheld preconcentrator for the rapid collection of cancerous cells using dielectrophoresis," *Biomicrofluidics*, vol. 5, no. 3, p. 034101, 2011. doi:10.1063/1.3609263. [Online]. Available: http://link.aip.org/link/BIOMGB/v5/i3/p034101/s1{&}Agg=doi

[281] C. Church, J. Zhu, G. Huang, T.-r. Tzeng, and X. Xuan, "Integrated electrical concentration and lysis of cells in a microfluidic chip." *Biomicrofluidics*, vol. 4, no. 4, p. 44101, jan 2010. doi:10.1063/1.3496358. [Online]. Available: http://www.pubmedcentral.nih.gov/articlerender.fcgi?artid=2962669{&}tool=pmcentrez{&}rendertype=abstract

[282] D. Hou, S. Maheshwari, and H.-c. Chang, "Rapid bioparticle concentration and detection by combining a discharge driven vortex with surface enhanced Raman scattering Additional information on Biomicrofluidics Rapid bioparticle concentration and detection by combining a discharge driven vortex wit," *Biomicrofluidics*, vol. 1, no. 1, p. 14106, jan 2007. doi:10.1063/1.2710191. [Online]. Available: http://www.pubmedcentral.nih.gov/articlerender.fcgi?artid=2709947{&}tool=pmcentrez{&}rendertype=abstract

[283] M. Koklu, S. Park, S. D. Pillai, and A. Beskok, "Negative dielectrophoretic capture of bacterial spores in food matrices." *Biomicrofluidics*, vol. 4, no. 3, jan 2010. doi:10.1063/1.3479998. [Online]. Available: http://www.pubmedcentral.nih.gov/articlerender.fcgi?artid=2937042{&}tool=pmcentrez{&}rendertype=abstract

[284] B. H. Lapizco-Encinas, R. V. Davalos, B. A. Simmons, E. B. Cummings, and Y. Fintschenko, "An insulator-based (electrodeless) dielectrophoretic concentrator for microbes in water," in *Journal of Microbiological Methods*, vol. 62, no. 3 SPEC. ISS., 2005, pp. 317–326.

[285] F. Schönfeld, A. Griebel, R. Konrad, S. Rink, and F. Karlsen, "Development of a μ-concentrator using dielectrophoretic forces," *JALA - Journal of the Association for Laboratory Automation*, vol. 7, no. 6, pp. 130–134, 2002.

[286] E. T. Lagally, S.-H. Lee, and H. T. Soh, "Integrated microsystem for dielectrophoretic cell concentration and genetic detection." *Lab on a chip*, vol. 5, no. 10, pp. 1053–1058, 2005.

[287] R. S. Kuczenski, H.-c. Chang, and A. Revzin, "Dielectrophoretic microfluidic device for the continuous sorting of Escherichia coli from blood cells," *Biomicrofluidics*, vol. 5, no. 3, p. 032005, 2011. doi:10.1063/1.3608135. [Online]. Available: http://link.aip.org/link/BIOMGB/v5/i3/p032005/s1{&}Agg=doi

[288] Y.-K. Cho, T.-h. Kim, and J.-G. Lee, "On-chip concentration of bacteria using a 3D dielectrophoretic chip and subsequent laser-based DNA extraction in the same chip," *Journal of Micromechanics and Microengineering*, vol. 20, no. 6, p. 065010, jun 2010. doi:10.1088/0960-1317/20/6/065010. [Online]. Available: http://stacks.iop.org/0960-1317/20/i=6/a=065010?key=crossref.98b30f72892fe39a08c19de359c3f145

[289] I.-F. Cheng, H.-C. Chang, D. Hou, and H.-C. Chang, "An integrated dielectrophoretic chip for continuous bioparticle filtering, focusing, sorting, trapping, and detecting." *Biomicrofluidics*, vol. 1, no. 2, p. 21503, jan 2007. doi:10.1063/1.2723669. [Online]. Available: http://www.pubmedcentral.nih.gov/articlerender.fcgi?artid=2717572{&}tool=pmcentrez{&}rendertype=abstract

[290] R. S. W. Thomas, P. D. Mitchell, R. O. C. Oreffo, and H. Morgan, "Trapping single human osteoblast-like cells from a heterogeneous population using a dielectrophoretic microfluidic device Additional information on Biomicrofluidics Trapping single human osteoblast-like cells from a heterogeneous population using a dielec," *Biomicrofluidics*, vol. 4, no. 2, jan 2010. doi:10.1063/1.3406951. [Online]. Available: http://www.pubmedcentral.nih.gov/articlerender.fcgi?artid=2917881{&}tool=pmcentrez{&}rendertype=abstract

[291] K. Zhu, A. S. Kaprelyants, E. G. Salina, and G. H. Markx, "Separation by dielectrophoresis of dormant and nondormant bacterial cells of Mycobacterium smegmatis." *Biomicrofluidics*, vol. 4, no. 2, jan 2010. doi:10.1063/1.3435335. [Online]. Available: http://www.pubmedcentral.nih.gov/articlerender.fcgi?artid=2917864{&}tool=pmcentrez{&}rendertype=abstract

[292] A. Castellanos, A. Ramos, A. González, N. G. Green, and H. Morgan, "Electrohydrodynamics and dielectrophoresis in microsystems: scaling laws," *Journal of Physics D: Applied Physics*, vol. 36, no. 20, pp. 2584–2597, oct 2003. doi:10.1088/0022-3727/36/20/023. [Online]. Available: http://stacks.iop.org/0022-3727/36/i=20/a=023?key=crossref.769b89e02baedeedab5b2c5cdd466452

[293] J. Oh, R. Hart, J. Capurro, and H. M. Noh, "Comprehensive analysis of particle motion under non-uniform AC electric fields in a microchannel." *Lab on a chip*, vol. 9, no. 1, pp. 62–78, 2009. doi:10.1039/b801594e

[294] D. Kohlheyer, G. a. J. Besselink, S. Schlautmann, and R. B. M. Schasfoort, "Free-flow zone electrophoresis and isoelectric focusing using a microfabricated glass device with ion permeable membranes." *Lab on a chip*, vol. 6, no. 3, pp. 374–80, mar 2006. doi:10.1039/b514731j. [Online]. Available: http://www.ncbi.nlm.nih.gov/pubmed/16511620

[295] H. Lu, S. Gaudet, M. A. Schmidt, and K. F. Jensen, "A microfabricated device for subcellular organelle sorting," *Analytical Chemistry*, vol. 76, no. 19, pp. 5705–5712, 2004.

[296] Y. A. Song, M. Chan, C. Cello, S. R. Tannenbaum, J. S. Wishnok, and J. Han, "Free-flow zone electrophoresis of peptides and proteins in PDMS microchip for narrow pi range sample prefractionation coupled with mass spectrometry," *Analytical Chemistry*, vol. 82, no. 6, pp. 2317–2325, 2010.

[297] S. Köhler, C. Weilbeer, S. Howitz, H. Becker, V. Beushausen, and D. Belder, "PDMS free-flow electrophoresis chips with integrated partitioning bars for bubble segregation." *Lab on a chip*, vol. 11, no. 2, pp. 309–314, 2011.

[298] C. R. Cabrera and P. Yager, "Continuous concentration of bacteria in a microfluidic flow cell using electrokinetic techniques." *Electrophoresis*, vol. 22, no. 2, pp. 355–62, jan 2001. doi:10.1002/1522-2683(200101)22:2¡355::AID-ELPS355¿3.0.CO;2-C. [Online]. Available: http://www.ncbi.nlm.nih.gov/pubmed/11288905

[299] K. Halle, J. Li, M. Munson, and J. Monteith, "Capture and release concentration of bacteria using free-flow-zone electrophoresis," in *Micro Total Analysis Systems*, 2003, pp. 559–562. [Online]. Available: http://scholar.google.com/scholar?hl=en{&}btnG=Search{&}q=intitle:Capture+and+release+concentration+of+bacteria+using+free-flow-zone+electrophoresis{#}0

[300] A. K. Balasubramanian, K. A. Soni, A. Beskok, and S. D. Pillai, "A microfluidic device for continuous capture and concentration of microorganisms from potable water." *Lab on a chip*, vol. 7, no. 10, pp. 1315–21, oct 2007. doi:10.1039/b706559k. [Online]. Available: http://www.ncbi.nlm.nih.gov/pubmed/17896016

[301] S. Podszun, P. Vulto, H. Heinz, S. Hakenberg, C. Hermann, T. Hankemeier, and G. A. Urban, "Enrichment of viable bacteria in a micro-volume by free-flow electrophoresis." *Lab on a chip*, vol. 12, no. 3, pp. 451–7, feb 2012. doi:10.1039/c1lc20575g. [Online]. Available: http://www.ncbi.nlm.nih.gov/pubmed/22008897

[302] W. W. Wilson, M. M. Wade, S. C. Holman, and F. R. Champlin, "Status of methods for assessing bacterial cell surface charge properties based on zeta potential measurements." *Journal of microbiological methods*, vol. 43, no. 3, pp. 153–64, jan 2001. [Online]. Available: http://www.ncbi.nlm.nih.gov/pubmed/11118650

[303] M. C. van Loosdrecht, J. Lyklema, W. Norde, G. Schraa, and A. J. Zehnder, "Electrophoretic mobility and hydrophobicity as a measured to predict the initial steps of bacterial adhesion." *Applied and Environmental Microbiology*, vol. 53, no. 8, pp. 1898–1901, 1987.

[304] M. Jackowski, J. Szeliga, E. Kodziska, and B. Buszewski, "Application of capillary zone electrophoresis (CZE) to the determination of pathogenic bacteria for medical diagnosis," *Analytical and Bioanalytical Chemistry*, vol. 391, no. 6, pp. 2153–2160, 2008.

[305] A. Pfetsch and T. Welsch, "Determination of the electrophoretic mobility of bacteria and their separation by capillary zone electrophoresis," pp. 198–201, 1997.

[306] H. Cui, K. Horiuchi, P. Dutta, and C. F. Ivory, "Isoelectric focusing in a poly(dimethylsiloxane) microfluidic chip," *Analytical Chemistry*, vol. 77, no. 5, pp. 1303–1309, 2005.

[307] N. W. Frost and M. T. Bowser, "Using buffer additives to improve analyte stream stability in micro free flow electrophoresis." *Lab on a chip*, vol. 10, no. 10, pp. 1231–6, may 2010. doi:10.1039/b922325h. [Online]. Available: http://www.pubmedcentral.nih.gov/articlerender.fcgi?artid=2903047{&}tool=pmcentrez{&}rendertype=abstract

[308] B. R. Fonslow, V. H. Barocas, and M. T. Bowser, "Using channel depth to isolate and control flow in a micro free-flow electrophoresis device," *Analytical Chemistry*, vol. 78, no. 15, pp. 5369–5374, 2006.

[309] P. Vulto, T. Huesgen, B. Albrecht, and G. a. Urban, "A full-wafer fabrication process for glass microfluidic chips with integrated electroplated electrodes by direct bonding of dry film resist," *Journal of Micromechanics and Microengineering*, vol. 19, no. 7, p. 077001, jul 2009. doi:10.1088/0960-1317/19/7/077001. [Online]. Available: http://stacks.iop.org/0960-1317/19/i=7/a=077001?key=crossref.960936a991db877df870480ec9529120

[310] C.-Y. Lee, C.-H. Lin, and L.-M. Fu, "Band spreading control in electrophoresis microchips by localized zeta-potential variation using field-effect." *The Analyst*, vol. 129, no. 10, pp. 931–7, oct 2004. doi:10.1039/b407627n. [Online]. Available: http://www.ncbi.nlm.nih.gov/pubmed/15457326

[311] J. R. Brody and S. E. Kern, "Sodium boric acid: A Tris-free, cooler conductive medium for DNA electrophoresis," *BioTechniques*, vol. 36, no. 2, pp. 214–216, 2004. [Online]. Available: http://www.biotechniques.com/multimedia/archive/00036/BTN{_}A{_}04362BM02{_}O{_}36180a.pdf

[312] R. E. Wooley and M. S. Jones, "Action of EDTA-tris and antimicrobial agent combinations on selected pathogenic bacteria," *Veterinary Microbiology*, vol. 8, no. 3, pp. 271–280, 1983.

[313] B. Herigstad, M. Hamilton, and J. Heersink, "How to optimize the drop plate method for enumerating bacteria," *Journal of Microbiological Methods*, vol. 44, no. 2, pp. 121–129, mar 2001. doi:10.1016/S0167-7012(00)00241-4. [Online]. Available: http://www.sciencedirect.com/science/article/pii/S0167701200002414http://linkinghub.elsevier.com/retrieve/pii/S0167701200002414

[314] R. Vijayakumar, V. Kannan, and C. Manoharan, "Molecular diagnosis of Pseudomonas aeruginosa contamination in ophthalmic viscosurgical devices," *International Journal of Research in Pharmaceutical Sciences*, vol. 2, no. 4, pp. 579–584, 2011. [Online]. Available: http://pharmascope.org/ijrps/downloads/Volume2/Issue4/16-101.pdf

[315] V. Oncescu, M. Mancuso, and D. Erickson, "Cholesterol testing on a smartphone." *Lab on a chip*, vol. 14, no. 4, pp. 759–63, feb 2014. doi:10.1039/c3lc51194d. [Online]. Available: http://xlink.rsc.org/?DOI=c3lc51194dhttp://www.ncbi.nlm.nih.gov/pubmed/24336861

[316] J. Yeon and J. Park, "Microfluidic cell culture systems for cellular analysis," *Biochip Journal*, vol. 1, no. 1, pp. 17–27, 2007. [Online]. Available: http://nanobio.kaist.ac.kr/papers/biochipj{_}1{_}17{_}2007.pdf

[317] A. van de Stolpe and J. den Toonder, "Workshop meeting report Organs on Chips: human disease models," *Lab on a Chip*, no. 207890, 2013. doi:10.1039/c3lc50248a. [Online]. Available: http://pubs.rsc.org/en/Content/ArticleLanding/2013/LC/c3lc50248a

[318] V. Charwat, M. Purtscher, S. F. Tedde, O. Hayden, and P. Ertl, "Standardization of microfluidic cell cultures using integrated organic photodiodes and electrode arrays." *Lab on a chip*, vol. 13, no. 5, pp. 785–97, feb 2013. doi:10.1039/c2lc40965h. [Online]. Available: http://www.ncbi.nlm.nih.gov/pubmed/23254868

[319] J. T. Nevill, R. Cooper, M. Dueck, D. N. Breslauer, and L. P. Lee, "Integrated microfluidic cell culture and lysis on a chip." *Lab on a chip*, vol. 7, no. 12, pp. 1689–95, dec 2007. doi:10.1039/b711874k. [Online]. Available: http://www.ncbi.nlm.nih.gov/pubmed/18030388

[320] K. Lei, "Review on Impedance Detection of Cellular Responses in Micro/Nano Environment," *Micromachines*, vol. 5, no. 1, pp. 1–12, jan 2014. doi:10.3390/mi5010001. [Online]. Available: http://www.mdpi.com/2072-666X/5/1/1/

[321] C. W. Gregory, K. L. Sellgren, K. H. Gilchrist, and S. Grego, "High yield fabrication of multilayer polydimethylsiloxane devices with freestanding micropillar arrays." *Biomicrofluidics*, vol. 7, no. 5, p. 56503, jan 2013. doi:10.1063/1.4827600. [Online]. Available: http://www.ncbi.nlm.nih.gov/pubmed/24396532

[322] S.-B. Huang, S.-S. Wang, C.-H. Hsieh, Y. C. Lin, C.-S. Lai, and M.-H. Wu, "An integrated microfluidic cell culture system for high-throughput perfusion three-dimensional cell culture-based assays: effect of cell culture model on the results of chemosensitivity assays." *Lab on a chip*, vol. 13, no. 6, pp. 1133–43, mar 2013. doi:10.1039/c2lc41264k. [Online]. Available: http://www.ncbi.nlm.nih.gov/pubmed/23353927

[323] C. P. Huang, J. Lu, H. Seon, A. P. Lee, L. a. Flanagan, H.-Y. Kim, A. J. Putnam, and N. L. Jeon, "Engineering microscale cellular niches for three-dimensional multicellular co-cultures." *Lab on a chip*, vol. 9, no. 12, pp. 1740–8, jun 2009. doi:10.1039/b818401a. [Online]. Available: http://www.pubmedcentral.nih.gov/articlerender.fcgi?artid=3758562{&}tool=pmcentrez{&}rendertype=abstract

[324] A. P. Wong, R. Perez-Castillejos, J. Christopher Love, and G. M. Whitesides, "Partitioning microfluidic channels with hydrogel to construct tunable 3-D cellular microenvironments." *Biomaterials*, vol. 29, no. 12, pp. 1853–61, apr 2008. doi:10.1016/j.biomaterials.2007.12.044. [Online]. Available: http://www.pubmedcentral.nih.gov/articlerender.fcgi?artid=2288785{&}tool=pmcentrez{&}rendertype=abstract

[325] M. B. Byrne, L. Trump, A. V. Desai, L. B. Schook, H. R. Gaskins, and P. J. a. Kenis, "Microfluidic platform for the study of intercellular communication via soluble factor-cell and cell-cell paracrine signaling." *Biomicrofluidics*, vol. 8, no. 4, p. 044104, jul 2014. doi:10.1063/1.4887098. [Online]. Available: http://www.ncbi.nlm.nih.gov/pubmed/25379089

[326] M.-C. Kim, Z. Wang, R. H. W. Lam, and T. Thorsen, "Building a better cell trap: Applying Lagrangian modeling to the design of microfluidic devices for cell biology," *Journal of Applied Physics*, vol. 103, no. 4, p. 044701, 2008. doi:10.1063/1.2840059. [Online]. Available: http://link.aip.org/link/JAPIAU/v103/i4/p044701/s1{&}Agg=doi

[327] P. J. Hung, P. J. Lee, P. Sabounchi, N. Aghdam, R. Lin, and L. P. Lee, "A novel high aspect ratio microfluidic design to provide a stable and uniform microenvironment for cell growth in a high throughput mammalian cell culture array." *Lab on a chip*, vol. 5, no. 1, pp. 44–8, jan 2005. doi:10.1039/b410743h. [Online]. Available: http://www.ncbi.nlm.nih.gov/pubmed/15616739

[328] K. Liu, R. Pitchimani, D. Dang, K. Bayer, T. Harrington, and D. Pappas, "Cell culture chip using low-shear mass transport." *Langmuir : the ACS journal of surfaces and colloids*, vol. 24, no. 11, pp. 5955–60, jun 2008. doi:10.1021/la8003917. [Online]. Available: http://www.ncbi.nlm.nih.gov/pubmed/18471001

[329] P. Sun, Y. Liu, J. Sha, Z. Zhang, Q. Tu, P. Chen, and J. Wang, "High-throughput microfluidic system for long-term bacterial colony monitoring and antibiotic testing in zero-flow environments." *Biosensors & bioelectronics*, vol. 26, no. 5, pp. 1993–9, jan 2011. doi:10.1016/j.bios.2010.08.062. [Online]. Available: http://www.ncbi.nlm.nih.gov/pubmed/20880691

[330] M. Kolnik, L. S. Tsimring, and J. Hasty, "Vacuum-assisted cell loading enables shear-free mammalian microfluidic culture." *Lab on a chip*, vol. 12, no. 22, pp. 4732–7, oct 2012. doi:10.1039/c2lc40569e. [Online]. Available: http://www.ncbi.nlm.nih.gov/pubmed/22961584

[331] N. J. Cira, J. Y. Ho, M. E. Dueck, and D. B. Weibel, "A self-loading microfluidic device for determining the minimum inhibitory concentration of antibiotics." *Lab on a chip*, vol. 12, no. 6, pp. 1052–9, mar 2012. doi:10.1039/c2lc20887c. [Online]. Available: http://www.ncbi.nlm.nih.gov/pubmed/22193301

[332] S. Sugiura, Y. Sakai, K. Nakazawa, and T. Kanamori, "Superior oxygen and glucose supply in perfusion cell cultures compared to static cell cultures demonstrated by simulations using the finite element method." *Biomicrofluidics*, vol. 5, no. 2, p. 22202, jun 2011. doi:10.1063/1.3589910. [Online]. Available: http://www.pubmedcentral.nih.gov/articlerender.fcgi?artid=3145228{&}tool=pmcentrez{&}rendertype=abstract

[333] S. Demming, B. Sommer, a. Llobera, D. Rasch, R. Krull, and S. Büttgenbach, "Disposable parallel poly(dimethylsiloxane) microbioreactor with integrated readout grid for germination screening of Aspergillus ochraceus." *Biomicrofluidics*, vol. 5, no. 1, p. 14104, jan 2011. doi:10.1063/1.3553004. [Online]. Available: http://www.pubmedcentral.nih.gov/articlerender.fcgi?artid=3060924{&}tool=pmcentrez{&}rendertype=abstract

[334] G. Pagano, M. Ventre, M. Iannone, F. Greco, P. L. Maffettone, and P. a. Netti, "Optimizing design and fabrication of microfluidic devices for cell cultures: An effective approach to control cell microenvironment in three dimensions," *Biomicrofluidics*, vol. 8, no. 4, p. 046503, jul 2014. doi:10.1063/1.4893913. [Online]. Available: http://scitation.aip.org/content/aip/journal/bmf/8/4/10.1063/1.4893913

[335] Y. C. Wei, F. Chen, T. Zhang, D. Y. Chen, X. Jia, J. B. Wang, W. Guo, and J. Chen, "Vascular smooth muscle cell culture in microfluidic devices," *Biomicrofluidics*, vol. 8, no. 4, p. 046504, jul 2014. doi:10.1063/1.4893914. [Online]. Available: http://scitation.aip.org/content/aip/journal/bmf/8/4/10.1063/1.4893914

[336] M. Gan, Y. Tang, Y. Shu, H. Wu, and L. Chen, "Massively parallel bacterial and yeast suspension culture on a chip." *Small (Weinheim an der Bergstrasse, Germany)*, vol. 8, no. 6, pp. 863–7, mar 2012. doi:10.1002/smll.201102322. [Online]. Available: http://www.ncbi.nlm.nih.gov/pubmed/22294524

[337] H. M. Hegab, A. Elmekawy, and T. Stakenborg, "Review of microfluidic microbioreactor technology for high-throughput submerged microbiological cultivation." *Biomicrofluidics*, vol. 7, no. 2, p. 21502, jan 2013. doi:10.1063/1.4799966. [Online]. Available: http://www.pubmedcentral.nih.gov/articlerender.fcgi?artid=3631267{&}tool=pmcentrez{&}rendertype=abstract

[338] M. Tehranirokh, A. Z. Kouzani, P. S. Francis, and J. R. Kanwar, "Microfluidic devices for cell cultivation and proliferation." *Biomicrofluidics*, vol. 7, no. 5, p. 51502, jan 2013. doi:10.1063/1.4826935. [Online]. Available: http://www.pubmedcentral.nih.gov/articlerender.fcgi?artid=3829894{&}tool=pmcentrez{&}rendertype=abstract

[339] D. Gao, H. Liu, Y. Jiang, and J.-M. Lin, "Recent developments in microfluidic devices for in vitro cell culture for cell-biology research," *TrAC Trends in Analytical Chemistry*, vol. 35, pp. 150–164, may 2012. doi:10.1016/j.trac.2012.02.008. [Online]. Available: http://linkinghub.elsevier.com/retrieve/pii/S0165993612000830

[340] E. W. K. Young and D. J. Beebe, "Fundamentals of microfluidic cell culture in controlled microenvironments." *Chemical Society reviews*, vol. 39, no. 3, pp. 1036–48, mar 2010. doi:10.1039/b909900j. [Online]. Available: http://www.pubmedcentral.nih.gov/articlerender.fcgi?artid=2967183{&}tool=pmcentrez{&}rendertype=abstract

[341] C. H. Chen, Y. Lu, M. L. Y. Sin, K. E. Mach, D. D. Zhang, V. Gau, J. C. Liao, and P. K. Wong, "Antimicrobial susceptibility testing using high surface-to-volume ratio microchannels." *Analytical chemistry*, vol. 82, no. 3, pp. 1012–9, feb 2010. doi:10.1021/ac9022764. [Online]. Available: http://www.pubmedcentral.nih.gov/articlerender.fcgi?artid=2821038{&}tool=pmcentrez{&}rendertype=abstract

[342] J. Zhou, A. V. Ellis, and N. H. Voelcker, "Recent developments in PDMS surface modification for microfluidic devices." *Electrophoresis*, vol. 31, no. 1, pp. 2–16, jan 2010. doi:10.1002/elps.200900475. [Online]. Available: http://www.ncbi.nlm.nih.gov/pubmed/20039289

[343] C. Y. Chan, V. N. Goral, M. E. DeRosa, T. J. Huang, and P. K. Yuen, "A polystyrene-based microfluidic device with three-dimensional interconnected microporous walls for perfusion cell culture," *Biomicrofluidics*, vol. 8, no. 4, p. 046505, jul 2014. doi:10.1063/1.4894409. [Online]. Available: http://scitation.aip.org/content/aip/journal/bmf/8/4/10.1063/1.4894409

[344] C. G. Sip and A. Folch, "Stable chemical bonding of porous membranes and poly(dimethylsiloxane) devices for long-term cell culture." *Biomicrofluidics*, vol. 8, no. 3, p. 036504, may 2014. doi:10.1063/1.4883075. [Online]. Available: http://scitation.aip.org/content/aip/journal/bmf/8/3/10.1063/1.4883075http://www.ncbi.nlm.nih.gov/pubmed/25379080

[345] E. Vereshchagina, D. Mc Glade, M. Glynn, and J. Ducrée, "A hybrid microfluidic platform for cell-based assays via diffusive and convective trans-membrane perfusion." *Biomicrofluidics*, vol. 7, no. 3, p. 34101, jan 2013. doi:10.1063/1.4804250. [Online]. Available: http://www.pubmedcentral.nih.gov/articlerender.fcgi?artid=3663865{&}tool=pmcentrez{&}rendertype=abstract

[346] D. Puchberger-Enengl, S. V. D. Driesche, C. Krutzler, F. Keplinger, and M. J. Vellekoop, "Microfluidic cell culturing by hydrogel-based diffusion/perfusion," in *Transducers 2013, Barcelona, SPAIN, 16-20 June 2013*, no. June, 2013, pp. 2094–2097. [Online]. Available: http://ieeexplore.ieee.org/xpls/abs{_}all.jsp?arnumber=6627213

[347] WHO, "Antimicrobial resistance: global report on surveillance 2014," World Health Organisation, Tech. Rep., 2014.

[348] F. Deiss, M. E. Funes-Huacca, J. Bal, K. F. Tjhung, and R. Derda, "Antimicrobial susceptibility assays in paper-based portable culture devices." *Lab on a chip*, vol. 14, no. 1, pp. 167–71, jan 2014. doi:10.1039/c3lc50887k. [Online]. Available: http://www.ncbi.nlm.nih.gov/pubmed/24185315

[349] C.-C. Chung, I.-F. Cheng, W.-H. Yang, and H.-C. Chang, "Antibiotic susceptibility test based on the dielectrophoretic behavior of elongated Escherichia coli with cephalexin treatment." *Biomicrofluidics*, vol. 5, no. 2, p. 21102, jun 2011. doi:10.1063/1.3600650. [Online]. Available: http://www.pubmedcentral.nih.gov/articlerender.fcgi?artid=3138792{&}tool=pmcentrez{&}rendertype=abstract

[350] Y.-H. Liu, C.-H. Wang, J.-J. Wu, and G.-B. Lee, "Rapid detection of live methicillin-resistant Staphylococcus aureus by using an integrated microfluidic system capable of ethidium monoazide pre-treatment and molecular diagnosis." *Biomicrofluidics*, vol. 6, no. 3, p. 34119, jan 2012. doi:10.1063/1.4748358. [Online]. Available: http://www.pubmedcentral.nih.gov/articlerender.fcgi?artid=3461804{&}tool=pmcentrez{&}rendertype=abstract

[351] K. P. Kim, Y.-G. Kim, C.-H. Choi, H.-E. Kim, S.-H. Lee, W.-S. Chang, and C.-S. Lee, "In situ monitoring of antibiotic susceptibility of bacterial biofilms in a microfluidic device." *Lab on a chip*, vol. 10, no. 23, pp. 3296–9, dec 2010. doi:10.1039/c0lc00154f. [Online]. Available: http://www.ncbi.nlm.nih.gov/pubmed/20938507

[352] M. Kalashnikov, J. C. Lee, J. Campbell, A. Sharon, and A. F. Sauer-Budge, "A microfluidic platform for rapid, stress-induced antibiotic susceptibility testing of Staphylococcus aureus." *Lab on a chip*, vol. 12, no. 21, pp. 4523–32, nov 2012. doi:10.1039/c2lc40531h. [Online]. Available: http://www.pubmedcentral.nih.gov/articlerender.fcgi?artid=3489182{&}tool=pmcentrez{&}rendertype=abstract

[353] Z. Hou, Y. An, K. Hjort, K. Hjort, L. Sandegren, and Z. Wu, "Time lapse investigation of antibiotic susceptibility using a microfluidic linear gradient 3D culture device." *Lab on a chip*, vol. 14, no. 17, pp. 3409–18, sep 2014. doi:10.1039/c4lc00451e. [Online]. Available: http://www.ncbi.nlm.nih.gov/pubmed/25007721

[354] J. Choi, Y.-G. Jung, J. Kim, S. Kim, Y. Jung, H. Na, and S. Kwon, "Rapid antibiotic susceptibility testing by tracking single cell growth in a microfluidic agarose channel system." *Lab on a chip*, vol. 13, no. 2, pp. 280–7, jan 2013. doi:10.1039/c2lc41055a. [Online]. Available: http://www.ncbi.nlm.nih.gov/pubmed/23172338

[355] C. D. Chin, V. Linder, and S. K. Sia, "Commercialization of microfluidic point-of-care diagnostic devices." *Lab on a chip*, vol. 12, no. 12, pp. 2118–34, jun 2012. doi:10.1039/c2lc21204h. [Online]. Available: http://www.ncbi.nlm.nih.gov/pubmed/22344520

[356] F. Cockerill, M. Wickler, and J. Alder, *Performance Standards for Antimicrobial Susceptibility Testing; Twenty-second Informational Supplement*, 32nd ed. Wayne, Pennsylvania: Clinical and Laboratory Standards Institute, 2012, vol. 32, no. 3. [Online]. Available: http://scholar.google.com/scholar?hl=en{&}btnG=Search{&}q=intitle:Performance+Standards+for+Antimicrobial+Susceptibility+Testing+;+Twenty-Second+Informational+Supplement{#}1

[357] P. V. D. Meeren, "Determination of oxygen profiles in agar-based gelled in vitro plant tissue culture media," *Plant Cell, Tissue and Organ Culture*, vol. 65, no. 3, pp. 239–245, 2001. doi:10.1023/A:1010698225362. [Online]. Available: http://link.springer.com/article/10.1023/A:1010698225362

[358] R. Sisieby, "Composition for diagnosing glucose," *US Patent 3,123,443*, 1964. [Online]. Available: http://www.google.com/patents/US3123443

[359] D. J. Mason, S. Shanmuganathan, F. C. Mortimer, and V. a. Gant, "A fluorescent Gram stain for flow cytometry and epifluorescence microscopy." *Applied and environmental microbiology*, vol. 64, no. 7, pp. 2681–5, jul 1998. [Online]. Available: http://www.pubmedcentral.nih.gov/articlerender.fcgi?artid=106444{&}tool=pmcentrez{&}rendertype=abstract

[360] C. Miller, L. E. Thomsen, C. Gaggero, R. Mosseri, H. Ingmer, and S. N. Cohen, "SOS response induction by beta-lactams and bacterial defense against antibiotic lethality." *Science (New York, N.Y.)*, vol. 305, no. 5690, pp. 1629–31, sep 2004. doi:10.1126/science.1101630. [Online]. Available: http://www.ncbi.nlm.nih.gov/pubmed/15308764

[361] M. a. Fonder, G. S. Lazarus, D. a. Cowan, B. Aronson-Cook, A. R. Kohli, and A. J. Mamelak, "Treating the chronic wound: A practical approach to the care of nonhealing wounds and wound care dressings." *Journal of the American Academy of Dermatology*, vol. 58, no. 2, pp. 185–206, feb 2008. doi:10.1016/j.jaad.2007.08.048. [Online]. Available: http://www.ncbi.nlm.nih.gov/pubmed/18222318

[362] S. Ramsay, L. Cowan, J. M. Davidson, L. Nanney, and G. Schultz, "Wound samples: moving towards a standardised method of collection and analysis." *International wound journal*, no. JANUARY, jan 2015. doi:10.1111/iwj.12399. [Online]. Available: http://www.ncbi.nlm.nih.gov/pubmed/25581688

[363] J. F. Tarlton, A. J. Bailey, E. Crawford, D. Jones, K. Moore, and K. D. Harding, "Prognostic value of markers of collagen remodeling in venous ulcers," *Wound Repair and Regeneration*, vol. 7, no. 5, pp. 347–355, sep 1999. doi:10.1046/j.1524-475X.1999.00347.x. [Online]. Available: http://doi.wiley.com/10.1046/j.1524-475X.1999.00347.x

About the Author

Dietmar Puchberger was born in Steyr, Austria in 1981. After graduating from the Federal Higher Technical Institute Steyr in electronics and computer engineering he studied electrical engineering at the Vienna University of Technology. In November 2009 he received his M.Sc. degree in automation and control engineering with distinction. In 2010 he worked as a temporary research assistant at the Institute of Microsystem Technology, University of Freiburg in the EU Marie Curie research training network Cellcheck. He joined the Institute of Sensors and Actuator Systems, Vienna University of Technology where he started working towards his Ph.D. in 2011. In 2013 he joined the Institute for Microsensors, -Actuators and -Systems at the University of Bremen to continue his research activities in biomedical sensing, microfluidic pathogen detection and physiological fluid analysis.